Tracking helminths : from molecular diagnostics to mechanisms behind immune polarization

Kaisar, M.M.

Tracking helminths:

from molecular diagnostics to
mechanisms behind immune polarization

ISBN: 978-94-6182-826-2

The work presented in this thesis was performed at the Department of Parasitology, at the Leiden University Medical Center in the Netherlands and the Department of Parasitology, Faculty of Medicine, Universitas Indonesia.

About the cover:
The cover illustrates, the recognition of *Schistosoma mansoni* or its molecules by dendritic cells and presentation to the T cells.

Cover design and artwork: Maria M. M. Kaisar and Ella Maru Studio (http://www.scientific-illustrations.com)

Layout: Maria M. M. Kaisar
Printing: Off Page (www.offpage.nl)

Printing of this thesis was financially supported by Dr P. F. C. Flu Foundation, Cayman Chemical, ChipSoft and SCIEX.

Tracking helminths: from molecular diagnostics to mechanisms behind immune polarization

Proefschrift

ter verkrijging van
de graad van Doctor aan de Universiteit Leiden,
op gezag van Rector Magnificus prof.mr. C.J.J.M. Stolker,
volgens besluit van het College voor Promoties
ter verdedigen op donderdag 19 september 2017
klokke 10.00 uur

door

Maria Mardalena Martini Kaisar
Geboren te Bengkulu (Indonesia) in 1986

Promotor	**:** Prof. Dr. M. Yazdanbakhsh
Co-promotor	**:** Dr. B. Everts
Leden promotiecommissie	**:** Prof. Dr. C. H. Hokke Prof. Dr. T. Supali (Universitas Indonesia) Prof. Dr. P. Soewondo (Universitas Indonesia) Prof. Dr. A. G. M. Tielens (Universiteit Utrecht, Utrecht) Prof. Dr. E. J. Kuijper Dr. A. Ioan-Facsinay

Dedicated to my husband Felix Liauw,
mama-papa and mami-papi
thank you for always love me

Contents:

Chapter 1

General Introduction

1. Helminth infections

Helminths are parasitic worms that live in their host for protection and to extract nutrients from, that allow them develop, grow, and reproduce. Among the 17 major neglected tropical diseases (NTDs), infections caused by soil transmitted helminths (STHs) and schistosomes are the most ubiquitous. In particular in tropical and subtropical areas, globally over 1.5 billion and 200 million people are infected with STHs and schistosomes, respectively [1, 2]. STHs are *Ascaris lumbricoides* (roundworm), *Trichuris trichiura* (whipworm), and two species of hookworms: *Necator americanus* and *Ancylostoma duodenale* [3]. The schistosome worms are *Schistosoma mansoni*, *Schistosoma heamatobium* and *Schistosoma japonicum* with *S. mansoni* the most prevalent [1].

Although people with light infections of STHs or *Shistosoma* spp normally have no symptoms, heavy infections are commonly associated with morbidity [4]. Using the disability-adjusted life years (DALYs) as a measure for burden of disease, STHs and schistosomiasis cause 5.2 million and 3.3 million DALYs, respectively, making them two major contributors to infection-induced DALYs [5]. Given that helminth infections can tremendously affect the quality of life, WHO together with several prominent global health organizations have implemented global deworming programs with the ultimate goal to eliminate these infections by 2020 [2].

Interestingly however, helminth infections do not only do harm. They are also known for their ability to dampen host immune responses, to allow their long term survival, and at the same time this can be beneficial to the host by helping to control excessive inflammation and thereby occurrence of inflammatory diseases. Several animal models and clinical trials have demonstrated beneficial effects of helminth infections on a broad range of diseases including celiac disease, inflammatory bowel disease (IBD), multiple sclerosis (MS), diabetes, asthma and atopy [6-11]. Therefore, besides combating helminth infections worldwide, investigating how helminths and molecules derived from these parasites can modulate the immune responses will be equally important.

2. Detecting helminth infections: moving toward a standardized molecular based diagnosis technique

Diagnosis of intestinal helminths has always relied on microscopy-based detection of egg, larva or cysts in human faecal samples. Although microscopic methods are sufficient to detect the most prominent parasite species with a high prevalence and load of infection, it is important to realize that there is currently no single method available that can diagnose all helminth infections with high sensitivity and specificity. Moreover, the current shifts in parasite distribution and successful results from control programmes increase the need for more sensitive and high-throughput diagnostic procedures to identify the remaining infectious reservoir [12]. For monitoring the progress of control or elimination programs and ongoing surveillance of helminth infections, new standardized diagnostics are critically important [2].

The use of real-time PCR for diagnosis of intestinal parasites has been implemented in several endemic countries as well as in clinical laboratories [13]. Real-time PCR has demonstrated to outperform microscopy in the detection of all helminths under study thus far [14-20]. However, further validation is necessary, such as direct comparison of the outcome between different endemic countries using the same pipeline (i.e. sample collection, DNA extraction methods and real-time PCR detection). Nonetheless, it is clear that real-time PCR holds promise as an alternative diagnostic tool and that it could ultimately become the first-line standardized screening method for the diagnosis of helminth infections.

Despite the rapid development and great potential of molecular based techniques to diagnose helminth infections, there are still some hurdles that need to be overcome before it could be used as standardized diagnostics both in the field and in the clinic. First, the need for technologically equipped laboratory to perform real-time PCR [21] makes this method currently mainly possible in research settings [22]. Moreover, current sample preparation techniques for DNA isolation are insufficiently optimized to detect all intestinal parasites. For instance, additional bead-beating treatment prior to DNA extraction has been suggested to improve *T. trichiura* DNA extraction [19]. However, population based data from high prevalence area is still lacking, making it difficult to evaluate the performance of the bead-beating. It is worth mentioning that the effect of bead-beating treatment on other intestinal parasites needs to be evaluated as well to assure that bead-beating will not affect the detection of other intestinal parasites.

3 Helminth-host immune system interplay

The immune system protects organisms from infections with layered defences of increasing specificity. The innate immune system provides an immediate but non-specific response and the long-term protection relies on adaptive immune responses mediated by T cells and B cells. Parasitic helminths have evolved together with the mammalian immune system and as a consequence they have developed numerous survival strategies that include secretion of molecules that can modulate the host immune system [23]. A key component of the immune system that has evolved to minimize the virulence of helminths is the type 2 (or T helper 2) immune response [24].

The generation of type 2 immune responses involves innate and adaptive immune cells as well as non-hematopoietic cells such as epithelial cells as illustrates in Figure 1. Upon infection with helminths, the first cells to be exposed to these pathogens are in many cases epithelial cells that start to produce a variety of type 2 alarmins and cytokines which include thymic stromal lymphopoietin (TSLP), IL-33, resistin-like molecule (RELM)-β and IL-25, of which the latter two are predominantly produced in the gut tuff and goblet cells. In response to TSLP and IL-33 mast cells and basophil are recruited from circulation to undergo degranulation releasing protease, histamine, IL-4 and TNF which can amplify type 2 inflammation and recruitment of leukocytes. Moreover, IL-33 and IL-25 are important for actviation of type 2 innate lymphoid cells (ILC2). Activated ILC2 secrete IL-5 and IL-13, which in turn induce eosinophilia and mucus secretion, respectively. Immature dendritic cells (DCs) reside in the peripheral tissues where they take up helminths antigens, undergo maturation while migrating to lymph nodes and then skew naive T cells toward a T helper 2 (Th2) profile which is characterized by production of IL-4, IL-5, IL-9 and IL-13. Additionally, alarmins such as TSLP also signal to DCs to express Th2-recruiting chemokines and to condition them to prime Th2 responses. Exposure to IL-4 and IL-13 skews macrophages towards a tissue repair phenotype, termed M2 or alternatively activated, characterized by the expression of factors such as arginase (Arg) 1, shitinase-like protein YM1 and RELM-α. Finally IL-4 produced by T cells is involved in B cell activation and Ig class switching towards IgE and IgG1 (in mice) or IgG4 (in humans).

Dendritic cells (DCs) are key players in bridging innate and adaptive immunity. Just like their crucial role in inducing Th1 and Th17 responses against intracellular pathogens (virus and bacteria) and extracellular unicellular pathogens (fungi and bacteria), respectively, the role of DCs in Th2 induction against helminth parasites is indispensable. In mouse models in which

CD11c^{+}DCs were depleted, Th2 priming in response to helminth infections was severely impaired [25-27].

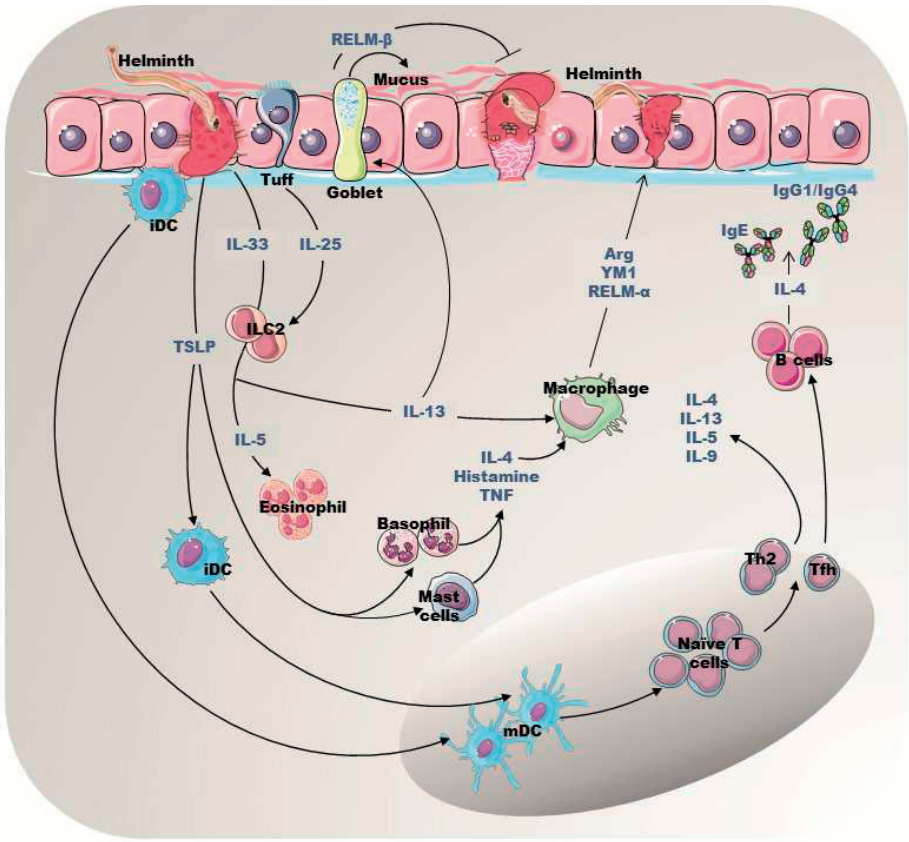

Figure 1. Type 2 immune responses induced by helminths
Helminth infections leads to the tissue damage and secretion of the cytokines IL-33 and TSLP. IL-33 signals on ILC2 leading to recruitment of eosinophils through the secretion of IL-5. ILC2 also sense the increased production of IL-25 by tuff cells and secrete IL-13, which feedback on goblet cells leading to increased mucus production. In response to TSLP, mast cells and basophils are recruited and start amplifying the type 2 inflammation by producing IL-4, histamine and TNF. Subsequently IL-13 and IL-4 contributed to skew macrophage in to M2 phenotype and produce RELM-α, Arg and YM1, which are important for tissue repair. Meanwhile, immature DC resides in the peripheral tissues take up helminths antigens or by sense the TSLP, undergo maturation while migrating to the lymphoid organs to polarize naive T cell into Th2. Th2 cell is characterized by the production of IL-4, IL-5, IL-9 and IL-13. Lastly, T follicular helper cells provide help to B cells for IgE and IgG production in IL-4 dependent manner.

Despite the well appreciated role of DCs in initiation of Th2 responses, several questions regarding the mechanisms underlying this response await to be fully addressed: first, what are the molecule(s) from helminths that is(are) responsible for Th2 priming and how are they recognized by DCs. Second how do these molecules condition DCs to induce Th2 responses. And finally, what are the characteristics of helminth-conditioned DCs that enable them to drive Th2. The current knowledge of these three aspects, will be summarized in the following sections and is schematically shown in Figure 2.

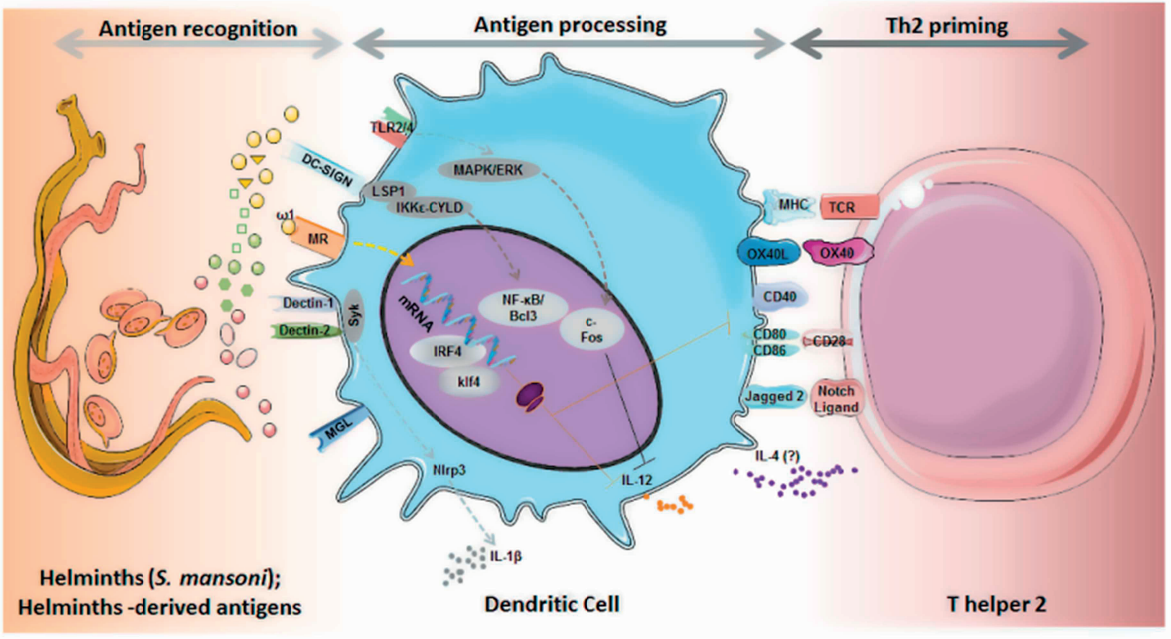

Figure 2. Molecular interaction involved in DC conditioning Th2 polarization by helminth

Antigen recognition: Helminth and helminth derived-antigens are recognized by DC via TLRs (TLR2 an TLR4) and CLRs (MGL, DC-SIGN, MR, Dectin-1 and -2). Antigen processing: Depending on helminth-derived antigens encountered via specific ligation of PRR results in; phosphorylation of MAPK/ERK which stabilized c-Fos and result in suppression of IL-12 production; phosphorylation of Syk that activate Nlrp3 which mediates IL-1β secretion; phosphorylation of LSP1 and subsequently the recruitment of IKKε-CYLD complex activate Bcl3/NF-κB which is important for controlling the CD40 and Jagged 2 expression; Klf4 is required for controlling the transcription factors necessary for Th2 induction in $IRF4^{+}$ DC; in parallel, ω-1 internalized by MR degrades rRNA and mRNA in RNase dependent manner, leading to inhibition of protein synthesis including co-stimulatory molecules (CD80 and CD86) as well as IL-12. Th2 priming: Altogether, via multiple signals which are: PPR-mediated interference of antigen presentation on MHC-II; lower expression of classical maturation markers; promotion of OX40L as well as Jagged 2; lower IL-12 production; and at last, possibly the production of IL-4 by DCs which is still questionable, thus all mediate Th2 polarization.

3.1. Recognition helminth-derived molecules by dendritic cells

Soluble *S. mansoni* egg antigen (SEA) and crude extracts prepared from nematode and cestode parasites [23] are often used in *in vivo* and *in vitro* models to study Th2 polarization by DCs. In addition, several excretory/secretory (ES) fractions from helminths have been found to harbour Th2 polarizing molecules [23, 28] and importantly, within those fractions a couple of helminths-derived single compounds with Th2-inducing capacity have been characterized. For instance a worm-derived lipid secreted by a roundworm, *Acanthocheilonema viteae*, termed ES-62 can condition DCs to prime a Th2 response [29]. Furthermore, lyso-phosphatidylserine (PS) derived from schistosome and *Ascaris* worms was shown to promote Th2 via DCs [30]. Finally an important contribution to this field was made by the discovery of omega-1 (ω-1), a single glycoprotein secreted by *S. mansoni* eggs which was found to harbour strong Th2-polarizing capacity [31, 32].

DCs are equipped with so-called pattern recognition receptors (PRRs) that are important in recognizing pathogens-associated molecular patterns (PAMPs). These receptors encompass several families including Toll-like (TLR), C-type lectin (CLR), nucleotide-binding oligomerization domain/NOD-like (NLR) and RIG-1-like (RLR) receptors [23]. Two out of 11 well-characterized TLRs in human, TLR2 and TLR4 are shown to be essential for Th2-specific DC response to SEA or PS from *S. mansoni* and ES-62 or phosphorylcholine (PC) from ES-62, respectively [29, 33, 34]. However, there is evidence suggesting that TLRs signalling might be dispensable for Th2 induction by helminth as shown by bone marrow-derived DCs (BMDCs) from TLR-2 and TLR-4 KO mice that can still induce a Th2 response [35]. CLRs, including DC-specific ICAM-3 grabbing non-integrin (DC-SIGN), macrophage galactose binding lectin receptor (MGL) and mannose receptor (MR), have been shown to be involved in the internalization of SEA [36]. Another DC CLR that has been shown to bind SEA is dectin-2. Although dectin-2 is primarily known for its ability to recognize fungal antigens, the complex of dectin-2 and FcRγ on BMDC was required for SEA-induced production of IL-1β [37]. Studies have shown that CLRs expressed on DCs that sense helminths glycans, play important role in Th2 induction. For instance, glycan found in SEA Lewis^X (Le^X) which contains Lacto-N-fucopentaose III (LNFIII) has been shown to bind to TLR4 as well as DC-SIGN [36]. DC-SIGN was also shown to be able to recognized glycans from *Toxocara canis* [38]. Another example is, ES from *Taenia crassiceps* (TcES), which can bind to MR and MGL on BMDCs and induce Th2 polarization in a glycan-dependent manner [39]. More recently, a study demonstrated that MR on DC is responsible for the binding and internalization of the *S. mansoni* secreted glycoprotein ω-1 [40]. Thus so far, the evidence suggests helminths glycans sensed by CLRs are generally important molecular patterns for Th2 induction by DCs.

3.2. Signalling by helminth-derived molecules in dendritic cells

Classically, TLR signalling involves the activation of mitogen activated protein kinases (MAPK) including p42/p44 (extracellular signal-regulated kinase, ERK1/2), Janus Kinase (JNK) and p38. Strong release of IL-12 by DC that favours Th1 differentiation is the result of p38 phosphorylation. In contrast, SEA and PS favour phosphorylation of ERK which is associated with induction of Th2, via stabilization of the c-fos transcription factor that suppresses IL-12 release [30, 41]. Likewise, ES-62 and LNFPIII were also shown to induce the activation of ERK in DCs via TLR4 ligation [42-44]. Moreover, a role for ERK in Th2 response development is indicated by the findings that ERK$^{-/-}$ mice exhibit increased susceptibility to experimental autoimmune encephalomyelitis and are Th1 prone. Together these suggest that ERK may play an important role in Th2 polarization [45].

However, the PRR that drive ERK activation in response to helminths and helminths-derived antigens including SEA stimulation remain to be elucidated.

Signalling via NF-κB was also shown to be involved in Th2 response. For instance, mice with the BMDCs from which NF- κB knockout failed to instruct Th2 cell differentiation in response to SEA and LNFPIII [46, 47]. Recently it was shown that Le^X residues derived from SEA can be recognized by DC-SIGN on moDCs. Thus recognition promotes the phosphorylation of LSP1 subsequently the recruitment of IKKε-CYLD that lead to the activation of Bcl3, atypical NF-κB family member which is crucial for inducing a Th2-priming phenotype [48]. Finally, SEA can activate the Nlrp3 inflammasome and increase IL-1β release by BMDCs via spleen tyrosine kinase (Syk) downstream of dectin-2 [37]. However, to what extent this pathway in DCs regulates Th2 priming remains to be investigated. With regards to the signalling events induced by single molecules from helminths, ω-1 was found to modulate DC function for induction of Th2 responses. Mechanistically, ω-1 interferes ribosomal function and protein synthesis in an RNase-dependent manner, following MR-driven translocation into the cytosol [40].

3.3. T helper 2 priming by dendritic cells

Proper priming and polarization of Th responses by DCs is dependent on three DC-derived signals: 1, presentation of cognate peptide antigens in the context of major histocompatibility complex (MHC) II; 2, co-stimulation; and 3, expression of T cell-polarizing factors. The nature of this latter signal is generally decisive for Th differentiation fate. A classic example is IL-12 secretion by DCs that promotes Th1 polarization. However, such a polarizing signal for priming of Th2 responses by helminths has remained elusive. This initially led to the so-called default concept which states that the absence of a Th1-priming signal will promote Th2 polarization. However, IL-12 deficient mice exposed to microbial pathogens failed to default to a Th2 pattern [49], indicating there are active signals involved in this process. A recent transcriptomics study has shown type I interferon to be a key transcriptional signature of murine skin DCs that enables them to drive Th2 induction in response to helminth antigens [50]. However, whether there are groups of type I interferon specifically associated with Th2 polarization or rather as the common signatures similar to Th1, thus need further studies. Another question is, whether the role of type I interferon is tissue and/or cell specific in terms of mounting a Th2 response by helminths. IL-4 can skew naive T cells toward Th2, but despite the importance of this signal, its origin is an area of much debate because it is still debated whether DCs can produce IL-4 [51-53]. It is possible that IL-4 or other Type 2 cytokines that can promote Th2 differentiation, originate from non-DC sources like ILC2s [25], that in conjunction with signal 1 and 2 from DCs can provide the necessary cues for Th2 differentiation.

Alterations in signal 1 and/or 2 have also been linked to Th2 polarization in the context of helminth infections. For instance, studies of early signalling events have shown that short-term or low-avidity interaction between DC and T cell favour Th2 differentiation due to low (avidity) antigen presentation (signal 1) [54]. Interestingly, this phenomenon has also been described for DCs exposed to SEA or ω-1 [31, 55]. Expression of CD40, as part of signal 2, is known to be important for Th2 induction by *S. manoni* [56]. Moreover, SEA has been shown to alter the balance between expression of co-stimulatory molecules CD80 and CD86 on DCs, which has been linked to favouring Th2 polarization as well [57]. Although DC expressing the notch ligand jagged2 have been implicated in Th2 priming, the expression of this molecule is not essential for Th2 response upon SEA stimulation, as Jagged-2-deficient BMDCs are still able to induce Th2 in response to SEA [58]. Finally, several groups have shown that in response both to SEA or TLSP, DC upregulated the

co-stimulatory molecule OX40 ligand (OX40L). T cells sense OX40L on DC through OX40 receptor and produce IL-4, IL-5 and IL-13 [59-63]. Although it has been shown that SEA-treated OX40L-KO DCs are still able to induce a Th2 responses, Th2 cell expansion was reduced, suggesting that the OX40L-OX40 signal contributes to the Th2 response by allowing for optimal expansion of Th2 cells [60].

The mechanisms behind the ability of helminth antigens to modulate DCs for priming of Th2 responses have been primarily studied in *in vitro* DC models, which fail to capture the complexity of the different DC subsets that exist *in vivo*. Recent studies have demonstrated the existence of a specific Th2-priming DC subset that is developmentally dependent on transcription factor (TF) IRF4 and Klf4 and is required for priming of Th2 responses including those in response to helminth antigens [64-66]. Future studies will be needed to determine the relative contribution of the ability of helminth antigens to conditions DCs for Th2 priming versus the intrinsic ability of certain DC subsets to prime Th2 responses, in *in vivo* upon helminth infections.

4. Interaction with microbe metabolites: the extended niche

4.1. The relationship between helminths and microbe

In recent years it has become increasingly clear that our microbiota play a key role in shaping our immune system. Given the fact that many helminths and microbiota inhabit the same niche, the intestine, it is likely that they interact and impact on each other [67]. Beside the ability of helminths to secrete a variety of products that directly affect host immune function, they also have the capacity to influence the composition of the microbiota [68-71], thereby possibility regulating immune function indirectly. *Vice versa,* changes in microbiota can affect susceptibility to helminth infection [70, 72, 73], indicating that the crosstalk between these two groups of endobiota can play an essential role in host intestinal immune function and homeostasis [74]. Importantly, this relationship between microbiota and helminths has been shown to have beneficial effects on inflammatory diseases including IBD, celiac diseases, multiple sclerosis, diabetes and allergy [67]. As an example, a recent study showed that the intestinal microbiota contributes to the ability of helminths to suppress allergic inflammation [75]. With respect to host defenses, helminth infections elicit type 2 immune responses as described in the previous section, while opportunistic bacterial infections can evoke Th1 or Th17 responses [74, 76, 77]. However, both microbiota and helminths have the additional capacity to promote regulatory immune responses, which are key to limit inflammation and associated tissue damage that could be caused by the aforementioned effector responses when left unchecked. The potential interaction between microbiota and helminths is illustrated in Figure 3.

4.2. Immune modulation by the bacterial metabolites

The human body is colonized by roughly 3.9×10^{13} bacteria [78] that can potentially interact with the immune system. There are more than 50 bacterial phyla, but human gut-associated microbiota is dominated by four main phyla: *Firmicutes*, *Bacteroidetes*, *Actinobacteria* and *Proteobacteria* [79]. Microbiota are able to produce numerous metabolites, among them are the short chain fatty acids [80]. A significant number of studies have highlighted the immunomodulatory potential of SCFAs with beneficial effects on a broad range of inflammatory diseases IBD, colitis, asthma, obesity and arthritis [80-84]. Mechanistically, SCFAs can affect immune cells via signaling through specific G protein-coupled receptors (GPRs) [85, 86] as well as through histone deacetylation (HDAC)

inhibition. This primarily leads to suppression of inflammatory responses (i.e. reduction in expression of pro-inflammatory cytokines) by DCs, macrophages and T cells [87-89]. With regard to DCs, it has been shown that SCFAs can promote tolerogenic properties in DCs resulting in increased ability to prime Treg cells [80, 86]. However, the exact molecular mechanisms through which SCFAs modulate the capacity of human DCs to induce Treg cells is not known.

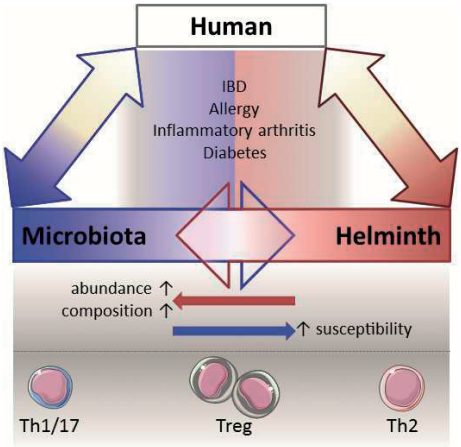

Figure 3. Interactions between human host, helminths and microbiota
Microbiota and helminths are co-inhabit the human gut with multi-way interactions. Helminths infections appear to be correlated with heightened microbiota diversity, and conversely, alteration of microbiota composition and abundance can alter susceptibility to helminths. Mechanistically, microbiota induce the Th1/Th17, whereas helminths are strong Th2 inducers. Moreover, both are capable of inducing Treg to keep immune responses under control. Thus can lead to protection against inflammatory diseases, such as IBD, diabetes, allergy and inflammatory arthritis.

5. Scope of the thesis

This thesis targets helminth infections and how they could affect the immune system in order to devise interventions that can help, on the one hand to control helminth infections and on the other to modulate inflammatory diseases. To start with, research is still needed to detect helminths with utmost sensitivity. Hence, the first two chapters of this thesis are focused on molecular diagnostics of helminth infections. Specifically, in **Chapter 2** the performance of real-time PCR *versus* microscopy in diagnosing STH infections are compared. The studies are performed in two STH endemic areas namely Beira, Mozambique and Nangapanda, East Nusa Tenggara, Indonesia. In **Chapter 3** a study is described that aims to improve the diagnosis of *T. trichiura* by optimizing sample preparation prior to DNA extraction from faces. The optimized procedures are then compared to the standard procedure.

Next, the issue of immune modulation by helminth infections, still requires in depth understanding of how helminths induce Th2 and Treg responses before new intervention strategies can be developed to combat these infections and to manipulate inflammatory diseases. Therefore the second part of the thesis deals with the interplay between helminths and the mammalian host immune system with particular emphasis on the mechanisms by which helminth-derived molecules promote Th2 responses. First, in **Chapter 4**, the lipid profile of different life cycle stages of *S. mansoni* is described, that can serve as a starting point to identify potential parasite lipid mediators that influence the host immune response. In **Chapter 5** the proteome of moDCs stimulated with helminth antigens is characterized using a mass spectrometry-based method to link expression of certain proteins by helminth-conditioned DCs to their ability to promote Th2 differentiation. As follow up to **Chapter 4**, the role of lipids, specifically prostaglandins, in SEA-driven Th2 polarization by DCs is studied in **Chapter 6.** Finally evidence is

accumulating that helminths interact with bacterial communities in the host, thereby shaping the SCFA profile these bacteria produce, which may impact immune cell function including DCs. Therefore, **Chapter 7** characterized the molecular mechanisms through which SCFAs produced by microbes condition human DCs to prime regulatory T cells.

REFERENCES

1. Colley, D.G., et al., *Human schistosomiasis.* Lancet, 2014. **383**(9936): p. 2253-64.
2. WHO, [cited 2017 Feb]. Available from: http://www.who.int/mediacentre/factsheets/fs366/en/.
3. Hotez, P.J., et al., *Helminth Infections: Soil-transmitted Helminth Infections and Schistosomiasis*, in *Disease Control Priorities in Developing Countries*, D.T. Jamison, et al., Editors. 2006, The International Bank for Reconstruction and Development/The World Bank Group.Washington (DC).
4. Hotez, P.J., et al., *Eliminating the Neglected Tropical Diseases: Translational Science and New Technologies.* PLoS Negl Trop Dis, 2016. **10**(3): p. e0003895.
5. GAHI, *Global Atlas of Helminth Infections*. [cited 2017 Feb]. Available from: http://www.thiswormyworld.org.
6. Cooper, P.J., et al., *Reduced risk of atopy among school-age children infected with geohelminth parasites in a rural area of the tropics*. J Allergy Clin Immunol, 2003. **111**(5): p. 995-1000.
7. Correale, J. and M.F. Farez, *The impact of environmental infections (parasites) on MS activity.* Mult Scler, 2011. **17**(10): p. 1162-9.
8. Giacomin, P., et al., *Experimental hookworm infection and escalating gluten challenges are associated with increased microbial richness in celiac subjects*. Sci Rep, 2015. **5**: p. 13797.
9. Helmby, H., *Human helminth therapy to treat inflammatory disorders - where do we stand?* BMC Immunol, 2015. **16**: p. 12.
10. Summers, R.W., et al., *Trichuris suis seems to be safe and possibly effective in the treatment of inflammatory bowel disease*. Am J Gastroenterol, 2003. **98**(9): p. 2034-41.
11. Summers, R.W., et al., *Trichuris suis therapy for active ulcerative colitis: a randomized controlled trial.* Gastroenterology, 2005. **128**(4): p. 825-32.
12. van Lieshout, L. and M. Roestenberg, *Clinical consequences of new diagnostic tools for intestinal parasites.* Clin Microbiol Infect, 2015. **21**(6): p. 520-8.
13. Verweij, J.J., *Application of PCR-based methods for diagnosis of intestinal parasitic infections in the clinical laboratory*. Parasitology, 2014. **141**(14): p. 1863-72.
14. Basuni, M., et al., *Detection of selected intestinal helminths and protozoa at Hospital Universiti Sains Malaysia using multiplex real-time PCR*. Trop Biomed, 2012. **29**(3): p. 434-42.
15. Cimino, R.O., et al., *Identification of human intestinal parasites affecting an asymptomatic peri-urban Argentinian population using multi-parallel quantitative real-time polymerase chain reaction.* Parasit Vectors, 2015. **8**: p. 380.
16. Gordon, C.A., et al., *Multiplex real-time PCR monitoring of intestinal helminths in humans reveals widespread polyparasitism in Northern Samar, the Philippines*. Int J Parasitol, 2015. **45**(7): p. 477-83.
17. Incani, R.N., et al., *Diagnosis of intestinal parasites in a rural community of Venezuela: Advantages and disadvantages of using microscopy or RT-PCR*. Acta Trop, 2017. **167**: p. 64-70.
18. Llewellyn, S., et al., *Application of a Multiplex Quantitative PCR to Assess Prevalence and Intensity Of Intestinal Parasite Infections in a Controlled Clinical Trial.* PLoS Negl Trop Dis, 2016. **10**(1): p. e0004380.
19. Mejia, R., et al., *A novel, multi-parallel, real-time polymerase chain reaction approach for eight gastrointestinal parasites provides improved diagnostic capabilities to resource-limited at-risk populations.* Am J Trop Med Hyg, 2013. **88**(6): p. 1041-7.
20. Wiria, A.E., et al., *The effect of three-monthly albendazole treatment on malarial parasitemia and allergy: a household-based cluster-randomized, double-blind, placebo-controlled trial.* PLoS One, 2013. **8**(3): p. e57899.
21. van Lieshout, L. and M. Yazdanbakhsh, *Landscape of neglected tropical diseases: getting it right*. Lancet Infect Dis, 2013. **13**(6): p. 469-70.
22. O'Connell, E.M. and T.B. Nutman, *Molecular Diagnostics for Soil-Transmitted Helminths.* Am J Trop Med Hyg, 2016. **95**(3): p. 508-13.
23. White, R.R. and K. Artavanis-Tsakonas, *How helminths use excretory secretory fractions to modulate dendritic cells*. Virulence, 2012. **3**(7): p. 668-77.
24. Girgis, N.M., U.M. Gundra, and P. Loke, *Immune regulation during helminth infections.* PLoS Pathog, 2013. **9**(4): p. e1003250.
25. Pelly, V.S., et al., *IL-4-producing ILC2s are required for the differentiation of TH2 cells following Heligmosomoides polygyrus infection*. Mucosal Immunol, 2016. **9**(6): p. 1407-1417.

26. Phythian-Adams, A.T., et al., *CD11c depletion severely disrupts Th2 induction and development in vivo.* J Exp Med, 2010. **207**(10): p. 2089-96.
27. Smith, K.A., et al., *Type 2 innate immunity in helminth infection is induced redundantly and acts autonomously following CD11c(+) cell depletion.* Infect Immun, 2012. **80**(10): p. 3481-9.
28. Lightowlers, M.W. and M.D. Rickard, *Excretory-secretory products of helminth parasites: effects on host immune responses.* Parasitology, 1988. **96 Suppl**: p. S123-66.
29. Goodridge, H.S., et al., *Immunomodulation via novel use of TLR4 by the filarial nematode phosphorylcholine-containing secreted product, ES-62.* J Immunol, 2005. **174**(1): p. 284-93.
30. van Riet, E., et al., *Combined TLR2 and TLR4 ligation in the context of bacterial or helminth extracts in human monocyte derived dendritic cells: molecular correlates for Th1/Th2 polarization.* BMC Immunol, 2009. **10**: p. 9.
31. Steinfelder, S., et al., *The major component in schistosome eggs responsible for conditioning dendritic cells for Th2 polarization is a T2 ribonuclease (omega-1).* J Exp Med, 2009. **206**(8): p. 1681-90.
32. Everts, B., et al., *Omega-1, a glycoprotein secreted by Schistosoma mansoni eggs, drives Th2 responses.* J Exp Med, 2009. **206**(8): p. 1673-80.
33. Gao, Y., et al., *Deficiency in TLR2 but not in TLR4 impairs dendritic cells derived IL-10 responses to schistosome antigens.* Cell Immunol, 2012. **272**(2): p. 242-50.
34. van der Kleij, D., et al., *A novel host-parasite lipid cross-talk. Schistosomal lyso-phosphatidylserine activates toll-like receptor 2 and affects immune polarization.* J Biol Chem, 2002. **277**(50): p. 48122-9.
35. Kane, C.M., E. Jung, and E.J. Pearce, *Schistosoma mansoni egg antigen-mediated modulation of Toll-like receptor (TLR)-induced activation occurs independently of TLR2, TLR4, and MyD88.* Infect Immun, 2008. **76**(12): p. 5754-9.
36. van Liempt, E., et al., *Schistosoma mansoni soluble egg antigens are internalized by human dendritic cells through multiple C-type lectins and suppress TLR-induced dendritic cell activation.* Mol Immunol, 2007. **44**(10): p. 2605-15.
37. Ritter, M., et al., *Schistosoma mansoni triggers Dectin-2, which activates the Nlrp3 inflammasome and alters adaptive immune responses.* Proc Natl Acad Sci U S A, 2010. **107**(47): p. 20459-64.
38. Schabussova, I., et al., *O-methylated glycans from Toxocara are specific targets for antibody binding in human and animal infections.* Int J Parasitol, 2007. **37**(1): p. 97-109.
39. Terrazas, C.A., L. Gomez-Garcia, and L.I. Terrazas, *Impaired pro-inflammatory cytokine production and increased Th2-biasing ability of dendritic cells exposed to Taenia excreted/secreted antigens: A critical role for carbohydrates but not for STAT6 signaling.* Int J Parasitol, 2010. **40**(9): p. 1051-62.
40. Everts, B., et al., *Schistosome-derived omega-1 drives Th2 polarization by suppressing protein synthesis following internalization by the mannose receptor.* J Exp Med, 2012. **209**(10): p. 1753-67, s1.
41. Agrawal, S., et al., *Cutting edge: different Toll-like receptor agonists instruct dendritic cells to induce distinct Th responses via differential modulation of extracellular signal-regulated kinase-mitogen-activated protein kinase and c-Fos.* J Immunol, 2003. **171**(10): p. 4984-9.
42. Goodridge, H.S., et al., *Differential regulation of interleukin-12 p40 and p35 induction via Erk mitogen-activated protein kinase-dependent and -independent mechanisms and the implications for bioactive IL-12 and IL-23 responses.* Immunology, 2003. **109**(3): p. 415-25.
43. Okano, M., et al., *Lacto-N-fucopentaose III found on Schistosoma mansoni egg antigens functions as adjuvant for proteins by inducing Th2-type response.* J Immunol, 2001. **167**(1): p. 442-50.
44. Thomas, P.G., et al., *Maturation of dendritic cell 2 phenotype by a helminth glycan uses a Toll-like receptor 4-dependent mechanism.* J Immunol, 2003. **171**(11): p. 5837-41.
45. Dillon, S., et al., *A Toll-like receptor 2 ligand stimulates Th2 responses in vivo, via induction of extracellular signal-regulated kinase mitogen-activated protein kinase and c-Fos in dendritic cells.* J Immunol, 2004. **172**(8): p. 4733-43.
46. Artis, D., et al., *Dendritic cell-intrinsic expression of NF-kappa B1 is required to promote optimal Th2 cell differentiation.* J Immunol, 2005. **174**(11): p. 7154-9.
47. Thomas, P.G., et al., *A helminth glycan induces APC maturation via alternative NF-kappa B activation independent of I kappa B alpha degradation.* J Immunol, 2005. **175**(4): p. 2082-90.
48. Gringhuis, S.I., et al., *Fucose-specific DC-SIGN signalling directs T helper cell type-2 responses via IKKepsilon- and CYLD-dependent Bcl3 activation.* Nat Commun, 2014. **5**: p. 3898.
49. Jankovic, D., et al., *In the absence of IL-12, CD4(+) T cell responses to intracellular pathogens fail to default to a Th2 pattern and are host protective in an IL-10(-/-) setting.* Immunity, 2002. **16**(3): p. 429-39.
50. Connor, L.M., et al., *Th2 responses are primed by skin dendritic cells with distinct transcriptional profiles.* J Exp Med, 2017. **214**(1): p. 125-142.
51. de Kouchkovsky, D.A., S. Ghosh, and C.V. Rothlin, *Negative Regulation of Type 2 Immunity.* Trends Immunol, 2017.

52. Ma, Y.L., et al., *IL-4-Producing Dendritic Cells Induced during Schistosoma japonica Infection Promote Th2 Cells via IL-4-Dependent Pathway.* J Immunol, 2015. **195**(8): p. 3769-80.
53. Na, H., M. Cho, and Y. Chung, *Regulation of Th2 Cell Immunity by Dendritic Cells.* Immune Netw, 2016. **16**(1): p. 1-12.
54. Constant, S., et al., *Extent of T cell receptor ligation can determine the functional differentiation of naive CD4+ T cells.* J Exp Med, 1995. **182**(5): p. 1591-6.
55. van Panhuys, N., F. Klauschen, and R.N. Germain, *T-cell-receptor-dependent signal intensity dominantly controls CD4(+) T cell polarization In Vivo.* Immunity, 2014. **41**(1): p. 63-74.
56. MacDonald, A.S., et al., *Cutting edge: Th2 response induction by dendritic cells: a role for CD40.* J Immunol, 2002. **168**(2): p. 537-40.
57. Brown, J.A., et al., *Blockade of CD86 ameliorates Leishmania major infection by down-regulating the Th2 response.* J Infect Dis, 1996. **174**(6): p. 1303-8.
58. Worsley, A.G., et al., *Dendritic cell expression of the Notch ligand jagged2 is not essential for Th2 response induction in vivo.* Eur J Immunol, 2008. **38**(4): p. 1043-9.
59. Ito, T., et al., *TSLP-activated dendritic cells induce an inflammatory T helper type 2 cell response through OX40 ligand.* J Exp Med, 2005. **202**(9): p. 1213-23.
60. Jenkins, S.J., et al., *Dendritic cell expression of OX40 ligand acts as a costimulatory, not polarizing, signal for optimal Th2 priming and memory induction in vivo.* J Immunol, 2007. **179**(6): p. 3515-23.
61. Soumelis, V., et al., *Human epithelial cells trigger dendritic cell mediated allergic inflammation by producing TSLP.* Nat Immunol, 2002. **3**(7): p. 673-80.
62. Wang, Y.H. and Y.J. Liu, *Thymic stromal lymphopoietin, OX40-ligand, and interleukin-25 in allergic responses.* Clin Exp Allergy, 2009. **39**(6): p. 798-806.
63. de Jong, E.C., et al., *Microbial compounds selectively induce Th1 cell-promoting or Th2 cell-promoting dendritic cells in vitro with diverse th cell-polarizing signals.* J Immunol, 2002. **168**(4): p. 1704-9.
64. Gao, Y., et al., *Control of T helper 2 responses by transcription factor IRF4-dependent dendritic cells.* Immunity, 2013. **39**(4): p. 722-32.
65. Kumamoto, Y., et al., *CD301b(+) dermal dendritic cells drive T helper 2 cell-mediated immunity.* Immunity, 2013. **39**(4): p. 733-43.
66. Tussiwand, R., et al., *Klf4 expression in conventional dendritic cells is required for T helper 2 cell responses.* Immunity, 2015. **42**(5): p. 916-28.
67. Zaiss, M.M. and N.L. Harris, *Interactions between the intestinal microbiome and helminth parasites.* Parasite Immunol, 2016. **38**(1): p. 5-11.
68. Lee, S.C., et al., *Helminth colonization is associated with increased diversity of the gut microbiota.* PLoS Negl Trop Dis, 2014. **8**(5): p. e2880.
69. Rausch, S., et al., *Small intestinal nematode infection of mice is associated with increased enterobacterial loads alongside the intestinal tract.* PLoS One, 2013. **8**(9): p. e74026.
70. Reynolds, L.A., et al., *Commensal-pathogen interactions in the intestinal tract: lactobacilli promote infection with, and are promoted by, helminth parasites.* Gut Microbes, 2014. **5**(4): p. 522-32.
71. Walk, S.T., et al., *Alteration of the murine gut microbiota during infection with the parasitic helminth Heligmosomoides polygyrus.* Inflamm Bowel Dis, 2010. **16**(11): p. 1841-9.
72. Dea-Ayuela, M.A., S. Rama-Iniguez, and F. Bolas-Fernandez, *Enhanced susceptibility to Trichuris muris infection of B10Br mice treated with the probiotic Lactobacillus casei.* Int Immunopharmacol, 2008. **8**(1): p. 28-35.
73. Holzscheiter, M., et al., *Lack of host gut microbiota alters immune responses and intestinal granuloma formation during schistosomiasis.* Clin Exp Immunol, 2014. **175**(2): p. 246-57.
74. Gause, W.C. and R.M. Maizels, *Macrobiota - helminths as active participants and partners of the microbiota in host intestinal homeostasis.* Curr Opin Microbiol, 2016. **32**: p. 14-8.
75. Zaiss, M.M., et al., *The Intestinal Microbiota Contributes to the Ability of Helminths to Modulate Allergic Inflammation.* Immunity, 2015. **43**(5): p. 998-1010.
76. Atarashi, K., et al., *Th17 Cell Induction by Adhesion of Microbes to Intestinal Epithelial Cells.* Cell, 2015. **163**(2): p. 367-80.
77. Ivanov, II, et al., *Specific microbiota direct the differentiation of IL-17-producing T-helper cells in the mucosa of the small intestine.* Cell Host Microbe, 2008. **4**(4): p. 337-49.
78. Sender, R., S. Fuchs, and R. Milo, *Revised Estimates for the Number of Human and Bacteria Cells in the Body.* PLoS Biol, 2016. **14**(8): p. e1002533.
79. Tlaskalova-Hogenova, H., et al., *The role of gut microbiota (commensal bacteria) and the mucosal barrier in the pathogenesis of inflammatory and autoimmune diseases and cancer: contribution of germ-free and gnotobiotic animal models of human diseases.* Cell Mol Immunol, 2011. **8**(2): p. 110-20.
80. Tan, J., et al., *The role of short-chain fatty acids in health and disease.* Adv Immunol, 2014. **121**: p. 91-119.

81. Kamada, N., et al., *Role of the gut microbiota in immunity and inflammatory disease.* Nat Rev Immunol, 2013. **13**(5): p. 321-35.
82. Koh, A., et al., *From Dietary Fiber to Host Physiology: Short-Chain Fatty Acids as Key Bacterial Metabolites.* Cell, 2016. **165**(6): p. 1332-45.
83. Minarrieta, L., et al., *Metabolites: deciphering the molecular language between DCs and their environment.* Semin Immunopathol, 2016.
84. Correa-Oliveira, R., et al., *Regulation of immune cell function by short-chain fatty acids.* Clin Transl Immunology, 2016. **5**(4): p. e73.
85. den Besten, G., et al., *The role of short-chain fatty acids in the interplay between diet, gut microbiota, and host energy metabolism.* J Lipid Res, 2013. **54**(9): p. 2325-40.
86. Singh, N., et al., *Activation of Gpr109a, receptor for niacin and the commensal metabolite butyrate, suppresses colonic inflammation and carcinogenesis.* Immunity, 2014. **40**(1): p. 128-39.
87. Chang, P.V., et al., *The microbial metabolite butyrate regulates intestinal macrophage function via histone deacetylase inhibition.* Proc Natl Acad Sci U S A, 2014. **111**(6): p. 2247-52.
88. Frikeche, J., et al., *Impact of HDAC inhibitors on dendritic cell functions.* Exp Hematol, 2012. **40**(10): p. 783-91.
89. Singh, N., et al., *Blockade of dendritic cell development by bacterial fermentation products butyrate and propionate through a transporter (Slc5a8)-dependent inhibition of histone deacetylases.* J Biol Chem, 2010. **285**(36): p. 27601-8.

Chapter 2

Multiplex real-time PCR as opposed to stool microscopy for studying and comparing the distribution of Soil-transmitted helminths within and between population living in endemic regions

MARIA M. M. KAISAR[1, 2], YENNY DJUARDI[2], FELISBERTO MENDES[3], FIRDAUS HAMID[1, 4], APRILIANTO E. WIRIA[1, 2], LINDA J. WAMMES[1], ERIC A. T. BRIENEN[3], ANTON M. POLDERMAN[1], ERLIYANI SARTONO[1], MARIA YAZDANBAKHSH[2], JACO J. VERWEIJ[1, 5], TANIAWATI SUPALI[2], LISETTE VAN LIESHOUT[1]

[1]Department of Parasitology, Leiden University Medical Center (LUMC), Leiden, The Netherlands
[2]Department of Parasitology, Faculty of Medicine, Universitas Indonesia, Jakarta, Indonesia
[3]Catholic University of Mozambique, Beira, Mozambique
[4]Department of Microbiology, Faculty id Medicine, Hasanuddin, Makassar, Indonesia
[5]Current address: Laboratory for Medical Microbiology and Immunology, St. Elisabeth Hospital, Tilburg, The Netherlands

Submitted

Backgroud cover: Helminths worms and eggs. Credit to Eric Brienen

ABSTRACT

Monitoring soil-transmitted helminth (STH) infections is usually done via stool microscopy. Although relatively simple, this approach is highly observer- and laboratory procedure-dependent. Here we evaluated data from two community-based surveys (Indonesia, Mozambique). Stool microscopy was compared with real-time PCR data. Subsequently, PCR findings were used to analyse potential risk-factors for STH infections in the Indonesian study population. In Indonesia a formol-ether concentration procedure was applied some months after stool collection at Flores-Island (N=1087), whereas in Beira (Mozambique) five different microscopy methods were used on the day of collection (N=303). Aliquots were transferred to a centralized laboratory for the detection and quantification of parasite-specific DNA of *Ancylostoma* spp., *Necator americanus, Ascaris lumbricoides* and *Strongyloides stercoralis*. For the Indonesian study population socio-demographic data and household properties were compared with parasitological outcomes. In the Indonesian samples, real-time PCR detected considerably more positive cases than microscopy, in particular for the hookworm species (73% vs. 17%, respectively). High DNA loads were noticed, indicating that this discrepancy could not be explained by mainly light infections missed by microscopy. In Mozambique, microscopy and PCR findings were highly comparable, showing a high prevalence for most of the helminth species tested. Based on PCR findings, behavioural risk factors were found to be associated with STH infections in Indonesia. Diagnosis based on DNA detection in stool seems a more reliable approach than stool microscopy for studying the distribution of helminth infections and to compare different target populations.

Keyword:
Soil-transmitted helminths, Indonesia, Mozambique, diagnostics, stool microscopy, real-time PCR, risk factors

INTRODUCTION

Soil-transmitted helminth (STH) infections are still a major global public health problem, despite many years of morbidity control through mass drug administration [1, 2]. It is estimated that currently approximately 1.4 billion people globally are infected with *Ascaris lumbricoides*, nearly 800 million people with *Trichuris trichiura*, and 740 million people with the hookworm species *Ancylostoma duodenale*, *A. ceylanicum* or *Necator americanus*. On top of that around 100 million people are estimated to be infected with *Strongyloides stercoralis*. This intestinal nematode species is often ignored, while its route of transmission is very similar to the hookworm species and infection is of significant clinical importance [3, 4]. All these soil-transmitted helminth infections affect, almost exclusively, the poorest populations within the tropics [1].

In Southeast Asia (SEA) numerous countries are endemic for STH infections and overall this region contributes approximately one-third of the global disease burden caused by these helminths [4]. In particular Indonesia, with an estimated 219 million infected cases, has the largest number of STH infected individuals within SEA [4]. Nevertheless, national figures about the precise distribution and prevalence show considerable scatter, with a reported prevalence of STH infections ranging from 10% to >50% and substantial gaps in the epidemiological data because certain regions of the archipelago are more intensely monitored than others [5, 6].

For the diagnosis of STH infections, faecal examination by microscopy is considered to be the "gold standard". The most widely applied microscopy method to identify the STH species as well as to quantify intensity of infection, is the Kato-thick smear (KS). This method is also recommended by the World Health Organization [5, 7]. Alternatively, the formol-ether concentration (FEC) method can be used. Although being more laboratory dependent, as it includes a centrifugation step, it has the major advantage of being the nearest to an all-round diagnostic procedure for the detection of a range of intestinal parasite species. To combine the advantages of each methods, several studies have applied both KS and FEC [8-11].

Although stool microscopy is a relatively simple diagnostic procedure, it poses many challenges, including the need to properly train microscopists and a lack of standardized protocols for collecting the sample, preparing the slide, performing the microscopic examination, and implementing external quality assessment schemes [12, 13]. This lack of standardization becomes most evident when comparing data collected at various study sites using different microscopy protocols [5, 14]. For example, the sensitivity of the detection of hookworm eggs can vary between microscopists, but is also largely depending on the number of stool samples collected, the number of microscopy examinations per stool samples and the overall intensity of infection within the population. In particular in populations where most individuals harbour light intensity of infection, some minor differences in the diagnostic protocol can have large consequences in the number of detected cases, and therefore on decisions to be made about the introduction or the continuation of helminth control programs [12, 13, 15].

Stool microscopy is also the most commonly used diagnostic procedure when analysing the risk factors that underlie helminth infections [16-20]. The prevalence of STH infections results from a complex interplay between multiple factors, including environmental settings and host related characteristics such as age, socioeconomic status, cultural habits, access to sanitation, and access to essential medication [1, 21-24]. Disentangling the relative contributions of each of the host-related risk factors associated with STH infections is relevant for a better understanding which socio-behavioural patterns influence infection and re-infection rates and for more insight into the beneficial effects of control strategies. The fact that most studies analysing risk factors associated

with STH infections are based on sub-optimal diagnostic procedures such as microscopy, might bias the overall conclusions.

Alternative diagnostic procedures have been developed in recent years, including methods to detect and quantify parasite DNA in stool samples using multiplex real-time PCR. These methods are both highly sensitive and highly specific [25-27]. Although real-time PCR has the practical limitation of requiring high-tech laboratory equipment, it can be standardized to a large extent, enabling researchers to pool and compare findings from various study populations [13]. Nevertheless, so far there is hardly any published data using the outcome of real-time PCR on stool samples collected in different countries to evaluate STH prevalence and intensity of infection, nor to specifically study risk-factors associated with STH infection [28].

In this study, we compared prevalence and infection intensity of STH between two unrelated community-based surveys, one conducted in Flores, Indonesia, the other in Beira, Mozambique. Part of the study data has been published before [29, 30]. Infection status was determined both by stool microscopy and by multiplex real-time PCR. Though similar approaches were used for the detection and quantification of parasite-specific DNA in stool, the microscopy procedures used at each of these two cross-sectional surveys differed substantially. Based on the outcome of the comparison, real-time PCR data was subsequently used to identify relevant risk factors associated with STH infections within the Indonesian study.

MATERIALS AND METHODS

Ethics statement

The two studies presented here have been approved by authorized ethic committees as described previously [29, 31, 32]. In Indonesia, the study protocol has been seen by the Faculty of Medicine of the Universitas Indonesia, in Mozambique by the Beira Committee of Medical Ethics and both protocols have been filed in the Netherlands by the Committee of Medical Ethics of the Leiden University Medical Center. Participants were informed about the objectives of the study prior to sample collection and all samples were anonymized before testing [29, 31, 32].

Indonesia: Study design, sample collection and microscopic examination

The Indonesian samples were collected as part of a larger double-blind randomized longitudinal study on the effect of treating inhabitants for two years with three monthly albendazole (400 mg) doses, looking at the effect of STH infections on malarial parasitemia and allergy. Study design and major outcomes have been described earlier [31-33]. The study was conducted in Nangapanda sub-district, a semi-urban area in Ende city, on Flores Island. This district consists of three villages, named Ndeturea, Ndorurea One and Ndorurea [31, 32]. Data regarding participant demographics (e.g., gender, age, parental education, occupation) and household properties (e.g., housing materials, floor materials, toilet, water supply) were collected by interviewing the individual participants. Parental education levels were categorized as "low" for parents who were illiterate or completed elementary school and "high" for parents who completed secondary school or higher. Because the vast majority of the population comprised of farmers, occupation was categorized as either "farmer" or "non-farmer".

A total of 1612 participants (including 510 children and 1102 adults) provided a stool sample during the 2008 dry season, from May through July. From each stool sample an aliquot of approximately one gram was stored at -20 $^{\circ}$C. The remaining stool was preserved in 4% formaldehyde, stored at room temperature, and transported to the Laboratory of Parasitology in Jakarta, Indonesia where microscopic examination was performed 2-3 month later. Following

formol-ether concentration (FEC), sediments were examined for the presence of eggs of STHs, including larvae of *Strongyloides stercoralis* [34]. The frozen aliquots were transported to the Netherlands, where DNA extraction and real-time PCR analysis was performed at each stool samples known to be matched with a blood sample for *Plasmodium* DNA detection [33]. In total 1087 samples were used for the current study, as 525 of the 1612 participants were excluded for the following reasons: (i) no paired blood sample was available; (ii) microscopy data was not available; or (iii) inhibition occurred during PCR amplification (Figure 1).

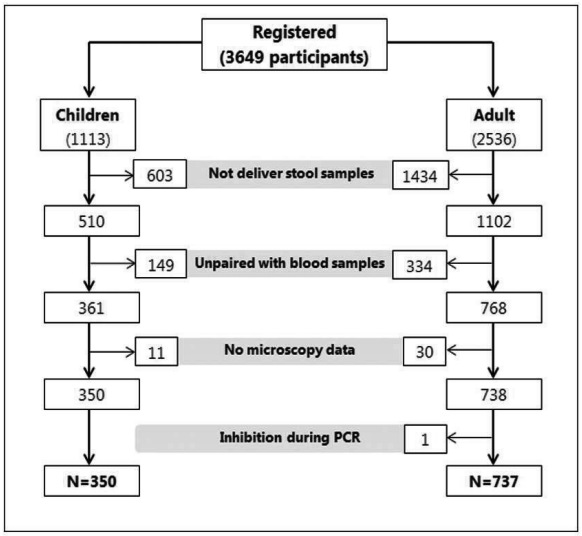

Figure 1. Flow-chart showing the sample selection of children and adults in the Nangapanda sub-district of Indonesia

Mozambique: Study design, sample collection and microscopic examination

The Mozambique samples were collected in Inhamudima, an informal settlement in Beira, Mozambique in order to study the distribution of intestinal parasites in the area. Similar to the Nangapanda, Indonesia population, study design and major outcomes have been describes previously [29]. In brief, a total of 303 stool samples were collected during a household randomized survey including 399 individuals from 63 households. The survey was performed during the dry season, June to August, of 2007. Within 24 hours after collection the samples were thoroughly examined for intestinal parasites at the laboratory of the University Hospital in Beira by a group of well-trained laboratory researchers. The microscopy methods included a direct smear, a formol-ether concentration (FEC) procedure, a single 25-mg Kato thick smear (KS) examination, a Baermann procedure and a copro-culture. Further details describing how these microscopy methods were applied within this study population have been described before [29].

The number of eggs or larvae present in each individual sample was recorded per helminth species, as well as per diagnostic test used. A stool aliquot of approximately 0.3 ml was mixed with 1 ml of 96% ethanol and transported to the Netherlands for DNA extraction and real-time PCR analysis.

DNA extraction and amplification

The procedure of DNA extraction and detection of parasite-specific DNA by real-time PCR was performed as described before [29, 32, 35]. In brief, DNA was isolated using DNeasy 96 Blood & Tissue Kit spin columns in accordance with the manufacturer's instructions (Qiagen, Hilden,

Germany). For the Mozambique samples this was done after removal of the ethanol via a washing procedure [36]. Real-time PCR was performed to detect the DNA from *Ancylostoma* spp. (including both *A. duodenale* and *A. ceylanicum*), *N. americanus*, *A. lumbricoides*, and *S. stercoralis* [29, 32, 35]. No assay was available yet for sensitive detection of *T. trichiura* DNA when the study samples were tested [37]. Negative and positive control samples for each species were included in each PCR run. A fixed amount of phocin herpes virus-1 (PhHV-1) was added within the isolation lysis buffer as an internal control and virus-specific primers and detecting probe were included in each reaction mixture. The PCR output consisted of a cycle threshold (Ct) value representing the amplification cycle in which the level of fluorescent signal exceeded the background fluorescence. Samples were considered positive showing a Ct-value below 50 [26, 29, 32]. The internal control PhHV-1 was detected at the expected Ct-value in all tested samples, with the exception of one stool originating from Indonesia (Figure 1).

Statistical analysis

Data were analysed using SPSS 20.0 (IBM, Chicago, IL). Descriptive frequency analysis was used to describe the overall characteristics of the participants, as well as the prevalence of each STH species based on microscopy and real-time PCR methods. The acronym ANAS describes those STH species included in the PCR detection, namely *Ancylostoma* spp., *N. americanus*, *A. lumbricoides*, and *S. stercoralis*. A chi-square (X^2) test was used to analyse the association between ANAS infection rates obtained using microscopy and the infection rates obtained using real-time PCR. The Mann-Whitney U test was used to detect a difference in median Ct-values between microscopically diagnosed ANAS positive and negative samples. Intensity of infection was arbitrarily categorized for each DNA target into low DNA load ($35 \leq Ct < 50$), moderate DNA load ($30 \leq Ct < 35$), or high DNA load ($Ct < 30$), while negative PCR results were recoded as $Ct = 50$ [38].

Based on the demographic data availability from the Indonesia study, a risk factor analysis was performed for STH infections. Infection status, defined as positive for at least one of the ANA PCR targets, was used as the binary outcome of risk factor analysis in each group. Children (≤15 years of age) and adult (>15 years of age) were analysed separately. To assess the risk factors associated with STH infections, logistic regression analysis under Generalized Linear Mixed Models (GLMM) was used in order to take into account clustering by household. Univariate analysis was applied to measure the correlation between STH infections detected using real-time PCR (dichotomous outcome) and potential risk factors (e.g., age, gender, village, occupation, parental education level, house materials, floor materials, toilet, water resource, and main staple). In the multivariate model, variables were included that were determined to be significant in the univariate analysis and the variables age, gender, and village were included as *a priori* confounders. In both the univariate and multivariate models, the data is presented as an odds ratio with 95% confidence interval (CI). Differences with a *p*-value <0.05 were considered to be statistically significant.

RESULTS

Population characteristics

Detailed characteristics of a total of 1087 participants from the Indonesia study, including demographics and household information, are summarized in Table 1. The age of the participants ranged from 4 to 78 years, with a median age of 31 years; 41.3% of the participants are male. Of the children who reported their parents' education level, 52.8% and 39.9% reported at least secondary school for their father and mother, respectively. Slightly more than 50% of the adults

classified themselves as farmers. Most of the households' walls were constructed of wood (73.3%) and contained a ceramic-covered floor (80.5%). The majority of households were equipped with an indoor toilet (65.5%) and pipeline water availability (54%). Rice was the main food staple in the majority of households (78.4%); cassava was the main food staple in the remaining households (21.6%).

In the Mozambique study, the age of the 303 participants ranged from 1 to 72 years, with a median age of 17 years; 47.5% of the participants are male. Additional demographics and household data were not available.

Table 1. Overview of the demographics and household data of the 1087 participants from the Nangapanda sub-district of Indonesia

	Children, n (%)	Adults, n (%)
N	350	737
Gender (male)	176 (50.3)	273 (37.0)
Age (years)		
4-7	111 (31.7)	NA
8-10	115 (32.9)	NA
11-15	124 (35.4)	NA
16-26	NA	147 (19.9)
27-36	NA	135 (18.3)
37-46	NA	186 (25.2)
47-56	NA	132 (17.9)
≥ 57	NA	137 (18.6)
Village		
Ndeturea	64 (18.3)	159 (21.6)
Ndorurea One	148 (42.3)	324 (44.0)
Ndorurea	138 (39.4)	254 (34.5)
Occupation (farmer)[1]	N/A	363 (50.6)
Father's education (high)[2]	118 (52.8)	ND
Mother's education (high)[3]	112 (39.9)	ND
Household data		
N	345	735
Wall material (stone)	82 (23.8)	206 (28.0)
Floor material (ceramic)	268 (77.7)	601 (81.8)
Water resource (piped)	182 (52.8)	401 (54.6)
Toilet (indoor)	216 (62.6)	491 (66.8)
Main food staple (rice)	276 (80.0)	571 (77.7)

[1] Data were available for a total of 717 participants
[2] Data were available for a total of 246 participants
[3] Data were available for a total of 281 participants
NA: not applicable; ND: not determined

Prevalence of STH infections in the populations

Table 2 summarizes the prevalence of each helminth species, or combination of species, detected either by microscopy or by real-time PCR, for both study populations, while Figure 2 focusses solely on those helminth species included in the multiplex real-time PCR and also depicts the relative parasite species–specific DNA loads measured.

Indonesia

In the Indonesia study, 47% (n=511) of the total study population were diagnosed with one or more STH species by using microscopy. Eggs of *A. lumbricoides*, hookworm, and *T. trichiura* were identified in 25.1, 16.7, and 27.5% of the samples, respectively (Table 2). No *S. stercoralis* larvae were seen. Multiple STH species were detected in 39.7% of the participants. In 163 (31.9%)

of the 511 STH-positive cases two different species were identified, with *A. lumbricoides* together with *T. trichiura* being the most common combination (n=102). In 2.5% of the positive cases three STH species were detected.

Real-time PCR revealed *N. americanus* DNA and *Ancylostoma* spp. DNA in 71.8% and 5.3% of the stool samples, respectively (Figure 2B). *A. lumbricoides* DNA was detected in 35.1% of cases, and *S. stercoralis* DNA was detected in 1.7% of cases (Figure 2B, Table 2). Multiple infections were detected in 396 (44.7%) of the 885 PCR positive stool samples, with the majority (n=391) harbouring a co-infection of two species. In total 81.4% of the samples were positive for at least one of the ANAS targets tested at the multiplex real-time PCR. This percentage is 2.3 fold higher than the percentage of cases diagnosed by microscopy as being positive for the same species (35.4%) (Table 2).

Slightly more than 60% of cases that were positive for *N. americanus* or *A. lumbricoides* based on real-time PCR analysis were categorized as having a high DNA load (Figure 2B). With respect to *Ancylostoma* spp., slightly fewer than 45% of the positive cases had a high species-specific DNA load. The positive cases of *S. stercoralis* were categorized primarily as having a low DNA load (n=9).

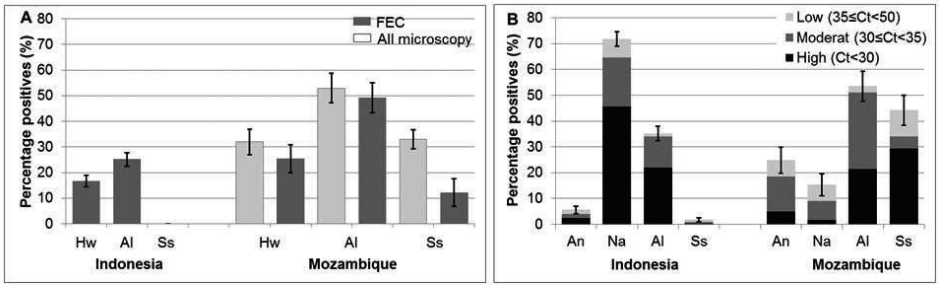

Figure 2. Summary of the percentage of positive STH infections in Indonesia (N=1087 participants) and Mozambique (N=303 participants) studies for the indicated soil-transmitted helminths (STHs)

(A) STH infections were measured using the formol-ether concentration (FEC) or a combination of five microscopy methods (direct smear, Kato-Katz, FEC, the Bearmann method, and copro-culture). (B) DNA load was measured using real-time PCR and stratified according to cycle threshold (Ct) value. Whiskers in each bar indicate 95% confidence intervals of the observed prevalence Hw= Hookworm; Na= *N. americanus*; An= *Ancylostoma* spp.; Al= *A. lumbricoides*; Ss= *S. stercoralis*.

Mozambique

In the Mozambique study, the FEC method revealed *A. lumbricoides*, hookworm, *S. stercoralis*, and *T. trichiura* infections in 49.2, 25.4, 12.2, and 90.8% of samples, respectively. Combining the outcome of all five microscopy procedures resulted in 296 positive cases (96.0%) for at least one of the target parasites, which is less than 3% higher than the 284 cases diagnosed using FEC only. The highest difference was seen for *S. stercoralis*, where the combined outcome of the five different microscopy procedures resulted in the detection of 63 additional cases (Table 2). Multiple helminth species were detected in 57.5% of the STH-positive cases. Primarily *A. lumbricoides* in combination with *T. trichiura* (n=69) was seen in the 115 cases with double infections. In the remaining multiple species-positive cases three (n=31) or four (n=33) helminths species were detected.

Real-time PCR detected *N. americanus* DNA in 15.2% of cases and *Ancylostoma* spp. DNA in 24.8% of cases (Figure 2B) and 5% (n=15) of the total study population showed a mixed infection with both species. *A. lumbricoides* DNA was detected in 53.5% of cases, and *S.*

stercoralis DNA was detected in 44.2% of cases (Figure 2B, Table 2). The overall percentage of STH infections detected using real-time PCR was 77.9% (n=236 positive cases), with multiple STH species in 129 cases, the majority of which were double infections (n=92).

Approximately half of the cases positive by PCR for *Ancylostoma* spp., *A. lumbricoides*, or *N. americanus* showed a Ct-value between 30 and 35 (moderate DNA load). Only for the *S. stercoralis* PCR 66.4% of the positive cases showed a Ct-value below 30, indicating a high DNA load.

Table 2. Positive number and percentage of soil-transmitted helminth (STH) infections determined using the indicated diagnostic methods in the Indonesia and Mozambique studies

	Indonesia (N=1087)			Mozambique (N=303)			
	FEC	Real-time PCR	All Techniques	FEC	All Microscopy[1]	Real-time PCR	All Techniques
Hookworms[2]	182 (16.7)	788 (72.5)	796 (73.2)	77 (25.4)	98 (32.3)	106 (35.0)	115 (38.0)
A. lumbricoides	273 (25.1)	381 (35.1)	415 (38.2)	149 (49.2)	161 (53.1)	162 (53.5)	169 (55.8)
S. stercoralis	0 (0.0)	19 (1.7)	19 (1.7)	37 (12.2)	100 (33.0)	134 (44.2)	146 (48.2)
Overall ANAS[3]	385 (35.4)	885 (81.4)	886 (81.5)	190 (62.7)	223 (73.6)	236 (77.9)	245 (80.9)
T. trichiura	299 (27.5)	ND	299 (27.5)	275 (90.8)	282 (93.1)	ND	282 (93.1)
Overall STH[4]	511 (47.0)	885 (81.4)	933 (85.8)	284 (93.7)	296 (96.0)	236 (77.9)	293 (96.7)

[1] All microscopy is the combined results from direct smear, Kato-Katz, FEC, the Baermann method, and copro-culture, see materials and methods section for further details
[2] *N. americanus* and *Ancylostoma spp*
[3] ANAS: *Ancylostoma* spp., *N. americanus*, *A. lumbricoides* and *S. stercoralis*
[4] Includes all soil-transmitted helminths examined in this study
ND: not determined

Parasite species–specific DNA load compared to the microscopy results

Indonesia

In the Indonesia study population, the highest level of discrepancy between PCR and microscopy outcome was seen for the hookworm species, with 614 samples (56.5%) in which hookworm DNA was detected while microscopy was negative and 8 samples (0.7%) where hookworm eggs were seen, while the PCR was negative. Those 8 microscopy positive samples all showed low egg counts, the maximum number of eggs observed in the sediment was four. The 614 samples diagnosed by PCR only, included samples with high DNA loads.

For *A. lumbricoides* the number of samples positive by PCR only was lower (142; 13.1%), but at the same time the number of samples positive by microscopy only was higher (34; 3.1%) in comparison to the hookworm. Again eggs counts were relatively low in those samples tested negative with the PCR, with a maximum of 68 eggs counted in the sediment. No significant difference was found in the Ct-value between the *A. lumbricoides* egg-negative stool samples (n=142, median Ct-value 29.2, with a range of 22.9-37.6) and the *A. lumbricoides* egg-positive stool samples (n=239, median Ct-value 28.6, with a range of 20.2-43.0) as determined by microscopy. In total 15 cases (1.4%) were positive by microscopy for at least one of the ANAS targets, while the PCR was negative for all targets tested.

Mozambique

In the Mozambique study population, in total 9 cases (3.0%) were positive by microscopy for at least one of the ANAS targets, while the PCR was negative for all targets. The highest level of discrepancy between PCR and microscopy outcome was seen with *S. stercoralis*, with 46 samples (15.2%) in which *S. stercoralis* DNA was detected while microscopy was negative and 12 samples (4.0%) in which L3 larvae were seen, while the PCR was negative. Each of those 12 microscopy positive samples were positive in only one of the five microscopy techniques used and the number of larvae were low. Within the group of *S. stercoralis* PCR positive samples, DNA loads were significantly higher in microscopy positive samples (n= 88, median Ct-value 26.2) in comparison to microscopy negative samples (n= 46, median Ct-value 34.4, $p<0.001$).

Risk factors associated with helminth infections in children and adults

Table 3 summarizes the putative risk factors for the helminth infections detected by the ANAS-PCR, stratified by the child and adult groups in the Nangapanda sub-district of Indonesia. A univariate analysis revealed that age, village, parental education level, and wall materials were all potentially factors associated with ANAS infection in children. With respect to age, children aged 8-10 years old had a higher risk to be infected with ANAS compared to those aged 4-7 years old (OR: 2.25; 95% CI: 1.06-4.76; $p=0.034$). Table 3 also showed that, living in the village of Ndeturea, living in Ndorurea One (OR: 0.24; 95% CI: 0.07-0.76; $p=0.017$) or Ndorurea (OR: 0.18; 95% CI: 0.05-0.63; $p=0.007$) significantly reduced the likelihood of having an ANAS infection. Children whose fathers had a low level of education had a significantly higher risk of ANAS infection than children whose fathers had a high level of education (OR: 2.29; 95% CI: 1.18-4.46; $p=0.015$); in contrast, the mother's education level had no effect on the child's likelihood of having an ANAS infection (OR: 1.55; 95% CI: 0.71-3.38; $p=0.267$). Finally, children who lived in a house built with bamboo or wood as the wall material had a significantly higher risk of having an ANAS infection compared to children who lived in a house with stone walls (OR: 2.82; 95% CI: 1.38-5.74; $p=0.005$).

In the adult group univariate analysis revealed that village, occupation, and all house components were positively associated with having ANAS infection. However, in multivariate analysis, only occupation (OR: 2.44; 95% CI: 1.57-3.81; $p<0.001$), the water resource (OR: 1.60; 95% CI: 1.04-2.46; $p=0.034$), and having an indoor toilet (OR: 2.51; 95% CI: 1.48-4.26; $p=0.001$) remained positively associated with ANAS infection (Table 3).

DISCUSSION

Recent estimates suggest that approximately 5.3 billion people worldwide are at risk of developing a chronic STH infections, with 69% living in Asia [4, 5, 22]. However, these estimates are based primarily on diagnostic procedures that have known limitations. Microscopic stool examination lacks sensitivity, meaning that light to moderate infection intensities are easily missed. In addition, this method is highly observer-dependent and poorly standardized. Because of these limitations, improving diagnostic methods has received high priority on the research agenda of helminth-related diseases in humans [14, 15, 39].

In the present study, the use of real-time PCR as a diagnostic tool for STH was further evaluated by comparing two distinct endemic communities, one in Ende, Indonesia, the other in Beira, Mozambique. In these two regions, the prevalence and intensity of four helminth species was measured both by microscopy and real-time PCR. Microscopy-based diagnostics was performed in accordance with the most feasible procedures within the given local setting, while a

Table 3. Risk factors associated with STH infections detected using real time PCR in the children and adults the Indonesia study

Indicators		Children (N=350)					Adults (N=737)				
		n (% STH positive)	Unadjusted		Adjusted[1]		n (% STH positive)	Unadjusted		Adjusted[1]	
			OR (95% CI)	p-value	OR (95% CI)	p-value		OR (95% CI)	p-value	OR (95% CI)	p-value
Gender	Female	174 (75.9)	1	0.616			464 (83.0)	1	0.654		
	Male	176 (79.0)	1.14 (0.68-1.90)				273 (83.9)	1.10 (0.73-1.65)			
Village	Ndeturea	64 (92.2)	1		1		159 (93.7)	1		1	
	Ndorurea One	148 (79.1)	0.34 (0.13-0.90)	**0.030**	0.24 (0.07-0.76)	**0.017**	324 (79.9)	0.30 (0.15-0.59)	**0.000**	0.54 (0.26-1.09)	0.085
	Ndorurea	138 (68.8)	0.20 (0.08-0.52)	**0.001**	0.18 (0.05-0.63)	**0.007**	254 (81.1)	0.32 (0.16-0.64)	**0.001**	0.58 (0.28-1.23)	0.156
Age (years)	4-7	111 (68.5)	1		1						
	8-10	115 (80.9)	2.06 (1.09-3.86)	**0.025**	2.25 (1.06-4.76)	**0.034**			NA		
	11-15	124 (82.3)	2.237 (1.20-4.18)	**0.012**	1.87 (0.85-4.13)	0.122					
	16-26						147 (87.7)	1			
	27-36						135 (78.5)	1.90 (1.00-3.63)	0.051		
	37-46			NA			186 (81.7)	1.50 (0.81-2.81)	0.199		
	47-56						132 (82.6)	1.38 (0.70-2.70)	0.353		
	≥57						137 (86.1)	1.10 (0.55-2.20)	0.797		
Occupation	Non-farmer			NA			354 (76.3)	1	**0.000**	1	**0.000**
	Farmer						363 (90.4)	2.85 (1.86-4.35)		2.44 (1.57-3.81)	
Father Education	High	118 (65.3)	1	**0.001**	1	**0.015**			NA		
	Low	128 (85.2)	3.00 (1.61-5.60)		2.29 (1.18-4.46)						
Mother Education	High	112 (66.1)	1	**0.002**	1	0.267			NA		
	Low	169 (82.8)	2.54 (1.43-4.51)		1.55 (0.71-3.38)						
Wall Materials	Stone	82 (64.6)	1	**0.001**	1	**0.005**	206 (77.7)	1	**0.021**	1	0.679
	Bamboo	263 (82.1)	2.68 (1.52-4.73)		2.82 (1.38-5.74)		529 (85.6)	1.63 (1.08-2.45)		1.10 (0.70-1.72)	
Floor Materials	Ceramic	268 (76.9)	1	0.752			601 (81.7)	1	**0.020**	1	0.321
	Mud	77 (81.8)	1.11 (0.57-2.17)				134 (91.0)	2.12 (1.13-4.00)		1.40 (0.72-2.71)	
Water Resource	Piped	182 (76.9)	1	0.569			401 (80.3)	1	**0.005**	1	**0.034**
	Non-Piped	163 (79.1)	1.16 (0.69-1.96)				334 (87.1)	1.81 (1.20-2.74)		1.60 (1.04-2.46)	
Toilet	Indoor	216 (76.4)	1	0.118			491 (79.4)	1	**0.000**	1	**0.001**
	Outdoor	129 (80.6)	1.57 (0.89-2.78)				244 (91.4)	2.75 (1.67-4.55)		2.51 (1.48-4.26)	
Main Staple	Rice	276 (74.6)	1	0.135			571 (80.6)	1	**0.000**	1	0.118
	Cassava	69 (91.3)	2.21 (0.78-6.27)				164 (93.3)	3.05 (1.63-5.68)		1.71 (0.87-3.30)	

[1] Adjusted by age, gender, and village
NA: not applicable

standardized real-time PCR method was used for all samples at a centralized laboratory. Unfortunately it was not possible to evaluate the use of real-time PCR for *T. trichiura* infections, as at that time no suitable method existed for extracting DNA from *T. trichiura* eggs [37].

Interestingly, significant differences were seen between the two study populations when comparing the outcome of each diagnostic procedure, in particular for hookworm infections. In the Indonesian study population hookworm eggs were detected in 16.7% of stool samples by using the FEC method, whereas real-time PCR analysis revealed the presence of hookworm DNA in the faeces of 72.5% of the participants. On the other hand, in in the Mozambique study population, hookworm eggs and DNA were detected in 25.4% and 35.0% of the participants, respectively. One possible explanation for this difference in outcomes could be the length of time elapsed between collecting the stool sample and performing the FEC procedure. In the Indonesian study, the preserved samples had to be sent to the local central laboratory, and the FEC examination was performed 2-3 months after sample collection. This is very different from the Mozambique situation where the FEC procedure was performed within 24 hours of sample collection. A delay between sample collection and specimen processing in the laboratory can affect the diagnostic performance of the FEC procedure, particularly for hookworm species [40]. In the Mozambique setting, four additional microscopy procedures were used besides the FEC. This somewhat increased the number of hookworm positive samples from 25.4% to 32.3%, a number which is still lower than de 35.0% of samples positive by PCR. Of all parasite species detected, *S. stercoralis* was the only one which showed a pronounced increase in the number of positive cases when all five techniques were used. This because two of the five techniques applied are specifically designed for the detection of *S. stercoralis* larvae, namely the Baermann method and the copro-culture. Previous studies already showed that single-method sampling fails to detect *S. stercoralis* larvae in as many as 70% of known positive cases [41].

Although overall PCR was found to be far more sensitive than microscopy, both study populations showed approximately 1-3% of the cases to be positive for at least one helminth species by microscopy while the ANAS PCR was negative for all targets. These so called false negative real-time PCR cases seem to occur more often when the intensity of infection, i.e. based on microscopy, is low. Most likely this is due to the fact that the DNA detection procedure is actually based on very small volumes. When intensity of infection is too low, parasite's eggs and free DNA might simply be lacking within the aliquot actually used for DNA isolation. In addition, the possibility of human error cannot be completely excluded, e.g. some structures of for instance plant-origin found in the faecal smear might have been erroneously identified as hookworm or *Ascaris* eggs [12].

In both studies only a single sample has been collected per participant. It has often been stated that examinations based on one stool sample only is inadequate, and at least three stool samples are required to increase the negative predictive value above 90% [42, 43]. However, in order to obtain more than one stool sample per participant, a range of practical and logistical issues need to be solved. A substantial number of people cannot deliver daily and in many cultural situations study subjects, in particularly teenagers, are embarrassed to provide a stool sample. The number of dropouts is also likely to increase if consecutive stool samples are requested. In order to diagnose *T. trichiura*, hookworm, and *S. stercoralis* infections accurately even as many as 20 stool samples should be examined in a low-intensity setting. With the exception of specialized, small-scale studies, such a higher sample number is totally not feasible [42]. Therefore, diagnostic methods that provide high sensitivity and have low technical demands are urgently needed.

A relatively new microscopy-based diagnostic method is the FLOTAC [9, 44, 45]. Several studies have been performed to evaluate this technique and found that FLOTAC can be more sensitive than both the Kato-smear and FEC methods at detecting STH eggs [9, 44-46]. However, the FLOTAC has the limitation it is a time-consuming procedure which also requires a large bucket centrifuge with a special adapter. The more recently introduced mini-FLOTAC method is a simplified version of the FLOTAC, which in addition allows the analysis of preserved stool samples. On the other hand, recent studies have shown that similar to the FEC procedure long-term storage of the faecal material in formalin decreases the diagnostic sensitivity of the mini-FLOTAC [47].

Hookworm infections were found to be abundant in both our study populations. Due to morphological similarities of the eggs, microscopy methods such as FEC and KS cannot be used to differentiate the hookworm species. Distinguishing between the two most common human hookworm species is important, as previous studies demonstrated that *Ancylostoma* spp. (i.e. *A. duodenale*) but not *N. americanus*, is independently associated with severe anaemia and iron deficiency [48]. Here we showed *Ancylostoma* spp. (including both *A. duodenale* and *A. ceylanicum*) to be more prevalent in the Mozambique study population, whereas *N. americanus* was considerably more prevalent in Indonesia.

High levels of polyparasitism were observed both in Nangapanda, Indonesia and in Beira, Mozambique. But different STH species predominated in each study. *N. americanus* was the most prevalent species in Nangapanda, Indonesia, whereas *A. lumbricoides* was the most prevalent species in Beira, Mozambique. Differences in the geo-climate might account for this finding, as surface temperature, altitude, soil type, and rainfall can strongly affect the distribution of STHs [1]. It is not known to what level the success of MDA is depending on the level of polyparasitism or on certain helminth species being predominant, but the increased usage of more sensitive diagnostic techniques, such as those based on DNA detection, will most likely provide more clarity on these issues [15].

Because real-time PCR seems to provide more accurate diagnostic data, PCR outcomes were used to analyse the risk factors associated with STH infections within the Indonesian study population. A correlation was found between the prevalence of STH and the materials used to construct the walls of the houses. However, this correlation was only seen in children and not in adults. Given that the better wall material was stone, this could have prevented environmental contamination from STH infections among the children but not the adults. The possible explanation could be that because more than half of the adults are farmers, the adult infection rate would not be as strongly affected by the type of material used to build their house. In addition, the father's level of education was found to be correlated with an decreased risk of STH infection in children, while no effect was seen for the mother. This is in contrast with several studies reporting a beneficial effect of the mother's level of education [49, 50]. Nevertheless, our study highlights the importance of obtaining information regarding the education level of both the mother and father in order to determine which had the higher influence. For example, in this study, the mothers do not always have an active role in caring for the children. This difference might also be related to the local culture. For example, a study in Latin America showed that men play a larger role in all aspects of life [21]. Similarly, in Nangapanda, Indonesia, men have a more active role in both the family and the community.

Working as a farmer highly increases one's risk of developing an STH infection [28], as reported recently in rural Bali, Indonesia [51]. Farmers are exposed to the soil almost continuously, which by definition is the way of transmission for soil-transmitted helminths. Several published

studies have reported that sanitary facilities such as water resources and an indoor toilet are strongly correlated with STH transmission, while good sanitation conditions lower the risk of STH infections [1, 24, 50, 52, 53]. Consistent with this correlation, we found that supplying water to the house through a pipeline and having an indoor toilet contributed to a significant decrease in STH infections in the adult group. On the other hand, even though schools can provide improved sanitation conditions, school children are at high risk for STH infections, as they play outdoors a large part of the day in high-risk settings such as rivers and the school yard [24, 52].

In conclusion, our findings confirm that real-time PCR is a sensitive method, suitable for high-throughput population-based screening for helminth infections. By using real-time PCR analysis in a highly standardized way at a centralized laboratory facility, it becomes feasible to compare STH infection rates between distinct study populations even when different microscopy procedures have been used in the field. Being a more reliable technique, DNA-based diagnostic methods are also more suitable to determine and evaluate potential risk factors associated with STH infections.

ACKNOWLEDGMENTS

We thank the participants from the Nangapanda-Flores region in Indonesia and the Inhamudima-Beira region of Mozambique. We also thank the Helminthology Group in the Department of Parasitology, Medical University, Indonesia; Natalie Vinkeles for helpful comments on earlier versions of the manuscript; and the students who were involved in the Indonesia and Mozambique studies. This study was funded by the Prof Dr P. F. C. Flu Foundation and The Royal Netherlands Academy of Arts and Science (KNAW), Ref 05-PP-35. The authors would also like to thank The Indonesian Directorate General of Higher Education (DIKTI)-Leiden University for providing a PhD scholarship.

REFERENCES

1. Hotez, P.J., et al., *Helminth infections: the great neglected tropical diseases.* J Clin Invest, 2008. **118**(4): p. 1311-21.
2. Vercruysse, J., B. Levecke, and R. Prichard, *Human soil-transmitted helminths: implications of mass drug administration.* Curr Opin Infect Dis, 2012. **25**(6): p. 703-8.
3. Olsen, A., et al., *Strongyloidiasis--the most neglected of the neglected tropical diseases?* Trans R Soc Trop Med Hyg, 2009. **103**(10): p. 967-72.
4. Jex, A.R., et al., *Soil-transmitted helminths of humans in Southeast Asia--towards integrated control.* Adv Parasitol, 2011. **74**: p. 231-65.
5. Dunn, J.C., et al., *Epidemiological surveys of, and research on, soil-transmitted helminths in Southeast Asia: a systematic review.* Parasit Vectors, 2016. **9**: p. 31.
6. GAHI, *This wormy wold. Global Atlas of Helminth Infections (GAHI).* http://www.thiswormyworld.org, 2017.
7. WHO, *Helminth control in scholl-age children- Second Edition. Geneva: World Health Organization.* 2012.
8. Endris, M., et al., *Comparison of the Kato-Katz, Wet Mount, and Formol-Ether Concentration Diagnostic Techniques for Intestinal Helminth Infections in Ethiopia.* ISRN Parasitol, 2013. **2013**: p. 180439.
9. Glinz, D., et al., *Comparing diagnostic accuracy of Kato-Katz, Koga agar plate, ether-concentration, and FLOTAC for Schistosoma mansoni and soil-transmitted helminths.* PLoS Negl Trop Dis, 2010. **4**(7): p. e754.
10. Steinmann, P., et al., *Occurrence of Strongyloides stercoralis in Yunnan Province, China, and comparison of diagnostic methods.* PLoS Negl Trop Dis, 2007. **1**(1): p. e75.
11. Yimer, M., et al., *Evaluation performance of diagnostic methods of intestinal parasitosis in school age children in Ethiopia.* BMC Res Notes, 2015. **8**: p. 820.
12. Bogoch, I., et al., *Differences in microscopic diagnosis of helminths and intestinal protozoa among diagnostic centres.* Eur J Clin Microbiol Infect Dis, 2006. **25**(5): p. 344-7.
13. van Lieshout, L. and M. Yazdanbakhsh, *Landscape of neglected tropical diseases: getting it right.* Lancet Infect Dis, 2013. **13**(6): p. 469-70.
14. McCarthy, J.S., et al., *A research agenda for helminth diseases of humans: diagnostics for control and elimination programmes.* PLoS Negl Trop Dis, 2012. **6**(4): p. e1601.

15. Medley, G.F., et al., *The Role of More Sensitive Helminth Diagnostics in Mass Drug Administration Campaigns: Elimination and Health Impacts*. Adv Parasitol, 2016. **94**: p. 343-392.
16. Gelaw, A., et al., *Prevalence of intestinal parasitic infections and risk factors among schoolchildren at the University of Gondar Community School, Northwest Ethiopia: a cross-sectional study.* BMC Public Health, 2013. **13**: p. 304.
17. Huat, L.B., et al., *Prevalence and risk factors of intestinal helminth infection among rural malay children*. J Glob Infect Dis, 2012. **4**(1): p. 10-4.
18. Khieu, V., et al., *Diagnosis, treatment and risk factors of Strongyloides stercoralis in schoolchildren in Cambodia*. PLoS Negl Trop Dis, 2013. **7**(2): p. e2035.
19. Kounnavong, S., et al., *Soil-transmitted helminth infections and risk factors in preschool children in southern rural Lao People's Democratic Republic*. Trans R Soc Trop Med Hyg, 2011. **105**(3): p. 160-6.
20. Sherkhonov, T., et al., *National intestinal helminth survey among schoolchildren in Tajikistan: prevalences, risk factors and perceptions*. Acta Trop, 2013. **126**(2): p. 93-8.
21. Karan, A., G.B. Chapman, and A. Galvani, *The influence of poverty and culture on the transmission of parasitic infections in rural nicaraguan villages*. J Parasitol Res, 2012. **2012**: p. 478292.
22. Pullan, R.L. and S.J. Brooker, *The global limits and population at risk of soil-transmitted helminth infections in 2010*. Parasit Vectors, 2012. **5**: p. 81.
23. Utzinger, J., et al., *Important helminth infections in Southeast Asia diversity, potential for control and prospects for elimination*. Adv Parasitol, 2010. **72**: p. 1-30.
24. Ziegelbauer, K., et al., *Effect of sanitation on soil-transmitted helminth infection: systematic review and meta-analysis*. PLoS Med, 2012. **9**(1): p. e1001162.
25. Verweij, J.J., et al., *Differentiation of Entamoeba histolytica and Entamoeba dispar cysts using polymerase chain reaction on DNA isolated from faeces with spin columns*. Eur J Clin Microbiol Infect Dis, 2000. **19**(5): p. 358-61.
26. Verweij, J.J., et al., *Simultaneous detection and quantification of Ancylostoma duodenale, Necator americanus, and Oesophagostomum bifurcum in fecal samples using multiplex real-time PCR*. Am J Trop Med Hyg, 2007. **77**(4): p. 685-90.
27. Verweij, J.J. and C.R. Stensvold, *Molecular testing for clinical diagnosis and epidemiological investigations of intestinal parasitic infections.* Clin Microbiol Rev, 2014. **27**(2): p. 371-418.
28. Arndt, M.B., et al., *Impact of helminth diagnostic test performance on estimation of risk factors and outcomes in HIV-positive adults*. PLoS One, 2013. **8**(12): p. e81915.
29. Meurs, L., et al., *Diagnosing Polyparasitism in a High-Prevalence Setting in Beira, Mozambique: Detection of Intestinal Parasites in Fecal Samples by Microscopy and Real-Time PCR*. PLoS Negl Trop Dis, 2017. **11**(1): p. e0005310.
30. Wiria, A.E., et al., *The effect of three-monthly albendazole treatment on malarial parasitemia and allergy: a household-based cluster-randomized, double-blind, placebo-controlled trial.* PLoS One, 2013. **8**(3): p. e57899.
31. Hamid, F., et al., *A longitudinal study of allergy and intestinal helminth infections in semi urban and rural areas of Flores, Indonesia (ImmunoSPIN Study).* BMC Infect Dis, 2011. **11**: p. 83.
32. Wiria, A.E., et al., *Does treatment of intestinal helminth infections influence malaria? Background and methodology of a longitudinal study of clinical, parasitological and immunological parameters in Nangapanda, Flores, Indonesia (ImmunoSPIN Study).* BMC Infect Dis, 2010. **10**: p. 77.
33. Kaisar, M.M., et al., *Epidemiology of Plasmodium infections in Flores Island, Indonesia using real-time PCR*. Malar J, 2013. **12**: p. 169.
34. Allen, A.V. and D.S. Ridley, *Further observations on the formol-ether concentration technique for faecal parasites*. J Clin Pathol, 1970. **23**(6): p. 545-6.
35. Verweij, J.J., et al., *PCR assay for the specific amplification of Oesophagostomum bifurcum DNA from human faeces.* Int J Parasitol, 2000. **30**(2): p. 137-42.
36. ten Hove, R., et al., *Detection of diarrhoea-causing protozoa in general practice patients in The Netherlands by multiplex real-time PCR*. Clin Microbiol Infect, 2007. **13**(10): p. 1001-7.
37. Kaisar, M.M., et al., *Improved diagnosis of Trichuris trichiura by using a bead-beating procedure on ethanol preserved stool samples prior to DNA isolation and the performance of multiplex real-time PCR for intestinal parasites*. Parasitology, 2017: p. 1-10.
38. Pillay, P., et al., *Real-time polymerase chain reaction for detection of Schistosoma DNA in small-volume urine samples reflects focal distribution of urogenital Schistosomiasis in primary school girls in KwaZulu Natal, South Africa*. Am J Trop Med Hyg, 2014. **90**(3): p. 546-52.
39. O'Connell, E.M. and T.B. Nutman, *Molecular Diagnostics for Soil-Transmitted Helminths.* Am J Trop Med Hyg, 2016. **95**(3): p. 508-13.
40. Krauth, S.J., et al., *An in-depth analysis of a piece of shit: distribution of Schistosoma mansoni and hookworm eggs in human stool.* PLoS Negl Trop Dis, 2012. **6**(12): p. e1969.

41. Siddiqui, A.A. and S.L. Berk, *Diagnosis of Strongyloides stercoralis infection.* Clin Infect Dis, 2001. **33**(7): p. 1040-7.
42. Knopp, S., et al., *Diagnosis of soil-transmitted helminths in the era of preventive chemotherapy: effect of multiple stool sampling and use of different diagnostic techniques.* PLoS Negl Trop Dis, 2008. **2**(11): p. e331.
43. Steinmann, P., et al., *Extensive multiparasitism in a village of Yunnan province, People's Republic of China, revealed by a suite of diagnostic methods.* Am J Trop Med Hyg, 2008. **78**(5): p. 760-9.
44. Barda, B., et al., *Mini-FLOTAC and Kato-Katz: helminth eggs watching on the shore of Lake Victoria.* Parasit Vectors, 2013. **6**(1): p. 220.
45. Barda, B.D., et al., *Mini-FLOTAC, an innovative direct diagnostic technique for intestinal parasitic infections: experience from the field.* PLoS Negl Trop Dis, 2013. **7**(8): p. e2344.
46. Albonico, M., et al., *Comparison of three copromicroscopic methods to assess albendazole efficacy against soil-transmitted helminth infections in school-aged children on Pemba Island.* Trans R Soc Trop Med Hyg, 2013. **107**(8): p. 493-501.
47. Barda, B., et al., *How long can stool samples be fixed for an accurate diagnosis of soil-transmitted helminth infection using Mini-FLOTAC?* PLoS Negl Trop Dis, 2015. **9**(4): p. e0003698.
48. Jonker, F.A., et al., *Real-time PCR demonstrates Ancylostoma duodenale is a key factor in the etiology of severe anemia and iron deficiency in Malawian pre-school children.* PLoS Negl Trop Dis, 2012. **6**(3): p. e1555.
49. Greenland, K., et al., *The epidemiology of soil-transmitted helminths in Bihar State, India.* PLoS Negl Trop Dis, 2015. **9**(5): p. e0003790.
50. Wang, X., et al., *Soil-transmitted helminth infections and correlated risk factors in preschool and school-aged children in rural Southwest China.* PLoS One, 2012. **7**(9): p. e45939.
51. Widjana, D.P. and P. Sutisna, *Prevalence of soil-transmitted helminth infections in the rural population of Bali, Indonesia.* Southeast Asian J Trop Med Public Health, 2000. **31**(3): p. 454-9.
52. Anuar, T.S., F.M. Salleh, and N. Moktar, *Soil-transmitted helminth infections and associated risk factors in three Orang Asli tribes in Peninsular Malaysia.* Sci Rep, 2014. **4**: p. 4101.
53. Campbell, S.J., et al., *Water, Sanitation and Hygiene (WASH) and environmental risk factors for soil-transmitted helminth intensity of infection in Timor-Leste, using real time PCR.* PLoS Negl Trop Dis, 2017. **11**(3): p. e0005393.

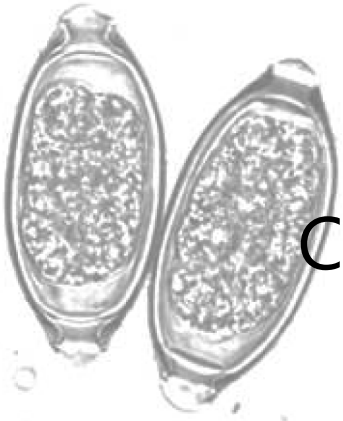

Chapter 3

Improved diagnosis of *Trichuris trichiura* by using a bead-beating procedure on ethanol preserved stool samples prior to DNA isolation and the performance of multiplex real-time PCR for intestinal parasites

MARIA M. M. KAISAR[1, 2], ERIC A.T. BRIENEN[1], YENNY DJUARDI[2], ERLIYANI SARTONO[1], MARIA YAZDANBAKHSH[1], JACO J. VERWEIJ[1, 3], TANIAWATI SUPALI[2], LISETTE VAN LIESHOUT[1]

[1]Department of Parasitology, Leiden University Medical Center, Leiden, The Netherlands
[2]Department of Parasitology, Faculty of Medicine, Universitas Indonesia, Jakarta, Indonesia
[3]Current address: Laboratory for Medical Microbiology and Immunology, St. Elisabeth Hospital, Tilburg, The Netherlands

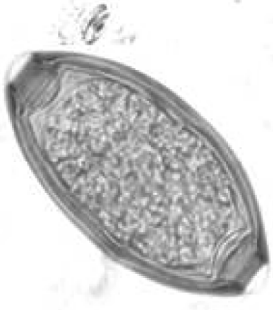

Parasitology, 14 March 2017
Doi: 10.1017/S0031182017000129

Backgroud cover: Trichuris trichiura eggs. Credit to Eric Brienen

ABSTRACT

For the majority of intestinal parasites, real-time PCR-based diagnosis outperforms microscopy. However the data for *Trichuris trichiura* has been less convincing and most comparative studies have been performed in populations with low prevalence. This study aims to improve detection of *T. trichuria* DNA in human stool by evaluating four sample preparation methods. Faecal samples (n=60) were collected at Flores island, Indonesia and examined by microscopy. Aliquots were taken and a bead-beating procedure was used both on directly frozen stool and on material preserved with 96% ethanol. PCR on frozen samples showed 40% to be positive for *T. trichiura*, compared to 45% positive by microscopy. The percentage positive increased when using ethanol preservation (45.0%), bead-beating (51.7%) and a combination (55.0%) and all three methods showed significantly higher DNA loads. The various procedures had a less pronounced effect on the PCR results of nine other parasite targets tested. Most prevalent were *Ascaris lumbricoides* (≈60%), *Necator americanus* (≈60%), *Dientamoeba fragilis* (≈50%) and *Giardia lamblia* (≈12%). To validate the practicality of the procedure, bead-beating was applied in a population-based survey testing 910 stool samples. Findings confirmed bead-beating before DNA extraction to be a highly efficient procedure for the detection of *T. trichiura* DNA in stool.

Keyword:
Trichuris trichiura, intestinal parasite, bead-beating, sample preparation, real-time PCR

INTRODUCTION

An estimated 1.45 billion people globally are infected with at least one or more of the soil transmitted helminths (STH). Within this group whipworm (*Trichuris trichiura)* infects around 450 million people, mostly school age children [1]. Although many cases show only mild symptoms or are even asymptomatic, trichuriasis still has significant health consequences. Anaemia and poor nutrition status, especially in children, are partially attributable to chronic *T. trichiura* infections, while heavy worm burdens can result in ulcerative colitis and rectal prolapse [2].

Diagnosis of STH as well as other intestinal parasites has always relied on the classical microscopic examination of stool samples as it is relatively simple to perform and does not require expensive laboratory equipment. However, microscopy is highly observer dependent, therefore lacking the opportunity to perform sufficient quality control. Moreover, the limited sensitivity has relevant consequences when monitoring the impact of mass drug administration as light infections are easily missed, hence population-based cure rates are overestimated [3, 4]. The widely used Kato-smear based stool examination for the detection of helminth eggs will miss most of the low intensity infections and therefore specifically lacks sensitivity when approaching the end of the elimination phase in a control setting [5, 6].

As an alternative to microscopy, DNA-based diagnostics have proved for over a decade to out-perform microscopy in the detection of gastro-intestinal parasites [7]. Real-time PCR (polymerase chain reaction) has been shown to be more specific and sensitive than direct parasitological techniques and its (semi) quantitative output also reflects the amount of parasite DNA present [3, 7, 8]. Moreover, within a multiplex format different parasite targets can be detected in a single procedure. An advantage of DNA-based detection methods is the fact that stool samples when directly mixed with a preservative like ethanol, can be stored without immediate need of a cold chain [9]. Therefore it is relatively simple to collect samples in remote rural areas and transport them to a central laboratory for further analysis without compromising the quality of the targeted DNA.

Nevertheless, despite its high-throughput screening potentials multiplex real-time PCR has not yet replaced microscopy for the diagnosis of STH in large-scale epidemiological surveys. Undoubtedly this can be explained by a range of logistical and financial challenges which might be faced when implementing DNA detection-based diagnostics in a low resource laboratory setting. But an additional explanation has been the lack of a more efficient, though simple-to-use procedure to detect *T. trichiura* DNA in human stool samples within a multiplex or multi-parallel real-time PCR context. The most likely explanation for the relatively poor performance of the *T. trichiura* PCR, as seen in several studies, seems to be the robustness of *T. trichiura* eggs, hampering optimal DNA isolation [10]. Further improvement of the DNA isolation steps is therefore important, because as long as not each of the target helminth species can be diagnosed by the highly sensitive DNA detection-based methodology in combination with a relatively simple-to-use uniform sample processing procedure, complementary microscopy examination of stool samples will remain indispensable [11-14]. To optimize DNA extraction for the detection of *T. trichiura*, several studies have suggested a supplementary bead-beating step proceeding a standard DNA extraction protocol [8, 15-19]. But only one short publication systematically evaluated the effect of bead-beating in relation to the microscopy outcome by comparing different procedures in a stool samples spiked with different concentrations of *T. trichiura* eggs. In this study bead-beating actually did not result in a higher sensitivity of the *T. trichiura* PCR [15].

Besides bead-beating, additional heating and centrifugation steps have been introduced specifically to enable efficient extraction of *T. trichiura* DNA [20]. Notably, nearly all studies applying these additional procedure showed a PCR-based prevalence of *T. trichiura* below 3 %, which obscures the actual beneficial effects of these [8, 11, 20, 21].

The aim of the current study is to evaluate different methods to improve the detection of *T. trichuria* DNA in human stool. We therefore compared the effect of a bead-beating procedure prior to DNA extraction in stool samples with and without ethanol preservation. Stool samples were collected at Nangapanda village, situated in an area highly endemic for soil transmitted helminths in Indonesia [13]. Samples were tested by multiplex real-time PCR for the presence of *T. trichiura* DNA as well as for nine other intestinal parasite targets and findings were compared with microscopy. In addition, to validate practical aspects of the procedure, bead-beating followed by *T. trichuria* DNA detection was applied in a large scale population-based survey before and after intense anthelmintic treatment.

MATERIALS AND METHODS

Study design and sample collection

Stool samples were obtained from a multidisciplinary community research project named "Improving the health quality based on health education in Nangapanda sub-district, East Nusa Tenggara", from the University of Indonesia. The study was approved by the ethics committee at the Faculty of Medicine, Universitas Indonesia with ethics number: 653/UN2.F1/ETIK/2014. In brief, this project focuses on the identification of factors that might contribute to food-borne diseases in young children living in Nangapanda sub-district, Ende, Flores Island, Indonesia. The study site has been selected partly based on the known high prevalence of STH [13]. The study started in January 2014. A total of 400 mothers were recruited together with their child, if within the age range of 1 to 5 years old. Participants gave written informed or parental consent. Each participant received an appropriate stool container and was asked to provide their faecal sample the following morning. The first 60 stool samples of at least 3 gram were included. This sample size was based on a convenience sample that was limited by budget and personnel. The 60 samples originated from 38 mothers, ranging in age from 20 to 47 years (median 34 years) and 22 children (median age 3 years).

Sample preparation and DNA isolation

Figure 1 shows the sample preparation procedures used. Within a few hours after collection of the containers, two 25 mg Kato-smears were made and examined within 30 to 60 minutes by two independent microscopists for the presence of helminth eggs. In addition, two aliquots were taken from each stool sample. One aliquot of approximately 1-1.5 gram was stored directly at -20 °C and kept frozen during transport. The other aliquot, equal to approximately 0.7 ml of volume, was mixed thoroughly with 2 ml of 96% ethanol by stirring with a wooden stick [9]. These faeces-ethanol solutions were initially stored at room temperature for around four weeks and thereafter stored and transported at 4 °C. Upon arrival at the Leiden University Medical Center (LUMC), the Netherlands, a custom-made automated liquid handling station (Hamilton, Bonaduz, Switzerland) was used for washing of samples, DNA isolation and the setup of the PCR plates. A washing step was applied to the preserved samples to remove the ethanol as described previously [9]. Thereafter, both the washed samples and the frozen samples were suspended in 250 µl of PBS containing 2% polyvinylpolypyrrolidone (pvpp) [Sigma, Steinheim, Germany] [22]. From each to

suspension 200 µl was transferred to two deep-well plates [96x2.0 ml round, Nerbe Plus, Germany]. From this point the following codes were used to label each of the four sample preparation procedures: C_PCR, which stands for controls, i.e. DNA extraction was performed on frozen samples without bead-beating; B_PCR, i.e. bead-beating was performed before DNA extraction on frozen samples; E_PCR, i.e. DNA extraction was performed on ethanol preserved samples; and E_B_PCR, bead-beating was performed before DNA extraction on ethanol preserved samples (Figure 1). For the bead-beating procedure, 0.25 gram of 0.8 mm garnet bead [Mobio US, SanBio Netherlands] was added to the B_PCR and E_B_PCR suspensions, followed by a beating process for 3 minutes at 1800 rotations per minute (rpm) using a homogenization instrument [Fastprep 96, MP Biomedical, Santa Ana California, USA]. The choice of garnet bead was based on a small pilot study comparing five different bead types (see supplementary Table S1). DNA extraction was performed using a spin column-based procedure as previously described [23]. In each sample 10^3 Plaque-forming unit (PFU)/ml Phocin herpes virus-1 (PhHV-1) was included in the isolation lysis buffer, to serve as an internal control.

Parasite DNA detection

Three different multiplex real-time PCR detection panels were used to detect and quantify parasite specific DNA of six helminth species and four species of intestinal protozoa. Panel I targets *Schistosoma sp.* and *T. trichiura*; Panel II targets *A. duodenale*, *N. americanus*, *A. lumbricoides*, and *S. stercoralis*; Panel III targets *E. histolytica*, *D. fragilis*, *G. lamblia* and *Cryptosporidium* spp.. The sequences of primers and probes and the set-up of the PCR were based on published information and are also summarized in the supplementary Table S2 and S3 [17, 23-32]. Amplification, detection, and analysis were performed using the CFX real-time detection system (Bio-Rad laboratories). Negative and positive control samples were included in each PCR run. Cycle threshold (Ct) value results were analysed using Bio-Rad CFX software (Manager V3.1.1517.0823). The Ct-value represents the amplification cycle in which the level of fluorescent signal exceeds the background fluorescence (10^2 Relative Fluorescents Units), reflecting the parasite-specific DNA load in the sample tested. The amplification of individual samples was considered to be hampered by inhibitory factors if the expected Ct-value of 31 in the PhHV-specific PCR was increased by more than 3.3 cycles. The PhHV PCR showed no significant reduction in Ct value as a result of the newly introduced sample preparation procedures. For each parasite-specific target, DNA loads were arbitrarily categorized into the following intensity groups: low ($35 \leq Ct < 50$), moderate ($30 \leq Ct < 35$) and high ($Ct < 30$) [33].

Application stage

An additional set of 910 stool samples was used to validate the practicality of *T. trichiura* DNA detection, in particular for the purpose of large scale population-based surveys. Details of the study design have been published in the study protocol [34]. In brief, faecal samples were collected at Nangapanda, on Flores Island, Indonesia, from 455 adults, age 16 to 83 years old (median 45 years), before and after a one-year period of three monthly household treatments on three consecutive days with a single dose of 400 mg albendazole. Following microscopic examination of duplicate 25 mg Kato-smears, an aliquot of each stool sample was frozen within 24 hours after collection and transferred to the Netherlands for laboratory analysis. For logistical reasons, explained in the discussion paragraph, it was decided in this study not to use ethanol preservation of stool samples. DNA isolation and detection of *T. trichiura* DNA was performed as

described above according to the B_ PCR procedure. Pre- and post-treatment samples were tested pairwise, blinded from microscopy data.

Data Management and Statistical analysis

All collected data were exported to the SPSS 20.0 (IBM, Chicago, IL) for statistical analysis and to Graph Pad 6 for visualization. Negative samples were re-coded into an arbitrary value, i.e. 0.5 for egg counts and Ct 50 for PCR. Microscopy results were expressed as eggs per gram (EPG) of stool. Descriptive analysis was used to characterise the outcome of each sample preparation procedure. The percentages of positives were compared by their 95% confidence intervals (95% CI). The Wilcoxon signed-rank test was used to analyse a difference in median Ct-value between C_PCR (DNA extraction performed on frozen samples without bead-beating) and each of the alternative preparation procedures. This analysis was performed on those samples positive for at least one of the two indicated procedures and only for those parasite targets with 9 or more positive samples. The Spearman's rho (ρ) value was used to indicate the strength of correlation between egg output (EPG) and DNA load (Ct-value) for *T. trichiura* and *A. lumbricoides,* as only these two have species specific microscopy as well as PCR data available. Samples negative for both procedures were excluded in the statistical analysis. The McNemar test was used to compare paired proportions of microscopy and PCR detected *T. trichiura* cases in the population-based survey. A *p*-value <0.05 was considered to be statistically significant.

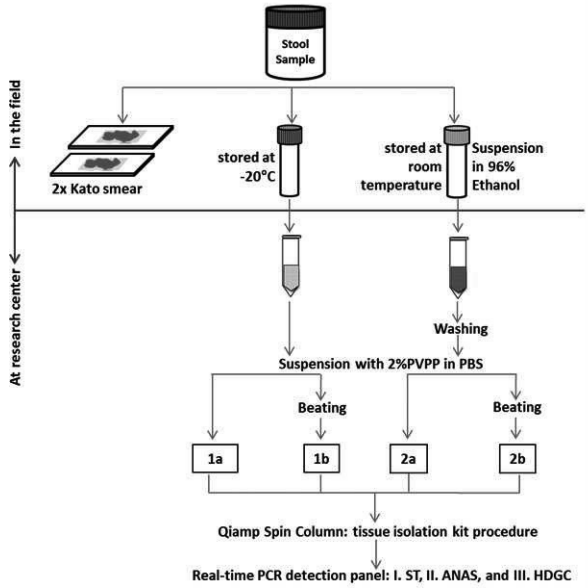

Figure 1. Flow-chart of the collection, preparations and measurements of 60 stool samples
Each preparation procedure is labelled as: 1a=C_PCR: PCR from directly frozen sample; 2a=E_PCR: PCR from ethanol preserved samples; 1b=B_PCR: PCR from bead-beating supplemented on frozen sample; 2b=E_B_PCR: PCR from bead-beating supplemented on ethanol preserved samples. Real-time PCR detection: Panel I=ST (targetting *Schistosoma* sp. and *T. trichiura*); Panel II=ANAS (targetting *A. duodenale, N. americanus, A. lumbricoides*, and *S. stercoralis*); Panel III=HDGC (targetting *E. histolytica, D. fragilis, G. lamblia* and *Cryptosporidium* spp.

RESULTS

Intestinal parasite detection

Table 1 shows parasite detection rates as determined by microscopy and real-time PCR following each of the four faecal sample preparation procedures. None of the samples were positive for *Schistosoma* sp., *Strongyloides stercoralis* or *Entamoeba histolytica.* Based on microscopy *Ascaris lumbricoides* (60%) was the most prevalent STH found, followed by hookworm (46.7%) and *T. trichiura* (45.0%). The real-time PCR results from frozen samples (C_PCR) showed a lower

percentage of *T. trichiura* positives (40.0%) compared to the Kato-smear (45.0%), while bead-beating (B_PCR), and the bead-beating on ethanol preserved samples (E_B_PCR) resulted in higher detection rates compared to microscopy, although the 95% CI did overlap. Using real-time PCR for the detection of hookworm, the number of positive cases ranged from 60.0% to 65.0%, with minor differences between the different samples preparation procedures. *Necator americanus* was found to be the dominant hookworm species. For *A. lumbricoides* the C_PCR procedure showed somewhat lower detection levels than microscopy, E_PCR, B_PCR and E_B_PCR, but none of the differences were significant. For intestinal protozoa the most prevalent species was *Dientamoeba fragilis* (55.0%) followed by *Giardia lamblia* (16.7%) and for both species the highest detection rates were found with the E_PCR procedure.

Table 1. Number and percentage of parasite positive cases detected either by microscopy or real-time PCR in 60 Indonesian stool samples

Parasite		No. positive (%) [95% CI]								
		Kato smear	C_PCR		E_PCR		B_PCR		E_B_PCR	
Schistosoma sp.		0	0		0		0		0	
T. trichiura		27 (45.0) [32-58]	24 (40.0) [27-53]		27 (45.0) [32-58]		31 (51.7) [39-65]		33 (55.0) [42-68]	
Hookworm	*A. duodenale*	28 (46.7) [34-60]	37 (61.7) [49-74]	4 (6.7) [3-16]	39 (65.0) [53-77]	5 (8.3) [4-18]	36 (60.0) [47-73]	4 (6.7) [3-16]	38 (63.3) [51-76]	4 (6.7) [3-16]
	N. americanus			36 (60.0) [47-73]		36 (60.0) [47-73]		34 (56.7) [44-70]		36 (60.0) [47-73]
A. lumbricoides		36 (60.0) [47-73]	34 (56.7) [44-70]		36 (60.0) [47-73]		36 (60.0) [47-73]		37 (61.7) [49-70]	
S. stercoralis		NA	0		0		0		0	
E. histolytica		NA	0		0		0		0	
D. fragilis		NA	31 (51.7) [39-65]		33 (55.0) [42-68]		26 (43.3) [30-56]		29 (48.3) [35-61]	
G. lamblia		NA	9 (15.0) [8-26]		10 (16.7) [9-28]		6 (10.0) [5-20]		7 (11.7) [6-22]	
Cryptosporidium spp.		NA	0		2 (3.3) [1-11]		0		1 (1.7) [0-9]	

CI= Confidence Interval. NA= Not applicable. The number of hookworm PCR from each preparation method were calculated based on *A. duodenale* plus *N. americanus* positives.

Stool parasite DNA load

Figure 2 displays the distribution of the PCR Ct-values for the five most common parasite targets for each of the sample preparation procedure, while table 2 shows the comparison between the median Ct values. For *T. trichiura*, the C_PCR procedure showed low DNA loads (Ct≥35) in the majority of 24 PCR positive samples. High DNA loads (Ct<30) were detected in 10 of 31 PCR positives (32.3%) after bead-beating on frozen samples (B_PCR) and in 20 of 33 PCR positives (75.8%) after bead-beating on ethanol preserved samples (E_B_PCR). All three modified sample preparation procedures showed significant higher *T. trichiura* DNA levels compared to control procedure (Table 2).

For *N. americanus* most PCR positive samples were categorized as having moderate to high DNA loads (Ct<35) in all four sample preparation procedures (Figure 2). The bead-beating procedure on ethanol preserved samples (E_B_PCR) resulted in significantly higher *N. americanus* DNA levels compared to the controls. In contrast, when the bead-beating procedure was applied

on frozen samples (B_PCR) *N. americanus* DNA levels were significantly lower compared to the controls (Table 2).

DNA loads in *A. lumbricoides* PCR-positive samples were mainly categorized as high (Figure 2). This was most prominent in the E_B_PCR group with 35 of 37 PCR positive samples (95.0%) showing a Ct below 30. The *A. lumbricoides* DNA load was significantly higher when comparing the E_B_PCR procedure with the control procedure, while no difference was seen for the two other sample preparation procedures (Table 2).

Table 2. Comparison of median cycle threshold (Ct) values between sample preparations procedures for the detected intestinal parasites

Species	Ct C_PCR vs E_PCR		N	*P*-value	Ct C_PCR vs B_PCR		N	*P*-value	Ct C_PCR vs E_B_PCR		N	*P*-value
T. trichiura	35.35	33.82	29	**	36.29	32.02	34	***	36.38	28.53	35	***
N. americanus	29.30	28.75	37	NS	28.86	32.65	36	***	29.30	26.53	37	***
A. lumbricoides	28.11	28.95	36	NS	28.11	29.55	36	NS	28.21	24.77	37	***
D. fragilis	32.16	30.21	33	***	32.16	34.26	31	***	32.16	31.53	32	NS
G. lamblia	34.40	34.33	10	NS	34.23	35.87	9	**	34.40	36.49	10	NS

NS: Not Significant; P value: *<0.05; **<0.01; ***<0.001

Using the bead-beating procedure (B_PCR) both the *D. fragilis* PCR and the *G. lamblia* PCR showed lower numbers of PCR positive samples, as well as reduced DNA loads compared to the frozen controls (Figure 2, Table 2). The same trend was seen when samples were preserved in ethanol.

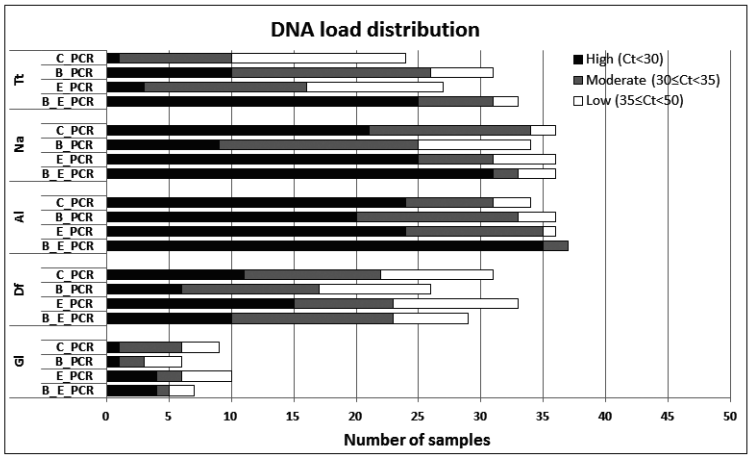

Figure 2. DNA load distribution of five most prominent intestinal parasites using four different preparation procedures on 60 stool samples

PCR results following the sample preparation procedure: C_PCR = directly frozen sample; E_PCR = ethanol preserved sample; B_PCR = bead-beating supplemented on frozen sample; E_B_PCR = bead-beating supplemented on ethanol preserved samples. Tt=*T. trichiura;* Na=*N. americanus*; Al=*A. lumbricoides*; Gl=*G. lamblia*; Df=*D. fragilis*.

Figure 3 shows the association between parasite DNA levels, represented by PCR Ct-value, and faecal egg count for *T. trichiura* and *A. lumbricoides*. *T. trichiura* egg counts ranged from 60 to 33.740 epg (median 780 epg) and *A. lumbricoides* egg counts ranged from 760 to 226.520 epg (median 19.330 epg). For each of the four sample preparation procedures a positive correlation

was found. For *T. trichiura*, the highest correlation coefficients were seen with the E_PCR procedure (Figure 2B; ρ=0.597, n=32, *p*<0.001) and the E_B_PCR procedure (Figure 2D; ρ=0.727, n=33, *p*<0.001). For *A. lumbricoides*, the highest correlation coefficients were seen when using the B_PCR procedure (Figure 2G; ρ=0.642, n=37, p<0.001) and the E_B_PCR procedure (Figure 2H; ρ=0.645, n=38, *p*<0.001).

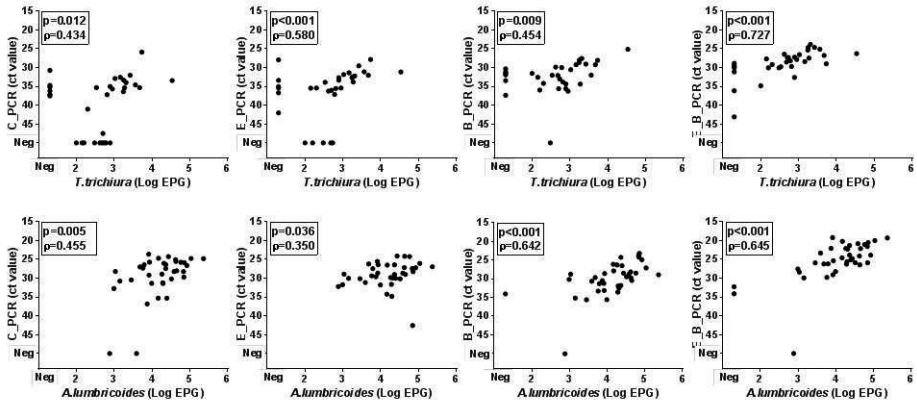

Figure 3. Association between egg output (Log EPG) and DNA load (Ct value) for *T. trichiura* (A-D) and *A. lumbricoide* (E-H)

PCR results following the sample preparation procedure: C_PCR = directly frozen sample; E_PCR = ethanol preserved sample; B_PCR = bead-beating supplemented on frozen sample; E_B_PCR = bead-beating supplemented on ethanol preserved samples. Samples negative for both microscopy and real-time PCR were excluded in the statistical analysis.

Application in an epidemiological survey

Figure 4 shows a comparison between the prevalence and intensity of *T. trichiura* infection determined by microscopy and by PCR using the bead-beating procedure (B_PCR) in a large scale population-based study. Based on microscopy 21.5% of this adult population (n=455) was found to be positive for *T. trichiura* (range 20-5,360 epg) prior to treatment, with 91 of the 98 positives showing less than 1,000 epg and a median egg count of 100 epg. Following a year of intense anthelmintic treatment, eggs of *T. trichiura* were seen in 18 individuals (4.0%) with egg counts ranging from 20 to 400 epg (median 40 epg). Significantly more cases were detected by PCR than by microscopy, both before (28.8%) and after (8.4%) repeated rounds of albendazole treatment (p=0.001).

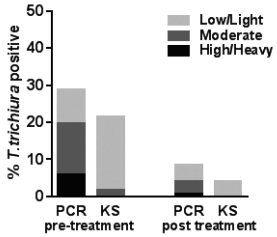

Figure 4. Prevalence and intensity of *T. trichiura* detected by PCR and Kato smear (KS) in 455 individuals before and one year after intense albendazole treatment

Ct values generated from real-time PCR were divided into three groups: high DNA load= Ct<30, moderate DNA Load= 30≤Ct<35 and low DNA load= 35≤Ct<50. EPG is calculated from Kato smear detection and divided into three categories based on WHO criteria: heavy-= ≥10,000, moderate-= 1,000-9,999, and light- infection= 1-999.

DISCUSSION

Molecular methods like real-time PCR are increasingly used in the diagnosis of intestinal helminths [10, 35]. However, large scale application of DNA detection procedures seems to be impaired, partly by the fact that the standard DNA extraction methods are not sufficient to release DNA from *T. trichiura* eggs [16]. The present study aimed to identify a simple-to-use sample preparation procedure which could replace our previous standard method of stool DNA isolation, thereby increasing the PCR detection rate of *T. trichiura* positive cases without uniformly changing the outcome of PCRs targeting other stool parasites.

In the pre-phase of the study several mechanical procedures (e.g. extensive heating, vortexing, blending, sonication), chemical procedures (e.g. alkaline supplementation, adding of lyticase, achromopeptidase or a higher amount of proteinase K) and a number of combinations were evaluated, to see which method performed best to enhance the release of DNA from *T. trichiura* eggs, but none of them was very successful (data not shown). Better results were seen by the introduction of a bead-beating step which facilitates the breakdown of the proteinaceous cellular wall, thereby making the DNA accessible [16, 36]. Several beads types of different manufacturers were compared and although tested in a small pilot only, differences were seen between the type of beads used (supplementary Table S1). Based on these findings garnet beads were selected for the further evaluation of the procedures.

Although the use of bead-beating to facilitate helminth DNA isolation has been mentioned in several publications, details of the performed procedures are mostly limited or even lacking. At most a comparison is made with the number of cases detected by PCR versus the number of cases detected by microscopy [8, 17-19, 37]. For example, in a study performed on 400 unpreserved stool samples collected from 13 month old children in Ecuador, 3% of the samples were positive for *T. trichiura* by PCR compared to 0.75% positive cases by microscopy [20]. In this study additional heating and centrifugation steps were introduced specifically to enable efficient extraction of *T. trichiura* DNA, but no details have been given and the overall low prevalence of *T. trichiura* makes it difficult to judge the importance of these additional procedures. Moreover, no adequate internal control was implemented to assess potential inhibition during DNA isolation and detection [20].

To our knowledge, Andersen and colleagues are the only group to have published details on the effect of adding beads on the detection of *T. trichiura* DNA by real-time PCR [15]. In this study three different types of beads, namely glass, garnet and zirconium, were evaluated. Bead-beating was compared to vortexing in the presence of beads. The authors concluded that glass beads were not very practical due to the increased risk of clotting of the tips and that none of the evaluated procedures increased the DNA yield from eggs of *T. trichiura* [15]. However, these findings have been based only on a stool sample artificially spiked with helminth eggs and on a single *T. trichiura* positive clinical sample.

In the current study 60 stool samples have been collected from a region in Indonesia known to be highly endemic for soil transmitted helminths. This high transmission level was confirmed by the detection of *T. trichiura* eggs in 45% of the stool samples after performing a duplicate 25 mg Kato-smear examination. However, egg excretion was not correspondingly high in this population with less than half of the positive samples showing more than 1000 epg. Despite the low intensity, this collection of stool samples was regarded as highly suitable for comparing different sample preparation procedures, noting that the majority of studies applying DNA detection-based diagnostic procedures work with a PCR-based prevalence of *T. trichiura* below 3% [8, 11, 20, 21]. In addition, the presented collection of stool samples showed high levels of co-infections with other

parasites, both helminths and protozoa, so the effect of different sample preparation procedures could be evaluated as well on DNA detection of *N. americanus*, *A. lumbricoides*, *D. fragilis* and *G. lamblia*.

Similarly to our previous, though unpublished, findings on stool samples which have been frozen only, the number of *T. trichiura* PCR positive cases was lower than the number of microscopy positive cases if no additional sample preparation procedures were applied. Indeed, without the addition of bead-beating the DNA yields of *T. trichiura* were generally low, with a minority of samples showing a Ct-value below 30. This in contrast to the effect of bead-beating, in particular on ethanol preserved samples, which resulted in the detection of additional helminth positive cases. Naturally the yield of *T. trichiura* DNA was also found to be substantially higher. The actual mechanism explaining why the addition of ethanol preservation resulted in higher DNA loads detected is not completely clear. The opposite might have been expected as the addition of ethanol requires a washing step, which discharges any free DNA present in the sample. The beneficial effect of combining bead-beating with ethanol preservation was found to be most distinct for the helminth species, in particular for *T. trichiura*, and not for the protozoa, suggesting the effect to be parasite specific.

Ethanol is widely used as a preservative of biological samples, including faecal material, when nucleic acid-based testing is needed and it was introduced several years ago to facilitate molecular diagnosis of helminth infections in remote populations where no cold-chain is available [9]. Despite the evident advantages of ethanol preservation shown in this study, we do not advocate the routine use of ethanol for all epidemiological studies dealing with stool collection. Three disadvantages of ethanol preservation have led to this new policy. Firstly, based on our experience in a number of population-based surveys, we noticed that the mixing of stool and ethanol in a field setting can be a critical process. Not only the ratio between the faecal material and the preservative is crucial, but the mixing must be thorough otherwise proper preservation will not take place. In case no vortex is available, this should be done by thoroughly stirring with a wooden stick. Secondly, the tubes should be well sealed to prevent leakage during transportation. Finally, the addition of a preservative will make the DNA extraction procedure more laborious and therefore more expensive as the ethanol has to be washed away before actual DNA extraction can proceed. This washing is an additional step in the sample handling procedure which increases the overall risk of human error, in particular if no automated sampling system is available.

In the past we have encountered errors resulting from each of the three points mentioned above, resulting in the loss of samples for molecular diagnosis, despite detailed instructions to field teams. In the case that no aliquots have been frozen and no supplementary microscopy has been performed, the loss of samples due to inappropriate preservation could be devastating. For these reasons we commonly advise our collaborators to directly freeze the samples whenever a proper cold-chain can be guaranteed or otherwise be extremely cautious concerning the point discussed above.

Because of the these practical limitations of ethanol preservation, direct freezing of stool samples has been applied in a recently performed survey on Flores Island, Indonesia, studying the effect of three monthly household treatments with albendazole [34]. Based on microscopy only, the prevalence of *T. trichiura* was found to be 21.5% at baseline, and with a median egg count of 100 epg, intensity of infection was already low before the intervention started. The relatively narrow range in egg excretion in this population probably explains why no correlation was found between the intensity of infection based on microscopy and the DNA load as determined by real-time PCR (data not shown). Following a year of intense treatment, a clear reduction was seen in the number

of *T. trichiura* positive cases, both based on microscopy and on DNA detection. Still, around twice as many *T. trichiura* positives cases were detected by PCR than by microscopy, confirming the higher sensitivity of molecular diagnosis assuming appropriate DNA isolation procedures have been performed [7, 38].

Our results overall illustrate that relatively minor differences in sample handling procedures can influence the output of real-time PCR. Consequently, comparison of studies, in particular when evaluating intensity of infections, should be interpreted with great care, especially if molecular testing has been performed in different laboratories or procedures have been changed over-time. The use of a standard curve, by adding genomic DNA at different concentrations or plasmids constructed to match the same target sequence, gives the impression that PCR yields standard results. But this does not allow for the effect of different isolation procedures. More progress is expected from defining an internationally recognized standard based on a fixed number of eggs per volume of stool.

In conclusion, the present findings confirm that a bead-beating procedure prior to DNA extraction increases the *T. trichiura* DNA yield in human faecal samples. Moreover, in combination with ethanol preservation this effect is most pronounced and also improves the detection rate of *N. americanus* and *A. lumbricoides*. Although ethanol preservation in itself has a positive effect, it also imposes several practical limitation. The effect of bead-beating on the detection of intestinal protozoa does not seem to be as uniform. Therefore bead-beating should be implemented with some caution, in particular when detecting *D. fragilis* in non-preserved samples. The general finding that sample handling procedures significantly influence detected DNA yield illustrates the potential impact of well-defined sample handling procedures and confirms the importance of standardisation. Exchange of proficiency panels between centralised reference laboratories seems an essential step in further harmonisation of molecular diagnosis of intestinal helminths.

ACKNOWLEDGMENTS

We thank all participants involved in this study as well as the team of the helminthology division, Department of Parasitology, Faculty of Medicine, Universitas Indonesia for their excellent help in samples collection and Kato-smear examination. We also acknowledge the SUGAR-spin team (http://sugarspin.org/), in particular Dicky Tahapary and Karin de Ruiter for their contributions. Finally we thank the students of the Department of Parasitology, LUMC, who were involved in the project and assisted in the laboratory analysis of the stool samples. This study was funded by the Prof Dr P. F. C. Flu Foundation ; The Royal Netherlands Academy of Arts and Science (KNAW), Ref 57-SPIN3-JRP and the Universitas Indonesia (Research Grant BOPTN 2742/H2.R12/HKP.05.00/2013). The authors would also like to thank The Indonesian Directorate General of Higher Education (DIKTI)-Leiden University for providing a PhD scholarship.

REFERENCES

1. Pullan, R.L., et al., *Global numbers of infection and disease burden of soil transmitted helminth infections in 2010.* Parasit Vectors, 2014. **7**: p. 37.
2. Knopp, S., et al., *Nematode infections: soil-transmitted helminths and trichinella.* Infect Dis Clin North Am, 2012. **26**(2): p. 341-58.
3. Knopp, S., et al., *Diagnostic accuracy of Kato-Katz, FLOTAC, Baermann, and PCR methods for the detection of light-intensity hookworm and Strongyloides stercoralis infections in Tanzania.* Am J Trop Med Hyg, 2014. **90**(3): p. 535-45.
4. van Lieshout, L. and M. Yazdanbakhsh, *Landscape of neglected tropical diseases: getting it right.* Lancet Infect Dis, 2013. **13**(6): p. 469-70.
5. Barda, B., J. Keiser, and M. Albonico, *Human Trichuriasis: Diagnostics Update.* Curr Trop Med Rep, 2015. **2**(4).

6. Utzinger, J., et al., *Progress in research, control and elimination of helminth infections in Asia.* Acta Trop, 2015. **141**(Pt B): p. 135-
7. Verweij, J.J., *Application of PCR-based methods for diagnosis of intestinal parasitic infections in the clinical laboratory.* Parasitology, 2014. **141**(14): p. 1863-72.
8. Easton, A.V., et al., *Multi-parallel qPCR provides increased sensitivity and diagnostic breadth for gastrointestinal parasites of humans: field-based inferences on the impact of mass deworming.* Parasit Vectors, 2016. **9**: p. 38.
9. ten Hove, R.J., et al., *Multiplex real-time PCR for the detection and quantification of Schistosoma mansoni and S. haematobium infection in stool samples collected in northern Senegal.* Trans R Soc Trop Med Hyg, 2008. **102**(2): p. 179-85.
10. Verweij, J.J. and C.R. Stensvold, *Molecular testing for clinical diagnosis and epidemiological investigations of intestinal parasitic infections.* Clin Microbiol Rev, 2014. **27**(2): p. 371-418.
11. Cimino, R.O., et al., *Identification of human intestinal parasites affecting an asymptomatic peri-urban Argentinian population using multi-parallel quantitative real-time polymerase chain reaction.* Parasit Vectors, 2015. **8**: p. 380.
12. Meurs, L., et al., *Is PCR the Next Reference Standard for the Diagnosis of Schistosoma in Stool? A Comparison with Microscopy in Senegal and Kenya.* PLoS Negl Trop Dis, 2015. **9**(7): p. e0003959.
13. Wiria, A.E., et al., *The effect of three-monthly albendazole treatment on malarial parasitemia and allergy: a household-based cluster-randomized, double-blind, placebo-controlled trial.* PLoS One, 2013. **8**(3): p. e57899.
14. Gordon, C.A., et al., *Multiplex real-time PCR monitoring of intestinal helminths in humans reveals widespread polyparasitism in Northern Samar, the Philippines.* Int J Parasitol, 2015. **45**(7): p. 477-83.
15. Andersen, L.O., et al., *Is supplementary bead beating for* 45*.DNA extraction from nematode eggs by use of the NucliSENS easyMag protocol necessary?* J Clin Microbiol, 2013. **51**(4): p. 1345-7.
16. Demeler, J., et al., *Discrimination of gastrointestinal nematode eggs from crude fecal egg preparations by inhibitor-resistant conventional and real-time PCR.* PLoS One, 2013. **8**(4): p. e61285.
17. Liu, J., et al., *A laboratory-developed TaqMan Array Card for simultaneous detection of 19 enteropathogens.* J Clin Microbiol, 2013. **51**(2): p. 472-80.
18. Platts-Mills, J.A., et al., *Association between stool enteropathogen quantity and disease in Tanzanian children using TaqMan array cards: a nested case-control study.* Am J Trop Med Hyg, 2014. **90**(1): p. 133-8.
19. Taniuchi, M., et al., *Etiology of diarrhea in Bangladeshi infants in the first year of life analyzed using molecular methods.* J Infect Dis, 2013. **208**(11): p. 1794-802.
20. Mejia, R., et al., *A novel, multi-parallel, real-time polymerase chain reaction approach for eight gastrointestinal parasites provides improved diagnostic capabilities to resource-limited at-risk populations.* Am J Trop Med Hyg, 2013. **88**(6): p. 1041-7.
21. Llewellyn, S., et al., *Application of a Multiplex Quantitative PCR to Assess Prevalence and Intensity Of Intestinal Parasite Infections in a Controlled Clinical Trial.* PLoS Negl Trop Dis, 2016. **10**(1): p. e0004380.
22. Verweij, J.J., et al., *Molecular diagnosis of Strongyloides stercoralis in faecal samples using real-time PCR.* Trans R Soc Trop Med Hyg, 2009. **103**(4): p. 342-6.
23. Wiria, A.E., et al., *Does treatment of intestinal helminth infections influence malaria? Background and methodology of a longitudinal study of clinical, parasitological and immunological parameters in Nangapanda, Flores, Indonesia (ImmunoSPIN Study).* BMC Infect Dis, 2010. **10**: p. 77.
24. Hamid, F., et al., *A longitudinal study of allergy and intestinal helminth infections in semi urban and rural areas of Flores, Indonesia (ImmunoSPIN Study).* BMC Infect Dis, 2011. **11**: p. 83.
25. Jothikumar, N., et al., *Detection and differentiation of Cryptosporidium hominis and Cryptosporidium parvum by dual TaqMan assays.* J Med Microbiol, 2008. **57**(Pt 9): p. 1099-105.
26. Niesters, H.G., *Clinical virology in real time.* J Clin Virol, 2002. **25 Suppl 3**: p. S3-12.
27. Obeng, B.B., et al., *Application of a circulating-cathodic-antigen (CCA) strip test and real-time PCR, in comparison with microscopy, for the detection of Schistosoma haematobium in urine samples from Ghana.* Ann Trop Med Parasitol, 2008. **102**(7): p. 625-33.
28. Verweij, J.J., et al., *Simultaneous detection of Entamoeba histolytica, Giardia lamblia, and Cryptosporidium parvum in fecal samples by using multiplex real-time PCR.* J Clin Microbiol, 2004. **42**(3): p. 1220-3.
29. Verweij, J.J., et al., *Simultaneous detection and quantification of Ancylostoma duodenale, Necator americanus, and Oesophagostomum bifurcum in fecal samples using multiplex real-time PCR.* Am J Trop Med Hyg, 2007. **77**(4): p. 685-90.
30. Verweij, J.J., et al., *Real-time PCR for the detection of Dientamoeba fragilis in fecal samples.* Mol Cell Probes, 2007. **21**(5-6): p. 400-4.
31. Verweij, J.J., et al., *Short communication: Prevalence of Entamoeba histolytica and Entamoeba dispar in northern Ghana.* Trop Med Int Health, 2003. **8**(12): p. 1153-6.

32. Verweij, J.J., et al., *Real-time PCR for the detection of Giardia lamblia.* Mol Cell Probes, 2003. **17**(5): p. 223-5.
33. Pillay, P., et al., *Real-time polymerase chain reaction for detection of Schistosoma DNA in small-volume urine samples reflects focal distribution of urogenital Schistosomiasis in primary school girls in KwaZulu Natal, South Africa.* Am J Trop Med Hyg, 2014. **90**(3): p. 546-52.
34. Tahapary, D.L., et al., *Helminth infections and type 2 diabetes: a cluster-randomized placebo controlled SUGARSPIN trial in Nangapanda, Flores, Indonesia.* BMC Infect Dis, 2015. **15**: p. 133.
35. O'Connell, E.M. and T.B. Nutman, *Molecular Diagnostics for Soil-Transmitted Helminths.* Am J Trop Med Hyg, 2016. **95**(3): p. 508-13.
36. Verollet, R., *A major step towards efficient sample preparation with bead-beating.* Biotechniques, 2008. **44**(6): p. 832-3.
37. Liu, J., et al., *Optimization of Quantitative PCR Methods for Enteropathogen Detection.* PLoS One, 2016. **11**(6): p. e0158199.
38. van Lieshout, L. and M. Roestenberg, *Clinical consequences of new diagnostic tools for intestinal parasites.* Clin Microbiol Infect, 2015. **21**(6): p. 520-8.

SUPPLEMENTARY DATA

Table S1. The comparison of cycle threshold (Ct) -values for different bead types tested in bead-beating procedure for *T. trichiura* detection

Sample ID	Egg count*	Real-time PCR (Ct-value)					
			Type of beads used in B_PCR**				
		C_PCR	Stainless Steel	Zirconium Oxide	Matrix A	Garnet	Matrix Y
A1284	61	34.18	27.13	24.69	25.14	26.58	26.40
A1311	42	34.33	27.15	26.91	27.13	26.00	0
D537	2	0	0	37.01	0	33.97	0
D680	0	0	0	0	0	0	0
H3404	162	37.06	32.48	34.98	31.52	29.15	35.03
H4022	374	37.75	32.87	28.06	26.32	27.72	27.55

C_PCR=PCR resulted from directly frozen sample; B_PCR=PCR resulted from bead-beating supplemented on frozen sample.
* A single slide microscopy examination performed using formol-ether concentration procedure
** The sizes of the beads are the following: Stainless steel [nextadvance, NY] is 0.5 mm; Zirconium Oxide [nextadvance, NY] is 0.5 mm; Matrix A is a 0.7 mm Garnet Lysing matrix [MP Biomedicals]; Garnet is 0.8 mm bead [Mobio US, SanBio Netherlands]; Matrix Y are 0.5 mm Yttria-Stabilized Zirconium Oxide beads [MP Biomedicals]. The volume of bead used per sample was 1.072 cm^3, this volume corresponds to 0.50 gram, 0.30 gram, 0.15 gram, 0.25 gram and 0.30 gram of beads which are, respectively, steel, zirconium oxide, matrix A, garnet and Matrix Y.

Table S2. Oligonucleotide primers and detection probes for real-time PCR for the simultaneous detection of intestinal helminth and protozoa

Target organism	Oligo name	Oligonucleotide sequences	Reference
***Schistosoma* sp.**	Ssp_ITS_48F	5'- GGTCTAGATGACTTGATYGAGATGCT -3'	(Obeng *et al.*, 2008)
	Ssp_ITS_124R	5'- TCCCGAGCGYGTATAATGTCATTA -3'	
	Ssp_ITS_78T_FAM	FAM-5'- TGGGTTGTGCTCGAGTCGTGGC -3'-BHQ1	
Trichuris trichiura	Tt_283F	5'- TTGAAACGACTTGCTCATCAACTT -3'	(Liu *et al.*, 2013)
	Tt_358R	5'- CTGATTCTCCGTTAACCGTTGTC -3'	
	Tt_308T_YY	Yakima Yellow-5'- CGATGGTACGCTACGTGCTTACCATGG -3'-BHQ1	
***Ancylostoma* sp.**	Ad_125F	5'- GAATGACAGCAAACTGCTTGTTG -3'	(Hamid *et al.*, 2011; Verweij *et al.*, 2009; Wiria *et al.*, 2010)
	Ad_195R	5'- ATACTAGCCACTGCCGAAACGT -3'	
	Ad_155_XS_TR	Texas red-5'- ATCGTTTACCGACTTTAG -3'BHQ2	
Necator americanus	Na_58F	5'- CTGGTTTGTCGAACGGTACTTGC -3'	
	Na_158R	5'- ATAACAGCGTGCACATGTTGC -3'	
	Na_81T_XS_FAM	FAM-5'- CTGTACTACGCATTGTATAC -3'-BHQ1	
Ascaris lumbricoides	Alum_96F	5'- GTAATAGCAGTCGGCGGTTTCTT -3'	
	Alum_183R	5'- GCCCAACATGCCACCTATTC -3'	
	Alum_124T_YY	Yakima Yellow-5'- TTGGCGGACAATTGCATGCGAT -3'-BHQ1	
Strongyloides stercoralis	Stro 18S-1530F	5'- GAATTCCAAGTAAACGTAAGTCATTAGC -3'	
	Stro 18S-1630R	5'- TGCCTCTGCATATTGCTCAGTTC -3'	
	Stro 18S-1586T	Quasar705-5'- ACACACCGGCCGTCGCTGC -3'-BHQ2	
Entamoeba histolytica	Ehd_F	5'- ATTGTCGTGGCATCCTAACTCA -3'	(Verweij *et al.*, 2003a)
	Ehd_R	5'- GCGGACGGCTCATTATAACA -3'	
	Eh_18S_XS_YY	Yakima Yellow-5'- TCATTGAATGAATTGGCCATTT -3'-BHQ1	

Table S2. Continue

Target organism	Oligo name	Oligonucleotide sequences	Reference
Dientamoeba fragilis	Df_124F	5′- CAACGGATGTCTTGGCTCTTTA -3′	(Verweij *et al.*, 2007)
	Df_221R	5′- TGCATTCAAAGATCGAACTTATCAC -3′	
	Df_172_XS_Quasar705	Yakima Yellow-5′- CAATTCTAGCCGCTTAT -3′-BHQ1	
Giardia lamblia	Giardia_18S_99F	5′- GACGGCTCAGGACAACGGTT -3′	(Verweij *et al.*, 2004; Verweij *et al.*, 2003b)
	Giardia_18S_125R	5′- TTGCCAGCGGTGTCCG -3′	
	Giardia_18S_FAM	FAM 5′- CCCGCGGCGGTCCCTGCTAG -3′-BHQ1	
***Cryptosporidium* spp.**	Cr_spp_JVAF	5′- ATG ACG GGT AAC GGG GAAT -3′	(Jothikumar *et al.*, 2008)
	Cr_spp_JVAR	5′- CCA ATT ACA AAA CCA AAA AGT CC -3′	
	Cr_spp_JVAP18S_TR	Texas Red 5′- CGC GCC TGC TGC CTT CCT TAG ATG -3′-BHQ2	
Phocin Herpes Virus (PhHV)	PhHV_267s	5′- GGGCGAATCACAGATTGAAT|C -3′	(Niesters, 2002)
	PhHV_337as	5′- GCGGTTCCAAACGTACCAA -3′	
	PhHV_305tq_Cy5	Cy5-5′- TTTTTATGTGTCCGCCACCATCTGGATC -3′-BHQ2	

Table S3. Mixtures composition in three real-time PCR panels used for intestinal parasites detection

Panel I: ST		
Reagents:	**Concentration:**	**1 Sample:**
H_20		2,025
$MgCl_2$	25 mM	3,50
BSA	5 mg/ml	0,50
Primer Ssp -F	25 µM	0,20
Primer Ssp -R	25 µM	0,20
Probe Ssp -FAM	10 µM	0,125
Primer Tt -F	25 µM	0,20
Primer Tt -R	25 µM	0,20
Probe Tt -YY	10 µM	0,125
Primer PHHV -S	25 µM	0,15
Primer PHHV -AS	25 µM	0,15
Probe PHHV - Cy5	10 µM	0,125
HotStar Taq Master Mix		12,50
Total		20,00
Add 5 µl DNA to the mix		

Panel II: ANAS		
Reagents :	**Concentration:**	**1 Sample:**
H_20		2,025
$MgCl_2$	25 mM	3,50
BSA	5 mg/ml	0,50
Primer Ad -F	25 µM	0,20
Primer Ad -R	25 µM	0,20
Probe Ad - TR	10 µM	0,25
Primer Na -F	25 µM	0,20
Primer Na -R	25 µM	0,20
Probe Na - FAM	10 µM	0,125
Primer Alum -F	10 µM	0,20
Primer Alum -R	10 µM	0,20
Probe Alum - YY	10 µM	0,125
Primer Stro -F	25 µM	0,10
Primer Stro -R	25 µM	0,10
Probe Stro -Quasar 705	10 µM	0,125
Primer PHHV -S	25 µM	0,15
Primer PHHV -AS	25 µM	0,15
Probe PHHV - Cy5	10 µM	0,125
HotStar Taq Master Mix		12,50
Total		20,00
Add 5 µl DNA to the mix		

Panel III: HDGC		
Reagents:	**Concentration:**	**1 Sample:**
H_20		1,61
$MgCl_2$	25 mM	3,50
BSA	5 mg/ml	0,50
Primer Ehd -F	25 µM	0,04
Primer Ehd -R	25 µM	0,04
Probe Eh - YY	10 µM	0,125
Primer Df -F	25 µM	0,20
Primer Df -R	25 µM	0,20
Probe Df - Quasar705	10 µM	0,25
Primer Giardia -F	25 µM	0,06
Primer Giardia -R	25 µM	0,06
Probe Giardia -FAM	10 µM	0,125
Primer Cr spp -F	25 µM	0,06
Primer Cr spp -R	25 µM	0,06
Probe Cr spp -TR	10 µM	0,25
Primer PHHV - S	25 µM	0,15
Primer PHHV -AS	25 µM	0,15
Probe PHHV - Cy5	10 µM	0,125
HotStar Taq Master Mix		12,50
Total		20,00
Add 5 µl DNA to the mix		

Chapter 4

The *Schistosoma mansoni* Lipidome: leads for immunomodulation

MARTIN GIERA[1], MARIA M. M. KAISAR[2, 3], RICO DERKS[1], EVELYNE STEENVOORDEN[1], YVONNE C. M. KRUIZE[2], CORNELIS H. HOKKE[2], MARIA YAZDANBAKHSH[2], BART EVERTS[2]

[1]Center of Proteomics and Metabolomics, LUMC, Leiden, The Netherlands
[2]Department of Parasitology, Leiden University Medical Center (LUMC), Leiden, The Netherlands
[3]Department of Parasitology, Faculty of Medicine, Universitas Indonesia, Jakarta, Indonesia

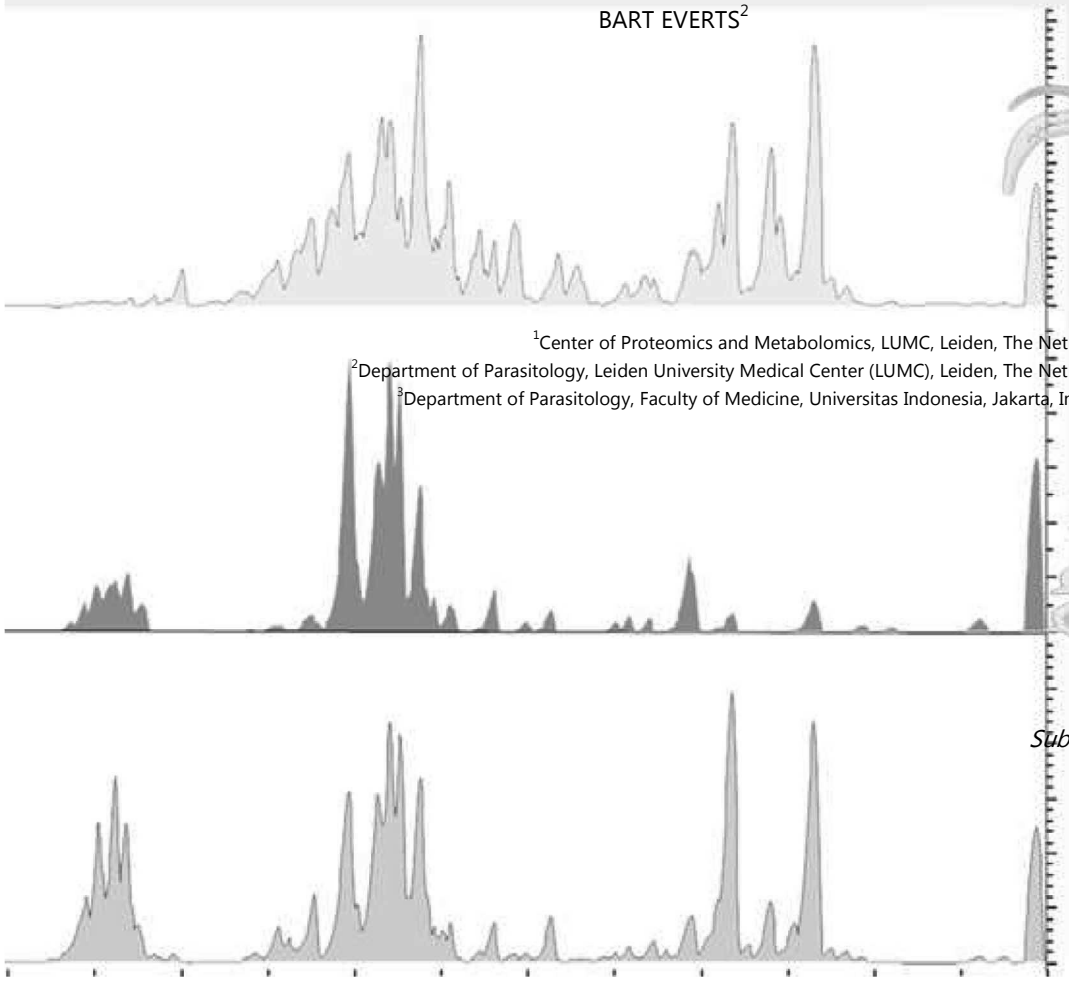

Submitted

ABSTRACT

Schistosoma mansoni is a parasitic helminth that infects millions of people mostly in tropical parts of the world. Different life cycle stages of *S. mansoni,* that infect or develop in the human host, promote distinct immune responses and are known for their ability to modulate host immune responses. However, the molecular mechanisms through which the parasites interact with, and modulate the host immune system remain incompletely understood. Despite the well-known ability of various lipids to modulate immune responses, a comprehensive analysis of the lipidome of the different life cycle stages has not been performed. Using three complementary MS-based platforms to detect and quantify around 400 lipid species, we here characterized the lipid profiles of *S. mansoni* cercariae, worms and eggs, as well as extracts and excretory/secretory (ES) products of different life cycle stages of *S. mansoni*. We identified life cycle stage specific signatures of lipid classes of which cercariae were found to have the most distinct profile. Moreover, we detected several immunolomodulatory oxylipids in the different life cycle stages. Specifically, prostaglandins were found to be most highly enriched in egg preparations, while resolvins were specifically detected in cercariae. Together, the generation of this detailed lipid database of the different life cycle stages of *S. mansoni* will not only be important for a better understanding of the biology of the parasite itself but also of host-parasite interactions and how that could result in immunomodulation.

Keyword:
Schistosoma mansoni, Lipidomics, Excretory/Secretory products, life cycle stages, immunomodulation

INTRODUCTION

Schistosoma mansoni is a parasitic trematode causing schistosomiasis in humans and occurs in mostly tropical parts of South America and Africa. According to the WHO more than 61 million people have been treated for this disease in 2014 [1] with estimates of between 20000 to 200000 deaths per year. The life cycle of this parasite is complex and involves both humans as a final host as well as freshwater snails as intermediate host. Infection of humans is initiated by the larval stage of these parasites, termed cercariae, through their ability to penetrate human skin. Upon penetration cercariae lose their tail, allowing their head to develop into schistosomula that migrate through the skin into the circulation. Two to 3 weeks after the initial infection, schistosomula end up in the hepatoportal circulation where they develop into sexually mature adults and pair for sexual reproduction. Subsequently, approximately 6 to 8 weeks into the infection, females start to produce eggs, of which around 50% through the wall of the intestine to reach the outside environment. However, a large fraction of the eggs get lodged in the intestinal wall or are instead carried by the blood flow into the liver, where they become trapped in hepatic sinusoids. This accumulation of eggs in tissues is the major cause of pathology in schistosomiasis [2].

The immune responses associated with this infection are equally complex. Infection with cercariae initially trigger an immune reaction characterized by a T helper 1 (Th1) response. However, upon egg production, a strong Th2 response is induced that subsequently orchestrates the development of granulomatous lesions surrounding the eggs. *S. mansoni* infections are often chronic in nature, which in part is thought to be due to the ability of these pasasites to promote regulatory responses that dampen type 2 inflammation that can lead to responses against their parasites [3, 4]. Importantly, evidence is accumulating that this induction of regulatory immune responses by *S. mansoni*, may not only impair effector responses directed against the parasite, but may also be beneficial to the host as it can concomitantly lead to bystander suppression of other inflammatory immune responses. For instance, population studies have revealed that these parasitic infections, can reduce various parameters associated with allergic responses [5, 6]. These observations have been corroborated in animal models [7, 8] and further extended to models of other inflammatory disorders including colitis [9] and type 2 diabetes [10]. This illustrates that different life cycle stages of *S. mansoni* that infect or develop in the human host, promote distinct immune responses, that are not only important in mediating immunity against the infection and in determining the immunopathological outcome of the disease, but that can also have beneficial effects on development of various unrelated inflammatory disorders. Therefore, it will be important to define the components and antigens from the different life cycle stages that may drive these distinct immune responses in humans. This could be of great value for vaccine development against *S. mansoni*, but could also contribute to the design of therapeutics to treat inflammatory diseases by exploiting the immunoregulatory potential of some helminth-derived molecules. Thus far, to identify *S. mansoni*-derived molecules with immunomodulatory potential, most studies have focused on proteomics [11, 12] or glycomics [13, 14]. Much less is known about *S. mansoni*-derived lipids in this context.

Already in the late 1960s studies were undertaken to characterize the major lipid classes present in *S. mansoni* worms [15]. Subsequent studies revealed that apart from being constituents of membranes, lipid metabolism in *S. mansoni* also has important roles in development of the different life cycle stages [16] and in evasion of immune responses by adult worms [17] or cercariae [18]. The potential role of lipids interacting with immune system comes from study that has directly linked *S. mansoni* Lyso-PS, to immunomodulation by induction of regulatory T cells [19]. Moreover, there is some evidence to suggest that *S. mansoni* can produce eicosanoids [20],

which are bioactive lipids well recognized for their immunomodulatory capacity. With these studies in mind, it is important to first conduct a comprehensive in-depth characterization of the lipid composition of the different classes of lipids of the distinct life cycle stages of *S. mansoni*. Studies that have performed lipid profiling of *S. mansoni* so far, were either based on a limited fingerprinting approach leading to the identification of a very small number of lipids [21-23] or focused specifically on the phospholipid content of only the worm itself [23, 24]. Using three complementary highly sensitive MS-based lipidomics platforms, we present a comprehensive lipidomics analysis of *S. mansoni* cercariae, adult worm and eggs, as well as of typical extracts of cercariae (cercarial antigen, CA), worms (adult worm antigen, AWA) and eggs of (soluble egg antigen, SEA) and their excretory and secretory products (ES), each widely used in immunological studies. We identified life cycle stage specific lipid signatures not only for membrane and storage lipids but in particular for bioactive lipid mediators, which provides potentially interesting new leads to study the link between the *S. mansoni* lipidome and immunomodulation.

MATERIALS AND METHODS

Chemicals

For all lipids the LipidMaps abbreviation system is used [25]. Oxylipid standards were from Cayman Chemicals (Ann Arbor, MI, USA), the internal standard solution for oxylipid analysis (oxIS) contained each of PGE2-d4, LTB4-d4, 15-HETE-d8 and DHA-d5 at a concentration of 50 ng/mL in methanol (MeOH). The internal standard for lipidomics analysis (lipIS) contained lysophosphatidylcholine LPC (19:0), phosphatidylcholine PC (11:0/11:0), phosphatidylethanolamine PE (15:0/15:0) (Avanti Polar Lipids, Alabaster, AL, USA) and triacylglyceride TG (15:0/15:0/15:0) (Sigma Aldrich) at a concentration of 0.5 µg/mL in 2-propanol. For GC-MS analysis the GLC-85 mix from Nu-check Prep (Elysian, MN, USA) in combination with the volatile acids mix from Sigma Aldrich was used for constructing calibration lines and as authentic standards for substance identification. Palmitic acid d31 1 µg/mL in ethanol was used as internal standard for GC-MS analysis (gcIS) (Cambridge isotopes, Cambridge, MA, USA). All other chemicals were from Sigma-Aldrich (St. Louis, MO, USA). All solvents were of *pro analysi* or LC-MS grade.

Animal and parasite materials

The full life cycle of the Puerto Rican strain of *S. mansoni* used in this study was maintained in *Biomphalaria glabrata* as snail intermediate host and male Golden hamsters (RjHan : AURA, Javier labs) as mammalian definitive host. For infections, male hamsters 9.5 weeks old and weighing ±100 g were exposed to an aqueous suspension containing 1200 cercariae of *S. mansoni* freshly shed by *B. glabrata* infected hamsters were maintained in a controlled environment at room temperature (RT) with normal night and daylight cycle. All hamster experiments were performed in accordance with local government regulations, and the EU Directive 2010/63EU and Recommendation 2007/526/EC regarding the protection of animals used for experimental and other scientific purposes and approved by the CCD. Preparation of parasite samples for lipidomics analysis is described below. For each sample three biological replicates were generated to account for possible parasite batch variations.

Cercariae. *S. mansoni*-infected *B. glabrata* snails kept in trays were transferred to a cup containing 30 mL of mineral water, and exposed to light at 28 °C for 2 h to trigger cercariae shedding. Cercariae were sedimented by cooling on ice, and stored in water at -80 °C until use. Alternatively, as described below, live cercariae were cultured to produce cercarial ES products.

Eggs. Eggs were obtained as described before (Dalton *et al*. 1997), with some modification. Briefly, the livers of 10 hamsters that were infected with *S. mansoni* 6 week before, were homogenised in 300 mL of wash buffer (1.7% NaCl PBS, to prevent hatching of eggs). The suspension was poured into a one-liter screw cap bottle containing 800 mL wash buffer, collagenase B (400 mg), streptomycin and penicillin (750 µl 200.000 U/ml, each) gently stirred at 37 °C overnight. Then the suspension was sequentially sieved through 355 and 200 micron sieves rinsed with wash buffer, and transferred to 50 mL tubes. After centrifugation for 5 min at 400 g, RT the pellets were collected, resuspended in wash buffer, transferred to new 50 mL tubes followed by centrifugation as above. These steps were repeated until the supernatant became clear, with intermediate application to an 80 micron sieve. The isolated eggs were resuspended in wash buffer containing EGTA and EDTA to inactivate collagenase, washed three times with this buffer at 60 g for 3 min, RT. The eggs were collected and counted prior to final wash with wash buffer at 1000 rpm, for 1 min, RT. Aliquots of approximately 50.000 eggs were stored at -80 °C in PBS until use. In addition, live eggs were cultured to generate egg ES, as described below.

Adult worms. Mixed male and female adult worms were obtained from hamsters sacrificed 6 weeks after infection with *S. mansoni*, through perfusion of the hepatic portal system and mesenteric veins. Collected live worms were washed with perfusion buffer (Dulbecco's buffered saline and sodium citrate) to remove blood and debris. Worms were then washed with PBS and stored at -80 °C until use, or cultured to collect worm ES as described in following section.

Preparation of extracts and ES products of *S. mansoni*: cercariae, worms and eggs

Parasite extracts

Cercarial Antigen (CA) and *Soluble Eggs Antigen (SEA)*. Frozen cercariae or eggs were thawed and manually homogenized in a sterilized glass homogenizer on ice. Homogenates were subsequently subjected to sonification (six rounds of 30 sec, with 20 sec intervals) (Branson sonifier) on ice. The extracts were kept overnight at -80 °C. Following thawing extracts were centrifuged twice cat 13000 rpm, 4 °C for 25 min. The supernatants were collected and filter-sterilized. Protein concentration was determined using BCA (Pierce BCA Protein assay kit, Thermo Scientific) according to the manufacturer's protocol. The protein concentrations of CA and SEA were adjusted to 80 µg/ml and samples were stored at -80 °C until use.

Adult Worm Antigen (AWA). Worms were lyophilized, suspended in cold PBS and manually homogenized in a sterilized glass homogenizer. The process was continued as for CA and SEA preparation.

Excretory/secretory (ES) products

Cercarial ES (CES). Approximately 100.000 freshly shed cercariae were suspended in 12.5 mL of M199 medium (Gibco) supplemented with HEPES, antimycotic and L-glutamine (Sigma-Aldrich). The cercariae were incubated for 20 min at 37 °C 5% CO_2, during this period they transform into schistosomula, after which the process continued with centrifugation at 1600 rpm, RT, 5 min, and then the supernatant (CES) was collected.

Egg ES (EES). Approximately 300.000 freshly isolated eggs were resuspended in 25 mL 20% percoll and centrifuged at 500 g for 6 min. The eggs were centrifuged for 4 min, at 1100 rpm, RT for four times: two times with 2 mL PBS (1.7% NaCl); one time with RPMI (Gibco) supplemented with penicillin and streptomycin; and one time with up to 40 mL of medium (RPMI supplemented with fungizone, penicillin and streptomycin—referred as E-medium). The eggs were resuspended in 1

mL of E-medium in 24 well plates and incubated for 48 h at 37 °C 5% CO_2. About 800 µL supernatant was collected (EES).

Worm ES (WES). Live worms were gently washed twice with S-medium (M199 medium (Gibco) supplemented with ABAM (Sigma) and HEPES—referred as S-medium). In total, approximately 200 mixed male and female worms were resuspended in 20 mL of S-medium and placed in a 75cm^3 flask. The flask was incubated at 37 °C 5% CO_2 for 48 h and the supernatant (WES) was collected.

All ES products were kept at -80 °C until further use. Prior to lipidomics analysis, ES preparation concentrations were adjusted to 80 µg/ml. For protein concentration determination by BCA, the medium used for culturing the cercariae, eggs and worms was taken as background.

Sample preparation

Three different types of samples were investigated in this study: 1) whole parasite life cycle stages (cercariae, worms and eggs); 2) water soluble extracts including: CA, AWA, SEA; and 3) ES products (CES, EES and WES). Whole parasite life cycle stages were extracted using 2-propanol after homogenization in a bullet blender for further analysis using mass-spectrometry . In the case of extracts or ES products, 20 µL of sample was directly used for the below described procedures. Briefly, to the parasite materials sample in 150 µL phosphate buffered saline was added 5 stainless steel beads and the sample homogenized for 5 min in a bullet blender. Subsequently 300 µL 2-propanol was added, the sample was vigorously shaken and centrifuged at 16100 ×*g* for 5 minutes. The supernatant was transferred to a glass vial. The residual sample was re-extracted using 300 µL of 2-propanol and the organic extracts combined. The combined organic extracts were dried under a gentle stream of nitrogen and dissolved in 200 µL 2-propanol, stored at -80 °C until analysis.

GC-MS analysis for total fatty acid analysis

GC-MS analysis was carried out as described elsewhere [1, 26], with some modifications. Briefly, to 20 µL sample in a glass vial was added 10 µL of 10 M NaOH and 250 µL acetone. The vial was flushed with nitrogen, tightly closed and incubated at 60 °C for one hour. After cooling to room temperature 10 µL of gcIS solution, followed by the addition of 100 µL of a 172 mM solution of PFBBr in acetone. The samples were subsequently incubated for 30 min at 60 °C. 250 µL of water and 500 µL of n-hexane was added and the hexane layer transferred to an auto sampler vial. GC-ECNI-MS analysis was carried out on a Bruker scion TQ (Bruker, Bremen, Germany) using methane (99.9995%) as CI gas, equipped with an Agilent VF-5MS (30 m × 0.25 mm × 0.25 mm) column. The temperature program was as follows: 1 min 50 °C, linear increase at 40 °C/min to 60 °C, held 3 min at 60 °C, linear increase at 25 °C/min to 237 °C, linear increase at 3 °C/min to 250 °C, linear increase at 25 °C/min to 315 °C held for 1.55 min. The transfer line and ionization source temperature were 280 °C. The pressure of the chemical ionization gas was set at 15 psi. The carrier gas was helium (99.9990%) at a flow rate of 1.2 mL/min.

LC-MS/MS analysis of eicosanoids and docosanoids

Eicosanoid and docosanoid analysis was carried out as described elsewhere [27]. For liquid samples 20 µL sample was mixed with 60 µL MeOH and 2 µL oxIS solution, the sample was centrifuged for 10 min at 16100 ×*g* and 4 °C. 50 µL of the supernatant was dried under a gentle stream of nitrogen and re-dissolved in 50 µL 40% MeOH for injection. Targeted lipidomics analysis was carried out as follows: analysis was achieved using a QTrap 6500 mass spectrometer in

negative ESI mode (ESI-) (Sciex, Nieuwerkerk aan den Ijssel, The Netherlands), coupled to a LC system employing two LC-30AD pumps, a SIL-30AC autosampler, and a CTO-20AC column oven (Shimadzu, 's-Hertogenbosch, The Netherlands). The employed column was a Kinetex C18 50 × 2.1 mm, 1.7 µm, protected with a C8 precolumn (Phenomenex, Utrecht, The Netherlands), kept at 50 °C. The following binary gradient of water (A) and MeOH (B) with 0.01% acetic acid was used: 0 min 30% B, held for 1 min, then ramped to 45% at 1.1 min, to 53.5% at 2 min, to 55.5% at 4 min, to 90% at 7 min, and to 100% B at 7.1 min, held for 1.9 min. The injection volume was 40 µL and the flow rate 400 µL/min. The MS was operated under the same conditions as in reference [28]. For quantification calibration lines, constructed with standard material were used and only peaks with a signal to noise (S/N) > 10 were quantified. For analytes where no calibration line was used, area ratios were used and a S/N > 3 was used as a detection limit. A list of all monitored oxylipids, corresponding lipidmaps IDs and calibration ranges can be found in supplementary (Table S1).

LC-MS analysis for lipid profiling

LC-MS/MS based lipid profiling was carried out as described elsewhere [29, 30] with some modifications. Briefly, a Dionex Ultimate 3000 (Thermo, Oberschleiβheim, Germany) delivered a gradient of water:acetonitrile 80:20 (eluent A) and water:acetonitrile:2-propanol 1:90:9, both containing 5 mM ammonium formate and 0.05% formic acid. The applied gradient was as follows: 0 min 40% B, 10 min 100% B, 12 min 100% B. The flow rate was set to 250 µL/min at a column temperature of 50 °C. The column used was a Phenomenex Kinetex C18, 2.7 µm, 50×2.1 mm (Phenomenex, Utrecht, The Netherlands). The MS was a Bruker Maxis Impact HD, operated in the positive ESI mode (ESI+), with the following conditions: capillary 3500 V, dry gas (nitrogen 99.9990%) 7 L/min, dry temperature 300 °C, nebulizer 2.1 bar, mass range m/z 150-1000. The injection volume was 20 µL.

Lipid identification

For targeted lipidomics employing GC-ECNI-MS and LC-MS/MS (QTrap) analysis, lipids were identified by comparing relative retention times (RRT) and either molecular ions [M]- monitored in selected ion monitoring mode for GC-ECNI-MS analysis or characteristic MRM transitions in case of LC-MS/MS (QTrap) analysis. In case of LC-MS based lipid profiling we made use of the following approach. Initially all MS and MS/MS spectra were recalibrated using the signal of a calibration solution consisting of sodium formate in 50:50 isopropanol:water. The calibration solution was post column injected into the LC effluent in order to elute before the dead time of every analysis. The recalibration was done in Data Analysis 4.2 build 395 (Bruker Daltonik GmbH, Germany). Subsequently, MS/MS acquisition was achieved using a data independent method. Analysis was done per sample per lipid class. For each lipid class characteristic parameters (i.e. retention time range, unique product ion or neutral lost) where set to filter the MS/MS spectra as shown in Table 1.

Within Data Analysis homemade Visual Basic scripts were used to filter all collected MS/MS spectra according to each lipid class separately. The results were exported to mgf format, resulting in a single mgf file per sample per lipid class. Each mgf file was used to search the LipidBlast databases [31]. LipidBlast contains several different libraries, some contain multiple lipid classes others are specific for one lipid class. The top results of all database searches were stored and further processed in R (CRAN R, version 3.3.2). For each sample type three biological sample replicates were measured and only lipids detected in at least two out of three samples were

deposited in our *S. mansoni* lipid database (supplementary Table S2). For calculating percentage (%) lipid composition of all samples we used the MS signals as follows: from the MS/MS data *m/z* and retention time for each lipid were extracted. Subsequently a homemade Visual Basic script was used to automate the following steps within data analysis: create extracted ion chromatogram (EIC) from the *m/z* with a narrow window of 5 mDa, set retention time window around the retention time and finally carry out peak detection and integration. Results of each sample were exported to a comma separated (csv) file. All result files were collected and further processed in R.

Table 1. Lipid class characteristics used for assignment

Lipid class	Retention time range [min]	Product ion	Neutral loss	Precursor
Phosphatidic Acid (PA)			97.9769	
Lyso-Phosphatidic Acid (LPA)		155.06638		
Lyso-Phosphatidylcholine (LPC)		184.0733		Even
Lyso-Phosphatidylethanolamine (LPE)	6.5 – 9.0		141.0191	
Phosphoglycerol (PG)			172.0137	
Phosphoinositol (PI)			260.0297	
Phosphatidylserine (PS)			185.0089	
Sphingomyelins (SM)		184.0733		Odd
Cholesteryl Ester (CE)	10.0 – 12.0	369.3516		Even
Diacylglycerol (DG)	7.0 – 9.5			Even
Triacylglycerol (TG)	10.0 – 12.0			Even

RESULTS

Analysis and identification of lipid species

Using three lipidomics platforms, which were: QToF based LC-MS/MS for major lipid classes, GC-MS for total fatty acid (FA) analysis as well as QTrap based LC-MS/MS for eicosanoid and docosanoid analysis and we investigated occurrence and quantity of several lipid classes in different life-cycle stages of *S. mansoni* that could be of relevance to interaction with human host. The investigated lipid classes, the employed platform and the number of detected species are given in Table 2.

Table 2. Analytical platforms and number of detected lipid species

Analytical Platform	Monitored Lipid Classes	Number of detected Species
GC-MS	Total FA	28
LC-MS/MS (QTrap)(ESI-)	Eicosanoids, Docosanoids, free FA	45
LC-MS/MS (QToF)(ESI+)	PA, LPA, LPC, LPE, PG, PI, PS, SM, CE, DG, TG	353

Global lipid class composition

It was our aim to investigate the lipid content of the different *S. mansoni* life cycle stages, not restricting our investigation to phospholipids, as done previously [24, 32], but also to include neutral lipids such as sterols, sterol esters and TG. Typical lipidomic profiles (ESI+ mode) obtained for cercariae, worms and eggs are shown in Figure 1. As can be appreciated from Figure 1, PC and TG lipids are the predominantly detected lipid classes. Specifically, we found PC(34:1), PC(36:1), and PC(36:2) to be the major phospholipid species present in all life cycle stages.

The fractional composition shown in Figure 2 indicates that particularly worms and eggs present similar lipid compositions while cercariae have a somewhat different lipid composition. A more detailed depiction comparing the overlapping individual lipid species within different lipid

classes between the distinct life-cycle stages is shown in Figure 3. Interestingly, we could only detect DG lipids in cercariae, but not in the eggs or worms. The same holds true for the species of lysophospholipids (LPC and LPE), which were mainly seen in cercariae and eggs but hardly in worms. On the other hand, there were lower amounts of neutral lipids of the CE and TG type in cercariae. Besides several very common lipids containing oleic or palmitic acid we could also detect some uncommon lipids, such as very long chain LPCs or PCs (i.e. PC(50:6) or LPC(26:2)) (Figure S1). A list of all identified lipids as well as the relative abundance of each lipid species of the total lipid pool from each life cycle stages can be found in supplementary Table S2.

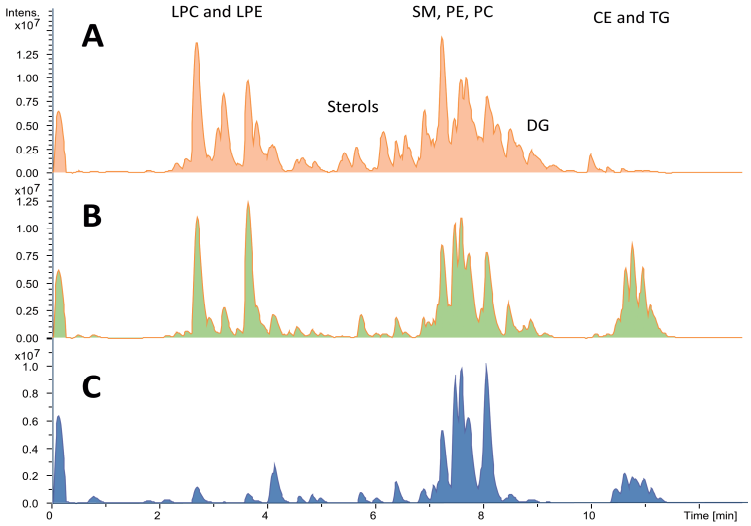

Figure 1. Lipidomic profiles of solid samples (base peak intensity chromatogram)
(A) Cercariae, (B) worms, (C) eggs. LPC (Lyso-Phosphatidylcholine); LPE (Lyso-Phosphatidylethanolamine); SM (Sphingomyelins); PE (Phosphatidylethanolamine); PC (Phosphatidylcholine), CE (Cholesteryl Ester); TG (Triacylglycerol).

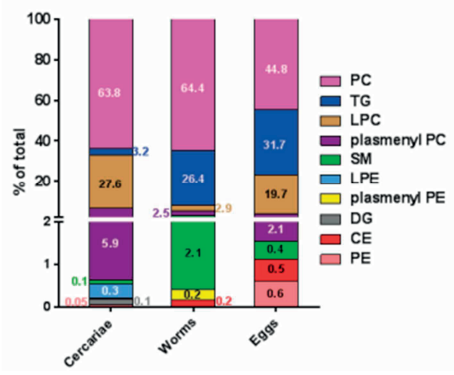

Figure 2. Fractional composition of *S. mansoni* life cycle stages
The percentage (%) fraction of each lipid class is given per life stage. PC (Phosphatidylcholine); TG (Triacylglycerol); LPC (Lyso-Phosphatidylcholine); SM (Sphingomyelins); LPE (Lyso-Phosphatidylethanolamine); DG (Diacylglycerol); CE (Cholesteryl Ester); PE (Phosphatidylethanolamine).

Total fatty acid composition

Next we investigated the total FA composition of the different *S. mansoni* life cycle stages. As can be seen from Table 3 particularly worms contained significant amounts of FA. As expected from the generally low solubility of FA in aqueous media, much lower amounts of FA per µg protein were obtained from AWA and WES.

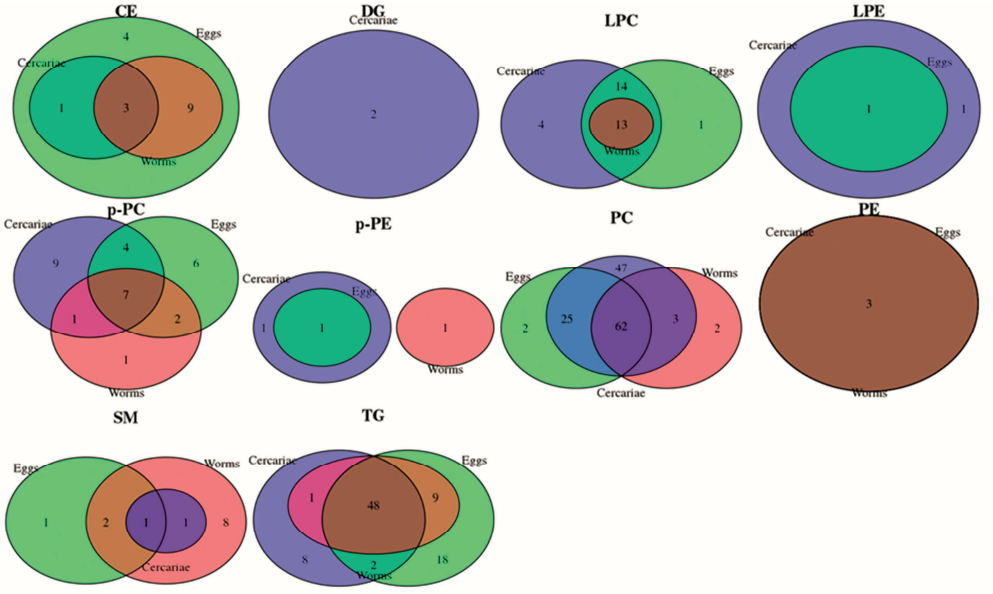

Figure 3. Overlapping lipid species detected in different *S. mansoni* life cycle-stages

CE (Cholesteryl Ester); DG (Diacylglycerol); LPC (Lyso-Phosphatidylcholine); LPE (Lyso-Phosphatidylethanolamine); p-PC (plasmenyl PC); p-PE (plasmenyl-PE); PC (Phosphatidylcholine), PE (Phosphatidylethanolamine), SM (Sphingomyelins), TG (Triacylglycerol).

A

Substance	RRT Standard	RRT Sample
RvE2	0.873	0.870
PDX	0.985	0.984
PD1	0.997	1.000

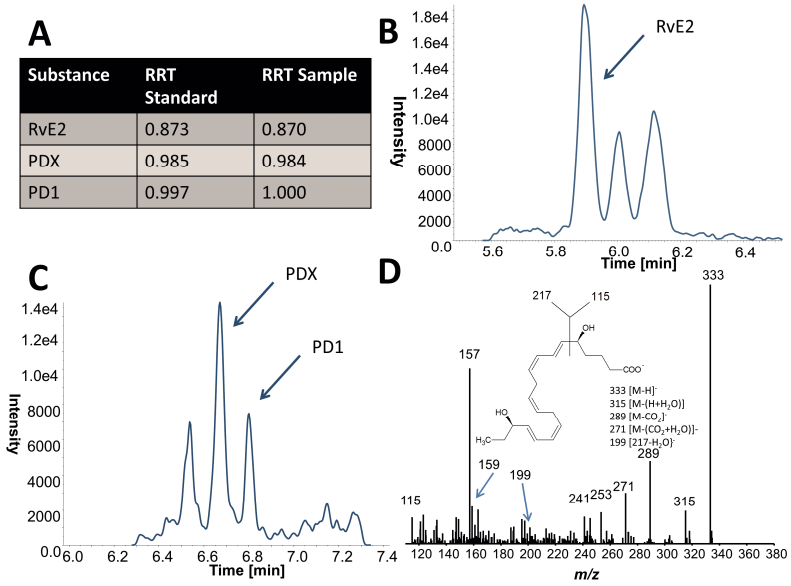

Figure 4. Identification of pro-resolving mediators in cercariae samples

Panel (A) comparison of relative retention times (RRT) between authentic standard material and signals observed in cercariae samples. (B) characteristic extracted ion chromatogram for RvE2 (Resolvin E2). (C) characteristic extracted ion chromatogram for PDX (Protectin DX) and PD1 (Protectin D1). (D) MS/MS spectrum used for the identification of RvE2. The obtained area ratios for PD1 and RvE2 can be found in the supplementary material.

Table 3. A heat-map of total fatty acids composition in ng per µg of protein

Sample type / Analyte	Cercaria	CA	CES	Worms	AWA	WES	Eggs	SEA	EES
FA 10:0	0.0	0.0	0.2	0.2	0.0	0.7	0.0	0.0	0.1
FA 11:0	0.0	0.2	0.8	0.4	0.0	1.9	0.0	0.0	0.5
FA 12:0	0.0	0.2	0.8	0.4	0.0	2.0	0.1	0.0	0.5
FA 13:0	0.0	0.2	0.8	0.4	0.0	1.9	0.0	0.0	0.5
FA 14:0	0.1	0.2	0.9	1.3	0.0	1.9	0.4	0.0	0.5
FA 14:1	0.0	0.2	0.8	0.3	0.0	1.7	0.0	0.0	0.5
FA 15:0	0.1	0.2	0.6	1.6	0.0	1.3	0.7	0.0	0.3
FA 15:1	0.0	0.2	0.6	0.2	0.0	1.3	0.0	0.0	0.3
FA 16:0	2.0	0.3	1.9	80.8	0.1	10.3	38.5	0.2	0.4
FA 16:1	0.1	0.1	0.5	5.0	0.0	0.9	1.4	0.0	0.2
FA 17:0	0.1	0.0	0.0	1.7	0.0	0.1	1.0	0.0	0.0
FA 17:1	0.0	0.0	0.0	0.6	0.0	0.1	0.0	0.0	0.0
FA 18:0	1.8	0.4	3.5	56.7	0.1	14.4	43.5	0.3	0.3
FA 18:1z	2.2	0.1	3.3	141.3	0.2	9.4	39.2	0.2	0.0
FA 18:1e	0.7	0.0	0.3	24.6	0.0	0.9	10.1	0.0	0.0
FA 18:2	3.3	0.1	0.3	100.9	0.1	4.2	70.5	0.3	0.0
FA 18:3 (GLA)	0.0	0.0	0.0	0.3	0.0	0.1	0.4	0.0	0.0
FA 18:3α (ALA)	0.2	0.0	0.1	4.0	0.0	0.2	2.5	0.0	0.0
FA 20:0	0.2	0.0	0.0	2.4	0.0	0.0	1.4	0.0	0.0
FA 20:1	2.0	0.0	0.1	54.1	0.1	6.8	5.0	0.1	0.0
FA 20:2	3.7	0.1	0.1	37.4	0.1	2.1	10.6	0.1	0.0
FA 20:3	0.0	0.0	0.1	6.3	0.0	0.2	1.9	0.0	0.0
FA 20:3α	0.4	0.0	0.3	0.8	0.0	3.1	0.5	0.0	0.1
FA 20:4 (AA)	1.0	0.1	0.6	79.3	0.1	3.7	17.4	0.1	0.2
FA 20:5 (EPA)	1.1	0.1	0.3	0.4	0.0	0.5	0.2	0.0	0.1
FA 22:0	0.1	0.0	0.0	0.5	0.0	0.0	0.2	0.0	0.0
FA 22:1	0.4	0.0	0.2	2.9	0.0	0.3	0.4	0.0	0.1
FA 22:2	0.8	0.0	0.0	2.6	0.0	0.1	0.9	0.0	0.0
FA 22:4 (AdA)	0.3	0.0	0.1	28.3	0.1	2.6	8.5	0.0	0.0
FA 22:5 (DPA)	1.1	0.1	0.4	5.5	0.0	0.8	2.1	0.0	0.1
FA 22:6 (DHA)	0.9	0.1	0.6	8.0	0.0	1.3	5.2	0.0	0.2
FA 24:1	0.1	0.0	0.0	3.2	0.0	0.2	0.3	0.0	0.0

Colour coding based on each parasite material
CA= Cercarial Antigen; CES= Cercarial ES; AWA= Adult Worms Antigen; WES= Worms ES; SEA= Soluble Eggs Antigen; EES= Egg ES

Oxylipid composition

Finally we analyzed the composition of oxylipids of the different life cycle stages and parasite extracts. Table 4 shows that large amounts of Polyunsaturated Fatty Acids (PUFAs) as well as downstream Cyclo-oxygenase (COX) and Lipoxygenase (LOX) derivatives could be detected in several parasite-derived material. Particularly, high levels of PUFA precursors such as Arachidonic Acids (AA), Linoleic Acids (LA) and Docosahexaenoic Acid (DHA) were found in all preparations, relative to their derivatives. Furthermore, the overall composition of COX and LOX derivatives of cercariae and eggs was largely similar but distinct to that of worms. However, an interesting difference between cercariae and eggs was the fact that we could detect several proresolvin lipids, including Protectin D1 (PD1) and (Resolvin E2) RvE2, as LOX derivatives specifically in cercariae, but not in eggs. Figure 4 illustrates the identification of these substances in the investigated samples and demonstrates that our structural assignments were based on several layers of analytical

characteristics. Firstly, we monitored characteristic tandem mass spectrometric transitions (MRM), secondly we compared relative retention times (RRT) with synthetic standard material and lastly we investigated the observed tandem mass spectra for the presence of several substance specific fragment ions.

Table 4. A heat-map of quantified oxylipids in *S. mansoni* preparations in ng per sample

	Sample type / Analyte	Cercaria	CA	CES	Worms	AWA	WES	Eggs	SEA	EES
Tri-hydroxy	LXA_4	0.002	0.000	0.000	0.000	0.000	0.010	0.002	0.030	0.043
	TxB_2	0.000	0.000	0.000	0.000	0.000	0.016	0.000	0.000	0.002
	PGD_2	0.004	0.000	0.000	0.001	0.000	0.012	0.006	0.018	0.029
	PGE_2 (and isomers)	0.018	0.001	0.001	0.012	0.001	0.087	0.019	0.172	0.359
	15-Keto-PGE_2	0.000	0.000	0.000	0.014	0.000	0.007	0.000	0.007	0.019
	8-iso-$PGF_{2\alpha}$	0.002	0.000	0.000	0.000	0.000	0.003	0.003	0.017	0.035
Di-hydroxy	14.15-diHETE	0.037	0.000	0.000	0.000	0.000	0.000	0.060	0.000	0.000
	19.20-DiHDPA	0.009	0.000	0.000	0.001	0.000	0.005	0.013	0.000	0.007
	Leukotriene B_4/5S.12S-diHETE	0.011	0.000	0.000	0.000	0.000	0.000	0.013	0.011	0.000
	6-trans-LTB_4	0.002	0.000	0.000	0.001	0.000	0.001	0.003	0.008	0.000
	PDX	0.019	0.000	0.000	0.000	0.000	0.000	0.025	0.003	0.000
	8S.15S-diHETE	0.017	0.000	0.000	0.000	0.000	0.000	0.021	0.018	0.001
	6t.12epi-LTB_4	0.002	0.000	0.000	0.002	0.000	0.003	0.004	0.012	0.002
	5.15-diHETE	0.040	0.000	0.000	0.000	0.000	0.000	0.051	0.061	0.003
Mono-hydroxy	5-HETE	0.23	0.00	0.01	0.20	0.01	0.05	0.31	0.37	0.01
	8-HETE	0.08	0.00	0.00	0.07	0.00	0.02	0.11	0.30	0.07
	11-HETE	0.13	0.00	0.00	0.05	0.00	0.02	0.16	0.19	0.00
	12-HETE	0.40	0.00	0.00	0.36	0.01	0.10	0.54	0.32	0.01
	15-HETE	0.68	0.00	0.00	0.14	0.01	0.09	0.92	0.54	0.02
	15-HEPE	0.86	0.00	0.00	0.00	0.00	0.00	1.35	0.00	0.00
	18-HEPE	0.80	0.00	0.00	0.00	0.00	0.00	1.09	0.01	0.00
	10-HDHA	0.11	0.00	0.00	0.01	0.00	0.00	0.17	0.07	0.01
	7-HDHA	0.04	0.00	0.00	0.01	0.00	0.01	0.06	0.04	0.00
	17-HDHA	1.18	0.00	0.00	0.03	0.00	0.02	1.89	0.18	0.00
PUFA	AA	638	3.00	8.00	445	15.0	29.0	931	13.0	5.00
	DHA	1586	3.00	7.00	9.03	9.00	8.00	2917	6.00	5.00
	EPA	733	1.00	1.00	5.00	1.00	0.00	1325	1.00	1.00
	AdA	299	1.00	0.00	100	1.00	5.00	499	1.00	0.00
	DPAn-3	573	0.00	0.00	23.0	0.00	2.00	1106	0.00	1.00
	LA	1328	15.0	30.0	357	34.0	53.0	2201	50.0	20.0
	ALA/GLA	128	1.00	1.00	52.0	0.00	3.00	211	2.00	2.00

Colour coding refers to each lipid subclass (mono-, di-, tri-hydroxy, PUFA) per worm preparation/life-stage
CA= Cercarial Antigen; CES= Cercarial ES; AWA= Adult Worms Antigen; WES= Worms ES; SEA= Soluble Eggs Antigen; EES= Egg ES

Conversely, we detected relatively high concentrations of COX products, including prostaglandin D2 (PGD_2) and PGE_2, in eggs and egg-derived antigen preparations. Moreover, apart from PGE_2 itself, several isomers were detected in high amounts in all egg-derived materials. The presence of geometric isomers can hamper substance identification, which is illustrated in Figure 5. When monitoring the PGE_2 characteristic MRM transition *m/z* 351->271 several closely eluting peaks were obtained. Due to the fact that geometric isomers such as the D- and E-series prostaglandins listed in Figure 5 give rise to almost identical tandem mass spectra we had to rely

on RRTs for substance identification. We compared the RRTs with the ones obtained for synthetic standard material as listed in Figure 5, showing the presence of several isomeric prostaglandins particularly present in eggs and egg-derived materials (SEA and EES).

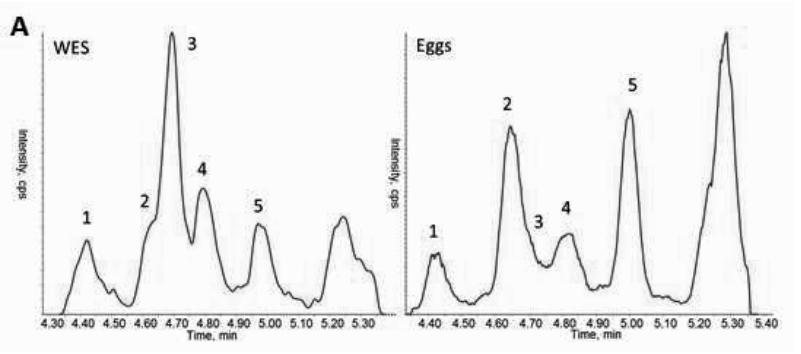

B

Standard	RRT	Compound	RRT	Detected
Δ^{12}-PGD_2	0.943	1	0.944	WES, Eggs
15R-PGE_2	0.947			
8-iso PGE_2	0.957			
15R-PGD_2	0.987	2	0.991	WES, Eggs
PGE_2	1.004	3	1.003	WES, Eggs
15-trans-PGD_2	1.011			
PGD_2	1.023			
11β-PGE_2	1.025	4	1.029	WES, Eggs
15-trans-PGE_2	1.057	5	1.067	WES, Eggs

Figure 5. PGE_2 and Isomer identification with MS/MS trace *m/z* 351 -> 271.

Finally, worms and AWA were found to have a particular enrichment for LTB_4. Although this was also detected in eggs, the signal found in SEA and cercariae could be attributed to isomeric 5S,12S-diHETE, which was revealed by small relative retention time (RRT) differences between the two components, as described by us previously [29, 33]. Concentrations and area ratios of all detected oxylipids can be found in Table 4 and supplementary data (Table S2).

DISCUSSION

In the current study we performed an in-depth lipidomic analysis of the different life cycle stages of *S. mansoni* using three complementary MS-based platforms. In addition, we defined the lipid profile of aqueous extracts from different life stages of *S. mansoni*, which are CA, AWA and SEA, as well as their excretory and secretory products (ES), which are all commonly used antigen preparations in immunoparasitological studies. In total we identified more than 400 lipid species including several bioactive molecules, which we organized in a *S. mansoni* lipid database (supplementary Table S2). For FA, eicosanoids and docosanoids we have generated quantitative data, while a compositional analysis with relative abundances was carried out for higher order lipids. Our data reveal that there are life-stage specific lipid signatures not only for structural lipids but also for bioactive lipid mediators that may be important in host-pathogen interactions.

Global lipid class composition analysis revealed that PC (34:1), PC (36:1), and PC (36:2) are the predominant phospholipid species present in all life cycle stages. In line with this work, Schariter *et al* have described the presence of PC in cercariae [34]. Moreover, our work is also consistent with

earlier work on adult worms by Retra *et al* [23] which also covered phosphoinositol (PI) and phosphatidylserine (PS) lipids and, as such, our work can be seen as complementary to theirs. Earlier work has found that a *S. mansoni*-specific PS fraction conditioned DCs to induce both Th2 and IL-10 producing T cells via TLR2 activation [19]. However, we were unable to detect significant amounts of PS in any of our preparations, this is likely due to the fact that our analytical approach focused on the ESI+ mode to detect PS while Retra *et al.* use the ESI- mode in their study. Furthermore, we observed that global composition of the major lipid classes present in worms and eggs were similar, while cercariae were found to have a distinct profile, with less neutral lipids such as CE and TG. This specific difference is likely to be a direct result of the fact that because *S. mansoni* is unable to synthesize fatty acids and sterols *de novo* [35], it relies on scavenging of lipid precursors from its host to generate complex lipids such as phospholipids and TG [36], a process that free swimming cercariae cannot resort to. In addition our observation that cercariae contain much lower amounts of a large range of free FA we quantified, would support the idea that cercariae, compared to worms and eggs that reside in the host, have limited lipid accessibility.

Oxylipids such as docosanoids and eicosanoids have pleiotropic functions that include shaping the function of immune cells [37]. Hence, mapping and analysis of these known immunomodulatory lipid classes including their precursors was an important part of the present study. We found that cercariae as well as eggs and the antigen preparation derived from these life cycle stages, but less so adult worms, contain significant amounts of PUFAs, such as n3-PUFA (DHA), Eicosapentaenoic Acid (EPA), Docosapentaenoic Acid (DPA) and n6-PUFA (AA), as well as many of their bioactive derivatives that are known to be generated through COX and LOX activity. While cercariae have been shown before to produce various eicosanoids [38], this has not been described for the egg stage. An interesting observation is that despite the absence of COX enzymes in the *S. mansoni* genome [20, 39], we detected various prostaglandins in both cercariae and eggs. This apparent discrepancy has been reported by others as well [40], and it has been postulated that this could be explained by an alternative mechanism for the generation of prostaglandin-like compounds, involving the non-enzymatic generation of molecules called isoprostanes, by auto-oxidation of AA by free-radicals. Indeed, we found evidence for production of isoprostanes in these parasites, which would allow for prostaglandin synthesis in the absence of COX activity. Of the prostaglandins we found PGD_2 and PGE_2 to be the most highly abundant species present in cercariae and eggs. Although PGD_2 may exert pro-inflammatory or anti-inflammatory effects in different biologic systems, in the context of *S. mansoni* it has primarily been linked to limiting the ability of the host to mount a protective immune response against cercariae [41], through its ability to suppress migration of langerhans cells in the skin [18]. Whether PGD_2 produced by eggs has similar immunomodulatory effects remains to be determined. PGE_2, like PGD_2, can have proinflammatory or anti-inflammatory effects depending on the context [42]. One particularly interesting property of PGE_2 is that is has been shown to condition DCs to prime Th2 responses [43]. This property, together with our observation that specifically eggs and SEA, which are well-known for their Th2 polarizing potential, contain high levels of PGE_2, would make it conceivable that PGE_2 contributes to Th2 induction by *S. mansoni* eggs. Further studies would be needed to test this hypothesis.

In addition, we found various potentially immunomodulatory LOX derived products to be present in the different life cycle stages. For instance, in line with other studies [20], the AA-derived LOX product 15-HETE was detected. 15-HETE is known to be a ligand for peroxisome proliferator-activated receptors [44], which when activated in immune cells generally leads to suppression of pro-inflammatory effector responses by these cells. As such, one could speculate that release of

15-HETE by the parasite may locally contribute to suppression of immune responses. Finally, our analyses for the first time reveal that cercariae contain several n3-PUFA derived LOX products including resolvin E2 (RvE2) protectin DX (PDX) and protectin D1 (PD1). These docosanoids are *specialized pro-resolving mediators* that can suppress inflammatory immune responses and are important for promoting resolution of inflammation [45]. Once cercariae have penetrated the skin, they stay in the skin for 3 to 4 days before they enter the circulation. We hypothesize that production of these pro-resolving mediators during this period increases their chances of survival as these factors can suppress recruitment of immune cells and anti-cercariael immune responses. More in depth studies are warranted to further explore the role of resolvin production by *S. mansoni* life cycle stages in host-pathogen interactions and subversion of host immunity.

In conclusion, we have generated a comprehensive dataset defining the lipidome of different life cycle stages of *S. mansoni* in unprecedented detail. Our analysis has revealed several important differences between the lipid composition of the different life cycle stages of *S. mansoni*, that provide new insights into the biology of the parasite itself as well as into how the various life cycle stages interact with and may modulate the host immune system. Moreover, an important observation was that lipid composition of parasite life cycle stages and the corresponding extracts were highly similar, which validates the use of those widely used parasite preparations as models to study host-parasite interactions in immunological studies. Altogether, we believe this work will be a highly useful resource to many researchers in the field of parasitology and immunoparasitology and may serve as a starting point for the identification of immunomodulatory lipids that could be used or targeted, to shape anti-parasite immune responses with regards to vaccination or to develop lipid-based therapeutics to treat inflammatory disorders.

ACKNOWLEDGEMENTS

The authors would like to thank Angela van Diepen, Janneke Kos-van Oosterhoud, Michelle Yang and Marije Kuipers for help with antigens preparations. This work was supported by The Indonesian Directorate General of Higher Education (DGHE/DIKTI)-Leiden University, the company of biologist-Diseases Model and Mechanisms (DMM)-travelling fellowship given to Maria M. M. Kaisar and LUMC fellowship to Bart Everts.

REFERENCES

1. Tomcik, K., et al., *Isotopomer enrichment assay for very short chain fatty acids and its metabolic applications.* Analytical Biochemistry, 2011. **410**(1): p. 110-117.
2. Pearce, E.J. and A.S. MacDonald, *The immunobiology of schistosomiasis.* Nat Rev Immunol, 2002. **2**(7): p. 499-511.
3. Pacifico, L.G., et al., *Schistosoma mansoni antigens modulate experimental allergic asthma in a murine model: a major role for CD4+ CD25+ Foxp3+ T cells independent of interleukin-10.* Infect Immun, 2009. **77**(1): p. 98-107.
4. van der Vlugt, L.E., et al., *Schistosomes induce regulatory features in human and mouse CD1d(hi) B cells: inhibition of allergic inflammation by IL-10 and regulatory T cells.* PLoS One, 2012. **7**(2): p. e30883.
5. Campolina, S.S., et al., *Effective anthelmintic therapy of residents living in endemic area of high prevalence for Hookworm and Schistosoma mansoni infections enhances the levels of allergy risk factor anti-Der p1 IgE.* Results Immunol, 2015. **5**: p. 6-12.
6. Mpairwe, H., et al., *Anthelminthic treatment during pregnancy is associated with increased risk of infantile eczema: randomised-controlled trial results.* Pediatr Allergy Immunol, 2011. **22**(3): p. 305-12.
7. Cardoso, L.S., S.C. Oliveira, and M.I. Araujo, *Schistosoma mansoni antigens as modulators of the allergic inflammatory response in asthma.* Endocr Metab Immune Disord Drug Targets, 2012. **12**(1): p. 24-32.
8. Smits, H.H., et al., *Protective effect of Schistosoma mansoni infection on allergic airway inflammation depends on the intensity and chronicity of infection.* J Allergy Clin Immunol, 2007. **120**(4): p. 932-40.

9. Hasby, E.A., et al., *FoxP3+ T regulatory cells and immunomodulation after Schistosoma mansoni egg antigen immunization in experimental model of inflammatory bowel disease.* Cell Immunol, 2015. **295**(1): p. 67-76.
10. Hussaarts, L., et al., *Chronic helminth infection and helminth-derived egg antigens promote adipose tissue M2 macrophages and improve insulin sensitivity in obese mice.* FASEB J, 2015. **29**(7): p. 3027-39.
11. Neves, L.X., et al., *What's in SWAP? Abundance of the principal constituents in a soluble extract of Schistosoma mansoni revealed by shotgun proteomics.* Parasit Vectors, 2015. **8**: p. 337.
12. Wilson, R.A., *Proteomics at the schistosome-mammalian host interface: any prospects for diagnostics or vaccines?* Parasitology, 2012. **139**(9): p. 1178-94.
13. Jang-Lee, J., et al., *Glycomics analysis of Schistosoma mansoni egg and cercarial secretions.* Mol Cell Proteomics, 2007. **6**(9): p. 1485-99.
14. Smit, C.H., et al., *Glycomic Analysis of Life Stages of the Human Parasite Schistosoma mansoni Reveals Developmental Expression Profiles of Functional and Antigenic Glycan Motifs.* Mol Cell Proteomics, 2015. **14**(7): p. 1750-69.
15. Smith, T.M. and T.J. Brooks, Jr., *Lipid fractions in adult Schistosoma mansoni.* Parasitology, 1969. **59**(2): p. 293-8.
16. Payares, G., et al., *Changes in the surface antigen profile of Schistosoma mansoni during maturation from cercaria to adult worm.* Parasitology, 1985. **91 (Pt 1)**: p. 83-99.
17. Parra, J.F., et al., *Schistosoma mansoni: phospholipid methylation and the escape of schistosomula from in vitro cytotoxic reaction.* Mol Biochem Parasitol, 1986. **21**(2): p. 151-9.
18. Angeli, V., et al., *Role of the parasite-derived prostaglandin D2 in the inhibition of epidermal Langerhans cell migration during schistosomiasis infection.* J Exp Med, 2001. **193**(10): p. 1135-47.
19. van der Kleij, D., et al., *A novel host-parasite lipid cross-talk. Schistosomal lyso-phosphatidylserine activates toll-like receptor 2 and affects immune polarization.* J Biol Chem, 2002. **277**(50): p. 48122-9.
20. Abdel Baset, H., G.P. O'Neill, and A.W. Ford-Hutchinson, *Characterization of arachidonic-acid-metabolizing enzymes in adult Schistisoma mansoni.* Mol Biochem Parasitol, 1995. **73**(1-2): p. 31-41.
21. Furlong, S.T. and J.P. Caulfield, *Schistosoma mansoni: Sterol and phospholipid composition of cercariae, schistosomula, and adults.* Experimental Parasitology, 1988. **65**(2): p. 222-231.
22. Ferreira, M.S., et al., *Screening the life cycle of Schistosoma mansoni using high-resolution mass spectrometry.* Analytica Chimica Acta, 2014. **845**: p. 62-69.
23. Retra, K., et al., *A simple and universal method for the separation and identification of phospholipid molecular species.* Rapid Communications in Mass Spectrometry, 2008. **22**(12): p. 1853-1862.
24. Retra, K., et al., *The tegumental surface membranes of Schistosoma mansoni are enriched in parasite-specific phospholipid species.* Int J Parasitol, 2015. **45**(9-10): p. 629-36.
25. Fahy, E., et al., *Update of the LIPID MAPS comprehensive classification system for lipids.* Journal of Lipid Research, 2009. **50**(Supplement): p. S9-S14.
26. Quehenberger, O., A.M. Armando, and E.A. Dennis, *High sensitivity quantitative lipidomics analysis of fatty acids in biological samples by gas chromatography–mass spectrometry.* Biochimica et Biophysica Acta (BBA) - Molecular and Cell Biology of Lipids, 2011. **1811**(11): p. 648-656.
27. Heemskerk, M.M., et al., *Prolonged niacin treatment leads to increased adipose tissue poly-unsaturated fatty acid synthesis and an anti-inflammatory lipid and oxylipin plasma profile.* Journal of Lipid Research, 2014.
28. Jónasdóttir, H.S., et al., *An Advanced LC–MS/MS Platform for the Analysis of Specialized Pro-Resolving Lipid Mediators.* Chromatographia, 2014. **78**(5-6): p. 391-401.
29. Giera, M., et al., *Lipid and lipid mediator profiling of human synovial fluid in rheumatoid arthritis patients by means of LC–MS/MS.* Biochimica et Biophysica Acta (BBA) - Molecular and Cell Biology of Lipids, 2012. **1821**(11): p. 1415-1424.
30. Jónasdóttir, H.S., et al., *Detection and Structural Elucidation of Esterified Oxylipids in Human Synovial Fluid by Electrospray Ionization-Fourier Transform Ion-Cyclotron Mass Spectrometry and Liquid Chromatography-Ion Trap-MS3: Detection of Esterified Hydroxylated Docosapentaenoic Acid Containing Phospholipids.* Analytical Chemistry, 2013. **85**(12): p. 6003-6010.
31. Kind, T., et al., *LipidBlast in silico tandem mass spectrometry database for lipid identification.* Nat Meth, 2013. **10**(8): p. 755-758.
32. Retra, K., et al., *A simple and universal method for the separation and identification of phospholipid molecular species.* Rapid Commun Mass Spectrom, 2008. **22**(12): p. 1853-62.
33. Jónasdóttir, H.S., et al., *Differential Mobility Separation of Leukotrienes and Protectins.* Analytical Chemistry, 2015. **87**(10): p. 5036-5040.
34. Schariter, J.A., et al., *Determination of neutral lipids and phospholipids in the cercariae of schistosoma mansoni by high performance thin layer chromatography.* J Liq Chrom & Rel Technol, 2002. **25**: p. 1615-22.
35. Meyer, F., H. Meyer, and E. Bueding, *Lipid metabolism in the parasitic and free-living flatworms, Schistosoma mansoni and Dugesia dorotocephala.* Biochim Biophys Acta, 1970. **210**(2): p. 257-66.

36. Brouwers, J.F., et al., *The incorporation, modification and turnover of fatty acids in adult Schistosoma mansoni.* Mol Biochem Parasitol, 1997. **88**(1-2): p. 175-85.
37. Dennis, E.A. and P.C. Norris, *Eicosanoid storm in infection and inflammation.* Nat Rev Immunol, 2015. **15**(8): p. 511-523.
38. Fusco, A.C., B. Salafsky, and M.B. Kevin, *Schistosoma mansoni: eicosanoid production by cercariae.* Exp Parasitol, 1985. **59**(1): p. 44-50.
39. Berriman, M., et al., *The genome of the blood fluke Schistosoma mansoni.* Nature, 2009. **460**(7253): p. 352-8.
40. Noverr, M.C., J.R. Erb-Downward, and G.B. Huffnagle, *Production of eicosanoids and other oxylipins by pathogenic eukaryotic microbes.* Clin Microbiol Rev, 2003. **16**(3): p. 517-33.
41. Abdel-Ghany, R., et al., *Blockade of Pge2, Pgd2 Receptors Confers Protection against Prepatent Schistosomiasis Mansoni in Mice.* J Egypt Soc Parasitol, 2015. **45**(3): p. 511-20.
42. Kalinski, P., *Regulation of immune responses by prostaglandin E2.* J Immunol, 2012. **188**(1): p. 21-8.
43. de Jong, E.C., et al., *Microbial compounds selectively induce Th1 cell-promoting or Th2 cell-promoting dendritic cells in vitro with diverse th cell-polarizing signals.* J Immunol, 2002. **168**(4): p. 1704-9.
44. Naruhn, S., et al., *15-hydroxyeicosatetraenoic acid is a preferential peroxisome proliferator-activated receptor beta/delta agonist.* Mol Pharmacol, 2010. **77**(2): p. 171-84.
45. Serhan, C.N. and N.A. Petasis, *Resolvins and Protectins in Inflammation Resolution.* Chemical Reviews, 2011. **111**(10): p. 5922-5943.

SUPPLEMENTARY DATA

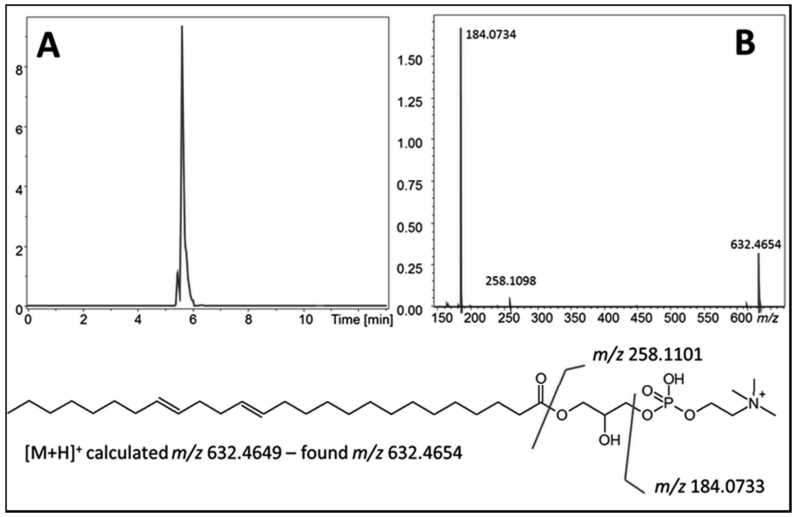

Figure S1. (A) Extracted ionchromatogram of *m/z* 632.465 and (B) Tandem mass spectrum of the very long chain LPC(26:2).

Table S1. A list of monitored oxylipids, corresponding lipidmaps IDs and calibration ranges

Lipid maps ID	Analyte	Calibration line range [ng/mL]
LMFA04000027	10-HDHA	0.025 – 10
LMFA03060085	11-HETE	0.025 – 10
LMFA03060088	12-HETE	0.025 – 10
LMFA02000228	13-HODE	N/A
LMFA02000051	13-HOTrE	N/A
LMFA03060077	14,15-diHETE	0.01 – 2
LMFA03070032	15-HEPE	0.025 – 10
LMFA03060087	15-HETE	0.025 – 10
LMFA04000032	17-HDHA	0.025 – 10
	17-HDoTE	N/A
LMFA03070033	18-HEPE	0.025 – 10
LMFA04000043	19,20-diHDPA	0.01 – 2
LMFA03020018	20-OH-LTB_4	0.01 – 2
LMFA03060084	5-HETE	0.025 – 10
LMFA03020014	6-trans-12-epi-LTB4	0.01 – 2
LMFA03020013	6-trans-LTB_4	0.01 – 2
LMFA04000025	7-HDHA	0.025 – 10
	7S,17S-diHDPA	0.025 – 2
LMFA03060086	8-HETE	0.025 – 10
LMFA03110003	8-iso-PGE_2	0.01 – 2
LMFA03110001	8-iso-$PGF_{2\alpha}$	0.01 – 2
LMFA02000151	9-HODE	N/A
LMFA02000024	9-HOTrE	N/A
LMFA01030001	AA	5 – 500
LMFA01030178	AdA	1 – 200
LMFA01030152	ALA/GLA	N/A
LMFA01030185	DHA	5 – 500
LMFA04000044	DPA_{n-3}	5 – 500
LMFA01030759	EPA	1 – 200
LMFA01030120	LA	5 – 500

Lipid maps ID	Analyte	Calibration line range [ng/mL]
LMFA03020001	LTB_4	0.01 – 2
LMFA03020006	LTD_4	0.01 – 2
LMFA03020002	LTE_4	0.01 – 2
LMFA03010004	PGD_2	0.01 – 2
LMFA03010003	PGE_2	0.01 – 2
LMFA03010002	$PGF_{2\alpha}$	0.025 – 2
LMFA03030002	TXB_2	0.01 – 2
LMFA04000047	10S,17S-diHDHA	0.01 – 2
LMFA03080004	11(12)EET	N/A
LMFA03010031	13,14-dihydro-15-keto-PGE_2	N/A
LMFA03010027	13,14-dihydro-15-keto-$PGF_{2\alpha}$	N/A
LMFA03080005	14(15)EET	N/A
LMFA03010021	15-deoxy-PGJ_2	N/A
LMFA03040010	15-epi-LXA_4	0.01 – 2
LMFA03010030	15-keto-PGE_2	0.01 – 2
LMFA04000074	17-epi-RvD1	N/A
LMFA03070049	18R-RvE3	N/A
LMFA03070048	18S-RvE3	N/A
LMFA03060010	5S,15S-diHETE	N/A
	7-epi-MaR1	N/A
LMFA03080003	8(9) EET	N/A
LMFA03060050	8S,15S-diHETE	0.01 – 2
LMFA03040001	LXA_4	0.01 – 2
LMFA03040002	LXB_4	0.01 – 2
LMFA04000048	MaR1	N/A
LMFA03010019	PGJ_2	N/A
LMFA04000006	RvD1	N/A
LMFA04000007	RvD2	N/A
LMFA03070019	RvE1	N/A
LMFA03070020	RvE2	N/A

Table S2. The relative abundance (%) of each lipid species of the total lipid pool from each life cycle stages of *S. mansoni* and parasites materials derived from *S. mansoni*

Lipid species	Cercariae	CA	CES	Worms	AWA	WES	Eggs	SEA	EES
CE.16.0.				0,01			0,02		
CE.18.0.				0,00			0,05		
CE.18.1.				1,95			0,99		
CE.18.2.	15,27			12,79			6,75	69,20	
CE.18.3.				3,21			2,15		
CE.20.0.							0,00		
CE.20.1.				2,27			3,05		
CE.20.2.				9,77			17,66		
CE.20.3.				3,09			3,44		
CE.20.4.	12,02			17,34			15,21	30,80	
CE.20.5.	19,06						0,65		
CE.22.1.				0,11			0,39		
CE.22.2.							3,16		
CE.22.4.				22,27			16,62		
CE.22.5.	21,41			9,33			7,47		
CE.22.6.	32,24			17,73			22,26		
CE.24.1.				0,12			0,11		
DG.42.3	42,90								
DG.42.4	44,49								
DG.44.3	12,61								
lysoPC.15.0	0,48						0,20		
lysoPC.15.1	0,10								
lysoPC.16.0	21,26		34,66	46,45		36,13	28,79	46,33	
lysoPC.16.1	0,13								
lysoPC.17.0	2,47			1,31			1,30		
lysoPC.17.1	0,15								
lysoPC.17.2	0,04						0,40		
lysoPC.18.0	0,22		49,65	26,18		48,53	0,54	53,67	
lysoPC.18.0.1	12,51						0,29		
lysoPC.18.0.2							32,86		
lysoPC.18.1	3,25		15,69	5,01			6,30		
lysoPC.18.2	1,34						1,67		
lysoPC.18.3	1,98								
lysoPC.20.0	2,08			1,68			2,92		
lysoPC.20.1	8,99			5,63		15,34	8,64		
lysoPC.20.2	11,35			3,25			7,06		
lysoPC.20.3	1,08						0,00		
lysoPC.20.4	0,23						0,77		
lysoPC.20.5	0,23						0,32		
lysoPC.21.0	0,95						0,13		
lysoPC.22.0	1,66			1,25			0,59		
lysoPC.22.1	2,86			0,98			1,08		
lysoPC.22.2	3,51			0,86			1,11		
lysoPC.22.4	0,13						0,45		
lysoPC.22.5	0,19						0,08		
lysoPC.22.6	0,22						0,36		
lysoPC.23.0	1,63			1,49			0,15		
lysoPC.24.0	3,73			3,31			0,80		
lysoPC.24.1	3,79			2,60			0,59		
lysoPC.24.4	0,04						0,13		
lysoPC.25.0	2,78						0,14		
lysoPC.26.0	2,12						0,62		
lysoPC.26.2	3,57						0,59		
lysoPC.O.16.0	4,87						1,12		
lysoPC.P.16.0	0,05								
lysoPE.20.1	33,01								
lysoPE.20.2	51,66								
lysoPE.22.2	15,33								
PC.28.0	0,15								
PC.29.0	0,33								

Lipid species	Cercariae	CA	CES	Worms	AWA	WES	Eggs	SEA	EES
PC.30.0	2,37			0,62			0,37		
PC.30.1	0,37								
PC.31.0	1,74			0,57		1,39	0,56		
PC.31.1	0,56			0,01			0,25		
PC.31.2	0,00			0,18			0,27		
PC.31.3	0,03								
PC.32.0	4,52		14,67	13,76	17,34	36,16	10,14	20,65	
PC.32.1	3,63			1,13			0,95		
PC.32.2	0,25						0,06		
PC.32.3	0,02			0,07					
PC.33.0	0,72			0,31			0,19		
PC.33.1	0,00			0,00			0,00		
PC.33.2	0,39			0,08			0,19		
PC.33.3	0,08			0,16			0,18		
PC.33.4	0,13								
PC.34.0	0,32			3,47	4,54	4,03	2,38		
PC.34.1	6,61		35,39	16,80	21,99	20,61	13,45	24,01	
PC.34.2	0,00			7,84	9,14	5,36	9,52	11,88	
PC.34.3	0,00			0,76			0,97		
PC.34.4	0,25			0,11			0,03		
PC.34.5	0,07								
PC.35.0	0,12			0,21			0,09		
PC.35.1	0,01			0,70			0,51		
PC.35.2	1,34			0,22			0,31		
PC.35.3	0,42						0,06		
PC.35.4	0,12			0,02			0,00		
PC.35.5	0,02			0,06			0,07		
PC.35.6	0,16			0,08			0,05		
PC.36.0	0,10			0,43			0,50		
PC.36.1	8,09		23,15	15,04	20,43	13,22	9,73	13,04	
PC.36.2	0,03		15,04	10,69	14,01	8,02	10,29	12,80	
PC.36.3	0,21			2,51			4,06	5,89	
PC.36.4	2,33			5,99	7,07	3,62	6,70	6,31	
PC.36.5	3,96			0,11			0,25		
PC.36.6	0,00								
PC.37.0	0,06			0,04					
PC.37.1	1,24			0,24			0,27		
PC.37.2	0,45			0,13			0,21		
PC.37.3	0,10			0,06			0,18		
PC.37.4	0,28			0,17			0,19		
PC.37.5	0,00			0,15					
PC.37.6	0,15						0,12		
PC.37.7	0,23								
PC.37.8	0,08								
PC.38.0	0,08			0,08			0,10		
PC.38.1	3,91			1,08		1,31	1,52		
PC.38.2	0,00			1,38		1,51	2,56		
PC.38.3	0,08			1,50			3,09		
PC.38.4	3,70		7,28	3,65	5,48	4,78	4,68	5,42	
PC.38.5	1,61			1,78			2,09		
PC.38.6	1,66			2,20			2,74		
PC.38.7	1,54			0,24			0,06		
PC.38.8	0,05								
PC.39.0	0,05			0,04					
PC.39.1	0,76			0,04			0,04		
PC.39.2	0,84						0,06		
PC.39.3	0,40								
PC.39.4	0,22			0,05			0,03		
PC.39.5	0,27			0,05			0,15		
PC.39.6	0,31			0,00			0,22		
PC.39.7	0,05						0,02		
PC.39.8							0,00		

Lipid species	Cercariae	CA	CES	Worms	AWA	WES	Eggs	SEA	EES
PC.40.0	0,09			0,08			0,07		
PC.40.1	1,82			0,18			0,23		
PC.40.10	0,06								
PC.40.2	3,00			0,19			0,46		
PC.40.3	4,51			0,24			0,82		
PC.40.4	3,58			1,31			0,47		
PC.40.5	1,37			1,07			1,62		
PC.40.6	0,88		4,47	0,51			1,11		
PC.40.7	2,84			0,08			0,32		
PC.40.8	1,52			0,10			0,56		
PC.40.9	0,24			0,04			0,07		
PC.41.0	0,05								
PC.41.1	0,44								
PC.41.2	0,50								
PC.41.3	0,28								
PC.41.4	0,17			0,04			0,05		
PC.41.5	0,12								
PC.41.6	0,18						0,05		
PC.41.7	0,11								
PC.41.8	0,07								
PC.42.0	0,06						0,04		
PC.42.1	0,59			0,06			0,13		
PC.42.10	0,13						0,13		
PC.42.11	0,17						0,00		
PC.42.2	1,72			0,10			0,16		
PC.42.3	2,44			0,08			0,17		
PC.42.4	1,60			0,15			0,32		
PC.42.5	0,79			0,30			0,47		
PC.42.6	1,02			0,30			0,53		
PC.42.7	0,72			0,12			0,07		
PC.42.8	1,70			0,15			0,46		
PC.42.9	0,45						0,09		
PC.43.0	0,02								
PC.43.1	0,20								
PC.43.2	0,28								
PC.43.3	0,19								
PC.43.4	0,06								
PC.43.5	0,06								
PC.43.6	0,08								
PC.44.0	0,02						0,02		
PC.44.1	0,24						0,06		
PC.44.10							0,03		
PC.44.11	0,06						0,01		
PC.44.12	0,05						0,02		
PC.44.2	0,77						0,07		
PC.44.3	1,21						0,07		
PC.44.4	0,39						0,02		
PC.44.5	0,23			0,06			0,14		
PC.44.6	0,60			0,04			0,18		
PC.44.7	0,32						0,03		
PC.44.8	0,26						0,04		
PC.44.9	0,06								
PC.45.1	0,08								
PC.45.2	0,11								
PC.45.3	0,10								
PC.45.4	0,08								
PC.45.5	0,11								
PC.45.6	0,04								
PC.46.1	0,09						0,02		
PC.46.2	0,30						0,04		
PC.46.3	0,44						0,03		
PC.46.4	0,41						0,03		

Lipid species	Cercariae	CA	CES	Worms	AWA	WES	Eggs	SEA	EES
PC.46.5	0,43						0,09		
PC.46.6	0,51						0,07		
PC.46.7	0,28								
PC.46.8	0,07								
PC.47.1	0,02								
PC.47.2	0,04								
PC.47.5	0,04								
PC.47.6	0,04								
PC.48.2	0,10						0,02		
PC.48.3	0,13						0,02		
PC.48.4	0,12						0,02		
PC.48.5	0,15						0,04		
PC.48.6	0,11						0,03		
PC.48.7	0,16								
PC.48.8	0,07								
PC.50.3	0,03								
PC.50.4	0,03								
PC.50.5	0,02						0,02		
PC.50.6	0,02								
PE.38.1							16,26		
PE.38.4							83,74		
PE.40.1	100,00								
plasmenyl.PC.26.0	33,01						12,03		
plasmenyl.PC.27.0	1,33						0,49		
plasmenyl.PC.28.0	5,28						7,25		
plasmenyl.PC.30.0	1,50						2,63		
plasmenyl.PC.30.1							4,41		
plasmenyl.PC.31.0	1,03								
plasmenyl.PC.32.0	3,01			5,47		23,16			
plasmenyl.PC.32.1	0,26								
plasmenyl.PC.33.0	2,52								
plasmenyl.PC.33.1	0,66						0,83		
plasmenyl.PC.33.2				2,59					
plasmenyl.PC.34.0	30,23			44,42		76,84	28,18		
plasmenyl.PC.34.1	0,00			11,30			11,93		
plasmenyl.PC.34.2	1,82			1,05					
plasmenyl.PC.34.3	0,61			1,65			1,86		
plasmenyl.PC.34.4				0,89					
plasmenyl.PC.35.0	2,75			0,61			0,19		
plasmenyl.PC.35.1	1,47			1,24					
plasmenyl.PC.35.2				3,45			0,78		
plasmenyl.PC.36.0	12,59			6,76			5,43		
plasmenyl.PC.36.1	0,00			11,26			11,09		
plasmenyl.PC.36.2	0,00			6,05			5,85		
plasmenyl.PC.36.3				0,67			2,02	100,00	
plasmenyl.PC.37.0	0,26			0,04			0,00		
plasmenyl.PC.37.1	0,19								
plasmenyl.PC.37.2	0,36								
plasmenyl.PC.38.0	1,12			0,77					
plasmenyl.PC.38.4				1,77			3,49		
plasmenyl.PC.42.0							0,30		
plasmenyl.PC.44.0							0,27		
plasmenyl.PC.44.1							0,44		
plasmenyl.PC.46.0							0,28		
plasmenyl.PC.46.1							0,24		
plasmenyl.PE.34.1	100,00								
plasmenyl.PE.36.1				100,00					
SM.33.1				0,87					
SM.34.0				0,89			6,36		
SM.34.1	10,61			51,41		48,77	78,64		
SM.34.2				2,01			1,93		
SM.36.1				5,23		9,62			

Lipid species	Cercariae	CA	CES	Worms	AWA	WES	Eggs	SEA	EES
SM.36.2				2,32					
SM.38.1				3,69		5,89			
SM.38.2				4,80		8,25			
SM.40.1				2,32			1,96		
SM.40.2				14,41		20,94			
SM.41.1				0,55			1,00		
SM.41.5	8,84								
SM.42.1				2,82			2,17		
SM.42.2	43,42			7,07		6,54	7,94		
SM.44.2	37,13			1,60					
TG.46.0							0,08		
TG.46.1							0,08		
TG.48.0				1,24			1,05		
TG.48.1				0,35			0,47		
TG.48.2							0,56		
TG.48.3							0,23		
TG.49.0							0,11		
TG.49.1							0,20		
TG.49.2							0,48		
TG.50.0				1,01			1,17		
TG.50.1	0,58			3,57			5,10	26,09	
TG.50.2	1,34			4,17			10,58	42,01	
TG.50.3				0,78			2,08		
TG.50.4							0,54		
TG.50.5							0,14		
TG.51.0				0,06			0,11		
TG.51.1				0,20			0,38		
TG.51.2	0,69			0,28			0,73		
TG.51.3				0,15			0,32		
TG.51.4							0,28		
TG.52.0				0,27			0,56		
TG.52.1	0,67			2,15			3,86		
TG.52.2	1,87			4,47			8,34	31,90	
TG.52.3	1,85			4,32			6,93		
TG.52.4	1,35			3,43			8,82		
TG.52.5				0,70			2,02		
TG.52.6							0,28		
TG.53.0							0,04		
TG.53.1	0,29			0,10			0,26		
TG.53.2	0,80			0,25			0,52		
TG.53.3	0,84			0,25			0,35		
TG.53.4	0,61			0,18			0,29		
TG.53.5							0,12		
TG.53.6							0,08		
TG.54.0							0,09		
TG.54.1	0,44			0,42			1,20		
TG.54.2	1,94			2,28			3,30		
TG.54.3	4,10			4,43			4,63		
TG.54.4	4,24			5,48			5,42		
TG.54.5	2,27			3,58			3,94		
TG.54.6	1,57			3,58			4,74		
TG.54.7	1,03			0,54			0,79		
TG.54.8							0,09		
TG.55.1	0,16						0,07		
TG.55.2	0,69			0,13			0,19		
TG.55.3	1,31			0,22			0,21		
TG.55.4	1,27			0,18			0,16		
TG.55.5	0,70			0,14					
TG.55.6	0,47			0,13			0,08		
TG.55.7	0,33								
TG.56.1	0,15			0,06			0,17		
TG.56.2	1,06			0,62			0,72		

Lipid species	Cercariae	CA	CES	Worms	AWA	WES	Eggs	SEA	EES
TG.56.3	3,24			2,57			1,31		
TG.56.4	4,44			4,23			1,91		
TG.56.5	4,08			4,61			1,86		
TG.56.6	3,34			5,40			2,02		
TG.56.7	2,28			5,54			1,40		
TG.56.8	1,44			2,96			2,05		
TG.56.9	0,75			0,23			0,27		
TG.57.2	0,33						0,05		
TG.57.3	0,85			0,11			0,07		
TG.57.4	1,01			0,12					
TG.57.5	0,70								
TG.57.6	0,54			0,12					
TG.58.1							0,05		
TG.58.10	1,10			2,35			0,63		
TG.58.11	0,70			0,05			0,07		
TG.58.12	0,35								
TG.58.2	0,36			0,18			0,15		
TG.58.3	1,53			0,89			0,33		
TG.58.4	3,56			1,62			0,48		
TG.58.5	5,02			1,90			0,56		
TG.58.6	4,71			2,62			0,56		
TG.58.7	3,68			3,43			0,49		
TG.58.8	3,27			2,70			0,65		
TG.58.9	2,24			3,18			0,51		
TG.59.2	0,10								
TG.59.3	0,31								
TG.59.4	0,44								
TG.59.5	0,38								
TG.60.10	1,34			0,82			0,20		
TG.60.11	0,87			0,29			0,16		
TG.60.12	0,67			0,41			0,19		
TG.60.13	0,35								
TG.60.2	0,09			0,04			0,06		
TG.60.3	0,46			0,19			0,12		
TG.60.4	1,35			0,38			0,14		
TG.60.5	2,22			0,46			0,14		
TG.60.6	2,27			0,63			0,14		
TG.60.7	1,96			0,72			0,13		
TG.60.8	2,16			0,59			0,16		
TG.60.9	1,90			0,80			0,13		
TG.62.11	0,40								
TG.62.12	0,32			0,11			0,06		
TG.62.13	0,24								
TG.62.14							0,05		

Table S3. The ratio of detected oxylipids from each life cycle stages of *S. mansoni* and parasites materials derived from *S. mansoni*

Oxylipid	Cercariae	CA	CES	Worms	AWA	WES	Eggs	SEA	EES
LXA4	0,01					0,04	0,57	0,08	0,11
5-HETE	0,67	0,01	0,01	0,42	0,02	0,11	10,79	0,79	0,03
8-HETE	0,29			0,18	0,01	0,04	4,12	0,81	0,27
11-HETE	2,03	0,01	0,01	0,62	0,04	0,24	23,80	2,33	0,06
12-HETE	1,75	0,01	0,04	1,18	0,04	0,31	20,17	1,05	0,02
15-HETE	3,32		0,04	0,51	0,05	0,32	41,46	1,95	0,08
15-HEPE	4,00				0,00		0,36		
18-HEPE	3,09	0,01		0,01		0,01	0,45	0,01	
LXB4									
Leukotriene B4	0,04						0,18	0,04	
17-HDHA	1,58		0,01	0,02		0,02	9,14	0,22	
14,15-diHETE	0,05								
19,20-DiHDPA	0,05			0,01		0,02	2,37		0,04
RvE1							0,04		
RvE2	0,10								
18S-RvE3									
18R-RvE3									
TxB2						0,08	0,04		0,03
6-trans-LTB4	0,01			0,00		0,01	0,14	0,02	
20-OH LTB4									
PGD2	0,04			0,01		0,07	0,93	0,10	0,17
PDX	0,06						0,01	0,01	
PD1	0,03							0,01	
MaR1_2									
AT-LXA4									
LTE4							0,03		
8S,15S-diHETE	0,02							0,02	0,00
LTD4									
Leukotriene B4 d4									
15-HETE d8									
PGE2-d4									
7,17-DiHDPA									
RvD1									
RvD2									
6t,12epi-LTB4	0,01	0,00		0,00		0,01	0,08	0,04	0,01
PGF2a				0,01	0,47		0,48		0,09
PGE2_2	0,27	0,03	0,03	0,18	0,03	1,19	16,90	2,33	4,87
17-OH-DH-HETE	0,54	0,01	0,01	0,15		0,06	6,14	0,57	0,01
13-HoTrE	0,77					0,01	0,42	0,08	
13-HoDE	30,60	0,31	0,33	0,91	0,41	0,67	65,06	16,18	0,75
7S-MaR1									
AT-RvD1	0,00	0,00	0,00	0,00	0,00	0,00	0,05	0,00	0,00
15-Keto-PGE2				0,07		0,03	0,80	0,03	0,10
13,14dihydro-15keto-PGE2	0,00	0,00	0,00	0,00	0,00	0,03	0,11	0,02	0,11
13,14dihydro-15keto-PGF2a									
8-iso-PGE2									
8-iso-PGF2a	0,01					0,01	0,50	0,04	0,09
9-HoTrE	0,37	0,01	0,01	0,03	0,01	0,02	1,41	0,15	0,02
9-HoDE	7,84	0,29	0,26	0,85	0,33	0,46	34,44	10,50	0,95
AA	8,37	0,04	0,08	4,00	0,14	0,27	44,79	0,12	0,06
DHA	51,68	0,06	0,13	1,66	0,16	0,14	135,66	0,12	0,09
EPA	37,45	0,02	0,04	0,13	0,04	0,01	10,14	0,04	0,02
AdA	5,43	0,01	0,01	1,08	0,01	0,06	67,85	0,01	0,01
DPAn-3	17,33	0,00	0,02	0,36	0,01	0,02	39,81	0,01	0,01
DHAd5									
LA	6,91	0,06	0,11	1,13	0,12	0,18	23,66	0,17	0,08

Oxylipid	Cercariae	CA	CES	Worms	AWA	WES	Eggs	SEA	EES
ALA	1,81	0,01	0,02	0,51	0,03	0,03	31,85	0,03	0,02
PGJ2	0,07								
5,15-diHETE	0,09						0,09	0,11	0,02
10-HDHA	0,50			0,03		0,01	3,11	0,19	0,02
7-HDHA	0,08			0,01		0,01	0,67	0,07	
5F3T IsoP	0,01	0,00	0,00	0,00	0,00	0,00	0,00	0,00	0,00
14(15)EET	0,11	0,03	0,02	0,41	0,03	0,03	3,04	0,04	0,02
11(12)EET	0,13	0,04	0,04	0,88	0,04	0,06	6,40	0,05	0,05
8(9)EET	0,04		0,02	0,34	0,02	0,02	2,41		0,03
15Deoxy PGJ2							0,08		
4F4T NP	0,03	0,00	0,00	0,00	0,00	0,00	0,61	0,02	0,03
17F2 Dihomo IsoP	0,02	0,00	0,00	0,00	0,00	0,03	1,82	0,15	0,17
10S17R-diHAdA									
ALA_2	0,30	0,00	0,00	0,08		0,01	3,01	0,00	0,00
GLA	0,32	0,00	0,00	0,09	0,01	0,01	6,04	0,01	0,00
4-HDHA	0,46		0,01	0,04		0,01	5,21	0,15	0,01
12-HEPE	2,13			0,02		0,01	0,30		
5-HEPE	1,22		0,00			0,00	0,15	0,01	
14(S)-HDHA	0,94		0,01	0,19		0,02	7,43	0,21	0,01
12-KETE	0,03			0,04			0,98		
DGLA	4,75		0,01	0,33		0,01	17,78	0,02	
5-KETE	0,05		0,03	0,54		0,04	13,30	0,12	
DPAn-6	11,58	0,01	0,01	0,80	0,01	0,04	132,75	0,01	0,01
19(20)EpDPA	0,32			0,07		0,02	6,33	0,08	
15-KETE	0,05		0,02	0,67	0,03	0,06	19,00	0,30	0,05
20-HETE_2	0,03			0,01			0,73		
20-HETE									

Chapter 5

Human dendritic cells with Th2-polarizing capacity: analysis using label-free quantitative proteomics

MARIA M. M. KAISAR[1, 2, #], LEONIE HUSSAARTS[1, #], ARZU TUGCE GULER[3], HANS DALEBOUT[3], BART EVERTS[1], ANDRÉ M. DEELDER[3], MAGNUS PALMBLAD[3], MARIA YAZDANBAKHSH[1]

[1]Department of Parasitology, Leiden University Medical Center (LUMC), Leiden, The Netherlands
[2]Department of Parasitology, Faculty of Medicine, Universitas Indonesia, Jakarta, Indonesia
[3]Center of Proteomics and Metabolomics, LUMC, Leiden, The Netherlands
[#]Contributed equally

International Archives of Allergy and Immunology. 2017

ABSTRACT

Dendritic cells (DCs) are the sentinels of the immune system. Upon recognition of a pathogen, they mature and migrate to draining lymph nodes to prime and polarize T cell responses. Although it is known that helminths and helminth-derived molecules condition DCs to polarize T helper (Th) cells towards Th2, the underlying mechanisms remain incompletely understood. The aim of this study was to conduct a proteome analysis of helminth antigen-stimulated DCs, in order to gain more insight into the cellular processes associated with their ability to polarize immune responses. We analyzed maturation and polarization of monocyte-derived DCs from nine donors at two different time points after stimulation with different Th1 and Th2-polarizing pathogen-derived molecules. The samples were measured using liquid chromatography-Fourier transform ion cyclotron resonance mass spectrometry (LC-FTICRMS) for relative quantitation. Lipopolysaccharide (LPS)-induced maturation promoted expression of proteins related to metabolic, cellular and immune system processes. Th1 polarizing DCs, conditioned by IFN-γ during maturation, displayed accelerated maturation by differentially expressing cytoskeletal proteins and proteins involved in immune regulation. Stimulation of DCs with Souluble Egg Antigents (SEA) and omega-1 derived from *Schistosoma mansoni*, two Th2-inducing stimuli, increased 60S acidic ribosomal protein P2 (RPLP2) and vesicle amine transferase 1 (VAT1) while decreasing the expression of proteins related to antigen processing and presentation. Our data indicate that not only proteins involved in interaction between T cells and DCs at the level of the immunological synapse but also those related to cellular metabolism and stress may promote Th2 polarization.

Keyword:
Dendritic cells, Helminths, Omega-1, Proteome, T helper 2 responses

INTRODUCTION

Dendritic cells (DCs) [1] are professional antigen-presenting cells located in peripheral tissues, that continuously sample the environment to capture antigens from invading microbes. Upon recognition of pathogens-associated molecules, DCs undergo maturation and migrate to the draining lymph nodes where they present antigen to antigen-specific T helper (Th) cells. Different classes of pathogens polarize DCs for the induction of different types of Th cell responses. In general, rapidly replicating intracellular microorganisms such as viruses and certain bacteria promote the differentiation of Th1 cells. The principal regulators of anti-helminth immunity are Th2 cells, and fungi and extracellular bacteria drive Th17 responses [2-4].

While much is known about the regulation of Th1 and Th17 responses, the mechanisms that control Th2 activation are still not fully understood [5]. Although helminths are strong inducers of Th2 responses, it has proven to be difficult to pinpoint the specific mechanisms involved due to the complex nature of many helminth-derived antigen preparations. For example, *Schistosoma mansoni* soluble egg antigen (SEA), among the most widely used preparations for studying immune responses to helminth antigens, contains more than 600 different proteins [6]. The identification of omega-1 as a major immunomodulatory component in SEA therefore provided an opportunity to further dissect the molecular mechanisms underlying Th2 skewing [7, 8]. We have previously shown that omega-1 (ω-1) is a glycosylated T2 RNase that conditions DCs for Th2 induction by suppressing protein synthesis [9]. However, it remains unclear which mechanisms subsequently enable Th2 skewing.

Maturation of DCs is characterized by changes in expression of a large number of proteins [10]. Therefore, as a representative indicator of cell function and phenotype, various groups have studied the proteome of pro-Th2 DCs. Using semi-quantitative gel-based techniques, three cytoplasmic proteins were found to be exclusive to the Th2-inducing proteome of human monocyte-derived DCs [11]. In mouse bone marrow-derived DCs (BMDCs), four proteins were significantly affected by stimulation with helminth antigens [12]. A third study on pro-Th2 BMDCs used iTRAQ labeling for relative quantitation of plasma membrane proteins, and showed that pro-Th2 BMDCs upregulated proteins related to cell metabolism and downregulated proteins associated with the cytoskeleton [13]. Although these studies provide valuable directions for future research, the use of 2-DE and iTRAQ does not allow for high-throughput analysis and direct comparison of a large number of biological replicates. This is especially relevant when donor-to-donor variation is expected, for example when working with DCs from human donors, and may explain why only very few proteins were found in common between different gel-based studies on lipopolysaccharide (LPS)-matured human DCs [10, 11, 14, 15].

As such, the introduction of a high-resolution label-free and gel-free method for quantitative analysis of DC proteomes would be highly beneficial. In this study, we analyzed DC maturation and polarization using liquid chromatography fourier transform ion cyclotron resonance mass spectrometry (LC-FTICRMS) for accurate mass measurement and relative quantitation [16, 17]. This method allowed us to include a total of nine DC donors and four different stimuli. We included an early (6 h) and a late (32 h) time point in addition to baseline (0 h), to reflect maturation stages associated with migration and antigen presentation. This experimental set-up enabled us to take in donor-to-donor variation in the global proteome into consideration and quantify the most abundant proteins across a large number of replicates. Using SEA, a complex antigen preparation, and ω-1, a single molecule for Th2 polarization, we here focused on the identification of proteins associated with the pro-Th2 DC proteome.

MATERIAL AND METHODS

Human DC culture, stimulation, and analysis

Monocytes isolated from venous blood of 9 healthy volunteers were differentiated as described previously [18]. On day 6 the immature DCs (iDCs) were stimulated with SEA (50 µg/mL), ω-1 (250 ng/mL) or IFN-γ (1000 U/mL) in the presence of 100 ng/mL ultrapure LPS (*E. coli* 0111 B4 strain, InvivoGen) and human rGM-CSF (20 ng/ml; Life Technologies). At the indicated time points, samples were collected for protein extraction and digestion as described below. Alternatively, after 48 h of stimulation, expression of surface molecules was determined by flow cytometry (FACSCanto, BD Biosciences) using the following antibodies: CD14 PerCP, CD86 FITC (both BD Biosciences), and CD1a PE (Beckman-Coulter). In addition, $1x10^4$ 48 h-matured DCs were co-cultured with $1x10^4$ CD40L-expressing J558 cells. Supernatants were collected after 24 h and IL-12p70 concentrations were determined by ELISA using mouse anti-human IL-12 (clone 20C2) as a capture antibody and biotinylated mouse anti-human IL-12 (clone C8.6) as a detection antibody (BD Biosciences). Volunteers signed informed consent forms and the samples were handled according to the guidelines described by the Dutch Federation of Medical Scientific Societies in the Code of Conduct for the responsible use of human tissue for medical research. Available from URL: www.fedra.org (accessed on September 2013).

Human T cell culture and analysis of T cell polarization

For analysis of T cell polarization, $5x10^3$ matured DCs were cultured with $2x10^4$ allogeneic naive $CD4^+$ T cells that were isolated from buffy coat (Sanquin) peripheral blood mononuclear cells using a $CD4^+/45RO^-$ Naive T Cell Enrichment Column (R&D Systems). Co-cultures were performed in the presence of staphylococcal enterotoxin B (10 pg/mL). On days 6 and 8, rhuIL-2 (10 U/mL, R&D Systems) was added and the T cells were expanded until day 11. Intracellular cytokine production was analyzed after restimulation with 100 ng/mL phorbol myristate acetate plus 1 µg/mL ionomycin for 6 h; 10 µg/mL brefeldin A was added during the last 4 h and the cells were fixed with 3.7% paraformaldehyde (all Sigma-Aldrich). The cells were permeabilized with 0.5% saponin (Sigma-Aldrich) and stained with PE- and FITC-labelled antibodies against IL-4 and IFN-γ, respectively (BD Biosciences).

Protein extraction and in-solution digestion

Cells were harvested with PBS at the indicated time points and centrifuged at 522×*g* for 8 minutes at 4 °C, after which they were transferred with 1 mL PBS to a micro centrifuge tube and centrifuged for 5 minutes at 5000 ×*g,* 4 °C. The supernatant was removed and pellets were snap-frozen in liquid nitrogen and stored at -80 °C. Samples were thawed in 30 µL lysis buffer consisting of 1% SDS, 125 U/mL benzonase nuclease (Sigma), 2 mM MgCl2, and protease inhibitors (complete ULTRA tablets, mini, EDTA-free, Roche) in 50 mM ammonium biocarbonate (ABC). Samples were placed at 95 °C for 5 min and following centrifugation at 16000 ×*g* for 30 min, the supernatant was collected. A BCA assay (Pierce Biotechnology) was conducted to determine the protein concentration. An equivalent of 10 µg protein was dissolved in 25 µL ABC and reduced using 10 mM DTT (Sigma) for 5 min at 95 °C, followed by 1 h alkylation using 40 mM iodoacetamide (Sigma) at room temperature. Using 3 kDa spin filters, the remainder of the lysis buffer was exchanged for ABC according to manufacturer's protocol (Millipore), and samples were digested for 17 h with sequencing-grade trypsin (Promega) at an enzyme to protein ratio of 1:50. The

digestion was quenched with 2% trifluoracetic acid to lower the pH. Peptide samples were stored at -35 °C until analysis.

Liquid chromatography - mass spectrometry

Accurate mass tags (AMTs) analysis was used to normalize the chromatograms for peptides and proteins identification across different stimulations and between different donors [19]. All samples were analyzed using a splitless NanoLC-Ultra 2D plus (Eksigent) system for parallel liquid chromatography (LC) with additional trap columns for desalting. The LC systems were configured with 300 µm-i.d. 5-mm PepMap C18 trap columns (Thermo Fisher Scientific) and 15-cm 300 µm-i.d. ChromXP C18 columns (Eksigent). Peptides were separated by a 90-minute linear gradient from 4 to 33% acetonitrile in 0.05% formic acid with the 4 µl/min flow rate. The LC systems were coupled on-line to amaZon speed ETD high-capacity 3D ion traps and a 12 T solariX FTICR system (all from Bruker Daltonics) in an FTICR-ion trap cluster [17]. For peptide identification in the ion traps, we generated three sample pools. Pool 1 contained a fraction of each sample that was stimulated for 32 h with LPS or LPS + IFN-γ. Pool 2 contained a fraction of each 0 h and 6 h iDC sample. Pool 3 contained a fraction of each uneven sample (all samples received a random number). These sample pools were run in triplicate on the ion traps. Up to ten abundant multiply charged precursors in *m/z* 300-1300 were selected for MS/MS in each MS scan in a data-dependent manner. After having been selected twice, each precursor was excluded for one minute. The LC systems were controlled using the HyStar 3.4 (Bruker) with a plug-in from Eksigent, the amaZon ion trap by trapControl 7.0, and the solariX FTICR system by solariXcontrol 1.3 (both Bruker).

Data analysis

The raw datasets from ion trap LC-MS/MS and LC-FTICRMS were converted to mzXML (48). The mzXML files were analysed using a scientific workflow called "Label-free proteomics using LC-MS" (http://www.myexperiment.org/workflows/4552.html). The workflow was designed using the Taverna workflow management system [20].

The LC-MS/MS data was used for identification. The TANDEM application [21] from the X! Tandem provided in Trans Proteomics Pipeline V4.7.7 was run to match the spectra with tryptic peptide sequences derived from UniProt *Homo sapiens* reference proteome database retrieved on 25.07.2014, for each pooled sample. The k-score plug-in was selected for the search with a minimum ion count of 1, and 2 maximum missed cleavage sites. The allowed parent monoisotopic mass error was ±5.0 Da, and the allowed fragment monoisotopic mass error was 0.4 Da. After peptide assignments to MS/MS spectra, the results were converted to pepXML format, an XML-based format that is used in peptide-level analysis [22], using the Tandem2XML application.

To use the high-resolution MS profiles for more precise quantification, each pepXML file was aligned with one master LC-FTICRMS data file. The alignment was done with pepAlign [23], which uses a genetic algorithm to align the two chromatographic time scales with a partial linear function. The output from pepAlign was the breakpoints of this function. The alignment was based on the X! Tandem expect scores and allowed a mass measurement error of ±50 ppm. The retention times in each pepXML file were changed according to the chromatographic alignment function by the pepWarp program. The accuracy of the peptide assignments to tandem mass spectra was assessed by PeptideProphet using the xinteract application provided in Trans Proteomics Pipeline V4.6.3 [24]. This application also combined the input datasets, so that all

identifications with assigned probabilities were contained in a single output file. This validated pepXML was then aligned with each individual LC-FTICRMS dataset. For quantitation of identified peptides, we used only peptides with PeptideProphet probabilities higher than 0.9369, giving a peptide-spectrum match false discovery rate of 1.0%. Modified peptides were not included.

The monoisotopic mass was calculated for each peptide of interest and the maximum intensity corresponding to this mass was extracted from a window ±60 seconds relative to the aligned retention time and ±25 ppm relative to the calculated mass. As the final output of the workflow, all peptide quantifications were combined into a single table where each row represents a peptide sequence and each column contains the intensity of that peptide in each sample. Missing values were imputed from a normal distribution representing the background signal removed during acquisition. A final matrix was created with proteins identified by more than two peptides, where the abundance of each protein was calculated as the median intensity of its peptides and normalized to the total signal intensity of all proteins in the entire LC-MS dataset. Fold changes in protein abundance between conditions were calculated in R based on the mean fold change of the nine different donors, and corresponding p-values were obtained from paired Student's t-testing of log-transformed protein intensities for each treatment and time point.

The heat-map for visualizing the regulated proteins of differently stimulated moDCs was generated using GENE-E software from the Broad Institute (https://software.broadinstitute.org/GENE-E/). Statistical analysis and visualization of differentially expressed proteins was performed using GraphPad Prism version 6.00 (GraphPad Software, La Jolla, CA USA) for Windows.

RESULTS

Functional characterization of human DCs

Immature DCs (iDCs) generated from nine donors were stimulated LPS in combination with IFN-γ as a Th1-inducing stimulus, and SEA or ω-1 as Th2-inducing conditions. The purpose of co-stimulation with LPS was to achieve a similar level of activation among the differently T polarizing DCs, to prevent the possibility that potential differences in activation status of the differently

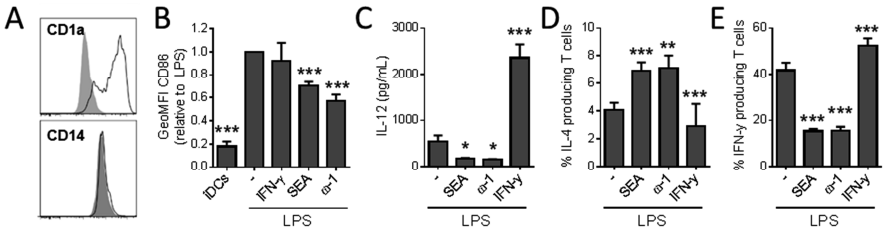

Figure 1. Functional characterization of pro-Th1 and pro-Th2 DCs

Monocyte-derived DCs were either left untreated or pulsed with LPS in the presence or absence of IFN-γ, SEA, or ω-1. After 48 h, expression of surface markers was analyzed by flow cytometry. (A) Representative histograms for expression of CD1a and CD14 are shown. (B) Expression levels of CD86, based on the geometric mean fluorescence, are shown relative to LPS, which was set to 1. (C) Following stimulation, moDCs were co-cultured with a CD40L-expressing cell line. Supernatants were collected after 24 h and IL-12p70 concentrations were determined by ELISA. (D) 48 h-matured DCs were cultured with allogeneic naive $CD4^+$ T cells for 11 days. Intracellular cytokine production as analyzed by flow cytometry after 6 h of stimulation with phorbol myristate acetate and ionomycin. The percentages of T cells uniquely positive for either IL-4 or (E) IFN-γ are shown. Box and whiskars ; *P<0.05; **P<0.01; ***<0.001 for significant differences with the LPS control based on a paired Student's t-test.

polarizing DCs would affect their T cell-polarizing characteristics. To functionally characterize these DCs, a co-culture system of human matured DCs and allogeneic naive $CD4^+$ T cells was used. Efficient differentiation of monocytes towards DCs was validated by expression high levels of CD1a and little CD14 (Figure 1A) and upregulation of CD86 expression upon LPS stimulation (Figure 1B). Additional stimulation with IFN-γ did not affect LPS-induced CD86 expression but strongly induced IL-12p70 production (Figure 1C), while SEA and ω-1 decreased expression of both CD86 and IL-12p70, as described previously (9). Analysis of T cell cytokine production confirmed that ω-1 and SEA induced a Th2 response, characterized by a high frequency of IL-4-producing T cells (Figure 1D), while stimulation of DCs with IFN-γ promoted a Th1 response (Figure 1E).

Protein Identifications

To establish the effect of maturation and polarization on the DC proteome, iDCs and LPS-matured DCs stimulated with IFN-γ, SEA or ω-1, were collected from each of the nine donors at three different time points: before stimulation (0 h), 6 hours after stimulation (6 h) and 32 h after stimulation (32 h). Proteins were digested after which peptides were identified using LC-MS/MS in an ion trap, resulting in the identification of 1159 unique peptides from 439 unique proteins with a false-discovery rate (FDR) of 1.0%. These were used for matching with and querying the LC-FTICRMS data for label-free quantitation [16, 17]. In total, 208 proteins corresponding to the most abundantly present proteins in these cells were quantified with multiple peptides in each biological replicate and at each time point. For analysis purposes we exclude one protein with the accession code Q9BZQ8 as the signal indicates that this protein was attributed to the VLTSEDEYNLLSDR peptide in NIBAN which is likely to come from the $^{13}C_1$-peak of the YCLQLYDETYER peptide from SEA-derived protein interleukin-4-inducing protein (IPSE). IPSE is known to be one of the most abundant proteins in SEA but has no Th2 polarizing activity [7], therefore irrelevant as a DC protein that constitutes pro-Th2 proteomes.

Effects of maturation on the human DC proteome

To identify proteins that were differentially expressed between the different stimulations, the stimulus-induced fold change in abundance was determined for each protein, by calculating the mean fold change of the nine donors. Corresponding *p*-values were obtained from a paired Student's t-test after log-transformation. Proteins were considered differentially expressed when $p<0.05$ and the stimulus induced fold change was more than 1.5-fold decreased or increased (i.e. fold change <0.67 or >1.5). LPS-induced maturation displayed a pronounced effect on the DC proteome. Compared to iDCs, LPS promoted differential expression of 10 proteins after 6 h (Table 1). Analysis of protein classification according to Gene Ontology terms indicated that the 8 upregulated proteins are mostly involved in transport or cell communication. The two downregulated proteins were both cytoskeletal proteins. After 32 h, LPS promoted differential expression of 22 proteins (Table 1). The majority of proteins was upregulated and related to different metabolic, cellular and immune system processes or transport. The protein most strongly upregulated by LPS stimulation was TNF receptor-associated factor 1 (TRAF1), an adapter molecule that regulates activation of NF-κB and JNK [25]. In addition, actin cross-linking proteins Fascin and Myristoylated alanine-rich C-kinase substrate (MARCS) were profoundly induced, as well as the MHC class I molecule HLA-B, involved in antigen presentation. Among the four downregulated proteins we identified Macrophage mannose receptor 1, that is involved in antigen uptake,

Table 1. Differentially expressed proteins in LPS-DCs versus iDCs

Accession	Protein	6 hours		32 hours	
		Fold	*p*-value	Fold	*p*-value
LPS-modulated, 6 hours					
P45880	Voltage-dependent anion-selective channel protein 2	2,74E+00	**4,40E-02**	1,81E+00	5,65E-01
P30040	Endoplasmic reticulum resident protein 29	2,59E+00	**3,12E-03**	1,67E+00	6,36E-01
Q13077	TNF receptor-associated factor 1	2,25E+00	**8,42E-03**	1,49E+01	**3,32E-06**
P61604	10 kDa heat shock protein. mitochondrial	2,23E+00	**3,28E-02**	1,68E+00	7,58E-01
P05362	Intercellular adhesion molecule 1	1,89E+00	**6,60E-04**	3,60E+00	**6,99E-03**
P30464*	HLA class I histocompatibility antigen, B-15 alpha chain	1,83E+00	**2,50E-02**	7,89E+00	**7,06E-04**
P29966	Myristoylated alanine-rich C-kinase substrate	1,77E+00	**2,18E-02**	1,08E+01	**8,81E-06**
Q9BQE5	Apolipoprotein L2	1,64E+00	**4,92E-02**	2,95E+00	**2,05E-03**
Q71U36	Tubulin alpha-1A chain	6,29E-01	**3,38E-02**	1,58E+00	8,17E-01
P06396	Gelsolin	6,21E-01	**5,29E-04**	1,96E+00	4,75E-01
LPS- modulated, 32 hours					
Q13077	TNF receptor-associated factor 1	2,25E+00	**8,42E-03**	1,49E+01	**3,32E-06**
P29966	Myristoylated alanine-rich C-kinase substrate	1,77E+00	**2,18E-02**	1,08E+01	**8,81E-06**
P30464*	HLA class I histocompatibility antigen, B-15 alpha chain	1,83E+00	**2,50E-02**	7,89E+00	**7,06E-04**
Q16658	Fascin	1,26E+00	6,06E-01	5,48E+00	**1,68E-04**
P04179	Superoxide dismutase [Mn], mitochondrial	1,20E+00	6,78E-01	4,66E+00	**7,52E-04**
P23381	Tryptophan--tRNA ligase, cytoplasmic	9,83E-01	5,47E-01	3,77E+00	**6,27E-06**
Q9UL46	Proteasome activator complex subunit 2	9,17E-01	2,54E-01	3,68E+00	**6,65E-04**
P05362	Intercellular adhesion molecule 1	1,89E+00	**6,60E-04**	3,60E+00	**6,99E-03**
P80723	Brain acid soluble protein 1	1,21E+00	5,38E-01	3,46E+00	**2,16E-03**
P27348	14-3-3 protein theta	9,58E-01	3,96E-01	3,00E+00	**4,39E-03**
Q9BQE5	Apolipoprotein L2	1,64E+00	4,92E-02	2,95E+00	**2,05E-03**
P19971	Thymidine phosphorylase	9,97E-01	7,64E-01	2,79E+00	**4,49E-02**
Q14974	Importin subunit beta-1	9,77E-01	3,78E-01	2,39E+00	**2,39E-02**
P02786	Transferrin receptor protein 1	1,14E+00	7,66E-01	2,20E+00	**4,70E-04**
P08107	Heat shock 70 kDa protein 1A/1B	1,19E+00	4,09E-01	1,93E+00	**1,61E-02**
P20700	Lamin-B1	1,34E+00	4,04E-01	1,85E+00	**3,84E-02**
P34931	Heat shock 70 kDa protein 1-like	1,16E+00	5,18E-01	1,55E+00	**4,28E-02**
Q9BZQ8	Protein Niban	1,14E+00	3,16E-01	1,54E+00	**6,54E-03**
P07339	Cathepsin D	1,68E+00	7,57E-01	6,26E-01	**3,15E-02**
P22897	Macrophage mannose receptor 1	9,76E-01	3,61E-01	6,31E-01	**1,62E-02**
P17900	Ganglioside GM2 activator	1,40E+00	1,85E-01	5,80E-01	**1,61E-02**
Q9UBR2	Cathepsin Z	1,30E+00	**1,23E-02**	5,64E-01	**2,42E-03**

*HLA serotypes originate from the same gene and share common peptides. The serotype attributed to the identification may therefore not be accurate. Red and blue coloured numbers represent higher and lower fold change of proteins compared to iDCs respectively. Statistically significant *p*-values are given in bold.

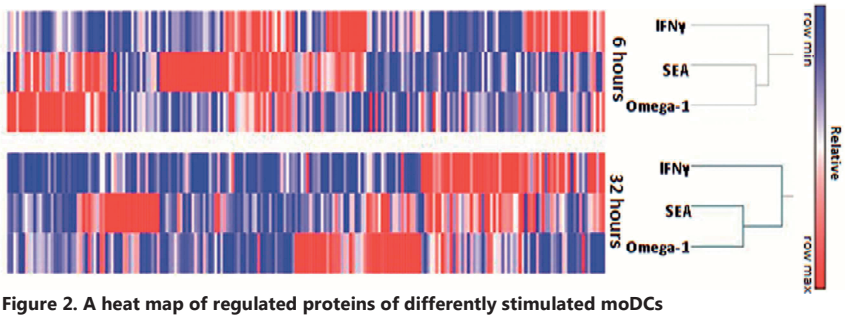

Figure 2. A heat map of regulated proteins of differently stimulated moDCs
Monocyte-derived DCs were stimulated as described in legend of Figure 1, and protein expression was analyzed by Gene E based on the fold change of proteins relative to LPS at 6 and 32 h. Colour indicates directionality of the change in protein expression (red=increase, blue= decrease).

cathepsins, that play a role in antigen processing, and Ganglioside GM2 activator (GM2A) that mediates presentation of lipids [22, 26, 27].

Effects of polarizing stimuli on the human DC proteome

Based on analysis of fold changes of proteins in the different polarizing conditions, compared to LPS, there was a hierarchical clustering based on time (Figure 2). This reflects the differential expression of proteins at 6 h and 32 h after initiation of polarization. The heat map showed that, at each time point, proteins expressed in DCs stimulated with the SEA and ω-1 clustered together, indicating distinct proteome profiles in pro-Th1 *versus* pro-Th2 DCs.

Table 2. Differentially expressed proteins in pro-Th1 and pro-Th2 DCs versus LPS-DCs

Accession	Protein	IFN-γ		SEA		Omega-1	
		Fold	*p*-value	Fold	*p*-value	Fold	*p*-value
IFN-γ-modulated, 6 hours							
P07900	Heat shock protein HSP 90-alpha	2,42E+00	**2,07E-02**	2,98E+00	**1,90E-02**	2,42E+00	1,39E-01
P23381	Tryptophan--tRNA ligase, cytoplasmic	2,13E+00	**3,93E-02**	1,20E+00	4,27E-01	1,07E+00	6,08E-01
P13639	Elongation factor 2	1,82E+00	**9,45E-03**	1,64E+00	1,17E-01	1,34E+00	3,31E-01
P30508*	HLA class I histocompatibility antigen, Cw-12 alpha chain	1,78E+00	**2,95E-02**	1,61E+00	4,08E-01	1,29E+00	9,68E-01
P09467	Fructose-1.6-bisphosphatase 1	1,69E+00	**2,11E-02**	1,54E+00	7,41E-02	1,53E+00	2,47E-01
Q01813	6-phosphofructokinase type C	1,39E+00	**2,10E-02**	1,13E+00	4,27E-01	1,65E+00	**6,14E-03**
P26038	Moesin	6,57E-01	**3,92E-02**	8,58E-01	1,59E-01	1,12E+00	5,77E-01
P67936	Tropomyosin alpha-4 chain	6,57E-01	**1,92E-02**	8,99E-01	1,79E-01	1,08E+00	3,63E-01
P02545	Prelamin-A/C	6,38E-01	**4,80E-03**	9,50E-01	2,09E-01	1,09E+00	7,34E-01
P16070	CD44 antigen	6,32E-01	**1,06E-02**	1,01E+00	3,96E-01	8,89E-01	2,11E-01
P10599	Thioredoxin	5,17E-01	**1,59E-02**	2,31E+00	3,27E-01	1,10E+00	6,85E-02
IFN-γ- modulated, 32 hours							
P09769	Tyrosine-protein kinase Fgr	6,47E-01	**2,73E-02**	6,80E-01	**9,46E-03**	9,47E-01	3,98E-01
P62937	Peptidyl-prolyl cis-trans isomerase A	5,88E-01	**2,87E-04**	9,94E-01	2,85E-01	9,75E-01	3,76E-01
P04908	Histone H2A type 1-B/E	5,77E-01	**1,94E-02**	2,38E+00	4,39E-01	3,71E+00	5,85E-01
P40926	Malate dehydrogenase. mitochondrial	5,53E-01	**4,74E-03**	1,07E+00	1,55E-01	1,31E+00	2,00E-01
SEA- modulated, 6 hours							
P62937	Peptidyl-prolyl cis-trans isomerase A	4,02E+00	4,45E-01	1,13E+01	**1,18E-02**	1,62E+00	5,41E-01
Q9BZQ8**	Protein Niban	1,10E+00	8,53E-01	9,78E+00	**4,42E-06**	1,03E+00	8,94E-01
P14625	Endoplasmin	1,47E+00	5,77E-01	4,14E+00	**3,95E-02**	2,31E+00	8,85E-01
P60842	Eukaryotic initiation factor 4A-I	1,83E+00	3,18E-01	3,21E+00	**4,20E-02**	1,17E+00	4,70E-01
P07900	Heat shock protein HSP 90-alpha	2,42E+00	**2,07E-02**	2,98E+00	**1,90E-02**	2,42E+00	1,39E-01
Q16658	Fascin	1,15E+00	9,19E-01	1,74E+00	**4,10E-02**	1,40E+00	3,18E-01
SEA- modulated, 32 hours							
P05387	60S acidic ribosomal protein P2	1,68E+00	1,75E-01	2,27E+00	**6,25E-03**	4,63E+00	**1,30E-02**
Q9BZQ8**	Protein Niban	1,19E+00	1,96E-01	2,20E+00	**1,10E-02**	1,20E+00	7,31E-01
Q99536	Synaptic vesicle membrane protein VAT-1 homolog	1,29E+00	2,04E-01	1,59E+00	**2,77E-02**	1,53E+00	**1,62E-02**
P09769	Tyrosine-protein kinase Fgr	6,47E-01	**2,73E-02**	6,80E-01	**9,46E-03**	9,47E-01	3,98E-01
P16070	CD44 antigen	1,47E+00	8,09E-01	6,25E-01	**2,34E-02**	4,71E-01	**1,92E-03**
P23381	Tryptophan--tRNA ligase, cytoplasmic	1,45E+00	3,41E-01	6,01E-01	**4,24E-03**	9,21E-01	1,88E-01
P02786	Transferrin receptor protein 1	7,54E-01	5,10E-02	5,65E-01	**1,65E-03**	4,86E-01	**1,54E-03**
P30464*	HLA class I histocompatibility antigen, B-15 alpha chain	1,27E+00	7,93E-01	4,52E-01	**3,34E-03**	3,99E-01	**1,64E-03**

Omega-1- modulated, 6 hours							
P30048	Thioredoxin-dependent peroxide reductase, mitochondrial	7,06E+00	1,43E-01	2,56E+00	6,36E-01	4,03E+00	**3,59E-02**
P05388	60S acidic ribosomal protein P0	1,47E+00	5,70E-02	1,31E+00	6,37E-01	1,86E+00	**2,05E-02**
P30041	Peroxiredoxin-6	1,33E+00	6,30E-01	1,44E+00	3,34E-01	1,77E+00	**2,00E-02**
Q01813	6-phosphofructokinase type C	1,39E+00	**2,10E-02**	1,13E+00	4,27E-01	1,65E+00	**6,14E-03**
P61158	Actin-related protein 3	1,47E+00	4,97E-01	2,11E+00	6,71E-01	1,61E+00	**3,78E-02**
Omega-1- modulated, 32 hours							
P05387	60S acidic ribosomal protein P2	1,68E+00	1,75E-01	2,27E+00	**6,25E-03**	4,63E+00	**1,30E-02**
P27824	Calnexin	1,32E+00	9,32E-01	1,76E+00	5,05E-01	2,64E+00	**4,73E-02**
P55084	Trifunctional enzyme subunit beta, mitochondrial	1,72E+00	1,44E-01	1,48E+00	1,34E-01	2,52E+00	**4,52E-02**
P63104	14-3-3 protein zeta/delta	1,60E+00	5,54E-01	1,51E+00	1,83E-01	2,33E+00	**3,52E-02**
P50502	Hsc70-interacting protein	1,29E+00	4,79E-01	1,45E+00	5,66E-02	2,05E+00	**2,43E-02**
P30041	Peroxiredoxin-6	9,44E-01	3,21E-01	1,46E+00	3,19E-01	2,02E+00	**1,97E-02**
Q99536	Synaptic vesicle membrane protein VAT-1 homolog	1,29E+00	2,04E-01	1,59E+00	**2,77E-02**	1,53E+00	**1,62E-02**
P17900	Ganglioside GM2 activator	1,04E+00	2,04E-01	1,26E+00	6,78E-01	6,54E-01	**2,57E-02**
P30508	HLA class I histocompatibility antigen, Cw-12 alpha chain	1,02E+00	2,89E-01	1,01E+00	5,45E-02	6,32E-01	**1,19E-02**
P29966	Myristoylated alanine-rich C-kinase substrate	1,19E+00	7,78E-01	7,32E-01	6,00E-02	5,84E-01	**1,46E-02**
P04179	Superoxide dismutase [Mn]. mitochondrial	1,30E+00	8,49E-01	1,24E+00	3,72E-01	5,21E-01	**6,19E-03**
P02786	Transferrin receptor protein 1	7,54E-01	5,10E-02	5,65E-01	**1,65E-03**	4,86E-01	**1,54E-03**
P16070	CD44 antigen	1,47E+00	8,09E-01	6,25E-01	**2,34E-02**	4,71E-01	**1,92E-03**
P30504*	HLA class I histocompatibility antigen, Cw-4 alpha chain	7,25E-01	9,92E-02	1,88E+00	2,10E-01	4,66E-01	**1,91E-02**
P30464*	HLA class I histocompatibility antigen, B-15 alpha chain	1,27E+00	7,93E-01	4,52E-01	**3,34E-03**	3,99E-01	**1,64E-03**

*HLA serotypes originate from the same gene and share common peptides. The serotype attributed to the identification may therefore not be accurate. **The signal attributed to the VLTSEDEYNLLSDR peptide in NIBAN is likely coming from $^{13}C_1$-peak of the YCLQLYDETYER peptide from SEA-derived protein IL-4-inducing protein (IPSE). Protein Niban was removed from further analysis. Red and blue coloured numbers represent higher and lower fold change of proteins compared to LPS-DCs respectively. Statistically significant *p*-value of protein change indicated by bold printed *p*-values.

The LPS-IFN-γ stimulated DCs differentially expressed eleven proteins after 6h of stimulation compared to stimulation with LPS alone (Table 2). Five proteins were downregulated, of which three were members of the cytoskeleton. The proteins most strongly upregulated were Heat Shock Protein HSP 90-alpha (HSP90AA1), which mediates inflammatory responses, and cytoplasmic tryptophan-tRNA ligase (WARS), also known as Interferon-induced protein 53 (p53). After 32 h, four proteins were downregulated (Table 2), including a tyrosine-protein kinase involved in regulation of immune responses (FGR), and Peptidyl-prolyl cis-trans isomerase A (PPIA), which plays an important role in protein folding, trafficking, and immune cell activation [28].

Following 6 h of stimulation with Th2-inducing SEA, five proteins were upregulated compared to stimulation with LPS alone (Table 2). SEA induced upregulation of PPIA which is involved in various cellular functions including protein folding, T cell activation and differentiation [28]. SEA also increased expression of Eukaryotic initiation factor 4A-I, which played a role in the initiation of the translation process. The expression of both chaperones of HSP90, namely Endoplasmin (HSP90B1) and HSP90AA1 were increased with SEA stimulation. Interestingly, HSP90 is a protein that is important for type I interferon production [29], which was recently found to be a key transcriptional signature of murine skin DCs and that enable them to drive Th2 responses in response to helminth antigens [30]. However, given that HSP90AA1 was also observed to be

upregulated by IFN-γ and that we could not find a clear type I interferon signature in the SEA or ω-1 stimulated DCs, makes it unlikely that this pathway is of importance for Th2 induction by SEA or ω-1-stimulated DCs. The fifth upregulated protein by SEA was seen at 6 h after SEA stimulation and was identified as Fascin, known to be involved in cell motility, migration and regulation of the cytoskeleton. After 32 h, SEA promoted differential expression of seven proteins (Table 2). Among those, five proteins were downregulated, including WARS which was upregulated by IFN-γ (at 6h), a MHC class I protein complex HLA-B and CD44 which are involved in antigen presentation and T cell activation, respectively [31]. The protein most strongly upregulated at 32 h of SEA stimulation was 60S acidic ribosomal protein P2 (RPLP2), which plays an important role in the elongation step of protein synthesis.

Omega-1 induced upregulation of five proteins after 6 h, and seven proteins after 32 h (Table 2), most of which were ribosomal proteins, chaperones or enzymes. Among those, several proteins were highly upregulated, including mitochondrial Thioredoxin-dependent peroxide reductase (6 h), a protein involved in redox regulation of the cell, RPLP2 (32 h), and the chaperone Calnexin (32 h). After 32 h of ω-1 stimulation, eight proteins were downregulated. In particular, ω-1 strongly decreased expression of HLA-B, HLA-C and CD44, as well as MARCS.

Analysis of proteins exclusive to the Th2-inducing proteome

The identification of proteins uniquely associated with the Th2-inducing DC proteome could provide valuable leads for understanding how DCs initiate Th2 responses. We therefore analyzed proteins affected by stimulation with SEA as well as ω-1, by looking at protein expression dynamics and individual donor responses. As can be appreciated from Table 2, ω-1 and SEA did not share proteins that indicate Th2 commitment after 6h of stimulation. After 32h, however, they shared five differentially expressed proteins. Among those five, Transferrin receptor protein 1 is seemingly downregulated by omega-1 and SEA, but also by IFN-γ (ρ=0.051), suggesting that this may not be a Th2-exclusive protein.

Analysis of protein expression dynamics of the four remaining Th2-associated proteins showed that RPLP2 was strongly upregulated by 32h of stimulation with SEA and omega-1 in at least eight out of nine donors (Figure 3A). Synaptic vesicle membrane protein VAT-1 homolog (VAT1) was upregulated by SEA and omega-1 in at least seven donors after 32h of stimulation (Figure 3B), but was also mildly increased by IFN-γ stimulation in the majority of donors. CD44 was significantly downregulated by SEA in seven donors, and by ω-1 in nine donors (Figure 3C). Lastly, LPS-induced upregulation of HLA-B was inhibited by SEA and ω-1 in eight donors (Figure 3D). These findings suggest that in particular upregulation of RPLP2, and downregulation of CD44 and HLA-B, are unique characteristics of pro-Th2 DCs.

DISCUSSION

Over the past decade, studies on the proteome of matured or polarized DCs relied on label- and gel-based techniques. Such approaches do not allow for high-throughput analysis of many different conditions or biological replicates, which might explain why only few proteins were found in common between different reports [10, 11, 14, 15, 32]. Here, we used ion traps for tandem mass spectrometry and LC-FTICRMS for label- and gel-free quantitation. The method is an AMTs-based analysis [17, 33], with the peptide identification being done in parallel with the FTICR measurement in the same instrument cluster. The bridging of peptide identification across LC-MS runs is performed through chromatographic alignment [19, 34]. This method had previously been used

for the analysis of the proteome from human plasma and the cells from a bacterium, *Deinococcus radiodurans* [16, 19]. This approach allowed us to analyze the most abundant proteins and to generate an overview of global proteome changes of LPS-matured and pro-Th1 versus pro-Th2 DCs from nine different human donors.

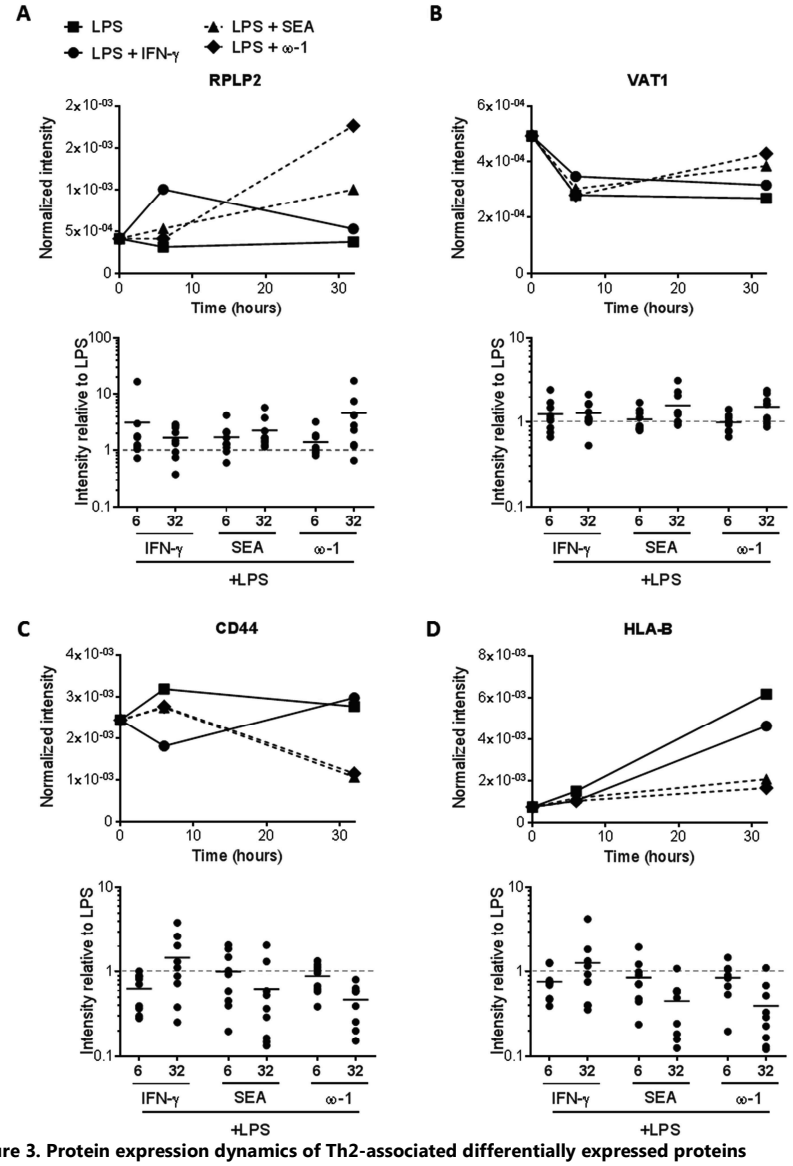

Figure 3. Protein expression dynamics of Th2-associated differentially expressed proteins
Monocyte-derived DCs were stimulated as described for the legend of Figure 1. Protein expression was analyzed by LC-FTICRMS. Differentially expressed proteins shared between 32 h of stimulation of with ω-1 and SEA are shown. The top panel of each figure shows the protein expression dynamics, the bottom panel shows the normalized intensity relative to LPS, which was set to 1 at 6 h and at 32 h (dashed line). (A) 60S acidic ribosomal protein P2. (B) Synaptic vesicle membrane protein VAT-1 homolog. (C) CD44 antigen. (D) HLA-B.

As expected, LPS-induced maturation resulted in a pronounced effect on the DC proteome. After 6 h of maturation, proteins involved in intracellular transport and cell communication were upregulated, and cytoskeletal proteins were either up- or downregulated. These processes may reflect that the DCs are preparing for migration, which requires profound alterations in cell morphology and motility [35]. The strongest effect on the DC proteome was observed after 32 h of LPS-induced maturation, when many proteins were upregulated at least 3-fold. Among the proteins most strongly induced was mitochondrial Superoxide dismutase (SODM). Indeed, DCs are known to upregulate reactive oxygen species in response to stimulation with LPS [36, 37], and subsequent upregulation of superoxide dismutases has also been reported [38]. In addition, stimulation with LPS induced Fascin, an actin cross-linking protein that plays a critical role in migration of mature DCs into lymph nodes. Specifically, actin bundling by Fascin was shown to promote membrane protrusions and mediates disassembly of podosomes, which are specialized structures for cell-matrix adhesion [39]. A second actin cross-linking protein, MARCS, was also profoundly induced, in line with a previous report [40]. The other two proteins most strongly affected by LPS stimulation were MHC class I molecule HLA-B, involved in antigen presentation, and TRAF1, an adapter molecule that regulates activation of NF-κB and JNK. Indeed, NF-κB activation was previously shown to be required for DC maturation [41]. The proteins downregulated after 32 h of LPS stimulation were involved in antigen uptake, processing and presentation of lipids. Together, these findings reflect that after 32 h of stimulation, LPS-DCs have become specialized for entering lymph nodes and presenting antigen to naive T cells, which identifies and validates the FTICR-ion trap cluster as an appropriate method to for high-throughput quantitative analysis of dendritic cell lysates.

Importantly, we find many differentially expressed proteins in common with a proteomics study by Ferreira *et al.* [14], which further validates our method. In our and their study, maturation reduces expression of cathepsins and GM2A, and increases expression of Apolipoprotein L2, Fascin, Proteasome activator complex subunit 2, and SODM. Furthermore, in line with another report [15], we observe an increase in Heath shock protein (Hsp) expression. Unique to our study, the FTICR method allowed us to perform statistical analysis on protein expression data from nine biological replicates. In addition, two time points were included, which provides information about protein expression dynamics. Indeed we were able to show that the detected proteins were differently regulated at earlier compared to the later time points after DC maturation. Our study therefore strengthens and expands previous reports on maturation of human DCs.

Using the cytokine IFN-γ, we polarized LPS-DCs for Th1 skewing, and observed that pro-Th1 DCs differentially expressed cytoskeletal proteins and proteins involved in inflammatory processes after 6 h of stimulation, compared to LPS-DCs. Among those proteins, HSP90AA1 and cytoplasmic tryptophan-tRNA ligase (WARS) were most strongly upregulated. Indeed, under inflammatory conditions, heat shock proteins (HSPs) can act as chaperones to facilitate antigen presentation and enhance the immune response [42]. In line with our results, Ferreira *et al.* also described upregulation of WARS in DCs following LPS + IFN-γ treatment [14]. WARS is an ubiquitous enzyme responsible for the association of tryptophan with its specific tRNA, resulting in Trp-tRNA complex used for protein synthesis. Therefore, IFN-γ seems to affect tryptophan metabolism in dendritic cells, which is also in line with the report that WARS mRNA expression in peripheral blood mononuclear cells is dependent on IFN-γ [43]. However, the exact role of WARS in DC-mediated T cell activation remains to be determined. After 32 h of IFN-γ stimulation, the effect on the DC proteome was less pronounced, as only 4 proteins were downregulated, including PPIA involved in

immune regulation and activation [28] and FGR, a tyrosine-protein kinase involved in cell migration regulating cytoskeletal reorganization [44]. Together these findings may suggest that IFN-γ treatment induces strong effects early after treatment, reminiscent of accelerated maturation, whereas at later time point, the changes reflect a less active state.

Interestingly, in contrast to 32 h of treatment with IFN-γ, short-term (6 h) stimulation of DCs with Th2-inducing SEA promoted strong expression of PPIA , also known as Cyclophilin A (CyA), which is the primary binding protein of Cyclosporin A, an immunosuppressive drug. The cyclophilin and cyclosporine complex, leads to anti-inflammatory responses [28, 45]. Increased levels of cyclophilin A have been reported following oxidative stress response [28] as well as during fibrosis [46]. Interestingly, a recent study found that CyA is highly expressed in both worm and SEA of *S. japonicum* and showed that injection of schistosome CyA facilited Th2 responses [47]. As both SEA, which is an antigenic mix, as well as ω-1, a pure SEA-derived protein, induce CyA, it is unlikely that in our model CyA is a parasite-derived protein. Moreover, the downregulation of CyA in IFN-γ conditioned DCs would also suggest that this is a molecule expressed by DCs, that is involved in DC polarization. The protein FGR was also downregulated after 32 h SEA treatment similar to that seen after IFN-γ stimulation.

The most profound effect of Th2-inducing stimuli was observed after 32h of stimulation, when SEA and ω-1 both strongly increased expression of ribosomal protein RPLP2. The ribosomal proteins are known for playing an important role in ribosome assembly and protein translation, suggesting that SEA and ω-1 are affecting these processes. However, they can also have extra-ribosomal functions. For instance, stress responses can be associated with increased levels of ribosomal proteins that in turn affect immune signaling [48]. Whether or not SEA- and ω-1-induced RPLP2 expression serves extra-ribosomal functions requires further investigation. Another upregulated protein was synaptic vesicle membrane protein VAT-1 homolog, known as negative regulator of mitochondrial fusion, which works in cooperation with mitofusin proteins (MFN1-2) [49]. Decrease in mitochondria fusion will lead to impairment of the oxidative phosporylation (OXPHOS) [50]. This finding suggests that SEA and ω-1 may affect cellular metabolism. Recent studies have indicated that modulation of metabolic pathways within dendritic cells can regulate DC function and the outcome of the immune response [51, 52]. Whether ω-1 and SEA skew responses towards Th2 through changing cellular metabolism, requires further studies. In addition, SEA and ω-1 decreased expression of CD44 and suppressed LPS-induced upregulation of HLA-B. Interestingly, CD44 expression by DCs was shown to promote CD4 T cell proliferation [31]. Together, these findings may suggest that Th2-inducing conditions interfere with efficient antigen presentation to T cells. It has been suggested that T cells are polarized towards Th2 if the interaction between DCs and T cells is weak [53-55]. In line with this, it was demonstrated that ω-1 reduces the capacity of bone marrow-derived DCs to form T cell-DC conjugates [8]. Also our own preliminary data point towards a reduced ability of SEA and ω-1-stimulated DCs to expand $CD4^+$ T cells, compared to Th1 polarizing DCs (data not shown).

In conclusion, our work has identified the FTICR-ion trap cluster as an appropriate method for quantitative high-throughput analysis of cell lysates. Our data on DC polarization suggest that pro-Th1 DCs undergo accelerated maturation compared to LPS-DCs, and indicate that pro-Th2 DCs may affect cellular metabolism and decrease expression of proteins involved in antigen processing and presentation. Future research should therefore focus on studying the contribution of metabolic pathways, TCR signaling, and the possible relation between the two, to further dissect the mechanisms of helminth-induced T helper 2 polarization via dendritic cells. Moreover, this

proteomic approach will also be a valuable tool in future studies to assess in unbiased manner the proteomes DCs that favor induction of Th17 and Tregs, that together with the current work could function as important resource for DC biologists. Finally, such investigations will not only improve our fundamental understanding of DC biology, but will also help in the identification of proteins or pathways that can targeted in DCs to shape their Th cell-polarizing characteristics. This could be particularly important for the rational design of DC-based immunotherapies as well as for development and/or improving efficacy of vaccines against parasitic as well as other infections.

ACKNOWLEDGEMENTS

This project was supported by the EU (HEALTH-F3-2009-241642). The authors thank The Indonesian Directorate General of Higher Education (DIKTI)-Leiden University for providing a PhD scholarship to Maria M. M. Kaisar.

REFERENCES

1. Steinman, R.M. and Z.A. Cohn, *Identification of a novel cell type in peripheral lymphoid organs of mice. I. Morphology, quantitation, tissue distribution.* J Exp Med, 1973. **137**(5): p. 1142-62.
2. Kapsenberg, M.L., *Dendritic-cell control of pathogen-driven T-cell polarization.* Nat Rev Immunol, 2003. **3**(12): p. 984-93.
3. Tato, C.M. and J.J. O'Shea, *Immunology: what does it mean to be just 17?* Nature, 2006. **441**(7090): p. 166-8.
4. Zelante, T., et al., *IL-17/Th17 in anti-fungal immunity: what's new?* Eur J Immunol, 2009. **39**(3): p. 645-8.
5. Hussaarts, L., M. Yazdanbakhsh, and B. Guigas, *Priming dendritic cells for th2 polarization: lessons learned from helminths and implications for metabolic disorders.* Front Immunol, 2014. **5**: p. 499.
6. Mathieson, W. and R.A. Wilson, *A comparative proteomic study of the undeveloped and developed Schistosoma mansoni egg and its contents: the miracidium, hatch fluid and secretions.* Int J Parasitol, 2010. **40**(5): p. 617-28.
7. Everts, B., et al., *Omega-1, a glycoprotein secreted by Schistosoma mansoni eggs, drives Th2 responses.* J Exp Med, 2009. **206**(8): p. 1673-80.
8. Steinfelder, S., et al., *The major component in schistosome eggs responsible for conditioning dendritic cells for Th2 polarization is a T2 ribonuclease (omega-1).* J Exp Med, 2009. **206**(8): p. 1681-90.
9. Everts, B., et al., *Schistosome-derived omega-1 drives Th2 polarization by suppressing protein synthesis following internalization by the mannose receptor.* J Exp Med, 2012. **209**(10): p. 1753-67, s1.
10. Pereira, S.R., et al., *Changes in the proteomic profile during differentiation and maturation of human monocyte-derived dendritic cells stimulated with granulocyte macrophage colony stimulating factor/interleukin-4 and lipopolysaccharide.* Proteomics, 2005. **5**(5): p. 1186-98.
11. Gundacker, N.C., et al., *Cytoplasmic proteome and secretome profiles of differently stimulated human dendritic cells.* J Proteome Res, 2009. **8**(6): p. 2799-811.
12. Ferret-Bernard, S., R.S. Curwen, and A.P. Mountford, *Proteomic profiling reveals that Th2-inducing dendritic cells stimulated with helminth antigens have a 'limited maturation' phenotype.* Proteomics, 2008. **8**(5): p. 980-93.
13. Ferret-Bernard, S., et al., *Plasma membrane proteomes of differentially matured dendritic cells identified by LC-MS/MS combined with iTRAQ labelling.* J Proteomics, 2012. **75**(3): p. 938-48.
14. Ferreira, G.B., et al., *Protein-induced changes during the maturation process of human dendritic cells: A 2-D DIGE approach.* Proteomics Clin Appl, 2008. **2**(9): p. 1349-60.
15. Richards, J., et al., *Integrated genomic and proteomic analysis of signaling pathways in dendritic cell differentiation and maturation.* Ann N Y Acad Sci, 2002. **975**: p. 91-100.
16. Johansson, A., et al., *Identification of genetic variants influencing the human plasma proteome.* Proc Natl Acad Sci U S A, 2013. **110**(12): p. 4673-8.
17. Palmblad, M., et al., *A novel mass spectrometry cluster for high-throughput quantitative proteomics.* J Am Soc Mass Spectrom, 2010. **21**(6): p. 1002-11.
18. Hussaarts, L., et al., *Rapamycin and omega-1: mTOR-dependent and -independent Th2 skewing by human dendritic cells.* Immunol Cell Biol, 2013. **91**(7): p. 486-9.
19. Smith, R.D., et al., *An accurate mass tag strategy for quantitative and high-throughput proteome measurements.* Proteomics, 2002. **2**(5): p. 513-23.

20. Wolstencroft, K., et al., *The Taverna workflow suite: designing and executing workflows of Web Services on the desktop, web or in the cloud.* Nucleic Acids Res, 2013. **41**(Web Server issue): p. W557-61.
21. Craig, R. and R.C. Beavis, *TANDEM: matching proteins with tandem mass spectra.* Bioinformatics, 2004. **20**(9): p. 1466-7.
22. Kolter, T. and K. Sandhoff, *Principles of lysosomal membrane digestion: stimulation of sphingolipid degradation by sphingolipid activator proteins and anionic lysosomal lipids.* Annu Rev Cell Dev Biol, 2005. **21**: p. 81-103.
23. Palmblad, M., et al., *Chromatographic alignment of LC-MS and LC-MS/MS datasets by genetic algorithm feature extraction.* J Am Soc Mass Spectrom, 2007. **18**(10): p. 1835-43.
24. Keller, A., et al., *Empirical statistical model to estimate the accuracy of peptide identifications made by MS/MS and database search.* Anal Chem, 2002. **74**(20): p. 5383-92.
25. Lee, S.Y. and Y. Choi, *TRAF1 and its biological functions.* Adv Exp Med Biol, 2007. **597**: p. 25-31.
26. Katunuma, N., et al., *Insights into the roles of cathepsins in antigen processing and presentation revealed by specific inhibitors.* Biol Chem, 2003. **384**(6): p. 883-90.
27. Martinez-Pomares, L., *The mannose receptor.* J Leukoc Biol, 2012. **92**(6): p. 1177-86.
28. Nigro, P., G. Pompilio, and M.C. Capogrossi, *Cyclophilin A: a key player for human disease.* Cell Death Dis, 2013. **4**: p. e888.
29. Saito, K., et al., *Heat shock protein 90 associates with Toll-like receptors 7/9 and mediates self-nucleic acid recognition in SLE.* Eur J Immunol, 2015. **45**(7): p. 2028-41.
30. Connor, L.M., et al., *Th2 responses are primed by skin dendritic cells with distinct transcriptional profiles.* J Exp Med, 2017. **214**(1): p. 125-142.
31. Termeer, C., et al., *Targeting dendritic cells with CD44 monoclonal antibodies selectively inhibits the proliferation of naive CD4+ T-helper cells by induction of FAS-independent T-cell apoptosis.* Immunology, 2003. **109**(1): p. 32-40.
32. Ferreira, G.B., C. Mathieu, and L. Overbergh, *Understanding dendritic cell biology and its role in immunological disorders through proteomic profiling.* Proteomics Clin Appl, 2010. **4**(2): p. 190-203.
33. Strittmatter, E.F., et al., *Proteome analyses using accurate mass and elution time peptide tags with capillary LC time-of-flight mass spectrometry.* J Am Soc Mass Spectrom, 2003. **14**(9): p. 980-91.
34. Jaitly, N., et al., *Robust algorithm for alignment of liquid chromatography-mass spectrometry analyses in an accurate mass and time tag data analysis pipeline.* Anal Chem, 2006. **78**(21): p. 7397-409.
35. Alvarez, D., E.H. Vollmann, and U.H. von Andrian, *Mechanisms and consequences of dendritic cell migration.* Immunity, 2008. **29**(3): p. 325-42.
36. Matsue, H., et al., *Generation and function of reactive oxygen species in dendritic cells during antigen presentation.* J Immunol, 2003. **171**(6): p. 3010-8.
37. Yamada, H., et al., *LPS-induced ROS generation and changes in glutathione level and their relation to the maturation of human monocyte-derived dendritic cells.* Life Sci, 2006. **78**(9): p. 926-33.
38. Rivollier, A., et al., *High expression of antioxidant proteins in dendritic cells: possible implications in atherosclerosis.* Mol Cell Proteomics, 2006. **5**(4): p. 726-36.
39. Yamakita, Y., et al., *Fascin1 promotes cell migration of mature dendritic cells.* J Immunol, 2011. **186**(5): p. 2850-9.
40. Buhligen, J., et al., *Lysophosphatidylcholine-mediated functional inactivation of syndecan-4 results in decreased adhesion and motility of dendritic cells.* J Cell Physiol, 2010. **225**(3): p. 905-14.
41. Rescigno, M., et al., *Dendritic cell survival and maturation are regulated by different signaling pathways.* J Exp Med, 1998. **188**(11): p. 2175-80.
42. Srivastava, P., *Roles of heat-shock proteins in innate and adaptive immunity.* Nat Rev Immunol, 2002. **2**(3): p. 185-94.
43. Boasso, A., et al., *Regulation of indoleamine 2,3-dioxygenase and tryptophanyl-tRNA-synthetase by CTLA-4-Fc in human CD4+ T cells.* Blood, 2005. **105**(4): p. 1574-81.
44. Suen, P.W., et al., *Impaired integrin-mediated signal transduction, altered cytoskeletal structure and reduced motility in Hck/Fgr deficient macrophages.* J Cell Sci, 1999. **112 (Pt 22)**: p. 4067-78.
45. Obchoei, S., et al., *Cyclophilin A: potential functions and therapeutic target for human cancer.* Med Sci Monit, 2009. **15**(11): p. Ra221-32.
46. Yuan, Y., et al., *Proteomic identification of cyclophilin A as a potential biomarker and therapeutic target in oral submucous fibrosis.* Oncotarget, 2016.
47. Li, J., et al., *Cyclophilin A from Schistosoma japonicum promotes a Th2 response in mice.* Parasit Vectors, 2013. **6**: p. 330.
48. Zhou, X., et al., *Ribosomal proteins: functions beyond the ribosome.* J Mol Cell Biol, 2015. **7**(2): p. 92-104.
49. Eura, Y., et al., *Identification of a novel protein that regulates mitochondrial fusion by modulating mitofusin (Mfn) protein function.* J Cell Sci, 2006. **119**(Pt 23): p. 4913-25.

50. Mishra, P. and D.C. Chan, *Metabolic regulation of mitochondrial dynamics*. J Cell Biol, 2016. **212**(4): p. 379-87.
51. Pearce, E.J. and B. Everts, *Dendritic cell metabolism*. Nat Rev Immunol, 2015. **15**(1): p. 18-29.
52. Pearce, E.L. and E.J. Pearce, *Metabolic pathways in immune cell activation and quiescence*. Immunity, 2013. **38**(4): p. 633-43.
53. Constant, S., et al., *Extent of T cell receptor ligation can determine the functional differentiation of naive CD4+ T cells*. J Exp Med, 1995. **182**(5): p. 1591-6.
54. Hosken, N.A., et al., *The effect of antigen dose on CD4+ T helper cell phenotype development in a T cell receptor-alpha beta-transgenic model*. J Exp Med, 1995. **182**(5): p. 1579-84.
55. van Panhuys, N., F. Klauschen, and R.N. Germain, *T-cell-receptor-dependent signal intensity dominantly controls CD4(+) T cell polarization In Vivo*. Immunity, 2014. **41**(1): p. 63-74.

Chapter 6

Dectin-1/2-induced autocrine PGE_2 signalling licenses dendritic cells to prime Th2 responses

MARIA M. M. KAISAR[1, 2], MARTIN GIERA[3], MANUEL RITTER[4], CARLOS DEL FRESNO[5], HULDA JÓNASDÓTTIR[3], ALWIN J. VAN DER HAM[1], LEONARD R. PELGROM[1], GABRIELE SCHRAMM[6], LAURA E. LAYLAND[7], DAVID SANCHO[5], CLARISSA P. DA COSTA[8], MARIA YAZDANBAKHSH[1, #], BART EVERTS[1, #]

[1]Department of Parasitology, Leiden University Medical Center (LUMC), Leiden, The Netherlands
[2]Department of Parasitology, Faculty of Medicine, Universitas Indonesia, Jakarta, Indonesia
[3]Center of Proteomics and Metabolomics, LUMC, Leiden, The Netherlands
[4]Institure of Medical Microbiology, Immunology and Parasitology (IMMIP), University Hospital of Bonn, Germany
[5]Centro Nacional de Investigaciones Cardiovasculares "Carlos III"(CNIC), Madrid, Spain
[6]Borstel Institute Germany
[7]IMMIP and German Center for Infection Research (DZIF), partner site, Bonn-Cologne, Bonn, Germany
[8]Institute for Microbiology, Immunology and Hygiene (MIH), Technische Universität München (TUM), Germany
[#]Contributed equally

Submitted

ABSTRACT

The molecular mechanisms through which dendritic cells (DCs) prime Th2 responses, including those elicited by parasitic helminths, remain incompletely understood. Here we report that egg antigens from *Schistosoma mansoni* (SEA), that are well known to drive potent Th2 responses, triggers DCs to produce Prostaglandin E2 (PGE_2), which subsequently in an autocrine manner induces OX40L expression to licence these DCs to drive Th2 responses. Mechanistically, SEA was found to promote PGE_2 synthesis through Dectin-1 and Dectin-2 and via a downstream signalling cascade involving Syk, ERK, $cPLA_2$, and COX-1/2. These findings were supported by *in vivo* data showing that Th2 priming by SEA was dependent on Syk expression by DCs and that Dectin-$2^{-/-}$, and to a lesser extent Dectin-$1^{-/-}$ mice, displayed impaired Th2 responses and reduced egg-driven granuloma formation following *S. mansoni* infection. In summary, we identified a novel pathway in DCs involving Dectin-1/2-Syk-PGE_2-OX40L through which Th2 immune responses are induced.

Keyword:
Dendritic cells, Soluble Egg Antigen, Omega-1, Prostaglandin E2, OX40L, Dectin-1, Dectin-2, Lipidomics

INTRODUCTION

Dendritic cells (DCs) are key players in the immune system because of their unique capacity to prime antigen-specific Th1, Th2, Th17 or regulatory T cell (Tregs) responses tailored against the pathogen they encounter [1-3]. It is well-known that allergens and parasitic helminths can evoke strong type 2 immune responses, that largely depends on DCs that prime Th2 responses [4-8]. However, the molecular mechanisms through which DCs prime Th2 responses are still not fully defined.

Soluble egg antigens (SEA) from *Schistosoma mansoni* are a widely used antigen mixture to study Th2 responses to helminths. SEA is well recognized for its ability to condition DCs for priming of Th2 responses [9-13]. Omega-1 (ω-1), a glycosylated T2 RNase [14], present in SEA was found to be a major Th2-polarizing molecule [9, 15-18]. Mechanistic studies revealed that ω-1 is bound and internalized via its glycans by the mannose receptor (MR) and that, following uptake, ω-1 impairs protein synthesis in an RNase-dependent manner that is essential for conditioning of DCs for Th2 polarization [9, 10]. However, while ω-1 by itself was sufficient to condition DCs for Th2 polarization, SEA from which ω-1 was depleted still retained most of its Th2 priming potential both *in vitro* and *in vivo*. Moreover, eggs in which ω-1 expression was silenced [19] retained most of their Th2-polarizing potential, suggesting that there are additional mechanisms through which DCs become conditioned by schistosome eggs to prime Th2 responses [20].

Lipid mediators (LMs), which arise from the enzymatic oxidation of polyunsaturated fatty acids (PUFAs), such as arachidonic acid (AA), docosahexaenoic acid or linoleic acid (DHA), play an important role in immunological responses. In particular, prostanoids such as tromboxanes and prostaglandins (PGs), that are derivatives of AA and that are primarily released by myeloid cells including macrophages and DCs, have been shown to have the capacity to influence immune cells by affecting their migration, differentiation, effector function and/or polarization [21-24]. Interestingly, just like their mammalian host, parasitic worms are able to synthesize PUFAs and LMs. Especially PGs and leukotrienes have been detected in many species of helminths including *S. mansoni* and are involved in different aspects of life cycle regulation and sexual maturation [25, 26]. Additionally, cercariae from *S. mansoni* have been shown to promote LM synthesis in host cells such as in keratinocytes [27]. Thus far, efforts to identify molecules responsible for Th2 polarization by helminths have primarily focused on glycans and (glyco)proteins. Whether LMs directly derived from schistosomes or derived from immune cells in response to infection by this parasite, may additionally affect immune polarization remains unknown.

To identify potential novel pathways through which Th2 responses are induced by *S. mansoni*, we set out to assess the role of PUFAs and LMs in *S. mansoni* egg-driven Th2 polarization. We here report that SEA contains various PUFAs and LMs, and that additionally SEA, independently of ω-1, induces DCs to generate a number of LMs, including Prostaglandin E2 (PGE_2). We show that this *de novo* synthesis of PGE_2 by SEA-stimulated DCs is driven by signalling through Dectin-1 and Dectin-2 and is crucial for Th2 priming. Mechanistically, we provide evidence that this PGE_2 through autocrine signalling induces OX40L expression, to licence DCs to prime Th2 responses. Finally, we show that this pathway is also crucial for Th2 priming by *S. mansoni in vivo*.

MATERIALS AND METHODS

Mice

Dectin-$1^{-/-}$ and Dectin-$2^{-/-}$ (C57BL/6 background) were housed and bred at the MIH, TUM, Germany, under SPF conditions. $Itgax^{cre}$ $syk^{fl/fl}$ mice [55] were housed and bred at the CNIC,

Madrid, Spain, under SPF conditions. All animal experiments were performed in accordance with local government regulations, and the EU Directive 2010/63EU and Recommendation 2007/526/EC regarding the protection of animals used for experimental and other scientific purposes and approved by the Regiuerung von Oberbayern, animal license number 55.2-1-54-2532-28-1.

Preparation and purification of *S. mansoni* egg-derived antigens

SEA, IPSE/α-1, ω-1 and SEAΔα-1/ω-1 from *S.mansoni* eggs were prepared and isolated as described previously [3, 20].

Human DC culture, stimulation and analysis

Peripheral blood mononuclear cells were isolated from venous blood of healthy volunteers by density centrifugation of Ficoll as described before [10]. Monocytes were isolated by positive magnetic cell sorting using CD14-microbeads (Miltenyi Biotech, Bergisch Gladbach, Germany) and cultured in 10% FCS RPMI medium supplemented with 20 ng/mL rGM-CSF (BioSource/Invitrogen, Carlsbad, CA, USA) and 0.86 ng/mL of rIL-4 (R&D System, Minneapolis, MN, USA). On day two, medium including supplements was replaced. In the presence or absence (if indicated) of 100 ng/mL ultrapure LPS (*E. coli* 0111 B4 strain, InvivoGen, San Diego, CA, USA), immature moDCs were stimulated on day 6 with indicated reagents: SEA (50 μg/mL), ω-1 (500 ng/mL), IPSE (500 ng/mL), SEAΔα-1/ω-1 (50 μg/mL), PGE_2 (2.5 ng/mL, Cayman), IFN-γ (1000 U/mL) as Th1 control, 0.1 mg/mL Zymosan (Sigma-Aldrich Z4250). Alternatively, moDCs were stimulated with 2.5 ng/mL LXA_4, 2.5 ng/mL PGD_2, 12.5 μg/mL 5-HETE, 12.5 μg/mL 8-HETE, 12.5 μg/mL 11-HETE, 25 μg/mL 9-HODE or 25 μg/mL 13-HODE (all Cayman). For blocking experiments cells were pre-incubated for 60 min at 37 °C with 20 μg/mL anti-DC-SIGN (clone AZN-D1, Beckman Coulter), anti-MR (clone 15.2, Biolegend), anti-Dectin-1 (clone #259931, R&D System, Minneapolis, MN, USA), anti-Dectin-2 (clone Q7-4B5, InvivoGen), 20 μg/mL IgG1 control antibody for both anti-DC-SIGN and anti-MR, IgG2a (clone RTK2758, Biolegend) control antibody for anti-Dectin-1 and anti-Dectin-2, 1 μM R406, 4 μM UO126 (Merk-Calbiochem), 1 μM Pyrrophenone (Merck-Calbiochem), 10 μM SC-236 (Sigma-Aldrich) in combination with 10 μM Indometachine (Sigma-Aldrich), 10 μg/mL neutralizing anti-PGE_2 antibody (2B5, Cayman Chemical, Ann Arbor, USA), 10 μM EP2 (AH6809, Cayman Chemical), 10 μM EP4 (AH23848, Cayman Chemical) receptor antagonist. After 24 or 48 h of stimulation, surface expression of co-stimulatory molecules was determined by flow cytometry (FACS-Canto, BD Biosciences, Breda, The Netherlands) using the following antibodies: CD14-HV450 (clone MΦP9), CD86-FITC (clone 2331 FUN-1), CD40-APC (clone 5C3), CD80 Horizon V450 (clone L307.4) (all BD Biosciences), HLA-DR APC-eFluor 780 (clone LN3) (eBioscience, San Diego, CA, USA), CD83 PE (clone HB15e), CD1a PE (clone BL6) (both Beckman-Coulter, Fullerton, CA, USA) and CD252/OX40L FITC (clone ANC10G1, Ancell). Only live cells, which were negative for 7-AAD (eBiosciences) were included in the analysis.

Cytokine detection

1×10^4 48 h-matured moDCs were co-cultured with $1x10^4$ CD40L-expressing J558 cells for 24 h and supernatants were collected to determine IL-12p70 levels, using mouse-anti-human IL-12 (Clone 20C2) as capture antibody and biotinylated mouse-anti-human IL-12 (Clone C8.6) (both BD Biosciences) in a sandwich ELISA.

Human DC and T cell co-culture and determination of T cell polarization

For analysis of T-cell polarization, 5×10^3 48 h-pulsed moDCs were cultured with 2×10^4 allogenic naive $CD4^+$ T cells for 11 days in the presence of *Staphylococcal enterotoxin B* (10 pg/mL). On day 6 and 8, rhuIL-2 (10 U/mL, R&D System) was added to expand the T cells. Intracellular cytokine production was analysed after re-stimulation with 100 ng/mL phorbol myristate acetate plus 2 μg/mL ionomycin for 6 h, 10 μg/mL brefeldin A was added during the last 4 h. Subsequently the cells were fixed with 1.9% paraformaldehyde (all Sigma-Aldrich). The cells were permeabilized with 0.5% saponin (Sigma-Aldrich) and stained with PE- and FITC-labelled antibodies against IL-4 and IFN-γ respectively (BD Biosciences). For blocking experiments moDC-T cell co-cultures were pre-incubated for 15 min with 10 μg/mL neutralizing PGE_2 antibody (2B5, Cayman Chemical, Ann Arbor, USA), 10 μM EP2 (AH6809, Cayman Chemical), 10 μM EP4 (AH23848, Cayman Chemical) receptor antagonist, 10 μg/mL anti-OX40L antibody (Clone 159403, R&D Systems), or IgG1 control antibody (clone P3.6.2.8.1, eBioscience).

Detection of reactive oxygen species

Detection of ROS was performed according to a published protocol (http://www.bio-protocol.org/e313) with minor modifications. In brief, after 6 h of stimulation moDCs were harvested and washed using 1% FCS RPMI and re-suspended in 50 μl of a mix containing 10 μM CM-H_2DCFDA (C6827, Invitrogen) and CD1a BV421 (clone HI149, Biolegend), followed by an incubation at 37 °C for 30 min. 7AAD was added prior to sample measurement. ROS levels were quantified by flow cytometry.

Western Blot

MoDCs were harvested after 8 h of stimulation. Then, cells were washed twice with PBS before being lysed in EBSB buffer (8% [w/v] glycerol, 3% [w/v] SDS and 100 mM Tris–HCl [pH 6.8]). Lysates were immediately boiled for 5 min and their protein content was determined using a bicinchoninic acid protein assay kit (Pierce). Proteins were separated by SDS-PAGE followed by transfer to a PVDF membrane. Membranes were blocked for 1 h at room temperature in TTBS buffer (20 mM Tris–HCl [pH 7.6], 137 mM NaCl, and 0.25% [v/v] Tween 20) containing 5% (w/v) fat free milk and incubated overnight with primary antibodies. The primary antibodies used were: COX-1 (Cell Signalling), COX-2 (Cell Signalling) and actin (Millipore). The membranes were then washed in TTBS buffer and incubated with horseradish peroxidase-conjugated secondary antibodies for 1 h at room temperature. After washing, blots were developed using enhanced chemiluminescence.

Syk and ERK phosphorylation

For detection of phosphorylation of Syk (pSyk) and ERK (pERK), 2.5×10^4 immature moDCs were seeded overnight in a 96 well flat bottom plate. moDC were stimulated with SEA (50 μg/ml), SEAΔα-1/ω-1 (50 μg/mL) or ω-1 (500 ng/mL) in the presence or absence of blocking antibodies or inhibitors (R406, anti-MR, anti-Dectin-1, anti-Dectin-2, combination of anti-Dectin-1 and anti-Dectin-2 or IgG1 and IgG2 control antibodies) for indicated periods and the moDCs were fixed for 15 min with 4% ultrapure formaldehyde (Polyscience) directly in the plate. The cells were harvested and washed first with PBS and then with 0.5% of saponin for permeabilization. Cell were Intracellularly stained with anti-phospo-Try525/526 Syk PE (clone C87C1) and anti-phospo-p44/42 MAPK (Erk1/2) AF488 (clone E10) (both Cell Signalling Technology). Following 2 h incubation at

room temperature, cells were washed with 0.5% of saponin and Syk and ERK phosphorylation was determined by flow cytometry.

cPLA$_2$ activity

Cytosolic phospholipase A_2 (cPLA$_2$) activity was determined according to the manufacturer's recommendation (Cayman Chemical). Briefly, 1×10^6 moDCs stimulated with indicated reagents for 8 h were harvested. MoDCs were lysed with lysis buffer (containing 50 mM Hepes, pH 7.4, 1 mM EDTA, NP-40, protease and phosphatase inhibitors) followed by 4 round of sonication for 10 second. The cells were then concentrated using a 30 KDa filter (Millipore, Amicon). To 10 µl cell lysate, 200 µl substrate solution was added to initiate the reaction, the plate was briefly shaken and incubated for 1 h at room temperature. To stop the reaction 10 µl DTNB/EGTA was added, the plate was briefly shaken, followed by 5 min incubation at room temperature. The cPLA$_2$ activity was measured using a plate reader with absorbance of 405 nm.

Antigen binding and uptake by moDCs

SEA was fluorescently labelled with PF-647 using promofluor labelling kit (Promokine) according to the manufacturer's recommendations. Approximately 2×10^4 immature moDCs per well were seeded in a flat bottom 96-well plate. Where indicated, cells were pre-incubated with 20 µg/mL of anti-MR, anti-DC-SIGN, anti-Dectin-1, anti-Dectin-2 or control antibodies at 37 °C for 45 min. Subsequently, cells were incubated with 2 µg/mL PF-647 labelled SEA at 37 °C for 45 min for testing both binding and uptake of the antigen. After 45 min cells were washed with PBS followed by flow cytometry measurement.

Liquid chromatography tandem mass spectrometry analysis of PUFAs and LMs

20 µl of SEA or supernatants from each condition were collected 0, 6, 12 and 24 h after stimulation and stored at -80 °C until analysis. A volume of 10 µl sample was mixed with 28.4 µL methanol (MeOH) and 1.6 µL of internal standard (IS, containing: Leukotriene B4-d4, 15-HETE-d8, PGE$_2$-d4, and DHA-d5 at a concentration of 50 ng/mL in MeOH). The samples were subsequently kept at -20 °C for 10 min for completion of protein precipitation, followed by centrifugation for 10 min, 16000 ×*g* at 4 °C. Subsequently samples were diluted 1:1 with water and transferred into auto-sampler vials. Liquid chromatography tandem mass spectrometry (LC-MS/MS) analysis using a QTrap 6500 (Sciex, OudekERK aan den Ijsel, The Netherlands) was carried out as described previously [56, 57].

SEA immunization and *S. mansoni* infection

Mice were injected s.c. with SEA (20 µg) in the hind footpad. Seven days later, cells from both draining and non-draining lymph nodes were isolated and analysed. For *S. mansoni* infection, mice were infected with 100 cercariae from a Brazilian strain of *S. mansoni* obtained from our in house cycle of infected *Biomphalaria glabrata* snails (also of Brazilian origin). Mice were killed after 8 weeks of infection. Liver samples were fixed in 4% buffered formalin and embedded in paraffin. Sections (4 µm) were stained with Masson blue and examined microscopically (Axioskop; Zeiss) for measuring the diameters to calculate the size of spherical granulomas. To determine the parasite burden, pieces of weighed liver and intestine samples from individual mice were digested in 4% KOH (Roth) at 37 °C for 4 h. After centrifugation, the released eggs were microscopically counted. The absolute number of eggs in the liver and intestine was then calculated in accordance to the

total organ weight. Worm burden was calculated as adult worm recovery after portal perfusion and microscopic examination of livers and intestines.

Analyses of murine T cell responses.

Antigen-specific recall responses were determined by culturing 3×10^5 LN or spleen cells per well in 96-well round bottom plates in 200 µl complete medium (RPMI containing 10% fetal calf serum, 100 U/ml penicillin/streptomycin, and 2 mM l-glutamine) in the presence of 20 µg/ml SEA or 1 µg/ml anti-CD3/CD28 antibody (eBioscience). 2.5 µg/ml IL-4R blocking antibody (M1) was added to the cultures to retain IL-4 in culture supernatants. 72 h later, culture supernatants were stored for cytokine determination. Cell culture supernatants were analysed for cytokines using the Cytokine Bead Array (BD) or the mouse Ready-Set-Go ELISA kits (eBioscience) according to the manufacturer's recommendation. Samples were analysed on a BD Canto II Flow Cytometer and Sunrise™ ELISA microplate reader (Tecan), respectively. Alternatively, assessment of cytokine production by intracellular staining of T cells from LNs was determined after polyclonal re-stimulation in 96-well round bottom plates for 5 h with PMA (phorbol 12-myristate 13-acetate; 50 ng/ml) and ionomycin (1 µg/ml) in the presence of brefeldin A (10 µg/ml; all from Sigma-Aldrich) for the last 3 h. Afterwards cells were fixed with 4% PFA and subsequently stained in 0.5% saponin with the following antibodies: αCD44 (IM7), αIL-4 (11B11), IFN-γ (XMG1.2) and CD4 (RM4-5) (all BD Bioscience). Samples were analysed on a BD Canto II Flow Cytometer.

Statistical analysis

The heatmap was generated using Microsoft Excel. Data were analysed for statistical significance using two-way ANOVA test, two-sided paired Student's T-test or unpaired Student's T-test. Statistical analysis was performed using GraphPad Prism version 6.00 (GraphPad Software, La Jolla, CA USA) for Windows.

RESULTS

LM composition of SEA and supernatants of SEA-conditioned moDCs

As a first step towards the identification of LMs that may play a role in *S. mansoni* egg-driven Th2 polarization we used a sensitive LC-MS/MS based platform to identify a total of 55 PUFAs and LMs in SEA (Table S1). We discovered that SEA contains 22 out of 55 monitored analytes, including docosahexaenoic acid, linoleic acid and AA and in relative high abundance but also PGs such as PGE_2 and PGD_2 (Figure 1A). To assess potential consumption or uptake of such lipids or synthesis by DCs in response to SEA stimulation, we tested supernatants of moDCs at 0, 6, 12, and 24 h after stimulation with LPS, LPS+SEA and LPS+ω-1. We observed that levels of the majority of the LMs present in SEA decreased over time in DC culture supernatants following SEA stimulation, indicative of consumption/uptake or degradation (Figure 1B). Interestingly, we also observed that some of these lipids (i.e. 13-HODE, LXA_4, PGD_2 and PGE_2) were accumulating over time in DC culture supernatants in response to SEA stimulation both in the presence (Figure 1B and quantitated for PGE_2 in Figure 1C) or absence of LPS (Figure S1), suggestive of active production by moDCs in response to SEA. Importantly, stimulation of moDCs with LPS alone or LPS+ω-1 did not drive accumulation of any of these compounds in the supernatants (Figure 1B). These results show that SEA contains a wide range of LMs as well as induces the release of particular LMs by DCs.

A

	Lipid mediators	ng/mg SEA
1	LA	387,09
2	AA	97,71
3	DHA	49,05
4	9-HODE	16,18
5	AdA	11,29
6	13-HODE	10,5
7	EPA	9,72
8	15-HETE	4,16
9	DPA_{n-3}	3,29
10	5-HETE	2,88
11	12-HETE	2,48
12	8-HETE	2,32
13	11-HETE	1,43
14	PGE_2	1,31
15	LXA_4	0,5
16	8*S*,15*S*-diHETE	0,14
17	PGD_2	0,13
18	8-*iso*-$PGF_2\alpha$	0,13
19	6*t*,12*epi*-LTB_4	0,09
20	6-*trans*-LTB_4	0,06
21	18-HEPE	0,04
22	PDX	0,02

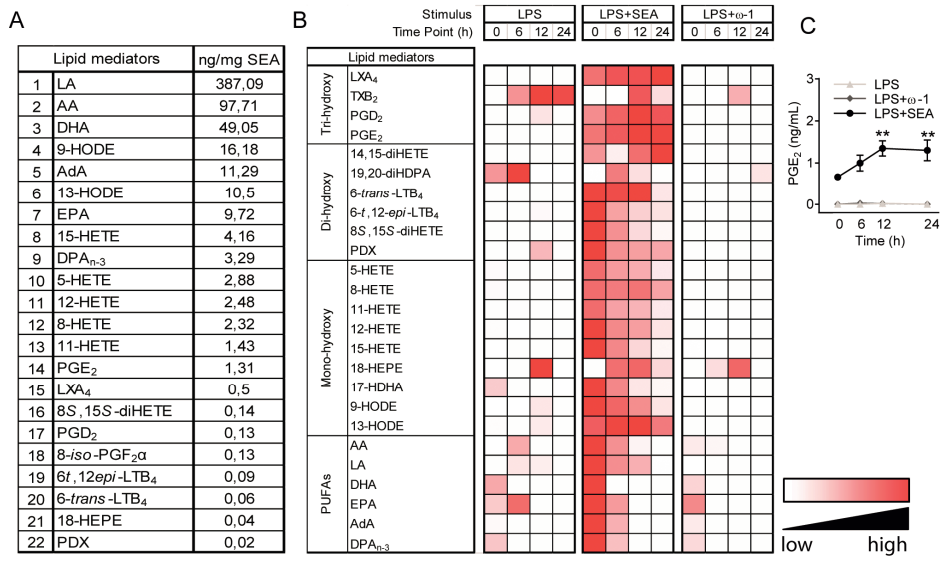

Figure 1. LM composition of SEA and in supernatants of SEA-conditioned moDCs
(A) Concentration of 22 LMs, out of 55 potentially detectable LMs, that are present in SEA from *S. mansoni* as determined by LC-MS/MS. LMs are ordered according to abundance and concentrations are determined based on internal standards. (B) MoDCs were pulsed with SEA or ω-1 in combination with LPS after which supernatants were collected at 0, 6, 12 and 24 h after stimulation. Relative amounts of PUFAs and LMs detected by LC-MS/MS in supernatants are shown in a heat-map. Data represents an average of three independent experiments. Colour coding is based on relative abundance of each lipid in comparison to other time points or stimulations. (C) PGE_2 concentration in supernatants from moDC cultures after stimulation with indicated reagents. Concentrations are determined based on an internal standard. Data represent mean ± SEM of four independent experiments. Statistical significance of different time points per condition compared to baseline (0 h) time point. *p<0.05, **p<0.01, ***p<0.001 based on two-way ANOVA test.

Th2 polarization by SEA is dependent on PGE_2 synthesis by moDCs in absence of ω-1

To test whether LMs present in SEA or generated by moDCs upon stimulation with SEA contribute to Th2 polarization by SEA, we stimulated moDCs with several of these LMs in concentrations similar to those found in SEA or in supernatants of SEA-stimulated moDCs and analysed their ability to condition DCs to induce Th2 polarization. Amongst all tested lipids, we identified PGE_2 as the only lipid capable of inducing Th2 polarization (Figure 2A). Based on this observation and given that ω-1 did not promote PGE_2 synthesis by moDCs (Figure 1B), we wondered whether PGE_2 may play a role in the previously observed ω-1-independent ability of SEA to prime Th2 responses [20]. To test this, we depleted ω-1 from SEA. Alongside ω-1, IPSE/α-1 was also depleted from this preparation, which is another glycoprotein present in SEA, but without Th2-priming capacity [20]. We found that treatment of moDCs with SEAΔα-1/ω-1 reduced expression of the Th1-polarizing cytokine IL-12 induced by LPS (Figure 2B) and promoted Th2 polarization, though less potently than total SEA (Figure 2C). In contrast to complete SEA, we could not detect PGE_2 in SEAΔα-1/ω-1 itself (time point 0 h in Figure 2D versus in Figure 1C), which suggests that during the depletion step of ω-1 and α-1 from SEA, PGE_2 was removed from SEA as well. Importantly, we observed that SEAΔα-1/ω-1 still promoted PGE_2 synthesis in moDCs (Figure 2D). This shows that SEA, in addition to containing PGE_2 itself, stimulates PGE_2 secretion by moDCs in an ω-1-independent fashion.

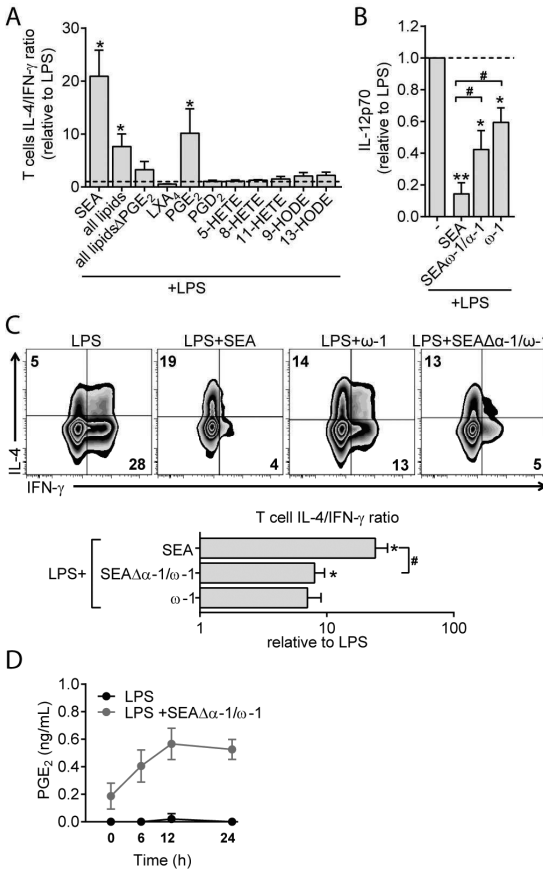

Figure 2. SEA stimulates PGE_2 secretion and primes Th2 responses independently from ω-1
(A) MoDCs stimulated with indicated lipids (concentration of 2.5 ng/mL for LXA_4, PGE_2 and PGD_2; 12,5 µg/mL for 5-HETE, 8-HETE and 11-HETE; 25 µg/mL 9-HODE and 13-HODE) were analysed for Th2 polarizing potential as described in Methods. The ratio of IL-4 over IFN-γ based on the intracellular cytokine staining was calculated relative to the control condition. (B) MoDCs were pulsed with indicated stimuli and subsequently co-cultured with a CD40L-expressing cell-line. Supernatants were collected after 24 h and IL-12p70 concentration were determined by ELISA. (C) T cell polarization was determined as in (A). Top and bottom panels show representative flow cytometry plots of intracellular staining of $CD4^+$ T cells for IL-4 and IFN-γ, and the ratio of IL-4 over IFN-γ ratio of these plots based on four experiments. Numbers in plots represent frequencies of cells in indicated quadrants. (D) PGE_2 levels as determined by LC-MS/MS in supernatants of moDCs stimulated with indicated stimuli. Data represent mean ± SEM of three independent experiments. *,#p<0.05 and **p<0.01 for significantly different with the LPS control (*) or between test condition (#) based on paired analysis (paired Student's T-test).

Next, we investigated the contribution of the synthesized PGE_2 by SEA-stimulated moDCs to ω-1-independent Th2 induction. Strikingly, when PGE_2 was neutralized using a specific anti-PGE_2 antibody during stimulation of moDCs with SEAΔα-1/ω-1, the ability of SEAΔα-1/ω-1-stimulated moDCs to drive Th2 polarization was totally lost (Figure 3A). In contrast, neutralization of PGE_2 in cultures of moDCs stimulated with ω-1 or complete SEA had no effect on the Th2-priming potential of these cells, which is consistent with our recently published study showing that ω-1, either alone or in the context of SEA can prime Th2 responses via other mechanisms [9, 10]. Moreover, we found that later neutralization of PGE_2 limited to the co-culture of SEAΔα-1/ω-1-stimulated moDCs with T cells did not impair Th2 polarization (Figure 3B), indicating that PGE_2 synthesized by moDCs does not act as a polarizing signal on T cells, but rather directly conditions moDCs in an autocrine manner to acquire a Th2-priming phenotype. In line with this observation, we found that simultaneous inhibition of the two major receptors of PGE_2, EP2 and EP4, on moDCs reduced the ability of SEAΔα-1/ω-1-stimulated moDCs to induce a Th2 response (Figure 3C). These results collectively demonstrate that SEA independently from ω-1 promotes PGE_2 synthesis by moDCs, which subsequently, in an autocrine manner, conditions these cells to acquire a Th2-polarizing phenotype.

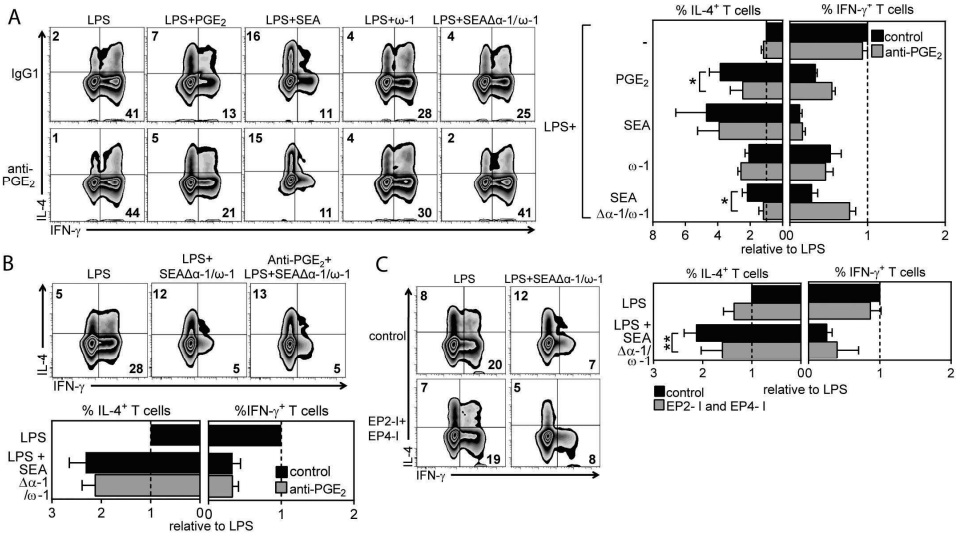

Figure 3. Omega-1-independent Th2 polarization by SEA is dependent on PGE_2 synthesis by moDCs
(A-C) T cell polarization assay as described in Figure 2A. (A) Neutralizing anti-PGE_2 antibody was added during stimulation of moDCs with indicated reagents or (B) during DC-T cell co-culture. (C) EP2 and EP4 receptor inhibitors were added during stimulation of moDCs with indicated stimuli. (A-C) Left: representative flow cytometry plots are shown of intracellular staining of $CD4^+$ T cells for IL-4 and IFN-γ. Numbers in plots represent frequencies of cells in indicated quadrants. Right: These data were used to calculate the fold change in frequency of $IL\text{-}4^+$ and $IFN\text{-}\gamma^+$ T cells polarized by moDCs stimulated with indicated stimuli relative the cytokine production by T cells polarized by LPS-stimulated moDCs, for which the values were set to 1. Bars represent mean ± SEM of at least four independent experiments. Significance was calculated based on the ratio of IL-4 over IFN-γ between conditions. *p<0.05 and **p<0.01 for significantly different from compared conditions based on paired analysis (paired Student's T-test).

OX40L is induced by SEA via PGE_2 signalling and is required for Th2 induction

MoDCs matured in the presence of PGE_2 are characterized by the expression of OX40L, a co-stimulatory molecule linked to Th2 polarization [28-30]. Moreover, an earlier study showed that moDCs stimulated with SEA express OX40L [3]. Indeed, we observed that stimulation of moDCs with PGE_2, SEA or SEAΔα-1/ω-1 induced expression of OX40L on moDCs, whereas ω-1 did not induce OX40L expression (Figure 4A). While both SEAΔα-1/ω-1 and SEA promote PGE_2 synthesis, OX40L induction by SEAΔα-1/ω-1 was lower than the levels induced by SEA. This might be explained by the fact that in contrast to SEAΔα-1/ω-1, SEA additionally contains pre-existing PGE_2 itself, resulting in higher overall concentrations of PGE_2 SEA-stimulated DCs are exposed to compared to SEAΔα-1/ω-1-primed DCs (Figure 1C versus Figure 2D). Importantly, neutralizing PGE_2 prevented the induction of OX40L expression by SEAΔα-1/ω-1 (Figure 4B). Finally, neutralizing OX40L during the co-culture with T cells significantly reduced the Th2-polarizing capacity of SEAΔα-1/ω-1-primed moDCs (Figure 4C). These data demonstrate that OX40L expression by SEAΔα-1/ω-1-conditioned-moDCs is dependent on PGE_2 and that subsequently induction of OX40L is important for Th2 polarization.

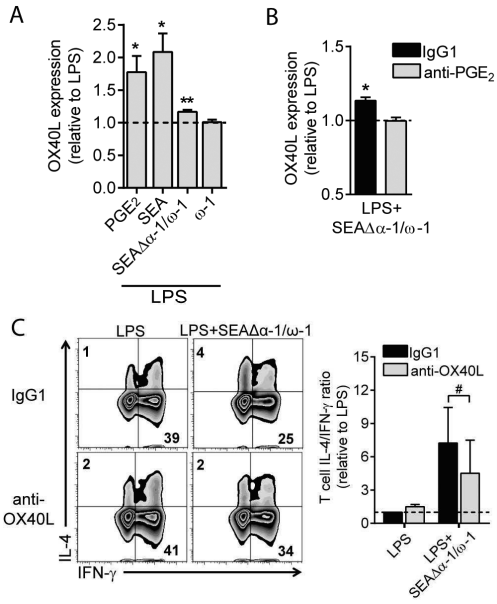

Figure 4. OX40L is induced by SEA via PGE_2 signalling and is required for Th2 induction
(A, B) MoDCs were stimulated as indicated for 48 h in the presence or absence of neutralizing anti-PGE_2 antibody after which expression of OX40L was analysed by flow cytometry. The fold change based on geometric mean fluorescence is shown relative to LPS, which is set to 1 (dashed line). (A) PGE_2 was taken along as positive control for OX40L expression. (C) T cell polarization assay as described in Figure 2C. Neutralizing OX40L antibody was added during the DC-T cell co-culture. Bar graphs represent means ± SEM of at least three independent experiments. *,#p<0.05, **,##p<0.01, ***,###p<0.001 for significant differences with the control conditions (*) or between test condition (#) based on paired analysis (paired Student's T-test).

SEA promotes PGE_2 synthesis and drives Th2 polarization via Dectin-1 and Dectin-2

Classically, central to the synthesis of PGE_2 is the release of AA from membrane phospholipids by $cPLA_2$, which can then be converted into PGs including PGE_2 through constitutively expressed COX-1 and stimulus-induced COX-2. We observed that SEA induced a small but consistent increase in $cPLA_2$ activity (Figure 5A). SEA did not change protein expression of COX-1 and was consistently expressed in all conditions. Moreover, SEA did not appear to promote COX-2 expression, nor to alter LPS-driven COX-2 expression (Figure 5B), suggesting that SEA primarily promotes PGE_2 synthesis through induction of $cPLA_2$ activation. Indeed, selective inhibition of $cPLA_2$ activity using pyrrophenone attenuated SEAΔα-1/ω-1-induced PGE_2 synthesis (Figure 5C). For these experiments in which we analysed the signalling events leading to PGE_2 synthesis we used PGE_2-free SEAΔα-1/ω-1 and not PGE_2-containing complete SEA, to be able to selectively assess *de novo* synthesis of PGE_2 by DCs. In addition, both COX-1 and COX-2 were important for PGE_2 synthesis by SEAΔα-1/ω-1, as treatment of moDCs with COX-1 and COX-2 inhibitors indomethacin and SC236 abrogated SEAΔα-1/ω-1-driven PGE_2 release (Figure 5C). Given that SEA has previously been reported to promote phosphorylation of extracellular-signal regulated kinase (ERK) [31] and that ERK can drive activation of $cPLA_2$ [32], we evaluated the role of ERK in SEA-driven PGE_2 synthesis. We found that SEA, in contrast to ω-1, induced phosphorylation of ERK (Figure 5D). and that inhibition of ERK signalling, using U0126, abrogated PGE_2 synthesis induced by SEAΔα-1/ω-1 (Figure 5E).

Next, we aimed to identify the receptors through which SEA activates this pathway leading to PGE_2 synthesis in moDCs. Previous studies have identified various CLRs through which SEA can be recognized by APCs. For human moDCs primarily fucose- and mannose-binding DC-SIGN and MR have been implicated in this process [13, 33-35]. Moreover, studies with murine APCs have also pointed to a possible role in recognition of components in SEA for Dectin-1 and Dectin-2, which are classically known for their ability to bind and respond to β-glucans and α-mannans from fungal origin, respectively [36]. Yet, whether components within SEA can be recognized and induce

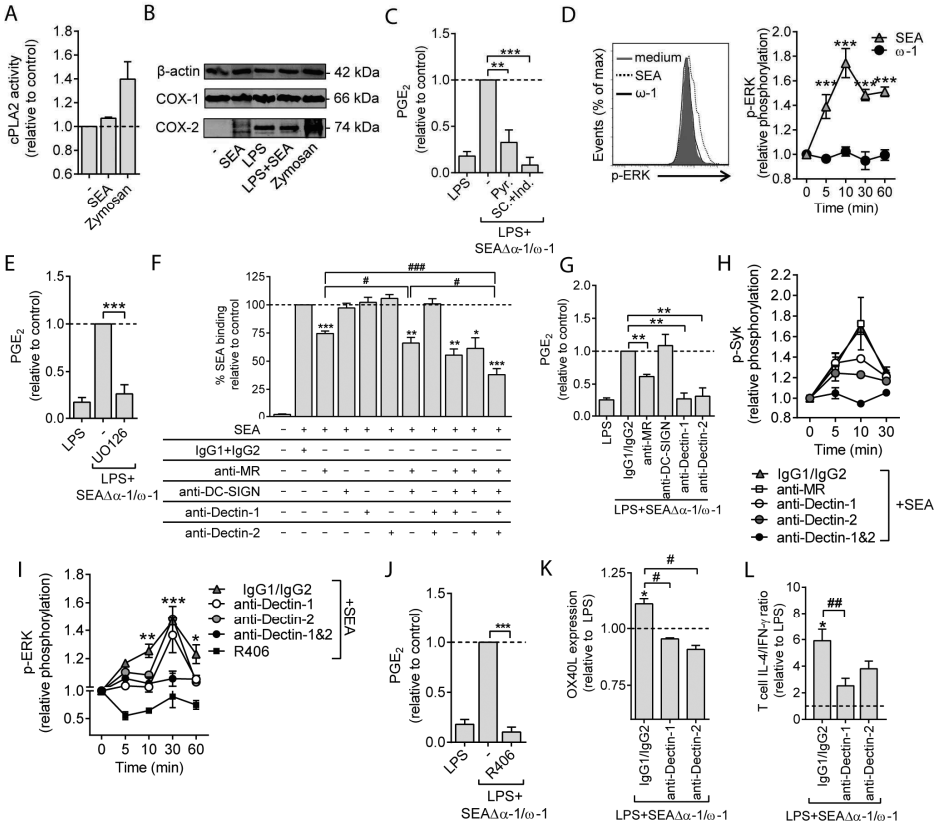

Figure 5. SEA promotes PGE_2 synthesis and drives Th2 polarization via signalling through Dectin-1 and Dectin-2

(A) $cPLA_2$ activity 8 h after stimulation. Zymosan was taken along as a positive control for $cPLA_2$ activation. (B) Protein expression of COX-1 and COX-2 were assessed by western blot. The β-actin was used as housekeeping protein. One of 3 experiments is shown. (C) Following 1 h pre-incubation with specific inhibitors for $cPLA_2$ (Pyrrophenone, [Pyr.]) or COX-1 and COX-2 (SC236 and Indometacin [SC.+ind.], respectively), moDCs were stimulated for 12 h with LPS+SEAΔα-1/ω-1 and supernatants were collected for PGE_2 determination by LC-MS/MS. (D) At the indicated time points after stimulation with depicted stimuli, phosphorylation of ERK was determined by flow cytometry. (E) PGE_2 levels were determined as in (C). U0216 was used as inhibitor of ERK. (F) MoDCs were treated 45 min with indicated blocking antibodies or isotype controls after which the cells were incubated with PF-647-labeled SEA. Antigen binding/uptake was analysed by flow cytometry and plotted as relative differences. (G) PGE_2 levels were assessed as in (C), following pre-incubation with blocking antibodies as described in (F). (H) Syk and (I) ERK phosphorylation were determined as described in (D) following pre-incubation with blocking antibodies as described in (F) or with Syk inhibitor R406. (J) PGE_2 levels were assessed as in (C). (K, L) MoDCs were pre-incubated with indicated blocking antibodies, followed by 48 h stimulation with LPS+SEAΔα-1/ω-1, after which OX40L expression was determined by flow cytometry. Data are based on geometric mean florescence. (L) Cells described in (K) were used for T cell polarization assay as described in Figure 2A. (A, C-L) data represent mean ± SEM of at least three independent experiments and are shown relative to control conditions, which are set to 1 (A, C-E, G-L) or 100% (F). *,#$p<0.05$, **,##$p<0.01$ and ***,###$p<0.001$ for significant differences with the control (*) or between test condition (#) based on paired analysis (paired Student's T-test).

signalling via human Dectin-1 and/or Dectin-2 expressed by DCs remains to be determined. As a first step towards the identification through which receptor(s) SEA induces PGE_2, we determined which of these receptors are involved in binding of SEA by moDCs. In line with earlier observations

[9, 13] blocking of MR reduced binding of fluorescently-labelled SEA, which could be further reduced when DC-SIGN binding was neutralized simultaneously. Interestingly, blocking of both Dectin-1 and Dectin-2 in conjunction with MR+DC-SIGN neutralization further reduced binding relative to blocking of just MR+DC-SIGN, suggesting that all 4 receptors contribute to recognition of glycans or glycoproteins present in SEA (Figure 5F). Next, we aimed to identify through which of these CLRs SEA promotes PGE_2 synthesis. We found that blocking of either Dectin-1 or Dectin-2, but not DC-SIGN, strongly attenuated PGE_2 synthesis induced by SEAΔα-1/ω-1, while blocking MR also resulted in reduced PGE_2 synthesis albeit to a lesser extent. This suggests a major role for Dectin-1 and Dectin-2 in SEAΔα-1/ω-1-driven PGE_2 synthesis (Figure 5G). Dectin signalling is mediated by the immunoreceptor tyrosine-based activation motifs (ITAMs) present in the cytoplasmic domains of Dectins that phosphorylate and activate spleen tyrosine kinase (Syk) either directly (Dectin-1) or following FcR recruitment (Dectin-2). Syk in turn can promote ERK phosphorylation [37]. Indeed, we observed that SEA stimulation resulted in phosphorylation of Syk, which was dependent on both Dectin-1 and Dectin-2 but not MR (Figure 5H), and found that SEA-driven ERK phosphorylation was dependent on Dectin-1, Dectin-2 and Syk signalling (Figure 5I). Of note, blocking of either Dectin-1 or Dectin-2 alone only had minor effects on Syk and ERK phosphorylation, while these signals were totally blunted when both Dectin-1 and Dectin-2 signalling were blocked simultaneously, suggesting that SEA depends on both receptors to activate this pathway. In line with these findings, inhibition of Syk signalling blunted SEAΔα-1/ω-1-induced PGE_2 synthesis (Figure 5J). Finally, blocking either Dectin-1 or Dectin-2 attenuated OX40L expression (Figure 5K) as well as the Th2 response induced by SEAΔα-1/ω-1 (Figure 5L). In conclusion, these data suggest that SEA promotes PGE_2 synthesis by moDCs through MR, Dectin-1 and -2 and via a signalling cascade involving Syk, ERK, $cPLA_2$, COX-1 and 2, that is required for Th2 induction by SEA.

PGE_2 isomer generation via autoxidation contributes to Th2 induction by SEA

The observations that PGE_2 promoted Th2 induction by SEA and that this PGE_2 synthesis was dependent on COX activity, led us to hypothesize that blocking of COX activity in SEAΔα-1/ω-1-stimulated moDCs would abrogate their ability to prime Th2 responses. Surprisingly however, inhibition of COX-1 and -2 only partly reduced the Th2 response induced by these SEAΔα-1/ω-1-conditioned DCs (Figure 6A). A possible explanation for this unexpected result came from a careful reanalysis of the extracted ion chromatogram of the PGE_2 trace (*m/z* 351 -> 271) in which we noted that alongside PGE_2, moDCs stimulated with SEA produced PGE_2 isomers, also known as isoprostanes (IsoPs) (Figure 6B). Several studies have suggested that isoPs may have similar properties as PGE_2, but that in contrast to the latter they are generated by an autoxidation process directly from AA fuelled by reactive oxygen species (ROS), independently from COX activity [26]. We found isomers '1' and '2' (Figure 6B) to have a fragment ion *m/z* 189 that is characteristic for 15-series IsoPs with identical relative retention times to commercially available 15*R*-PGD_2 and 11β-PGE_2, respectively, suggesting these isomers are 15*R*-PGD_2 and 11β-PGE_2 (Figure 6C) [38]. Isomer '3' showed a somewhat different tandem MS spectrum indicating it belongs to the class of 5-series IsoPs, but this could not be confirmed due to a lack of standard material (Figure 6D) [39].

To provide a mechanistic explanation for how SEA stimulation results in IsoP generation by moDCs, we test whether SEA could induce ROS production. Consistent with earlier observations in murine DCs [33, 36], we observed that human moDCs stimulated with SEA and SEAΔα-1/ω-1, but not with ω-1, resulted in ROS production (Figure 6E) that was dependent on signalling through Syk

(Figure 6F). To determine the biological significance of the generation of these two 15-series IsoPs in response to SEA, we first determined whether 15*R*-PGD_2 and 11β-PGE_2 IsoPs could affect T cell polarization. Interestingly, these two IsoPs could condition moDCs for priming of a Th2 response, which could be blocked by treatment with anti-PGE_2 (Figure 6G). Importantly, in contrast to COX inhibition alone, pre-treatment with COX inhibitors in conjunction with ROS scavenger *N*-acetyl-*L*-cysteine (NAC), abrogated the ability of SEAΔα-1/ω-1-stimulated moDCs to prime a Th2 response (Figure 6H), suggesting that enzymatically generated PGE_2 and its isomers act in concert to condition moDCs for Th2 polarization.

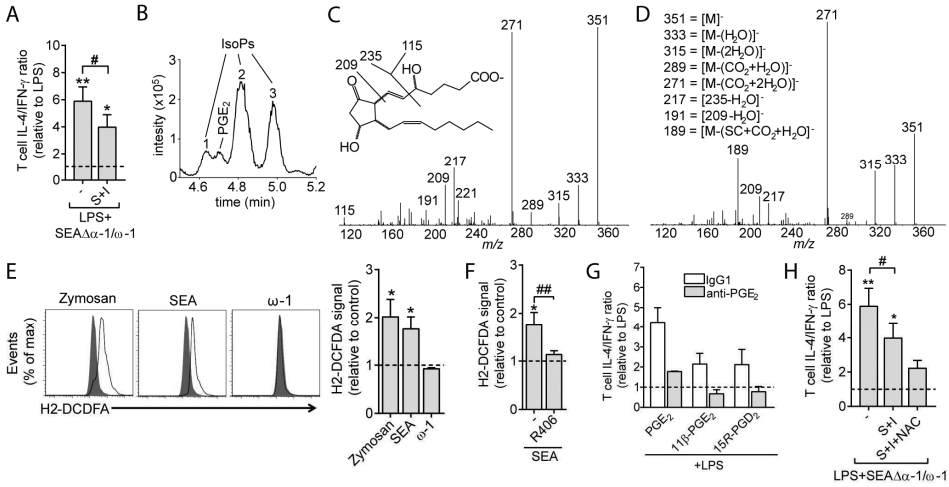

Figure 6. SEA-induced ROS production by moDCs results in PGE_2 isomers synthesis that contribute to Th2 polarization

(A) T cell polarization assay as described in Figure 2A in the presemce of COX inhibitors SC236 (S) and indomethacin (I). Bars represent mean ± SEM of at least three independent experiments. (B) LC-MS/MS trace showing the transition *m/z* 351 -> 271, the detected IsoPs are indicated by numbers. (C) Tandem MS spectrum of isomer 2, showing the fragment ion *m/z* 189, characteristic for 15-series IsoPs. (D) Showing the MS/MS spectrum of isomer 3, possibly identifying this isomer as a 5-series isoP, based on the fragment ions *m/z* 115, 217 and 191. (E) ROS generation was determined by flow cytometry (H2-DCFDA) of moDCs pulsed for 6 h with indicated reagents. On the left representative histograms for ROS induction are shown. On the right the geometric mean fluorescence of these signals is enumerated and shown as fold change relative to unstimulated moDCs (dashed line set to 1). (F) ROS production was quantified as in (E) following pre-treatment with general ROS scavenger Nac or R406 for 1 h. (G) MoDCs were stimulated with indicated PGs with or without anti-PGE_2 after which a T cell polarization assay was performed as described in Figure 2A. (H) MoDCs were stimulated with indicated reagents in the presence following 1 h pre-incubation with COX inhibitors (S+I) and NAC after which a T cell polarization assay was performed as described in Figure 2A. Bars represent mean ± SEM of at least three independent experiments. *,#$p<0.05$ and **$p<0.01$ for significant differences with the LPS control (*) or between test conditions (#) based on paired analysis (paired Student's T-test).

S. mansoni egg-driven Th2 polarization *in vivo* depends on Dectin-2 and Syk

We next aimed to assess the importance of this Dectin-Syk signalling in mediating Th2 polarization by *S. mansoni* egg antigens *in vivo*. First, to test the importance of Syk in Th2 polarization by DCs in response to egg antigen challenge *in vivo*, we made use of $Itgax^{cre}$ $syk^{fl/fl}$ mice ($CD11c^{\Delta syk}$), which selectively lack Syk expression in $CD11c^{+}$ DCs. We found that following subcutaneous immunization with SEA, $CD4^{+}$ T cells from draining LNs from $CD11c^{\Delta syk}$ mice, compared to $CD11c^{WT}$ controls, produced less Th2 cytokines *ex vivo* in response to both polyclonal (Figure 7A) and antigen-specific restimulation (Figure 7B), while IFN-γ production was not different between the

two groups of mice. These data validate our *in vitro* findings and suggest that Syk signalling in DCs plays a key role in Th2 priming by *S. mansoni* egg antigens *in vivo*.

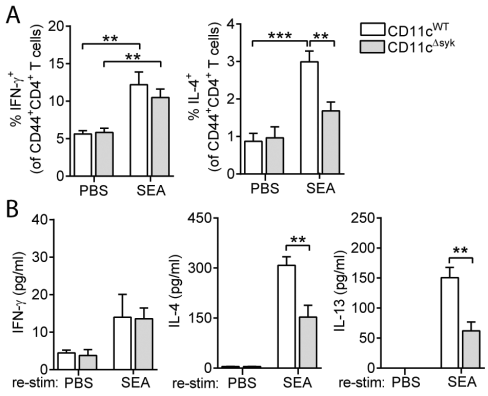

Figure 7. Th2 polarization induced by SEA mediated partly via Syk signalling *in vivo*
(A, B) WT or CD11c$^{\Delta syk}$ mice were injected with SEA in the hind footpad and draining pLNs were analysed 7 d later. (A) pLN cells were re-stimulated with PMA/Ionomycin in the presence of brefeldin A and CD4$^+$ T cells were stained for indicated intracellular cytokines. (B) pLN cells were re-stimulated with SEA for 72 h, and cytokine levels in culture supernatants were determined. Bars represent mean ± SEM of one of two independent experiments with 5 mice per group. *p<0.05, **p<0.01 and ***p<0.001 for significant differences relative to PBS treated mice based on un-paired analysis (un-paired Student's T-test).

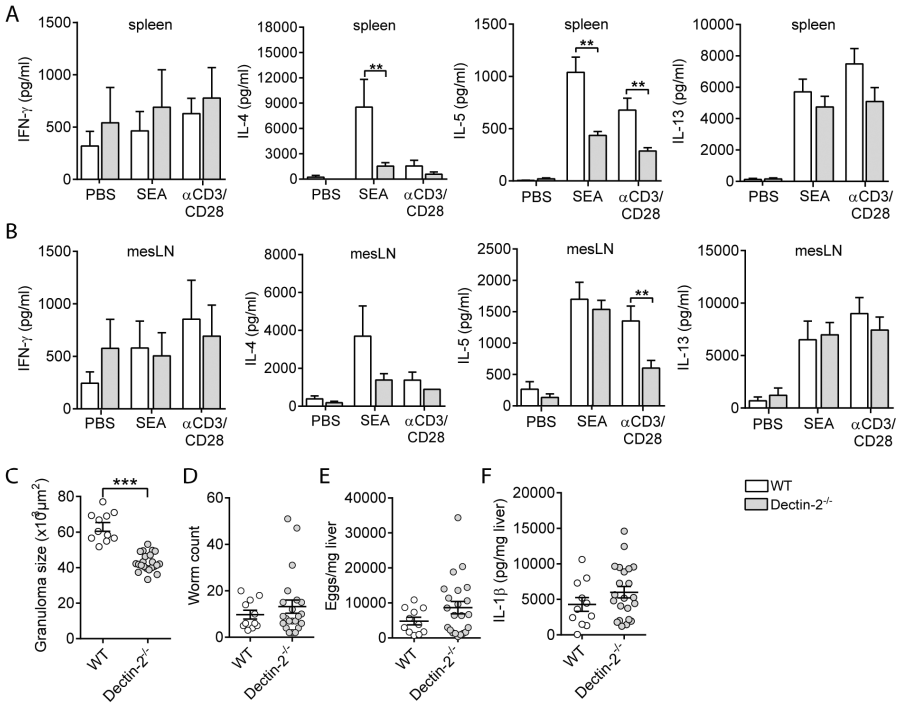

Figure 8. Dectin-2 signalling is required for induction of a Th2 response during *S. mansoni* infection
WT and Dectin-2$^{-/-}$ mice were infected with *S. mansoni*. After 8 weeks of infection cells from (A) spleens or (B) mLNs were re-stimulated with SEA or anti-CD3/CD28 for 72 h and cytokine levels were analysed in supernatants by luminex or ELISA. Bars represent mean ± SEM of combined data of at least two or three independent experiments with 5 to 10 mice per group. (C) Granuloma sizes around eggs trapped in the liver of 8 weeks infected mice were assessed in masson blue stained liver sections. Data are based on 10 mice per group. Number of worms (D) and liver and intestinal eggs (E) in 8 weeks *S. mansoni*-infected mice. (F) IL-1β protein levels in livers of 8 weeks *S. mansoni*-infected mice. **p<0.01 and ***p<0.001 for significant differences relative to the control mice based on un-paired analysis (un-paired Student's T-test).

Finally, we set out to assess the importance of this signalling axis in Th2 differentiation and Th2-driven immunopathology during a natural infection with *S. mansoni*, using Dectin-1 and Dectin-2 knock out mice (Dectin-$1^{-/-}$ and Dectin-$2^{-/-}$). During *S. mansoni* infection adult worms residing in the portal vasculature release eggs that get trapped in the liver where they induce strong Th2 responses that orchestrate the development of granulomatous lesions surrounding the eggs [8]. The intensity of the Th2 response and associated granulomatous inflammation peaks at 8 weeks after infection. To compare the Th2 response induced by this infection in WT and Dectin-$1^{-/-}$ and Dectin-$2^{-/-}$ mice, cells from mesenteric LNs and spleens from 8 weeks infected mice were re-stimulated with SEA or anti-CD3/CD28. We found that infected Dectin-$2^{-/-}$ mice displayed lower production of Th2 cytokines IL-4 and IL-5 in both lymphoid organs in comparison to their infected WT counterparts, while IFN-γ production was not different between the two groups (Figure 8A, B). In infected Dectin-$1^{-/-}$ mice only IL-5 production by splenocytes was reduced (Figure S2A, S2B). Importantly, in line with the reduced Th2 responses found in the infected Dectin-$2^{-/-}$ mice, granuloma size around the eggs trapped in the liver was smaller relative to infected WT mice (Figure 8C). Of note, this difference in Th2 response was not due to differences in infection load, as both Dectin-$2^{-/-}$ and WT mice were found to harbour similar numbers of eggs and adult worms (Figure 8D, E). Dectin-$1^{-/-}$ mice did not show an altered granulomatous response towards liver eggs (Figure S2C), nor did they show differences in numbers of adult worms and eggs (Figure S2D, S2E). We previously found that inflammasome activation, which can be triggered by SEA via Dectin-2 signalling, can alter T cell polarization and contributes to granuloma formation during *S. mansoni* infection [33]. However, levels in IL-1β protein, as readout for inflammasome activity, in liver were similar between Dectin-$2^{-/-}$ and WT mice (Figure 8F). Altogether, these findings highlight an important role for Dectin-2 in promoting Th2 differentiation and immuno-pathological outcome of this response during *S. mansoni* infection.

DISCUSSION

The molecular mechanisms through which DCs prime Th2 responses, including those elicited by helminths, are still incompletely understood. We here explored the role of PUFAs and LMs in Th2 induction by *S. mansoni eggs*, that are well known for their potent ability to elicit strong Th2 responses. This enabled us to identify a novel signalling axis in DCs involving Dectin-Syk-PGE_2-OX40L through which Th2 responses are induced *in vitro* and *in vivo*.

Some studies have been documented that different life stages of *S. mansoni* are able to produce LMs from both COX products (e.g: PGE_1, PGE_2, PGD_2 and PGA_2) and Lipoxygenase products (e.g: LTB_4, 5-HETE, 12-HETE)[26, 40]. However, the existence of LMs in eggs or SEA had not been examined before. Here we uncovered that SEA itself contains various PUFAs and LMs with potential immunomodulatory properties. In particular, the presence of the well-studied immunomodulatory eicosanoid PGE_2 caught our attention, since among the pleiotropic properties that have been attributed to this lipid, it has been associated with promoting Th2 polarization by functional modulation of DCs [3, 29]. Moreover, we found PGE_2 not only to be present in SEA, but also to be synthesized by DCs themselves in response to SEA stimulation. While, other life cycle stages of *S. mansoni* have been shown to promote PGE_2 synthesis in host cells such as cercariae in keratinocytes [27], we are the first to report and mechanistically investigate the ability of egg-derived antigens to promote PGE_2 synthesis in immune cells. Importantly, we found that this PG, in contrast to several other LMs secreted by SEA-stimulated DCs, was not only sufficient to condition moDCs for Th2 polarization, but also crucial for mediating ω-1-independent Th2 polarization by

SEA. This identifies PGE_2 as a key factor through which SEA, independently from ω-1, primes Th2 responses. A question that remains to be answered is what the relative contribution is of the pre-existing PGE_2 (present in SEA) *versus* PGE_2 synthesized by moDCs in mediating the Th2-polarizing effect. The observation that SEA from which ω-1 was depleted, was fully dependent on *de novo* synthesized PGE_2 by the moDCs for Th2 polarization, at least shows that moDC-derived PGE_2 can be sufficient for promoting a Th2 response. Moreover, the fact that SEA requires Syk signalling in DCs to prime a Th2 response *in vivo*, would argue that PGE_2 derived from SEA itself is insufficient to condition DCs for Th2 priming and that SEA instead rather depends on Syk-driven *de novo* PGE_2 synthesis for this response.

Mechanistically, we found that PGE_2 derived from moDCs acts in an autocrine manner to promote Th2 polarization by promoting the expression of OX40L in moDCs. OX40L expression has been shown to be important for Th2 polarization by DCs stimulated with various other Th2-priming stimuli, such as allergens and TSLP [30, 41, 42]. Congruent with these studies we found that OX40L expression was crucial for Th2 polarization by SEA from which ω-1 was depleted. While expression of OX40L in response to SEA has been documented before [3, 12], we now provide evidence that SEA-induced OX40L expression in moDCs is secondary to its ability to induce PGE_2 synthesis by these cells.

Moreover, we found that SEA from which ω-1 was depleted was dependent on signalling through both Dectin-1 and Dectin-2 to condition moDCs to drive Th2 polarization. Dectin-2 has been linked to Th2 polarization before in the context of allergic responses induced by house dust mite [43, 44]. In these studies Dectin-2 was found to mediate Th2 induction through the generation of cysteinyl leukotrienes by murine DCs. However, we did not observe induction of cysteinyl leukotrienes by SEA. Instead, we found that SEA interacts with Dectin-1, Dectin-2 and MR to promote PGE_2 synthesis. Downstream of these receptors we identified a pathway involving, Syk, ERK, and $cPLA_2$, that leads to the release of AA, which subsequently acts as a substrate for COX to produce PGE_2. The observation that MR also seems to play a role in SEA-driven PGE_2 synthesis, despite the fact that MR itself in contrast to Dectin-1 and Dectin-2 does not harbour an intracellular signalling motif, leads us to speculate that MR may collaborate with Dectin-1 and/or Dectin-2 to form complexes that effectively bind glycans or glycoproteins in SEA that allow for efficient activation of the signalling cascade downstream of Dectins resulting in PGE_2 synthesis. Associations of different CLRs to potentiate glycan-induced signalling have been described before for Dectin-2 and Dectin-3 [45]. Glycans derived from the cell wall of fungi such as *Candida albicans* [32] are well known to promote PGE_2 synthesis through this pathway via activation of Dectin-1, Dectin-2 and MR [46, 47]. However, in this context the production of PGE_2 seems to contribute to Th17 priming by APCs and not Th2 [46]. This difference might be explained by differences in glycan repertoire between fungi and schistosome eggs. For instance, classical β-glucans expressed by fungi are not present in SEA [48]. Therefore, the carbohydrates in SEA that mediate Dectin binding, may interact differently with, or have a lower affinity for these receptors than fungal carbohydrates do. This may induce a qualitatively and/or quantitatively different signalling cascade that could trigger sufficient PGE_2 synthesis to allow for Th2 induction to occur, without promoting the expression of high level of Th17-promoting cytokines. Secondly, fungal Dectin agonists may trigger additional PRRs to induce pro-inflammatory cytokine expression that are not activated by SEA [49]. Finally, the immunological outcome of Dectin engagement can also be cell type-dependent. For instance, Dectin-1 ligand curdlan was found to promote Th2 responses via plasmacytoid DCs while this same ligand conditioned myeloid DCs to inhibit Th2 responses [50] or

to promote Th9 responses [51]. Interestingly, similar to our observations with SEA, the conditioning of plasmacytoid DCs by curdlan to promote Th2 responses was dependent on induction of OX40L expression [50]. Currently, studies are ongoing to identify the glycoproteins or glycan moieties present in SEA that bind to Dectin-1, Dectin-2 and MR to promote this response.

We provide evidence that COX-independent generation of several PGE_2 isomers (isoPs) by SEA, independently from enzymatically synthesized PGE_2 are capable of conditioning moDCs for Th2 priming. While COX-independent generation of these isomers has been described before, as a result of auto-oxidation of AA by free radicals [26], we now here show a role for these isoPs in regulation of an immune response. In line with the free radical-dependent synthesis of isoPs, we found that SEA could drive ROS production in a Syk-dependent manner, which corroborates a recent study showing that SEA can induce ROS in murine DCs [33]. However, the latter study focused on the role of ROS in SEA-driven inflammasome activation, and did not report on other ROS-mediated effects. Our data suggest that that enzymatically synthesized PGE_2 and its ROS-induced isomers act in concert in Dectin-mediated conditioning of moDCs for Th2 priming by SEA. Moreover, we found that the widely used neutralizing anti-PGE_2 antibody [52] that we have used in this study not only neutralizes PGE_2, but also harbours cross-reactivity towards two of the main isoPs that we found to be generated by SEA-stimulated DCs. This can explain our observation that PGE_2 neutralization, in contrast to COX inhibition, did fully block Th2 polarization.

We found that mice which were deficient for Syk in their DCs, failed to mount a Th2 response following SEA immunization *in vivo*, which provides strong support for a key role of the dectin-Syk-PGE_2-OX40L axis in Th2 polarization by *Schistosoma* egg-derived antigens *in vivo*. Moreover, our studies with *S. mansoni*-infected Dectin-$2^{-/-}$ mice suggest that also during natural infection this signalling axis seems to be crucial for induction of Th2 responses. SEA has previously been reported to activate the Nlrp3-inflammasome in a Dectin-2-dependent manner and inflammasome-deficient mice were shown to have an altered T cell polarization profile and a reduction in granuloma size during *S. mansoni* infection similar to our observations reported here in infected Dectin-$2^{-/-}$ mice. However, the fact that in contrast to what was observed in inflammasome deficient mice [33], there was no reduction in total IL-1β levels in livers of Dectin-$2^{-/-}$ mice during *S. mansoni* infection, would suggest that downstream of Dectin-2 the PGE_2-OX40L axis, rather than inflammasome activation, plays a key role in Th2 priming during, and in the immuno-pathological outcome of, this infection. Nonetheless, additional studies will be needed to definitively determine the individual contribution of each pathway to the immunopathology *in vivo*. Somewhat surprising was the observation that in contrast to the *in vitro* data Dectin-1 appears to be less important for Th2 polarization *in vivo*. This may suggest that murine Dectin-1, as opposed to its human counterpart, does not play a major role in recognition of glycans present in SEA, which, although currently still speculation, might be due to differences in glycan-specificity or in expression of Dectin-1 isoforms between murine and human DCs [53, 54]. More detailed comparative studies between the SEA-binding characteristics of human and murine Dectin-1 could provide more molecular insight in the mechanisms underlying the difference in requirement for Dectin-1 in Th2 polarization by SEA between the human *in vitro* and murine *in vivo* models.

In summary, we propose a model (Figure 9) in which SEA can condition DCs for Th2 polarization independently from ω-1 by triggering Dectin-1, Dectin-2 and MR to induce in a Syk-dependent fashion the synthesis of PGE_2 and isoPs, that subsequently promote OX40L expression in an autocrine manner. OX40L then enables the SEA-stimulated moDCs to prime a Th2 response. Importantly, the fact that neutralization of PGE_2 and its isomers completely blunted the Th2-

priming ability of moDCs that had been stimulated with SEA from which ω-1 had been depleted, provides strong support for the notion that this pathway can fully account for 'residual' ability of SEA to prime Th2 polarization in the absence of ω-1. However, the fact that this same intervention had little or no effect on the Th2-priming capacity of complete SEA in our *in vitro* DC assay, suggests that the Dectin-PGE_2-OX40L signalling axis can be compensated for by the presence of ω-1, which employs distinct mechanisms to condition moDCs for Th2 polarization, and that this novel axis is only unmasked *in vitro* when ω-1 is removed from SEA. *In vivo*, however, the contribution of Dectin-PGE_2-OX40L signalling axis in egg antigen-driven Th2 polarization appears to be much more dominant, given that interference with Syk or Dectin signaling, did result in an impaired Th2 response induced by complete SEA or by a natural infection with *S. mansoni,* respectively. This would be corroborated by our previous work showing that SEA from which ω-1 was depleted was still potent in inducing a Th2 response as complete SEA *in vivo* [20] and that ω-1 knockdown in *S. mansoni* eggs by lentiviral transduction did not reduce Th2 responses induced by the eggs *in vivo* [19]. Together this leads us to speculate the Dectin-PGE_2-OX40L signalling axis plays a more important role in schistosome egg-driven Th2 polarization that *in vivo* than the one that is driven by ω-1 in which MR and suppression of protein synthesis play a central role [9].

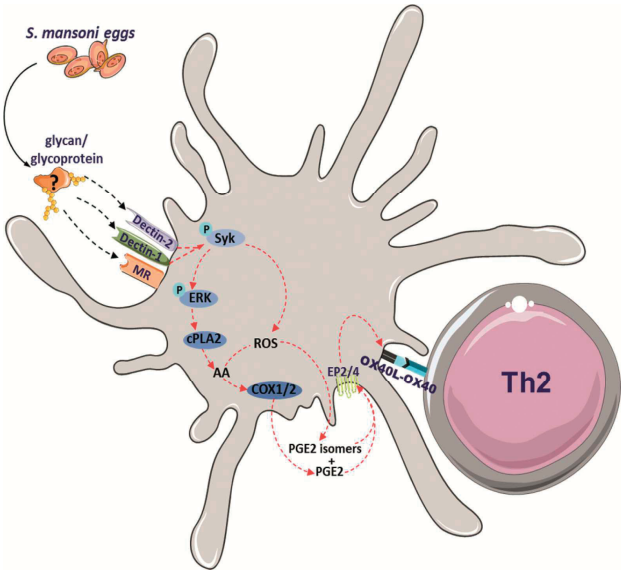

Figure 9. Proposed model of *S. mansoni* egg-driven Th2 polarization
The molecules derived from SEA recognized by Dectin-1, Dectin-2 further activate Syk and lead to two intracellular pathways in moDCs: ERK-$cPLA_2$-COX and ROS activity result in PGE_2 and PGE_2 isomers synthesis respectively. Both PGE_2 and its isomers bind to EP2 and EP4 in an autocrine loop. These series of signalling pathways give rise to a Th2-inducing phenotype of moDCs by promoting OX40L expression.

In conclusion, we have delineated a previously unrecognized pathway involving Dectin-1/2, PGE_2 and OX40L through which Th2 immunity is induced. Targeting this axis may hold promise as an approach to regulate type 2 immune responses for therapeutic purposes, not only in the context of *S. mansoni* and other helminth infections, but possibly also in major diseases of the western world, such as allergies and type 2 diabetes, that are caused by overzealous and defective type 2 immune responses, respectively.

ACKNOWLEDGMENTS

We thank the volunteers for their participation in this study. The authors thank Hilde Brouwers for help with $cPLA_2$ assay in this study. This work was supported by The Indonesian Directorate General of Higher Education (DGHE/DIKTI)-Leiden University and LUMC fellowship to Bart Everts.

REFERENCES

1. Gause, W.C., T.A. Wynn, and J.E. Allen, *Type 2 immunity and wound healing: evolutionary refinement of adaptive immunity by helminths.* Nat Rev Immunol, 2013. **13**(8): p. 607-14.
2. Kapsenberg, M.L., *Dendritic-cell control of pathogen-driven T-cell polarization.* Nat Rev Immunol, 2003. **3**(12): p. 984-93.
3. de Jong, E.C., et al., *Microbial compounds selectively induce Th1 cell-promoting or Th2 cell-promoting dendritic cells in vitro with diverse th cell-polarizing signals.* J Immunol, 2002. **168**(4): p. 1704-9.
4. Connor, L.M., et al., *Helminth-conditioned dendritic cells prime CD4+ T cells to IL-4 production in vivo.* J Immunol, 2014. **193**(6): p. 2709-17.
5. Cook, P.C., et al., *Alternatively activated dendritic cells regulate CD4+ T-cell polarization in vitro and in vivo.* Proc Natl Acad Sci U S A, 2012. **109**(25): p. 9977-82.
6. Everts, B., et al., *Functional impairment of human myeloid dendritic cells during Schistosoma haematobium infection.* PLoS Negl Trop Dis, 2010. **4**(4): p. e667.
7. Pearce, E.J., et al., *Downregulation of Th1 cytokine production accompanies induction of Th2 responses by a parasitic helminth, Schistosoma mansoni.* J Exp Med, 1991. **173**(1): p. 159-66.
8. Pearce, E.J. and A.S. MacDonald, *The immunobiology of schistosomiasis.* Nat Rev Immunol, 2002. **2**(7): p. 499-511.
9. Everts, B., et al., *Schistosome-derived omega-1 drives Th2 polarization by suppressing protein synthesis following internalization by the mannose receptor.* J Exp Med, 2012. **209**(10): p. 1753-67, s1.
10. Hussaarts, L., et al., *Rapamycin and omega-1: mTOR-dependent and -independent Th2 skewing by human dendritic cells.* Immunol Cell Biol, 2013. **91**(7): p. 486-9.
11. Jankovic, D., et al., *Mechanisms underlying helminth- induced Th2 polarization: default, negative or positive pathways?* Chem Immunol Allergy, 2006. **90**: p. 65-81.
12. Klaver, E.J., et al., *Schistosoma mansoni Soluble Egg Antigens Induce Expression of the Negative Regulators SOCS1 and SHP1 in Human Dendritic Cells via Interaction with the Mannose Receptor.* PLoS One, 2015. **10**(4): p. e0124089.
13. van Liempt, E., et al., *Schistosoma mansoni soluble egg antigens are internalized by human dendritic cells through multiple C-type lectins and suppress TLR-induced dendritic cell activation.* Mol Immunol, 2007. **44**(10): p. 2605-15.
14. Fitzsimmons, C.M., et al., *Molecular characterization of omega-1: a hepatotoxic ribonuclease from Schistosoma mansoni eggs.* Mol Biochem Parasitol, 2005. **144**(1): p. 123-7.
15. Steinfelder, S., et al., *The major component in schistosome eggs responsible for conditioning dendritic cells for Th2 polarization is a T2 ribonuclease (omega-1).* J Exp Med, 2009. **206**(8): p. 1681-90.
16. Dunne, D.W., F.M. Jones, and M.J. Doenhoff, *The purification, characterization, serological activity and hepatotoxic properties of two cationic glycoproteins (alpha 1 and omega 1) from Schistosoma mansoni eggs.* Parasitology, 1991. **103 Pt 2**: p. 225-36.
17. Cass, C.L., et al., *Proteomic analysis of Schistosoma mansoni egg secretions.* Mol Biochem Parasitol, 2007. **155**(2): p. 84-93.
18. Mathieson, W. and R.A. Wilson, *A comparative proteomic study of the undeveloped and developed Schistosoma mansoni egg and its contents: the miracidium, hatch fluid and secretions.* Int J Parasitol, 2010. **40**(5): p. 617-28.
19. Hagen, J., et al., *Omega-1 knockdown in Schistosoma mansoni eggs by lentivirus transduction reduces granuloma size in vivo.* Nat Commun, 2014. **5**: p. 5375.
20. Everts, B., et al., *Omega-1, a glycoprotein secreted by Schistosoma mansoni eggs, drives Th2 responses.* J Exp Med, 2009. **206**(8): p. 1673-80.
21. Harizi, H., *The immunobiology of prostanoid receptor signaling in connecting innate and adaptive immunity.* Biomed Res Int, 2013. **2013**: p. 683405.
22. Hirata, T. and S. Narumiya, *Prostanoids as regulators of innate and adaptive immunity.* Adv Immunol, 2012. **116**: p. 143-74.
23. Dalli, J. and C.N. Serhan, *Specific lipid mediator signatures of human phagocytes: microparticles stimulate macrophage efferocytosis and pro-resolving mediators.* Blood, 2012. **120**(15): p. e60-72.
24. Sreeramkumar, V., M. Fresno, and N. Cuesta, *Prostaglandin E2 and T cells: friends or foes?* Immunol Cell Biol, 2012. **90**(6): p. 579-86.

25. Kubata, B.K., et al., *Molecular basis for prostaglandin production in hosts and parasites.* Trends Parasitol, 2007. **23**(7): p. 325-31.
26. Noverr, M.C., J.R. Erb-Downward, and G.B. Huffnagle, *Production of eicosanoids and other oxylipins by pathogenic eukaryotic microbes.* Clin Microbiol Rev, 2003. **16**(3): p. 517-33.
27. Ramaswamy, K., P. Kumar, and Y.X. He, *A role for parasite-induced PGE2 in IL-10-mediated host immunoregulation by skin stage schistosomula of Schistosoma mansoni.* J Immunol, 2000. **165**(8): p. 4567-74.
28. Flynn, S., et al., *CD4 T cell cytokine differentiation: the B cell activation molecule, OX40 ligand, instructs CD4 T cells to express interleukin 4 and upregulates expression of the chemokine receptor, Blr-1.* J Exp Med, 1998. **188**(2): p. 297-304.
29. Krause, P., et al., *Prostaglandin E(2) enhances T-cell proliferation by inducing the costimulatory molecules OX40L, CD70, and 4-1BBL on dendritic cells.* Blood, 2009. **113**(11): p. 2451-60.
30. Ito, T., et al., *TSLP-activated dendritic cells induce an inflammatory T helper type 2 cell response through OX40 ligand.* J Exp Med, 2005. **202**(9): p. 1213-23.
31. van Riet, E., et al., *Combined TLR2 and TLR4 ligation in the context of bacterial or helminth extracts in human monocyte derived dendritic cells: molecular correlates for Th1/Th2 polarization.* BMC Immunol, 2009. **10**: p. 9.
32. Rodriguez, M., et al., *Polarization of the innate immune response by prostaglandin E2: a puzzle of receptors and signals.* Mol Pharmacol, 2014. **85**(1): p. 187-97.
33. Ritter, M., et al., *Schistosoma mansoni triggers Dectin-2, which activates the Nlrp3 inflammasome and alters adaptive immune responses.* Proc Natl Acad Sci U S A, 2010. **107**(47): p. 20459-64.
34. van Die, I., et al., *The dendritic cell-specific C-type lectin DC-SIGN is a receptor for Schistosoma mansoni egg antigens and recognizes the glycan antigen Lewis x.* Glycobiology, 2003. **13**(6): p. 471-8.
35. Ferguson, B.J., et al., *The Schistosoma mansoni T2 ribonuclease omega-1 modulates inflammasome-dependent IL-1beta secretion in macrophages.* Int J Parasitol, 2015. **45**(13): p. 809-13.
36. Saijo, S. and Y. Iwakura, *Dectin-1 and Dectin-2 in innate immunity against fungi.* Int Immunol, 2011. **23**(8): p. 467-72.
37. Hangai, S., et al., *PGE2 induced in and released by dying cells functions as an inhibitory DAMP.* Proc Natl Acad Sci U S A, 2016. **113**(14): p. 3844-9.
38. Brose, S.A., B.T. Thuen, and M.Y. Golovko, *LC/MS/MS method for analysis of E(2) series prostaglandins and isoprostanes.* J Lipid Res, 2011. **52**(4): p. 850-9.
39. Milne, G.L., et al., *Isoprostane generation and function.* Chem Rev, 2011. **111**(10): p. 5973-96.
40. Abdel Baset, H., G.P. O'Neill, and A.W. Ford-Hutchinson, *Characterization of arachidonic-acid-metabolizing enzymes in adult Schistisoma mansoni.* Mol Biochem Parasitol, 1995. **73**(1-2): p. 31-41.
41. Agrawal, K., S.L. Kale, and N. Arora, *Protease activity of Per a 10 potentiates Th2 polarization by increasing IL-23 and OX40L.* Eur J Immunol, 2015. **45**(12): p. 3375-85.
42. Hoshino, A., et al., *Critical role for OX40 ligand in the development of pathogenic Th2 cells in a murine model of asthma.* Eur J Immunol, 2003. **33**(4): p. 861-9.
43. Barrett, N.A., et al., *Dectin-2 recognition of house dust mite triggers cysteinyl leukotriene generation by dendritic cells.* J Immunol, 2009. **182**(2): p. 1119-28.
44. Barrett, N.A., et al., *Dectin-2 mediates Th2 immunity through the generation of cysteinyl leukotrienes.* J Exp Med, 2011. **208**(3): p. 593-604.
45. Zhu, L.L., et al., *C-type lectin receptors Dectin-3 and Dectin-2 form a heterodimeric pattern-recognition receptor for host defense against fungal infection.* Immunity, 2013. **39**(2): p. 324-34.
46. Smeekens, S.P., et al., *The Candida Th17 response is dependent on mannan- and beta-glucan-induced prostaglandin E2.* Int Immunol, 2010. **22**(11): p. 889-95.
47. Suram, S., et al., *Regulation of cytosolic phospholipase A2 activation and cyclooxygenase 2 expression in macrophages by the beta-glucan receptor.* J Biol Chem, 2006. **281**(9): p. 5506-14.
48. Smit, C.H., et al., *Glycomic Analysis of Life Stages of the Human Parasite Schistosoma mansoni Reveals Developmental Expression Profiles of Functional and Antigenic Glycan Motifs.* Mol Cell Proteomics, 2015. **14**(7): p. 1750-69.
49. Rogers, N.C., et al., *Syk-dependent cytokine induction by Dectin-1 reveals a novel pattern recognition pathway for C type lectins.* Immunity, 2005. **22**(4): p. 507-17.
50. Joo, H., et al., *Opposing Roles of Dectin-1 Expressed on Human Plasmacytoid Dendritic Cells and Myeloid Dendritic Cells in Th2 Polarization.* J Immunol, 2015. **195**(4): p. 1723-31.
51. Zhao, Y., et al., *Dectin-1-activated dendritic cells trigger potent antitumour immunity through the induction of Th9 cells.* Nat Commun, 2016. **7**: p. 12368.
52. Mnich, S.J., et al., *Characterization of a monoclonal antibody that neutralizes the activity of prostaglandin E2.* J Immunol, 1995. **155**(9): p. 4437-44.

53. Carvalho, A., et al., *Dectin-1 isoforms contribute to distinct Th1/Th17 cell activation in mucosal candidiasis.* Cell Mol Immunol, 2012. **9**(3): p. 276-86.
54. Fischer, M., et al., *Isoform localization of Dectin-1 regulates the signaling quality of anti-fungal immunity.* Eur J Immunol, 2017.
55. Caton, M.L., M.R. Smith-Raska, and B. Reizis, *Notch-RBP-J signaling controls the homeostasis of CD8- dendritic cells in the spleen.* J Exp Med, 2007. **204**(7): p. 1653-64.
56. Heemskerk, M.M., et al., *Prolonged niacin treatment leads to increased adipose tissue PUFA synthesis and anti-inflammatory lipid and oxylipin plasma profile.* J Lipid Res, 2014. **55**(12): p. 2532-40.
57. Schlegel, M., et al., *The neuroimmune guidance cue netrin-1 controls resolution programs and promotes liver regeneration.* Hepatology, 2016. **63**(5): p. 1689-705.

SUPPLEMENTARY DATA

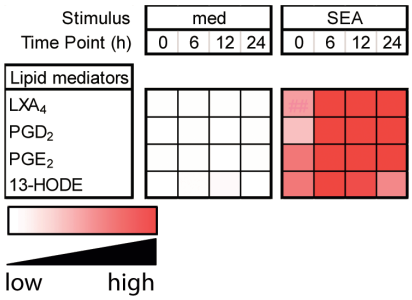

Figure S1. Heat-map of lipid changes in supernatants of SEA-stimulated moDCs

Monocyte-derived DCs were pulsed with SEA after which supernatant were collected at 0, 6, 12 and 24 h after stimulation. Relative amounts of indicated PUFAs detected by LC-MS/MS in supernatants are shown in a heat-map. Data represent one of two independent experiments.

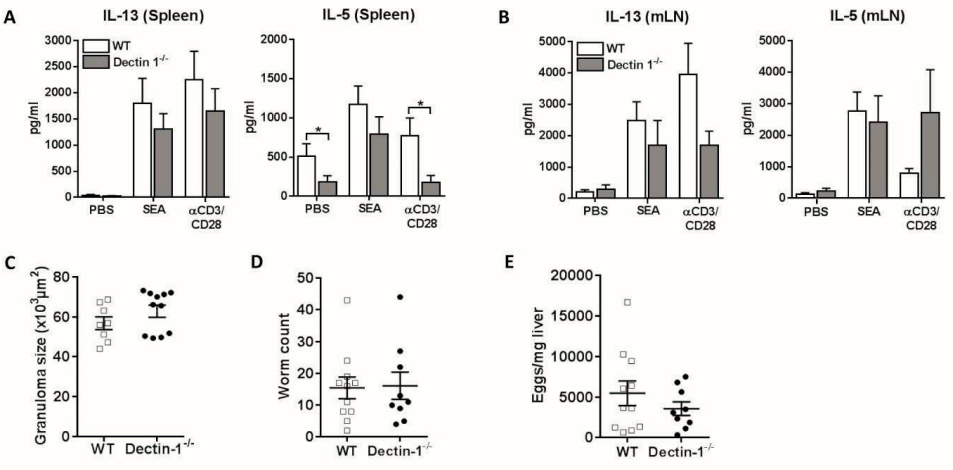

Figure S2. Dectin-1 signalling plays a minor role in Th2 priming during *S. mansoni* infection

WT and Dectin-1$^{-/-}$ mice were infected with *S. mansoni*. After 8 weeks of infection cells from (A) spleens or (B) mLNs were re-stimulated with SEA or anti-CD3/CD28 for 72 h and cytokine levels were analysed in supernatants by ELISA. Bars represent mean ± SEM of combined data of at least two or three independent experiments with 5 to 10 mice per group. (C) Granuloma sizes around eggs trapped in the liver of 8 weeks infected mice were assessed in Masson blue stained liver sections. Data are based on 10 mice per group. Number of worms (D) and liver and intestinal eggs (E) in 8 weeks *S. mansoni*-infected mice. *p<0.05 for significant differences relative to the control mice based on un-paired analysis (un-paired Student's T-test).

Table S1. Lipid Mediators (LM) including Polyunsaturated Fatty Acids (PUFAs) that were measured using LC-MS/MS.

LMs analyzed by GC-MS/MS					
1	10-HDHA	10-hydroxy Docosahexaenoic acid	29	8*S*,15*S*-diHETE	18S, 15S-dihydroxyeicosatetraenoic acid
2	11-HETE	11-hydroxyeicosatetraenoic acid	30	9-HODE	9-hydroxyoctadecadienoic acid
3	12-HETE	12-hydroxyeicosatetraenoic acid	31	9-HoTrE	9-hydroxyoctadecatrienoic acid
4	13,14dihydro-15-keto-PGE_2	13, 14dihidro-15-keto-Prostaglandin E2	32	AA	Arachidonic acid
5	13,14dihydro-15-keto-$PGF_2\alpha$	13, 14dihidro-15-keto-Prostaglandin F2α	33	AdA	Adrenic acid
6	13-HODE	13-hydroxyoctadecadienoic acid	34	ALA	α-linolenic acid
7	13-HoTrE	13-hydroxyoctadecatrienoic acid	35	AT-LXA_4	AT-Lipoxin A4
8	14,15-diHETE	14, 15-dihydroxyeicosatetraenoic acid	36	AT-RvD1	AT-Resolvin D1
9	15-HEPE	15-hydroperoxyeicosapentanoic acids	37	DHA	Docosahexaenoic
10	15-HETE	15-hydroxyeicosatetraenoic acid	38	DPA_{n-3}	Docosapentaenoic acid n-3
11	15-Keto-PGE_2	15-Keto-Prostaglandin E2	39	EPA	Eicosapentaenoic acid
12	17-HDHA	17-hydroxy Docosahexaenoic acid	40	LA	Linoleic acid
13	17-OH-DH-HETE	17-OH-DH- hydroxyeicosatetraenoic acid	41	LTB_4	Leukotriene B4
14	18-HEPE	18-hydroperoxyeicosapentanoic acids	42	LTD_4	Leukotriene D4
15	18*R*-RvE3	18R-Resolvin E3	43	LTE_4	Leukotriene E4
16	18*S*-RvE3	18S-Resolvin E3	44	LXA_4	Lipoxin A4
17	19,20-diHDPA	19, 20-dihydroxydocosapentanoic acid	45	MaR1_2	Maresin 1_2
18	20-OH-LTB_4	20-OH-Leukotrine B4	46	PDX	Protectin DX
19	5,15-diHETE	5, 15-dihydroxyeicosatetraenoic acid	47	PGD_2	Prostaglandin D2
20	5-HETE	5-hydroxyeicosatetraenoic acid	48	PGE_2	Prostaglandin E2
21	6*t*,12*epi*-LTB_4	6t, 12epi-Leukotrine B4	49	$PGF_2\alpha$	Prostaglandin F2α
22	6-*trans*-LTB_4	6-trans-Leukotrine B4	50	PGJ_2	Prostaglandin J2
23	7,17-diHDPA	7, 17-dihydroxydocosapentanoic acid	51	RvD1	Resolvin D1
24	7-HDHA	7-hydroxy Docosahexaenoic acid	52	RvD2	Resolvin D2
25	7*S*-MaR1	7S-Maresin 1	53	RvE1	Resolvin E1
26	8-HETE	8-hydroxyeicosatetraenoic acid	54	RvE2	Resolvin E2
27	8-iso-PGE2	8-iso-Prostaglandin E2	55	TxB_2	Thromboxane-B2
28	8-*iso*-$PGF_2\alpha$	8-iso-Prostaglandin F2α			

Chapter 7

Butyrate conditions human dendritic cells to prime type 1 regulatory T cells via histone deacetylase inhibitions and GPR109A signalling

MARIA M. M. KAISAR[1, 2], LEONARD R. PELGROM[1], ALWIN J. VAN DER HAM[1], MARIA YAZDANBAKHSH[1, #], BART EVERTS[1, #]

[1]Department of Parasitology, Leiden University Medical Center (LUMC), Leiden, The Netherlands
[2]Department of Parasitology, Faculty of Medicine, Universitas Indonesia, Jakarta, Indonesia
[#]Contributed equally

Submitted

ABSTRACT

Recently it has become clear that short chain fatty acids (SCFAs), in particular butyrate, have anti-inflammatory properties. Murine studies have shown that butyrate can promote regulatory T cells (Tregs) via induction of tolerogenic Dendritic cells (DCs). However, the effects of SCFAs on human DCs and how they affect their capacity to prime and polarize T cell responses has not been addressed. Here we report that butyrate and to a lesser extent proprionate, suppress LPS-induced maturation and metabolic changes of human monocyte-derived DCs and condition them to induce IL-10-producing type 1 regulatory T cells (Tr1). This effect was dependent on butyrate-induced rethinaldehyde dehydrogenase (RALDH) activity and retinoic acid (RA) production by DCs. The induction of RALDH activity and Tr1 cell differentiation by butyrate required both inhibition of histone deacetylases (HDACs) and signaling through G protein-coupled receptor (GPR)109A. Taken together, butyrate was shown to be a potent inducer of tolerogenic human DCs, thereby shedding new light on the cellular and molecular mechanisms through which SCFAs can exert their immunomodulatory effects in humans.

Keyword:

Short chain fatty acids, Butyrate, Dendritic cells, Type 1 regulatory T cells, Histone deacetylase, G-coupled protein receptor 109A, RALDH, Retinoic acids

INTRODUCTION

Dendritic cells (DCs) play a crucial role in the development of adaptive immune responses during infections and inflammatory diseases, as well as in the regulation of immune homeostasis during steady state, by governing the activation and maintenance of T cell responses. In response to many viral and bacterial infections, DCs promote the generation of immune responses that are dominated by $CD4^+$ T helper 1 (Th1) cells and cytotoxic $CD8^+$ T cells. In contrast, fungal and parasitic worm infections are predominantly associated with Th17 and Th2 responses respectively. In addition to these effector responses, DCs can be instructed to become tolerogenic and promote regulatory T cells (Tregs) responses, a process that is crucial for maintenance of immune homeostasis and control of autoimmune disorders and allergies [1-3].

Over the years, there has been a growing appreciation that microbiota are central players in the education and maintenance of a well-balanced immune system. Among the various mechanisms through which intestinal microbiota have been described to modulate the immune system, the production of short chain fatty acids (SCFAs) is a major one [4]. SCFAs are organic fatty acids with acyle chains constisting of 1 to 6 carbon atoms (C1-C6) that are the fermentation products of nondigestible polysaccharides by gut microbiota. Acetate (C2), propionate (C3) and butyrate (C4) are amongst the most abundant species found in the intestine [5]. Given their ability to be transported into the circulation, SCFAs can exert functions in organs distal to the intestine [2, 4, 6, 7]. In line with this, SCFAs have beneficial effects on a broad range of inflammatory diseases in animal models of inflammatory bowel disease (IBD), colitis, asthma, obesity and arthritis [2, 4, 8, 9].

SCFAs have diverse functions depending on the tissue or cell type involved. For instance, SCFAs are crucial for the maintenance of intestinal epithelium physiology by regulating the cellular turnover and barrier functions. SCFAs can also regulate the activation, recruitment and differentiation of immune cells, including neutrophils, DCs, macrophages, and T lymphocytes. In general, SCFAs have anti-inflammatory effects on immune cells. For instance, SCFAs reduce expression of pro-inflammatory cytokines such as tumor necrosis factor (TNF)-α, IL-6 and IL-12 by macrophages and DCs. In addition, SCFAs, in particular butyrate, can condition murine DCs to promote the differentiation and expansion of Tregs. SCFAs can additionally act on T cells directly, resulting in reduced proliferation and polarization towards a regulatory phenotype [10-12].

Two main mechanisms have been described thus far through which SCFAs can modulate immune cell function. SCFAs can affect immune cells via signaling through specific G protein-coupled receptors (GPRs). The most well-characterized SCFAs-sensing GPRs are GPR41, GPR43 and GPR109A [5, 13, 14]. In addition, following transport across the plasma membrane via monocarboxylate transporter Slc5a8 [15-17], proprionate and butyrate can act as inhibitors of histone deacetylase (HDAC) 1 and 3. HDACs together with histone acetylase (HATs) control histone acetylation, which plays a key role in epigenetic regulation of gene expression by serving as a switch between permissive (via HAT-induced acetylation) and repressive chromatin (through HDAC-driven deacetylation). While inhibition of HDAC activity can have a wide range of effects including changes in gene expression, chemotaxis, differentiation, proliferation and apoptosis [9, 11, 18], studies on immune cells have linked HDAC inhibition by SCFAs primarily to suppression of inflammatory responses [19-22]. Finally, SCFAs can also act as direct substrates for metabolic processes in cells. For instance, butyrate is known to be a major energy source for gut epithelium [23]. However, whether SCFAs also feed into core metabolic pathways of immune cells in a similar manner to regulate their bio-energetic status and whether this has an immunomodulatory effect still needs to be investigated.

Despite the advances in the field, there is still an incomplete understanding of the mechanisms through which SCFAs promote tolerogenic DCs and how these DCs drive Tregs. While one study found that butyrate-driven Treg cell induction by murine DCs is dependent on signaling through GPR109A [13], others have refuted this [16, 24]. These latter studies instead implicated the requirement for transport through Slc5a8 and subsequent inhibition of HDAC activity in promoting tolerogenic murine DCs. These butyrate-conditioned murine DCs were found to have increased expression of known immunosuppressive enzymes retinaldehyde dehydrogenase (RALDH)2 and indoleamine-pyrrole 2,3-dioxygenase (IDO) [16]. However, whether RALDH and/or IDO were important in tolerance induction by these DCs was not assessed. Importantly, to date there has only been a single study assessing the effects of SCFAs on human DCs, in which particularly butyrate was found to suppress LPS-induced maturation [14]. Yet, whether or how SCFAs can condition human DCs to prime Tregs remains to be addressed. Given these inconsistencies in murine literature and the paucity in our understanding of how SCFAs affect the functional properties of human DCs, we here set out to assess whether and through which molecular mechanisms SCFAs affect T cell polarization by human DCs. We find that butyrate through a combination of signaling via GPR109A and HDAC inhibition drives RALDH1 expression in human DCs which licenses them to prime Tr1 cells. This provides important new insights into the cellular and molecular mechanisms through which SCFAs can exert their immunomodulatory effects in humans.

MATERIALS AND METHODS

Ethics statement

Human monocytes and T cells were obtained from blood that was donated to the Bloodbank (Sanquin, Amsterdam) by healthy volunteers. The donated material was processed and analyzed anonymously. As such, not ethical approval was required for these studies.

Human DC culture, stimulation, and analysis

Monocytes were isolated from venous blood and differentiated into moDCs as described previously [25]. On day six immature DCs were left untreated or were stimulated with 2 mM short chain fatty acids namely: acetate, butyrate (both sigma-Aldrich, kind gift from Dr. Martin Giera) or propionate (Sigma-Aldrich); 2.5 μM Vitamin D3 (Sigma-Aldrich), Trichostatin A (100 ng/mL), Niacin (2 mM) (Sigma-Aldrich), Soluble Egg Antigens (SEA) (50 μg/mL), IFN-γ (1000 U/mL). SEA was prepared as previously described [26]. All stimulations were done in the presence of 100 ng/mL ultrapure LPS (*E. coli* 0111 B4 strain, InvivoGen, San Diego, CA, USA), unless indicated otherwise. The DCs were incubated with 10 μM RALDH inhibitor diethylaminobenzaldehyde (DEAB) (Stem cell Technologies) in the indicated conditions. After 48 h of stimulation, surface expression of co-stimulatory molecules was determined by flow cytometry (FACS-Canto, BD Biosciences, Breda, The Netherlands) using the following antibodies: CD14 HV450 (MΦP9), CD86 FITC (2331 FUN-1), CD40 APC (5C3), CD80 Horizon V450 (L307.4), CD274/PDL1 PECy7 (MIH1) (all BD Biosciences), HLA-DR APC-eFluor 780 (BL6), CD273/PDL2 PE (MIH18) (eBioscience, San Diego, CA, USA), CD83 PE (HB15e), CD1a PE (BL6) (all Beckman-Coulter, Fullerton, CA, USA), LAP APC (TW4-2FB) (BioLegend). In addition, $1x10^4$ matured moDCs were co-cultured with $1x10^4$ CD40L-expressing J558 cells. Supernatants were collected after 24 h and the concentration of IL-10 (Sanquin) and IL-12p70 (using mouse anti-human IL-12, clone 20C2 and biotinylated mouse-anti-human IL-12 clone 8.6, both BD Bioscience) were determined by ELISA.

Aldefluor assay
Aldefluor kit (Stemcell Technologies) was used, according to the manufacture's protocol, to determine RALDH activity.

Histone 3 (H3) and H4 acetylation by flow cytometry
H3 and H4 acetylation was determined by flow cytometry according to the protocol described elsewhere [27].

HDAC activity assay
HDAC activity was determined using a commercial HDAC cell-based activity assay kit (Cayman Chemical, Ann Arbor, MI) according to the manufacture's guidelines. The HDAC activity was measured with the Wallac 1420 (PerkinElmer Life and Analytical Sciences, Turku, Finland).

Functional metabolic analyses
The metabolic characteristics of moDCs were analyzed using a Seahorse XF^{e}96 Extracellular Flux Analyzer (Seahorse Bioscience) as described previously [28, 29]. In brief, after 48h of pulsing, 4x10^4 DCs were plated in unbuffered, glucose-free RPMI supplemented with 5% dialyzed FCS and left to rest one hour before the assay. Subsequently ECAR and OCR were analyzed in response to glucose (10 mM; port A), oligomycin (1 μM; port B), fluoro-carbonyl cyanide phenylhydrazon (FCCP, 3 μM; port C), rotenone/antimycin A (1/1 μM; port D) (all Sigma-Aldrich). Baseline ECAR = increase in ECAR in response to injection A. Spare ECAR = increase in ECAR in response to injection B. Baseline OCR = difference in OCR between readings following port A injection and readings after port D injection. Spare OCR is difference between basal and maximum OCR which is calculated based on the difference in OCR between readings following port C injection and readings after port A injection.

Human T cell culture and analysis of T cell polarization
For analysis of T-cell polarization, 48 h-pulsed moDCs were cultured with allogenic naive CD4$^+$ T cells for 11 days in the presence of *staphylococcal enterotoxin B* (10 pg/mL). On day 6 and 8, rhuIL-2 (10 U/mL, R&D System) was added to expand the T cells. Intracellular cytokine production was analyzed after re-stimulation with 100 ng/mL phorbol myristate acetate and 2 μg/mL ionomycin for a total 6 h; 10 μg/mL brefeldin A was added during the last 4 h. Subsequently the cells were fixed with 3.7% paraformaldehyde (all Sigma-Aldrich). The cells were permeabilized with 0.5% saponin (Sigma-Aldrich) and stained with PE-, FITC- and APC-labelled antibodies against IL-4 (8D4-8), IFN-γ (25723,11) (both BD Biosciences) and IL-10 (JES3-19F1) (BioLegend), respectively. Alternatively, 1x10^5 T cells were re-stimulated using anti-CD3 and anti-CD28 (both BD Biosciences), 24 h after re-stimulation supernatants were collected and IL-10 production by T cells was measured by ELISA (Sanquin).

T cell suppression assay
For analysis of suppression of proliferation of bystander T cells by test T cells, 5x10^4 SCFA-pulsed DCs were co-cultured with 5x10^5 naive CD4$^+$ T cells for 6 days. These T cells (test T cells) were harvested, washed, counted, stained with the cell cycle tracking dye 1 μM Cell Trace Violet dye (Thermo Fisher Scientific) and irradiated (3000 RAD) to prevent expansion. Bystander target T cells (responder T cells), which were allogeneic memory T cells from the same donor as the test T cells, were labeled with 0.5 μM cell tracking dye 5,6-carboxy fluorescein diacetate succinimidyl ester

(CFSE). Subsequently, $5x10^4$ test T cells, $2.5x10^4$ responder T cells and $1x10^3$ LPS-stimulated DCs were co-cultured for 6 days. Proliferation was determined by flow cytometry, by co-staining with CD4 PE-Cy7 (clone SK3) and CD25 APC (clone 2A3) (both BD Bioscience). To some cultures, where indicated, 10 µg/mL anti-IL-10 antibody (Biolegend), 10 µM ALK5 (Sigma-Aldrich), 10 µM DEAB, 20 ng/mL recombinant human TGF-β1 (Biolegend) (kind gift from Dr. L. Boon) or control antibody IgG1 (Biolegend) was added during the DC-T cell co-culture or during the test-responder T cell co-culture.

Quantitative real-time PCR

RNA was extracted from snap-frozen 16 h-stimulated DCs. The isolation of mRNA was performed according to manufacturer's instruction using RNeasy plus micro kit (Qiagen). cDNA was synthesized with reverse transcriptase kit (Promega) and PCR amplification by the SYBER Green method were done using CFX (Biorad). Specific primers for detected genes are listed in supplemental experimental procedures. Relative expression was determined using the $2^{-\Delta\Delta CT}$ method.

siRNA electroporation

On day 4 of the DC culture, the cells were harvested and transfected with either no siRNA (R buffer only, provided by Invitrogen), 20 nM control siRNA or 20 nM GPR109A siRNA (both Dharmacon) using Neon Transfection System (Invitrogen) with the following setting: 1600 V, 20 ms width, one pulse. Following electroporation, $3.5x10^5$ cells were seeded per well in to a 24-well plate containing RPMI media without antibiotics. After 24 h, culture medium (RPMI) supplemented with 10% HI-FCS, rIL4 (0.86 ng/mL. R&D system Minneapolis, MN, USA) and rGM-CSF (20 ng/mL, Invitrogen, Carlsbad, CA, USA) was added. The transfection efficiency was routinely greater than 80%. *GPR109A* silencing efficiency was determined by quantitative RT PCR.

ATAC-seq analysis

$5x10^4$ moDCs stimulated for 6 h with indicated reagents were subjected to ATAC-seq as described elsewhere [30]. For analysis of the ATAC-seq data the Biopet Carp pipeline was used (http://biopet-docs.readthedocs.io/en/latest/pipelines/carp/).

Statistical analysis

Data were analyzed for statistical significance using GraphPad Prism 7.0 statistical software (GraphPad Software, La Jolla, CA, USA). Comparison between groups was performed using the Student's t test or two way ANOVA test. All data are shown as means ± SEM. Differences were considered significant if $p<0.05$.

RESULT

Butyrate suppresses LPS-induced activation and metabolic reprogramming in human DCs

Tolerogenic compounds are often able to interfere with DC activation induced by pro-inflammatory signals. Therefore, we first examined how acetate, propionate and butyrate influenced several markers of activation of human monocyte-derived DCs (moDCs) during co-stimulation with LPS, a toll-like receptor (TLR)-4 ligand. Treatment with butyrate, and to a lesser extent with acetate and propionate, antagonized the LPS-induced upregulation of costimulatory markers CD83, CD80 and CD40 (Figure 1A). In line with this, all SCFAs lowered production of both IL-10 and IL-12 induced by LPS, with the strongest suppression induced by butyrate (Figure 1B).

Given the importance of metabolic rewiring for DC activation [31] and the fact that SCFAs can act as direct substrates for several core metabolic pathways in the intestinal epithelium [23], we also analyzed the effects of SCFAs on DC metabolism. As previously reported [28], LPS stimulation enhanced the extra-cellular acidification rate (ECAR), a measure of glycolysis, of human DCs.

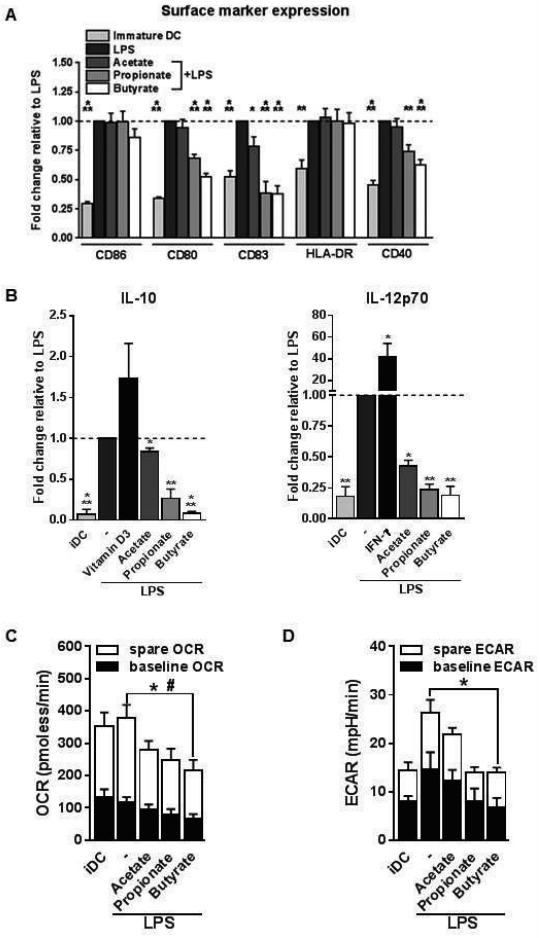

Figure 1. Butyrate suppresses LPS-induced activation and metabolic changes in human DCs

(A and B) Monocyte-derived DCs were left un-treated (iDC) or stimulated as indicated for 48 h after which (A) expression of maturation markers was analysed by flow cytometry and (B) supernatants were collected and concentrations of indicated cytokines were determined by ELISA. (A) The expression levels of maturation markers are based on the geometric mean fluorescence and are shown relative to DCs stimulated with LPS, which was set to 1 for each marker (dashed line). (B) Vitamin D3 and IFN-γ-stimulated DCs were taken along as IL-10 - and IL-12-inducing controls, respectively. (C and D) Metabolic phenotype of differently stimulated DCs was assed using a Seahorse extracellular flux analyser. (C) Baseline and spare mitochondrial OCR were determined as described in materials and methods, with significant differences in baseline or spare OCR indicated with * and #, respectively. (D) baseline and spare ECAR were determined as described in materials and methods, with significant differences in baseline ECAR indicated with *. (A-D) Bar graphs represent means ± SEM of at least five experiments. *-# $p<0.05$, ** $p<0.01$, *** $p<0.001$ based on paired Student's T-test.

Interestingly, we observed that in contrast to acetate and propionate, butyrate significantly antagonized this response. Moreover, we found that butyrate significantly reduced baseline mitochondrial oxygen consumption rate (OCR) (Figure 1C) as well as the spare respiratory capacity (SCR) of LPS-stimulated DCs (Figure 1D), suggesting that butyrate reduces the overall metabolic activity of DCs. Together, these findings indicate that propionate and more strongly butyrate, have the capacity to suppress LPS-induced DC activation and that butyrate additionally renders DCs metabollically less active.

Butyrate conditions human DCs to induce type 1 regulatory T (Tr1) cells

We next set out to address how these phenotypic and metabolic changes induced by SCFAs on DCs would translate into their ability to prime T helper (Th) cell responses. To assess this, we co-

cultured the SCFAs-pulsed DCs with naive $CD4^+$ T cells and measured the intracellular cytokine production by the T cells. We found that all three SCFAs did not condition DCs to drive Th1 or Th2 responses, since neither IFN-γ nor IL-4 production was altered (Figure 2A). Instead, we found that butyrate-stimulated DCs significantly promoted IL-10 production by T cells after re-stimulation with either PMA and ionomycin (Figure 2B) or anti-CD3/CD28 (Figure 2C). Because IL-10 is a well-known immunosuppressive cytokine released by Tregs, we next examined whether these IL-10-producing T cells were bona-fide Tregs, by determining their capacity to suppress the proliferation of other T cells. T cells that had been primed by butyrate-conditioned DCs strongly suppressed proliferation of target T cells. Propionate had a similar effect, although to a lesser extent (Figure 2D). To further characterize the phenotype of Tregs primed by butyrate-treated DCs, protein expression of three common Treg markers were measured, namely glucocorticoid induced TNF receptor (GITR), cytotoxic T-lymphocyte-associated protein 4 (CTLA4) and forkhead box P3 (FOXP3) [1, 32]. In contrast to Tregs that were primed by DCs rendered tolerogenic by vitamin D3, Tregs induced by butyrate-stimulated DCs did not display increased expression of these markers (Figure 2E). This phenotype of a Treg with high IL-10 production but low FOXP3 expression is typical for Tr1 cells, which are defined by their dependency on IL-10 production to suppress bystander T cell proliferation [32]. Indeed, when IL-10 (Figure 2F), but not transforming growth factor beta-1 (TGF-β1) (Figure S1), was neutralized in the T cell suppressor assay, the suppressive capacity of these Tregs was significantly reduced. Together, these data demonstrate that butyrate conditions human DCs to prime IL-10-secreting Tr1 cells.

Tr1 cell induction by butyrate-conditioned DCs depends on RALDH1 expression.

We next aimed to determine through which mechanism(s) butyrate-conditioned DCs prime Tr1 cells. To address this, we analyzed gene expression of several immune-regulatory factors that are known to be expressed by tolerogenic DCs and have been shown to be induced by SCFAs in immune cells, namely *IL-10*, *IDO1*, *TGFB1*, and *RALDH1* and *RALDH2* (also known as aldehyde dehydrogenase 1 family member A1 and A2 respectively) [33] (Figure 3A). We found that *TGFB1* mRNA was up-regulated by both butyrate and propionate, while *RALDH1* was selectively induced by butyrate. This prompted us to further study the role of TGF-β and RALDH1 in Tr1 cell induction by butyrate-conditioned DCs. To this end, we quantified latency-associated peptide (LAP) expression, which is a protein derived from the N-terminal region of the *TGFB1* gene product and binds TGF-β on the cell surface to keep it in its inactive form. In line, with the mRNA expression data, we found that the level of LAP protein expression was significantly increased by both propionate- and butyrate-stimulated DCs (Figure 3B and S2A). However, while blocking of TGF-β signaling using the SMAD2/3 inhibitor ALK5 did reverse Treg induction by exogenously added TGF-β, it did not affect the Tr1-priming capacity of butyrate-conditioned DCs (Figure 3C). This suggests that butyrate does not license DCs to prime Tr1 cells through induction of TGF-β.

We next assessed the role of RALDH1. RALDH1 converts vitamin A into retinoic acid (RA), that through the activation of retinoic acid receptor (RAR) has been shown to induce tolerogenic properties in DCs as well as to directly drive Treg differentiation of T cells [34]. We found that in line with the increased mRNA expression of *RALDH1*, DCs stimulated with butyrate, but nor with acetate or propionate, increased the enzymatic activity of RALDH in a time-dependent manner both in the presence (Figure 3D) and absence of LPS (Figure S2B and S2C). To test the role of RALDH activity in Tr1 cell induction by butyrate-treated DCs, we used diethylaminobenzaldehyde (DEAB), a reversible inhibitor of RALDH [35] during the DC-T cell co-culture. This treatment

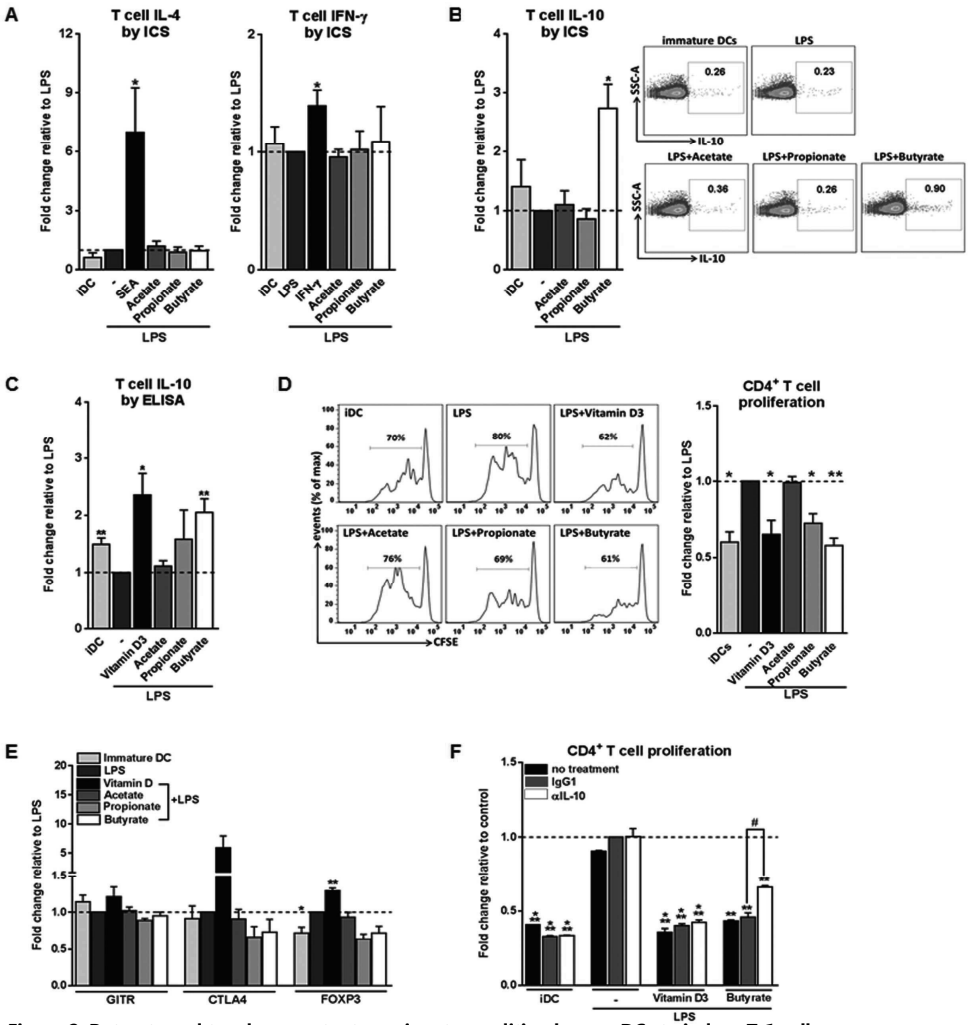

Figure 2. Butyrate and to a lesser extent propionate condition human DCs to induce Tr1 cells

(A-C) Differently stimulated DCs were co-cultured with allogenic naive $CD4^+$ T cells. After 11 days cytokine production by T cells was analysed (A and B) by flow cytometry after 6 h of stimulation with PMA and ionomycin or (C) by ELISA after 24 h re-stimulation with αCD3/αCD28. (A-C) Data represent fold change in (A and B) percentage of T cells that stain positive for indicated cytokines or in (C) IL-10 levels in culture supernatants, relative to data from LPS-stimulated DCs which was set to 1 for each cytokine (dashed line). (B) Representative flow cytometry plots are shown on the right. (D) T cell suppression assay in which irradiated test T cells were co-cultured with activated CFSE-labelled responder $CD4^+$ T cells. On day 6 CFSE dilution of the responder T cells was assessed by flow cytometry. The left panels are representative histograms of CFSE dilution by responder T cells. Quantification of these data is shown in the bar graph and is depicted as fold change relative to data from LPS-stimulated DCs which was set to 1 (dashed line). (E) Expression of regulatory markers by T cells was analysed by flow cytometry. Bar graphs represent relative differences based on geometric mean fluorescence for GITR and CTLA4 or frequency of T cells that express FOXP3. (F) For the duration of the assay as described in (D) indicated antibodies were added. Data are from one experiment representative of two, shown as means ± SEM of triplicates. (A-E) Bar graphs represent means ± SEM of at least three experiments. $^{*,\#}p<0.05$, $^{**}p<0.01$, $^{***}p<0.001$ for significant differences with the control (*) or between test conditions (#) based on paired Student's T-test.

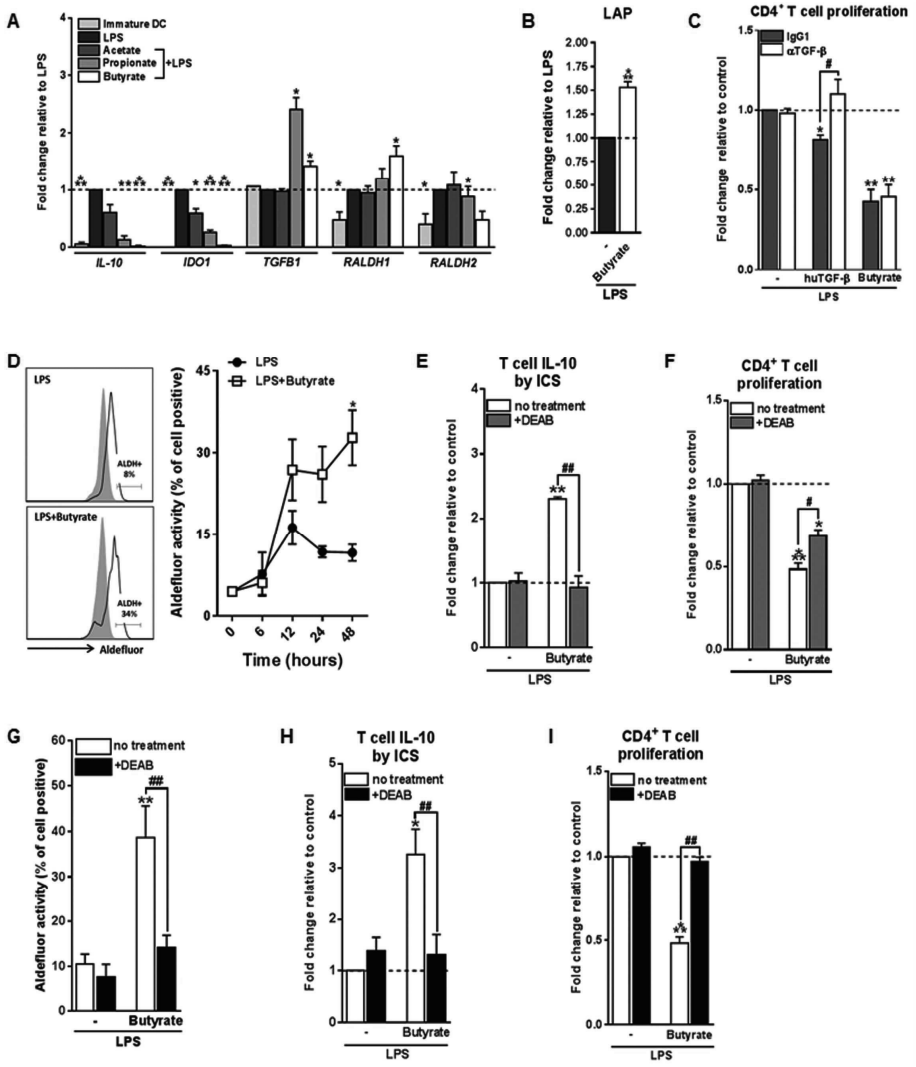

Figure 3. Tr1 cell induction by butyrate-conditioned human DCs depends on RALDH1 expression
(A) mRNA expression of indicated genes was quantified using real time-qPCR of moDCs stimulated for 16 h. (B) Relative membrane bound LAP expression on DCs stimulated with indicated reagents as determined by flow cytometry. (C) T cell suppression assay as described in Figure 2D, F. Blocking antibody of human TGF-β was added during the co-culture of DCs with T cells. Human TGF-β was taken along as positive control. (D) RALDH activity in DCs was assessed using an aldefluor assay with a readout by flow cytometry. Representative histograms of RALDH activity 48 h after stimulation are shown on the left, with grey shaded histograms and black lines representing DCs in which RALDH activity was assessed in the presence or absence of reversible RALDH inhibitor DEAB, respectively. Right graph: RALDH activity was measured at different times after stimulation and frequencies of DCs positive for RALDH activity are depicted. *p<0.005 based on two-way ANOVA test. (E) IL-10 production by T cells as described in Figure 2B or (F) T cell suppression assay as described in Figure 2D, but with the addition that DEAB or vehicle control was added during the DC-T cell co-culture. (G) RALDH activity assay as described in Figure 3D, but during stimulation DEAB or vehicle control were added. (H and I) Same as E and F, but now DEAB was added during stimulation of DCs with LPS +/- butyrate. (A-I) Bar graphs represent means ± SEM of at least three experiments and (A-C, F, G, I, J) are shown as fold change relative to control conditions. *, #p<0.05, **, ##p<0.01, ***p<0.001 for significant differences with the control (*) or between test conditions (#) based on paired Student's T-test.

abolished IL-10 production and reduced the suppressive capacity of the T cells (Figure 3E and 3F), indicating that RALDH activity is a key factor expressed by DCs to promote Tr1 cells and that DC-derived RA acts on T cells to prime their regulatory properties. In addition, we wondered whether RA produced by DCs may also act in an autocrine fashion to enforce their tolerogenic potential. Blocking RA generation by DCs from the beginning of the stimulation with butyrate blunted the ability of butyrate to increase RALDH activity in these cells (Figure 3G) and, as a consequence, in the inability of these cells to promote Tr1 cells (Figure 3H and 3I). Together, these findings suggest that initial butyrate-driven RALDH activity by means of production of RA is required to maintain its own expression, which licenses these DCs to subsequently prime Tr1 cells.

HDAC inhibition by butyrate is not sufficient for inducing tolDCs

We next set out to investigate the mechanisms through which butyrate drives RALDH1 expression in human DCs. Two mechanisms have been described in other immune cells, namely HDAC inhibition and GPR signaling [5, 11, 12, 36, 37]. To first establish whether butyrate could affect HDAC activity in human DCs, we performed an HDAC activity assay on differently stimulated moDCs. As expected, trichostatin A (TSA), a well-known HDAC inhibitor with broad specificity [20, 36], was effective in inhibiting HDAC activity in DCs (Figure 4A). Butyrate, and to a lesser extent propionate, also displayed a robust capacity to inhibit HDAC activity in human DCs. Importantly,

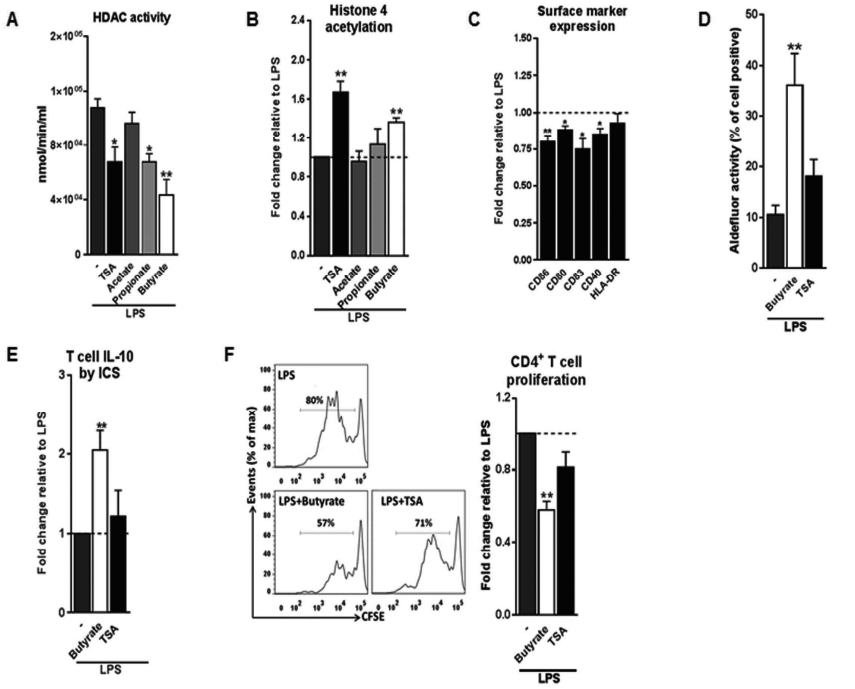

Figure 4. HDAC inhibition by butyrate is not sufficient for inducing Tr1 cells-promoting tolDCs

(A) DCs were stimulated for 24 h with indicated reagents and then assayed for HDAC activity. (B) Analysis of histone 4 acetylation by flow cytometry of DCs stimulated with indicated reagents for 6 h. (C) The expression of maturation markers of DCs stimulated for 48 h with TSA was analyzed using flow cytometry. The expression of surface marker levels is based on the geometric mean fluorescence. (D) RALDH activity assay as described in Figure 3D. (E) IL-10 production by T cells as described in Fig. 2B. (F) T cell suppression assay as described in Figure 2D. (A-F) Bar graphs represent means ± SEM of at least three experiments and (B, C, E, F) are shown as fold change relative to control conditions. *p<0.05, **p<0.01, ***p<0.001 based on paired Student's T-test.

this finding was corroborated by the observation that histone 4 acetylation was increased in DCs exposed to butyrate (Figure 4B). We did not see major changes in histone 3 acetylation as determined by flow cytometry (Figure S3). We hypothesized that if HDAC inhibition would be underlying the ability of butyrate to induce tolDCs, then TSA would be able to recapitulate the effects of butyrate. Indeed, TSA suppressed LPS-induced expression of several DC activation markers (Figure 4C). However, TSA treatment only marginally promoted RALDH activity in DCs (Figure 4D) and concordantly, failed to significantly induce IL-10-producing (Figure 4E) functional Tr1 cells (Figure 4F). These data indicate that while HDAC inhibition alone is sufficient to recapitulate some of the modulatory effects of butyrate (e.g. suppression of LPS-induced maturation marker expression), it is insufficient in inducing Tr1 cells by DCs.

Signaling through GPR109A by butyrate is required but not sufficient for inducing Tr1 cell-promoting tolDCs

The inability of HDAC inhibition to induce Tr1 cell-priming tolDCs, led us to assess the role of GPRs in this process. The major GPRs activated by SCFAs are GPR41, GPR43 and GPR109A [4, 10, 11]. Acetate and propionate are the most potent activators of GPR41 and GPR43, while butyrate more effectively binds to GPR109A [4, 9]. Consistent with a recent report [14], we found that *GPR109A* but not *GPR41* or *GPR43* are expressed by moDCs (Figure 5A). To investigate the role of GPR109A in mediating the modulatory effects of butyrate on human DCs, *GPR109A* was silenced using siRNA, resulting in >85% silencing at the mRNA level (Figure 5B) and a corresponding loss of the ability of niacin, a natural ligand of GPR109A, to suppress LPS-induced TNF-α production [13] (Figure S4A). silencing of *GPR109A* did not interfere with the capacity of butyrate to modulate LPS-induced DC maturation (Figure S4B). Importantly, however, we found that butyrate failed to induce RALDH activity in DCs in which *GPR109A* was silenced (Figure 5C). As a result, these DCs largely lost the ability to promote IL-10 production by T cells (Figure 5D) and functional Tr1 cells (Figure 5E). Interestingly however, stimulation with niacin was not sufficient to promote RALDH activity in DCs nor did it enhance their ability to induces Tr1 cells. This suggests that GPR109A signaling is required yet not sufficient for human tolDC induction by butyrate.

Butyrate depends on the combination of histone deacetylase inhibition and GPR109A signaling to prime Tr1 cell-inducing tolDCs

Given that butyrate inhibited HDAC activity in human DCs and that it dependents on GPR109A signaling to promote tolDCs, but that neither stimulation of GPR109A signaling nor HDAC inhibition alone was sufficient for induction of tolDCs, we evaluated whether butyrate requires both HDAC inhibition and GPR109A activation for its optimal modulatory effect. To test this, we co-incubated human DCs with both HDAC inhibitor TSA and GPR109A ligand niacin. Strikingly, in contrast to the single treatments, the combinatorial treatment synergistically induced RALDH activity to a level similar to what was induced by butyrate (Figure 6A). Consistent with these findings, T cells that were primed by DCs that had been treated with the combination of TSA and niacin, displayed a stronger suppressive capacity compared to the single treatment conditions Accessible Chromatin with high-throughput sequencing (ATAC-seq) analysis on the promotor region of RALDH1 to assess the level of chromatin accessibility following stimulation with butyrate, TSA, niacin or TSA in combination with Niacin. We found that TSA treatment, relative to unstimulated cells, resulted in a stronger ATAC-seq signal in the promotor region of *RALDH1,* which was comparable to the profile induced by butyrate (Figure 6C). In contrast, niacin treatment alone did not lead to opening of the chromatin in this locus, nor did it significantly alter the ATAC

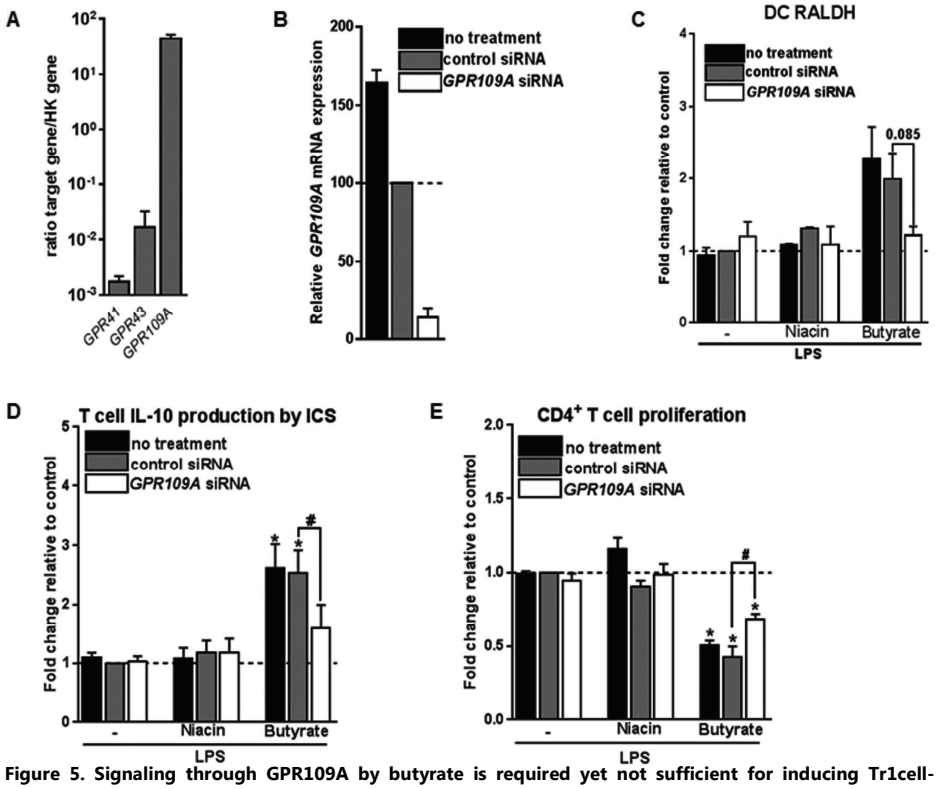

Figure 5. Signaling through GPR109A by butyrate is required yet not sufficient for inducing Tr1cell-promoting tolDCs

(A) mRNA expression of indicated genes was quantified using real time qPCR of unstimulated DCs. Expression is shown relative to housekeeping gene β-actin. (B-E) *GPR109A* expression was silenced by small interfering RNA (siRNA) on day 4 of DC differentiation after which (B) silencing efficacy was determined by real time-qPCR on day 6. (C) RALDH activity induced by butyrate and GPR109A ligand niacin was assessed as described in Figure 3D. (D) IL-10 production by T cells as described in Figure 2B was determined and (E) T cell suppression assay was performed as described in Figure 2D. (A-F) Bar graphs represent means ± SEM of at least three experiments and (B-E) are shown as fold change relative to control conditions. *, $^{\#}p<0.05$, $^{**}p<0.01$, $^{***}p<0.001$ for significant differences with the control (*) or between test conditions (#) based on paired Student's T-test.

seq profile induced by TSA. These findings point to two distinct roles of HDAC inhibition and GPR109A signaling in driving RALDH1 expression. Together with the observation that only the combined treatment with TSA and niacin significantly induced RALDH activity in DCs, this suggests that HDAC activity is needed for opening of the chromatin of the locus encoding RALDH1, while GPR109 signaling is required for initiation of transcription once the locus is accessible for transcription factors. Taken together, our data suggest that butyrate depends on both HDAC inhibition as well as GPR109A signaling to efficiently drive RALDH1 expression and to promote an anti-inflammatory phenotype in human DCs.

DISCUSSION

SCFAs produced by commensal bacteria, such as butyrate, have been well-documented to promote anti-inflammatory responses through the modulation of a variety of immune cells such as neutrophils, DCs, macrophages and T cells. However, the effects of SCFAs on human DC phenotype and function have remained elusive. Here we find that SCFAs, in particular butyrate,

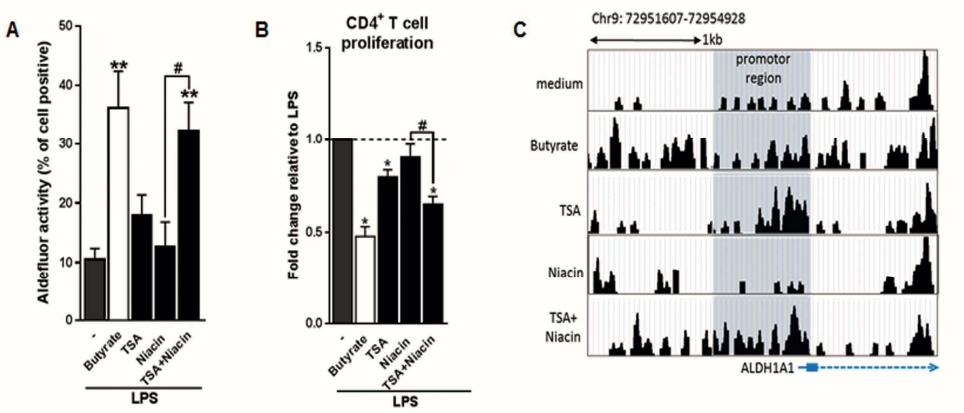

Figure 6. Butyrate depends on the combination of HDAC inhibition and GPR109A signaling to prime Tr1-inducing human tolDC

(A) RALDH activity assay as described in Figure 3D. (B) T cell suppression assay as described in Figure 2D. (C) ATAC-seq analysis of the promotor region (highlighted in grey) of RALDH1 gene locus 6 h after stimulation of DCs with indicated reagents. (A) Bar graphs represent means ± SEM of at least three experiments and (B) are shown as fold change relative to control conditions. (C) Data from one of three experiments is shown. $^{*,\#}p<0.05$, $^{**}p<0.01$ for significant differences with the control (*) or between test condition (#) based on paired Student's T-test.

suppresses LPS-induced activation and licenses them to prime functional Tr1 cells. Mechanistically, we provide evidence that butyrate, through the concerted action of both GPR109A activation and HDAC inhibition, drives the induction of RALDH1 expression and activity in human DCs. The resultant RA production on the one hand acts in autocrine manner to reinforce RALDH expression and maintain the tolerogenic properties of the DCs themselves, and on the other hand acts in a paracrine manner on T cells to differentiate them into regulatory IL-10-producing Tr1 cells (Figure 7). Our observation that SCFAs, especially butyrate, downregulate LPS-induced expression of DC activation markers as well as cytokines released by DCs is consistent with earlier studies in murine

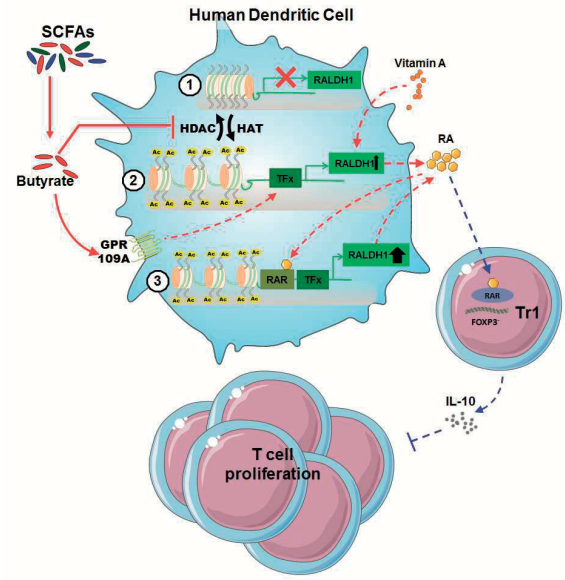

Figure 7. Proposed model of how butyrate conditions human DCs to prime Tr1 cells

(1) Butyrate inhibits HDAC activity in DCs to enhance net histone acetylation, resulting in opening of the gene locus of RALDH1 in human DCs. (2) The now open promotor region of RALDH1 enables butyrate through signaling via GPR109A to promote transcription and expression of RALDH1. (3) This initial RALDH1 expression results in RA synthesis that further reinforces RALDH1 expression. Butyrate-induced RALDH1 expression endows human DCs with the capacity to prime IL-10-producing Type 1 regulatory T cells.

DCs and more recently human DCs [14, 38, 39]. This observation has been linked to the ability of butyrate to interfere with LPS-induced translocation of NF-κB in macrophages and DCs [39, 40]. Here we additionally find that this inhibitory effect of butyrate on LPS-driven changes in DC biology can be extended to cellular metabolism, by showing that butyrate lowers activity of core metabolic pathways, i.e glycolysis and oxidative phosphorylation (OXPHOS), in human DCs. Since LPS-induced glycolysis, which occurs independently of NF-κB signaling is known to be crucial for DC activation [31], it is possible that one of the mechanisms through which butyrate interferes with LPS-driven DC activation is via modulation of DC metabolism. It remains to be determined how butyrate affects metabolism in DCs, but it is interesting to consider that SCFAs including butyrate can directly act as substrates for core metabolic pathways as has been well-documented in intestinal epithelial cells (IECs) [5, 11]. Additionally, butyrate has been shown to affect hypoxia induced factor (HIF), which is a transcription factor that amongst others is transcriptional regulator of glycolytic enzymes [23]. This low metabolic activity of butyrate-conditioned tolDCs appears to be different from what has been described for DCs that were rendered tolerogenic by vitamin D3, which were found to be metabolically characterized by increased glycolysis and OXPHOS [41, 42], suggesting that not all tolerogenic DCs share a common metabolic signature.

Several studies have demonstrated that SCFAs, in particular butyrate, are potent inducers of Tregs through the functional modulation of murine DCs [13, 24]. While butyrate was recently reported to suppress pro-inflammatory cytokine expression of human DCs, the consequence of this in terms of T cell polarization or Treg induction remained unclear. We now show that butyrate-conditioned DCs promote the *de novo* induction of Tregs from naive T cells. Specifically, we found that butyrate-exposed DCs prime IL-10 secreting Tr1 cells. However, it should be noted that IL-10 neutralization did no completely block their suppressive effect in our model, suggesting that additional mechanisms are involved. Our findings are in line with study of Jeon *et al.* who found that murine colonic DCs, when exposed to butyrate, also promote Tr1 cells differentiation [43]. Given that butyrate can also directly act on T cells to favor differentiation of $Foxp3^+$ Tregs [24], it is likely that Tregs induced by butyrate *in vivo* through both DC-dependent and independent pathways, are comprised of different subsets that mediate their immune-regulatory effects through a number of different mechanisms.

Mechanistically, our data reveal that specifically induction of *RALDH1* expression and activity is the key mechanism through which butyrate-conditioned human DCs prime Tr1 cells. RALDH enzymes are necessary for RA production by DCs from retinol (vitamin A) [44]. The role of DC-derived RA in promoting Tregs responses has been well documented, especially in the gut in both mouse [45] and human DC models [34]. However, the link between butyrate and the induction of RALDH1 expression in DCs has only been recently made. In this respect, our observation is in line with a recent study showing that the expression of *RALDH1* gene is induced by butyrate in human moDCs [14]. However, its role in T cell priming was not assessed. In addition, consistent with our *in vitro* findings with human DCs, high dietary fiber intake and butyrate synthesis have been linked to increased activity of RALDH in murine intestinal $CD103^+$ DCs, which was found to be important for protection against colitis [13] and food allergy [46]. A striking observation was that blocking of the enzymatic activity of RALDH in DCs during exposure to butyrate resulted in loss of butyrate-induced RALDH activity and Tr1-inducing ability, suggesting that RALDH-derived RA acts in an autocrine loop on DCs to reinforce their own RALDH activity required to maintain their tolerogenic potential. We additionally found that inhibition of RALDH activity during DC-T cell co-culture also reduced their Treg priming ability, implying that RALDH-derived RA subsequently acts as a key

signal from DCs to differentiate naive T cells into Tregs. Independent support for this model comes from a recent study showing that treatment of moDCs with RA itself is indeed sufficient to induce RALDH expression and to endow these cells with the capacity to induce IL-10-producing Tregs in an RA-dependent manner [34].

Two of the most well-studied mechanisms through which butyrate has been shown to modulate immune cell function are inhibition of HDAC activity and signaling through GPRs [4, 5, 9, 10, 18]. Our data suggest that butyrate depends on both mechanisms together to efficiently induce RALDH expression and promote functional tolDCs. This is based on the following observations: 1) silencing of *GPR109A*, resulted in the inability of butyrate to drive RALDH activity in DCs and to licence them to induce Tr1 cells; 2) yet signaling through this receptor induced by a GPR109A ligand, niacin could not recapitulate the tolerogenic effects of butyrate; 3) likewise, TSA, a general HDAC inhibitor, failed to do so as well; and 4) only simultaneous treatment of DCs with niacin and TSA could functionally mimic the effects of butyrate. Other studies, using murine models, have either highlighted a role for signaling via GPR109A or a role for inhibition of HDAC activity in the ability of butyrate to promote tolDCs [13, 24]. However, to our knowledge we now for the first time show that both modes of action are equally important and act in concert to drive RALDH expression and a tolerogenic phenotype in human DCs. These findings, together with the ATAC-seq data, lead us to speculate that inhibition of HDAC activity drives the opening of the chromatin encoding RALDH, while concurrent signaling via GPR109A promotes the activation of transcription factors that then can efficiently access the promotor region of this gene to drive transcription of RALDH1. Further studies would be warranted to identify which transcription factors downstream of GPR109A would mediate *RALDH1* expression.

In summary, we found human DCs treated with butyrate acquire a tolerogenic phenotype, which is dependent on RALDH activity driven by the combined action of HDAC inhibition and GPR109A signaling. Our findings provide key new mechanistic insights into the immunomodulatory effects of SCFAs on human cells and highlight the importance of a well-balanced composition of our gut microbiota with sufficient SCFA-generating genera to ensure maintenance of an immune tolerant state. In addition, in line with the well documented therapeutic potential of SCFAs for a wide range of diseases [2, 4, 8, 9, 11], our work could spur the design of targetable drugs that exploit the synergetic effect of GPR109 signaling and HDAC activity in DCs to favor tolerogenic responses to treat inflammatory disorders.

ACKNOWLEDGEMENTS

We thank Dr. Martin Giera for providing us SCFAs used in this project and Dr. Stefan White for help with the ATAC-seq analysis. This work was supported by the Indonesian Directorate General of Higher Education (DGHE/DIKTI)-Leiden University to Maria M. M. Kaisar and a Veni grant from Netherlands Organisation for Scientific Research to Bart Everts.

REFERENCES

1. Lutz, M.B., *Induction of CD4(+) Regulatory and Polarized Effector/helper T Cells by Dendritic Cells.* Immune Netw, 2016. **16**(1): p. 13-25.
2. Minarrieta, L., et al., *Metabolites: deciphering the molecular language between DCs and their environment.* Semin Immunopathol, 2016.
3. Yoo, S. and S.J. Ha, *Generation of Tolerogenic Dendritic Cells and Their Therapeutic Applications.* Immune Netw, 2016. **16**(1): p. 52-60.
4. Tan, J., et al., *The role of short-chain fatty acids in health and disease.* Adv Immunol, 2014. **121**: p. 91-119.
5. den Besten, G., et al., *The role of short-chain fatty acids in the interplay between diet, gut microbiota, and host energy metabolism.* J Lipid Res, 2013. **54**(9): p. 2325-40.

6. Murase, M., Y. Kimura, and Y. Nagata, *Determination of portal short-chain fatty acids in rats fed various dietary fibers by capillary gas chromatography.* J Chromatogr B Biomed Appl, 1995. **664**(2): p. 415-20.
7. Topping, D.L. and P.M. Clifton, *Short-chain fatty acids and human colonic function: roles of resistant starch and nonstarch polysaccharides.* Physiol Rev, 2001. **81**(3): p. 1031-64.
8. Kamada, N., et al., *Role of the gut microbiota in immunity and inflammatory disease.* Nat Rev Immunol, 2013. **13**(5): p. 321-35.
9. Koh, A., et al., *From Dietary Fiber to Host Physiology: Short-Chain Fatty Acids as Key Bacterial Metabolites.* Cell, 2016. **165**(6): p. 1332-45.
10. Thorburn, A.N., L. Macia, and C.R. Mackay, *Diet, metabolites, and "western-lifestyle" inflammatory diseases.* Immunity, 2014. **40**(6): p. 833-42.
11. Correa-Oliveira, R., et al., *Regulation of immune cell function by short-chain fatty acids.* Clin Transl Immunology, 2016. **5**(4): p. e73.
12. Trompette, A., et al., *Gut microbiota metabolism of dietary fiber influences allergic airway disease and hematopoiesis.* Nat Med, 2014. **20**(2): p. 159-66.
13. Singh, N., et al., *Activation of Gpr109a, receptor for niacin and the commensal metabolite butyrate, suppresses colonic inflammation and carcinogenesis.* Immunity, 2014. **40**(1): p. 128-39.
14. Nastasi, C., et al., *The effect of short-chain fatty acids on human monocyte-derived dendritic cells.* Sci Rep, 2015. **5**: p. 16148.
15. Donohoe, D.R., et al., *The Warburg effect dictates the mechanism of butyrate-mediated histone acetylation and cell proliferation.* Mol Cell, 2012. **48**(4): p. 612-26.
16. Gurav, A., et al., *Slc5a8, a Na+-coupled high-affinity transporter for short-chain fatty acids, is a conditional tumour suppressor in colon that protects against colitis and colon cancer under low-fibre dietary conditions.* Biochem J, 2015. **469**(2): p. 267-78.
17. Miyauchi, S., et al., *Functional identification of SLC5A8, a tumor suppressor down-regulated in colon cancer, as a Na(+)-coupled transporter for short-chain fatty acids.* J Biol Chem, 2004. **279**(14): p. 13293-6.
18. Rooks, M.G. and W.S. Garrett, *Gut microbiota, metabolites and host immunity.* Nat Rev Immunol, 2016. **16**(6): p. 341-52.
19. Chang, P.V., et al., *The microbial metabolite butyrate regulates intestinal macrophage function via histone deacetylase inhibition.* Proc Natl Acad Sci U S A, 2014. **111**(6): p. 2247-52.
20. Frikeche, J., et al., *Impact of HDAC inhibitors on dendritic cell functions.* Exp Hematol, 2012. **40**(10): p. 783-91.
21. Singh, N., et al., *Blockade of dendritic cell development by bacterial fermentation products butyrate and propionate through a transporter (Slc5a8)-dependent inhibition of histone deacetylases.* J Biol Chem, 2010. **285**(36): p. 27601-8.
22. Tao, R., et al., *Deacetylase inhibition promotes the generation and function of regulatory T cells.* Nat Med, 2007. **13**(11): p. 1299-307.
23. Kelly, C.J., et al., *Crosstalk between Microbiota-Derived Short-Chain Fatty Acids and Intestinal Epithelial HIF Augments Tissue Barrier Function.* Cell Host Microbe, 2015. **17**(5): p. 662-71.
24. Arpaia, N., et al., *Metabolites produced by commensal bacteria promote peripheral regulatory T-cell generation.* Nature, 2013. **504**(7480): p. 451-5.
25. Hussaarts, L., et al., *Rapamycin and omega-1: mTOR-dependent and -independent Th2 skewing by human dendritic cells.* Immunol Cell Biol, 2013. **91**(7): p. 486-9.
26. Everts, B., et al., *Omega-1, a glycoprotein secreted by Schistosoma mansoni eggs, drives Th2 responses.* J Exp Med, 2009. **206**(8): p. 1673-80.
27. Rigby, L., et al., *Methods for the analysis of histone H3 and H4 acetylation in blood.* Epigenetics, 2012. **7**(8): p. 875-82.
28. Everts, B., et al., *Commitment to glycolysis sustains survival of NO-producing inflammatory dendritic cells.* Blood, 2012. **120**(7): p. 1422-31.
29. Pelgrom, L.R., A.J. van der Ham, and B. Everts, *Analysis of TLR-Induced Metabolic Changes in Dendritic Cells Using the Seahorse XF(e)96 Extracellular Flux Analyzer.* Methods Mol Biol, 2016. **1390**: p. 273-85. 30. Buenrostro, J.D., et al., *ATAC-seq: A Method for Assaying Chromatin Accessibility Genome-Wide.* Curr Protoc Mol Biol, 2015. **109**: p. 21 29 1-9.
31. Everts, B. and E.J. Pearce, *Metabolic control of dendritic cell activation and function: recent advances and clinical implications.* Front Immunol, 2014. **5**: p. 203.
32. Hoeppli, R.E., et al., *The environment of regulatory T cell biology: cytokines, metabolites, and the microbiome.* Front Immunol, 2015. **6**: p. 61.
33. Li, H. and B. Shi, *Tolerogenic dendritic cells and their applications in transplantation.* Cell Mol Immunol, 2015. **12**(1): p. 24-30.
34. Bakdash, G., et al., *Retinoic acid primes human dendritic cells to induce gut-homing, IL-10-producing regulatory T cells.* Mucosal Immunol, 2015. **8**(2): p. 265-78.

35. Koppaka, V., et al., *Aldehyde dehydrogenase inhibitors: a comprehensive review of the pharmacology, mechanism of action, substrate specificity, and clinical application*. Pharmacol Rev, 2012. **64**(3): p. 520-39.
36. Park, J., et al., *Short-chain fatty acids induce both effector and regulatory T cells by suppression of histone deacetylases and regulation of the mTOR-S6K pathway.* Mucosal Immunol, 2015. **8**(1): p. 80-93.
37. Vinolo, M.A., et al., *Suppressive effect of short-chain fatty acids on production of proinflammatory mediators by neutrophils.* J Nutr Biochem, 2011. **22**(9): p. 849-55.
38. Berndt, B.E., et al., *Butyrate increases IL-23 production by stimulated dendritic cells.* Am J Physiol Gastrointest Liver Physiol, 2012. **303**(12): p. G1384-92.
39. Saemann, M.D., et al., *Bacterial metabolite interference with maturation of human monocyte-derived dendritic cells.* J Leukoc Biol, 2002. **71**(2): p. 238-46.
40. Maa, M.C., et al., *Butyrate reduced lipopolysaccharide-mediated macrophage migration by suppression of Src enhancement and focal adhesion kinase activity.* J Nutr Biochem, 2010. **21**(12): p. 1186-92.
41. Ferreira, G.B., et al., *Vitamin D3 Induces Tolerance in Human Dendritic Cells by Activation of Intracellular Metabolic Pathways.* Cell Rep, 2015.
42. Malinarich, F., et al., *High mitochondrial respiration and glycolytic capacity represent a metabolic phenotype of human tolerogenic dendritic cells.* J Immunol, 2015. **194**(11): p. 5174-86.
43. Jeon, S.G., et al., *Probiotic Bifidobacterium breve induces IL-10-producing Tr1 cells in the colon.* PLoS Pathog, 2012. **8**(5): p. e1002714.
44. Schilderink, R., et al., *The SCFA butyrate stimulates the epithelial production of retinoic acid via inhibition of epithelial HDAC.* Am J Physiol Gastrointest Liver Physiol, 2016. **310**(11): p. G1138-46.
45. Vitali, C., et al., *Migratory, and not lymphoid-resident, dendritic cells maintain peripheral self-tolerance and prevent autoimmunity via induction of iTreg cells.* Blood, 2012. **120**(6): p. 1237-45.
46. Tan, J., et al., *Dietary Fiber and Bacterial SCFA Enhance Oral Tolerance and Protect against Food Allergy through Diverse Cellular Pathways.* Cell Rep, 2016. **15**(12): p. 2809-24.

SUPPLEMENTARY DATA

Table S1. Primer sequences used for RT-qPCR

Gene	Forward (5'-3')	Reverse (5'-3')
ACTB	GCTACGAGCTGCCTGACGG	CAGCGAGGCCAGGATGGAGCC
IL10	ACCTGCCTAACATGCTTCGAG	CCAGCTGATCCTTCATTTGAAAG
IDO1	GGTCTGGTGTATGAAGGGTTCTG	GAGGAACTGAGCAGCATGTCCT
TGFB1	CCCAGCATCTGCAAAGCTC	GTCAATGTACAGCTGCCGCA
RALDH1	TGGCTTATCAGCAGGAGTGT	ACCGTACTCTCCCAGTTCTCTTC
RALDH2	GAGCAGGGTCCCCAGATTGA	CCCAGTCCTTTGCCTCCACA
GPR41	TCTCAGCACCCTGAACTCCT	TTCTGCTCCTTCAGCTCCAT
GPR43	GCCTGGTGCTCTTCTTCATC	AGGTGGGACACGTTGTAAGG
GPR109	TGCCGCCCTTCCTGATGGACA	TGTTCAGGGCGTGGTGGGGA

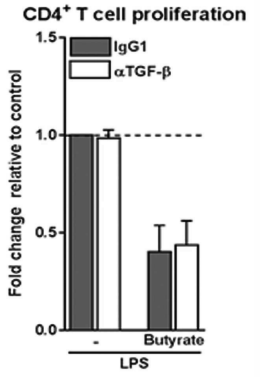

Figure S1. T cell suppression by butyrate-conditioned DCs is independent from TGF-β signalling
T cell suppression assay as described in Figure 2D. Blocking antibody against TGF-β or IgG1 control antibody was added during the DC-T cell co-culture. Bar graphs represent means ± SEM of two experiments and are shown as fold change relative to control condition.

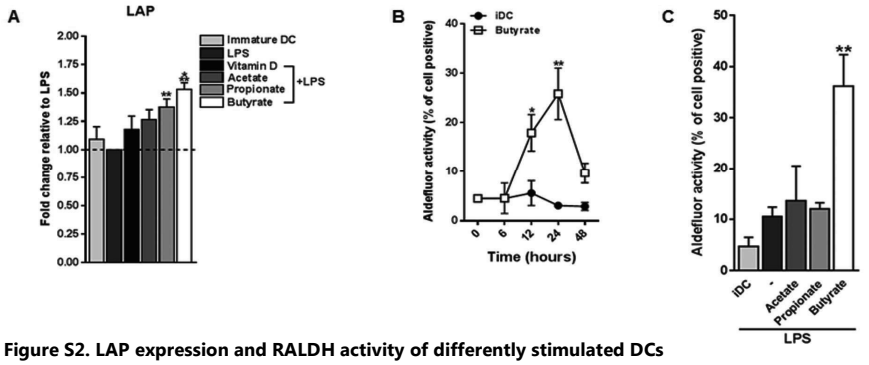

Figure S2. LAP expression and RALDH activity of differently stimulated DCs
(A) Surface LAP expression on stimulated DCs was determined as described in Figure 3B. (B and C) RALDH activity was assessed in stimulated DCs as described in Figure 3D and 3E. In (B) the kinetic of RALDH activity was assessed on iDC and butyrate stimulated DCs (in the absent of LPS) at 0, 6, 12, 24 and 48 h after stimulation and in (C) RALDH activity was measured on 6 h-differently stimulated DCs. (B) Bars represent means ± SEM, statistically significance of different time points per condition compared to 6 h time point. *p<0.05, **p<0.01 based on two-way ANOVA test. (A and C) Bar graphs represent means ± SEM of at least three experiments and (A) are shown as fold change relative to control conditions. **p<0.01, ***p<0.001 based on paired Student's T-test.

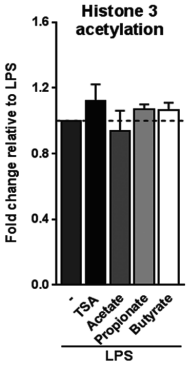

Figure S3. Histone 3 acetylation in differently stimulated DCs
Analysis of histone 3 acetylation by flow cytometry of DCs stimulated with indicated reagents for 6 h. Bar graphs represent means ± SEM of at least three experiments and are shown as fold change relative to LPS control which is set to 1 (dashed line).

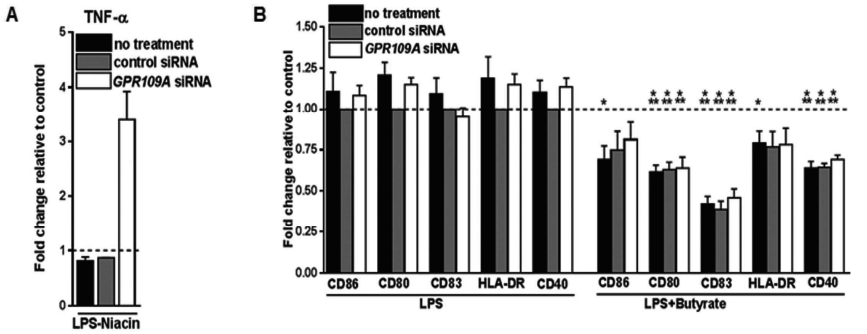

Figure S4. Effect of *GPR109A* silencing on niacin and butyrate conditioned-DCs
GPR109A expression was silenced by small interfering RNA (siRNA) on day 4 of DC differentiation after which (A) the ability of niacin, as a natural ligand of GPR109A, to suppress LPS-induced TNF-α production was determined in supernatants by ELISA. (B) Expression of maturation markers of stimulated DCs was analysed by flow cytometry. (A and B) Bar graphs represent means ± SEM of at least three experiments and are shown as fold change relative to control conditions. *p<0.05, ***p<0.001 based on paired Student's T-test.

Chapter 8

General Discussion

Conceptual framework of this thesis

Knowing that helminth infections can have both detrimental and beneficial effects on host physiology and wellbeing, these consequences should be taken into account when one aims to implement programs to eradicate these infections. In this regard, decisions on when and where intervention strategies are initiated is on the one hand dependent on the availability of sensitive diagnostic methods to detect helminth infections, and on the other, on how these parasites influence the host immune system, directly or indirectly for instance via microbiota, as a major determining factor of disease outcome. Thus helminth diagnostics and immunological interplay between helminth and host can be seen as *two sides of the same coin* as they are distinct topics but also interrelated. The common denominator of the studies described in this thesis is tracking helminths, either, at the level of diagnostics or at the level of the immunological footprint they leave behind in the host. Together this thesis, provides valuable new insights for the design of more effective intervention strategies as well as for the development of therapeutic agents against inflammatory diseases. The conceptual frameworks of this thesis, is shown in the Figure 1. In this chapter, we will integrate the findings of different chapters. We discuss what novel insights this thesis has generated in the light of current knowledge and highlight directions for future research.

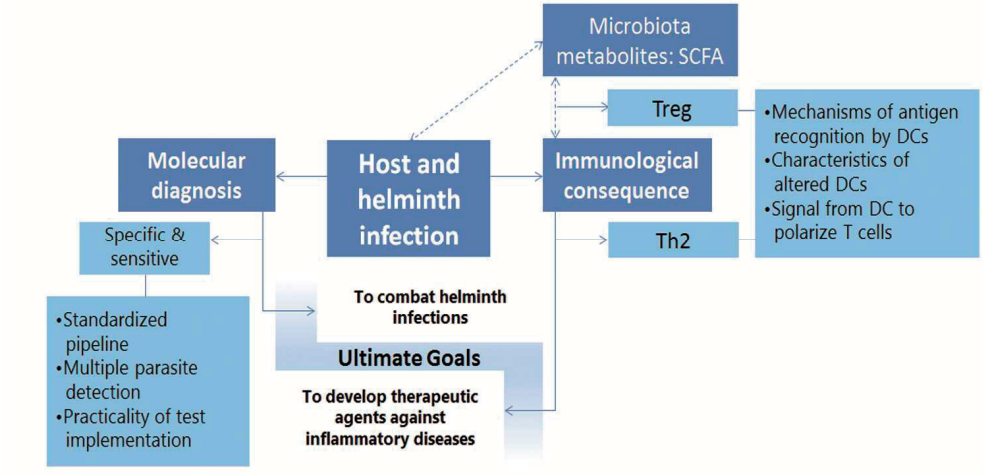

Figure 1. The conceptual framework of this thesis

Tracking helminths using molecular diagnostics, in a standerdized pipeline that allows for detection of multiple helminth species simulatioulsy with improved sensitivity and specificity over conventional methods, will be crucial for effective implementation and monitoring of deworming programs. The second part of this thesis focuses on tracking the immunological footprint of heliminths, particularly on the mechanisms of how helminths prime Th2 and Treg responses, either through direct functional modulation of DCs by helminth derived antigens, or indirectly by promoting changes in composition of gut microbiota and microbial products, such as SCFAs. Delineating the molecular mechanims through which helminths polarize Th2 and Treg response may now open up new avenues for anti-helminth therapies, but could also help in the developing of approaches to shape these immune responses for treatment of non-infectious inflammatory diseases.

Tracking helminths in the context of diagnostics

What we know and have learned from this thesis

Epidemiological studies have shown that the prevalence of infections caused by helminths, especially soil transmitted helminths (STHs) and schistosomes remain high in developing countries

and thus could have detrimental effects on the quality of life for humans [1, 2]. Although so far the diagnosis of helminth infections has relied on microscopy-based methods [3, 4], the importance of molecular based diagnostics has started to be appreciated. The lack of standardized protocols in performing microscopy-based methods to diagnose helminth infections [3, 5, 6], make it difficult to compare the data collected between studies [4, 7]. By evaluating the performance of multiplex real-time PCR, using samples collected in two helminths endemic areas, in which the microscopy procedures used were different, we have now shown that real-time PCR-based diagnosis can make the comparison between different endemic areas possible (**Chapter 2**). In addition, within a multiplex format, different parasite targets can be detected in a single procedure. We were also able to demonstrate that using real-time PCR two different species of hookworm namely *Necator americanus* and *Ancylostoma duodenale* can be distinguished, which is impossible by microscopy. This is important, because recently it was found that *A. duodenale,* but not *N. americanus*, is associated with severe anaemia and iron deficiency [8]. Moreover, *Strongyloides stercorales* can readily be detected by real-time PCR, whereas this is challenging using microscopy [9]. This may be particularly relevant, since it was recently shown that although 60% of infected people remain asymptomatic [10], immunosuppression in patients with chronic *S. stercorales* infection can precipitate a life-threatening hyper-infection characterized by increased parasite burden [11]. Finally, we have also demonstrated that the real-time PCR method is useful to analyse the risk factors associated with helminth infections. A recent study focusing on water, sanitation and hygiene (WASH) and environmental risk factors for infections with STHs, successfully used real-time PCR to identify strong risk associations with environmental variables [12].

Although real-time PCR-based methods to diagnose helminth infections have been reported to outperform microscopy-based methods [13-19], detection of *T. trichiura* by real-time PCR has often been unreliable until now because the current methods were insufficient to efficiently extract DNA from *T. trichiura* eggs. Therefore, specific sample preparation is required to extract the DNA of *T. trichiura* eggs prior to PCR detection. Bead-beating prior to DNA extraction has been used to improve DNA recovery. However, the studies using this method showed a PCR-based prevalence of *T. trichiura* below 3% [14, 17, 18, 20], which is a too low frequency to detect any beneficial effect that the beating method may have. Therefore, we performed in **Chapter 3** a comprehensive comparison of different sample preparation procedures prior to DNA extraction for helminth infections to establish a protocol to maximize *T. trichiura* DNA yield. We found that for optimal *T. trichiura* DNA extraction, sample preservation with ethanol in combination with bead-beating prior to parasite DNA extraction was the best procedure. This has already been successfully implemented in a recent population-based study where the effect of anthelmintic treatment on insulin resistance was examined [21].

Key points regarding current knowledge and the advances described in this thesis regarding the molecular diagnosis of helminth infections are summarized in Box.1, in section A and B, respectively.

Future perspective: A standardized operating procedure to perform epidemiological studies of helminth infections

The ability to reliably monitor the distribution of helminth infections is key to evaluate the success of mass drug administration programs [1, 2]. This critically depends on standardized diagnostic techniques for these infections and the implementation of strict guidelines of the operating procedures for diagnosis. We in chapter 2 and 3, not only indicate that diagnosis based on DNA detection is as a more reliable approach than microscopy, but also show that operating

procedures, which include sample collection, storage, preparation and helminth detection may affect the outcome of helminth diagnostics. However, it is well understood that each centre might have their own standard operating procedure in performing the diagnostics of helminth infections, raising the question, how can this be standardized? This will require, engagement of multiple research centres, the support from developed countries as well as consultation with WHO. Moreover, there is an emerging need for rapid diagnosis to support the WHO programs that strive to eliminate neglected tropical diseases (NTDs) in general and STHs and schistosomiasis, specifically. In this respect, recombinase polymerase amplification has recently been developed as an alternative molecular-based rapid diagnostic tool [22], that although still being evaluated in a population-based study, it is likely to become of great value for this field.
See for a summary of the direction for future research regarding molecular diagnostics of helminth infections Box.1, section C.

Tracking the immunological footprint of helminths in their host: Dendritic cell-driven T cell polarization by helminths

What we know and have learned from this thesis

Helminths induce Th2 polarization, in which DCs play a pivotal role. This is a complex process that is initiated by the recognition of antigens derived from helminths by DCs, via a variety of PRRs that in both signalling-dependent and independent mechanisms can condition DCs for Th2 polarization [23-27]. Yet the molecular mechanisms through which helminths instruct DCs to prime Th2 responses and how helminth-conditioned DCs drive Th2 polarization are still incompletely understood. In chapters 4, 5 and 6 we used various approaches to study this in detail by focusing on Th2 polarization by egg-derived antigens from *S. mansoni*.

In a first attempt to find markers important for Th2 induction by DCs we performed a proteomics analysis on DCs that were stimulated with SEA and ω-1 (**Chapter 5**). Although some groups have used proteomics to characterize DCs stimulated with helminth antigens, the studies were primarily gel-based [28-30]. However, gel-based methods do not allow for high-throughput analysis and direct comparison of biological replicates is not possible. In our study, we analysed the proteomes using LC-FTICRMS, a high-throughput gel-free technique based on accurate mass tag (AMT) analysis [31, 32]. This method enabled us to take into account donor-to-donor variation. We observed that DCs stimulated with SEA or ω-1 were clustered together and separated from IFN-γ-stimulated pro-Th1 DCs, indicative of distinct proteomics profiles in pro-Th1 *versus* pro-Th2 DCs. We found that both SEA and ω-1 strongly increased expression of 60S acidic ribosomal protein P2 (RPLP2) and vesicle membrane protein (VAT-1) which are involved in ribosome and mitochondrial regulation respectively [33, 34]. This finding might indicate that SEA and ω-1 could affect cellular metabolism in DCs. Additionally, DC stimulated with SEA or ω-1 downregulated HLA-B and CD44 expression, which are important for efficient antigen presentation by DCs to T cells. The latter finding is supporting the dogma that Th2 differentiation may be favoured by a weak interaction between T cells and DCs at the immunological synapse [35, 36]. While this chapter pinpointed a set of proteins that may contribute to Th2 polarization by helminth-stimulated DCs, there are also indications that other factors, such as lipids, derived from helminths or induced by DCs upon recognition of helminths antigens, might be important for Th2 polarization by DCs.

All parasites contain lipids [37] which are not only of great importance to parasites as the chief form of stored energy, but also for their role as building units for cell membranes and various intracellular and paracrine signaling functions [38]. Parasite-derived lipids are not only important

for the biology of parasites themselves but might also affect immune polarization of the host. With this in mind, we performed a lipidomics analysis of the different life cycle stages of *S. mansoni* (**Chapter 4**). Although the lipid contents of different life cycle stages of *S. mansoni* has been studied [39], the lipid content of ES as well as the crude antigens has not been characterized. Using three complementary MS-based analytical platforms, our study has resulted in the establishment of a lipid profile database of both the different life cycle stages as well as what is found in extracts from *S. mansoni* that are often used for cellular immunological studies. This detailed lipid database can be used as a valuable resource to further study helminth biology in general and specifically that of *S. mansoni*. We found that different life cycle stages have distinct lipid signatures; for example diacylglycerols (DGs) are present predominantly in cercariae. DGs are important for promoting protein kinase C (PKC) activity, which regulates cellular function such as differentiation, cell growth and metabolism [40], processes that are known to be crucial for development of cercariae to worms [39]. In addition, a striking finding is the presence of prostaglandins (PGs) specifically in preparations from eggs (ES form eggs and soluble egg antigens). This ability to synthesize PGE_2 may not be limited to S. mansoni as it was recently found that also the whipworm *Trichuris suis* was able to secrete substantial amounts of PGE_2 [47]. Since egg deposition in the host during *Schistosoma* infection is strongly associated with Th2 induction [41] and members of PGs such as PGE_2 and PGD_2 have been shown to condition DCs for Th2 induction [42-44], this observation prompted us in chapter 6 to assess the role of these PGs in promotion of Th2 polarization by *S. mansoni* eggs.

In **Chapter 6**, we reported that that SEA not only contains PGE_2 but also stimulates DCs to synthesize PGE_2 and its isomers, and this occurred independently from ω-1. We additionally found that SEA binds to dectin-1 and dectin-2 on human moDCs, to trigger a signalling cascade involving Syk-Erk-$cPLA_2$ and COX1/2 to promote PGE_2 synthesis. Subsequently, our data shows, that this PGE_2 then acts in an autocrine fashion to drive OX40L expression on DCs to licence these cells to prime a Th2 response. In addition, we discovered that the non-enzymatic generation of PGE_2 isomers through reactive oxygen species (ROS)-driven auto-oxidation by DCs in response to SEA contributes to conditioning of DCs for Th2 priming. Finally, these findings were extended *in vivo*, showing that Syk and dectin-2 are essential for Th2 polarization *in vivo* as well as for Th2-driven granuloma formation around eggs in the liver during *S. mansoni* infection. Altogether, the data presented in this chapter reveal a previously unrecognized pathway that operates independently from ω-1 through which Th2 responses are induced by *S. mansoni*. Importantly, this pathway appears to play an instrumental role in the immunopathological outcome of schistosomiasis. The observations that antigens from *Fasciola hepatica* as well as from house dust mite have been shown to be recognized by dectin-1 [45] and dectin-2 [46], respectively, make it tantalizing to speculate that this dectin-PGE_2 dependent signalling axis in DCs is possibly not only triggered by *S. mansoni* but also by other helminths or allergens to promote Th2 responses.

To add to the complexity, increasing evidence implicates a role for microbiota in mediating immune regulation by helminths. A characteristic feature of helminth infections is that they elicit a type 2 immune response, alongside a regulatory response, especially in the setting of chronic, asymptomatic infections [48]. The stimulation of Treg activity has emerged as a central explanation certain microbiota and helminth infections, in ameliorating inflammatory diseases such as allergy and autoimmune diseases [49]. Interestingly, a recent publication showed a dependency of a gastrointestinal helminths on gut microbiota in modulating allergic inflammation [50], an effect that was mediated through the production of SCFAs by the microbiota. Although, microbiota are

the most well studied source of SCFAs, helminths are also known to generate acetate [51], which through specific enzymatic processes, can also be converted into butyrate, generally considered the most potent immunomodulatory SCFA [52]. Therefore, we aimed to elucidate the mechanism of action through which SCFAs induce regulatory responses in **Chapter 7**, by specifically focusing on the still poorly studied modulatory effects of SCFAs on human DCs. In this chapter, we demonstrate that butyrate suppresses LPS-induced maturation on DCs and conditions these cells to drive the differentiation of IL-10-producing type 1 regulatory T cells (Tr1). Mechanistically we found, butyrate to induce expression of RALDH by DCs, a key enzyme involved in retinoic acid (RA) production. This was required for both the priming of Tr1 cells and the maintenance of a tolerogenic DC (tolDC) phenotype. Finally, we observed that the conditioning of DCs by butyrate in our model depends on the combination of HDAC inhibition and GPR109A signalling. In chapter 7 for the first time we delineate the molecular mechanisms through which the SCFA butyrate conditions human DCs to prime Tregs. These findings do not only reveal additional mechanisms through which helminth may promote Treg activity in their hosts, but may also help in developing approaches to modulate regulatory immune responses for therapeutic purposes by targeting this butyrate-driven signalling pathway in DCs.
Key points of current knowledge and the advances described in this thesis regarding the molecular interplay between the immune system and helminths are summarized in Box.1, in section D and E respectively.

Future perspectives:

Uncovering novel mechanisms through which helminths modulate DCs

In the chapter 4 we identified different lipids in different cycle stages of *S. mansoni*. Some lipids are known for their capacity to induce Th2 such us PGD_2 and PGE_2 [42, 44]. However others lipids have not been investigated and the possible contribution of these other lipids to Th2 polarization awaits further investigation. Furthermore, how the helminths and microbiota can influence each other is still not fully understood. It has been postulated that antimicrobial peptides produced by helminths may shift microbial composition in the gut [51]. Moreover, it will be important to dissect the relative contributions of helminth- and microbiota-elicited Tregs in mediating immune modulation.

Entering unexplored territories in studying Th2- and Treg-priming by DCs in the context of helminth infections

Our proteomics (chapter 5) and lipidomics (chapter 6) studies have advanced our understanding of how DCs prime Th2 responses. For instance, in our DC-proteomics study, we have found the upregulation of protein HSP90AA1 in SEA- and ω-1- stimulated DCs, which is a protein important for type I interferon (IFN) production [53]. Interestingly, a recently published study showed that parasite-induced Th2 response depends on type I IFN signalling in murine skin DC [54]. This clearly warrants further investigation to assess whether this protein and type I IFN signalling in general is involved in Th2 priming by human DCs in response to *S. mansoni* antigens.

Evidence is accumulating that the capacity of immune cells to perform particular functions is controlled by their cellular metabolic state [55]. Also, the role of cellular metabolism in shaping the biology of immune cells that are involved in type 2 immune response is an active area of investigation. For instance, *in vitro* studies of Th2 metabolism showed that Th2 cell differentiation depend on glycolysis, and that inhibition of glycolysis interferes with the expression of GATA3 as well as IL-4 receptor [56, 57]. In contrast, to this date little is known about role of DC metabolism in

Th2 or Treg polarization, but would be a very interesting angle to uncover potential novel molecular mechanisms through which DCs prime these types of T cell responses.

From a methodological standpoint, we could foresee that the use of omics approaches will be crucial to fully unravel the molecular mechanisms through which DCs prime Th2 and Treg responses, as they allow for unbiased characterization of cellular phenotypes. In particular the integration of data from multiple omics approaches holds great promise to significantly move this field forward. For example, the integration of transcriptomics and metabolomics has resulted in the identification of distinct key metabolic pathways involved in classic and alternative activation of macrophages [58], which would not have been possible from analysis of either single omics approach.

Finally, a very important aspect to consider is that neighbouring cells may also influence the capacity of DC to induce Th2 polarization. As an example, B cells have been suggested to be important in the initiation of Th2 response by enabling the right localization of DCs in the lymph node [59]. Moreover, recent observations suggest that ILC2s contribute to Th2 responses by promoting DC migration, by interacting with T cells via MHC-II and by production of type 2 cytokines. This is an important concept as it suggests that studying Th2 polarization by merely looking at DC-T cell interactions, may be too simplistic as it fails to model the *in vivo* interdependency of multiple cell types to efficiently initiate Th2 responses [60, 61].

A summary of the direction for future research regarding molecular interplay of immune system and helminth infections are illustrated in figure 2 and summarized in Box.1 (section F).

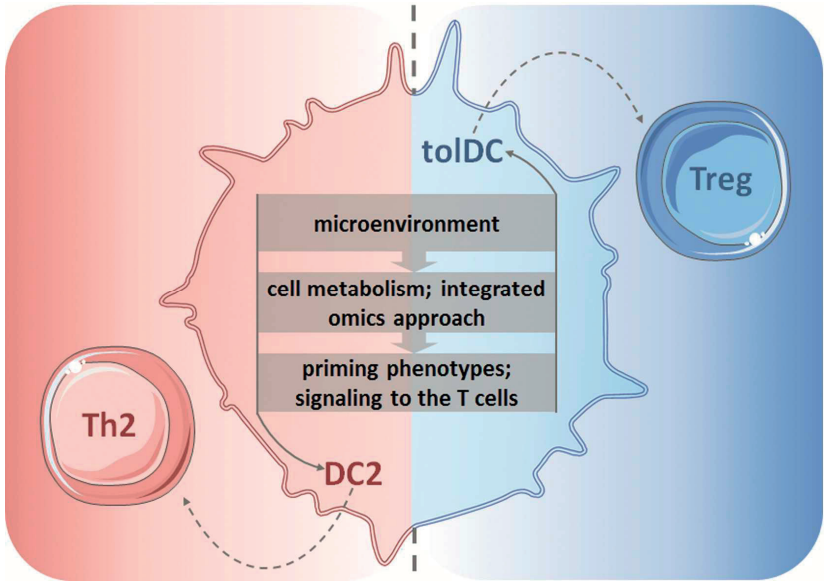

Figure 2. The proposed concept of how dendritic cells can be programmed to prime Th2 and Treg responses by helminths

DC biology is shaped by the microenvironment, including the cytokine milieu, signals from accessory cells, antigens and metabolites derived from helminth and microbiota. This will lead to changes in DC phenotype that can be studied by various integrated –omics approaches. Together this will determine the T cell polarization.

Box.1. Summary of the: current knowledge, contribution of the research in this thesis and future direction in the context of tracking helminths

	Molecular diagnosis	Immunological interplay
	A	**D**
Current knowledge	• Most of epidemiological studies of helminth infections have relied on microscopic techniques. • Study to study comparison based on microscopic diagnosis for helminth infections is challenging due to lack of standardization. • Real-time PCR-based diagnosis for detection of helminth infections has been shown to be more sensitive and specific than microscopy. • The current sample preparation following real-time PCR detection for gastrointestinal parasites is inadequate for detection of *T. trichiura*, which is one of most prevalent STHs.	▪ Helminth antigens can bind to receptors on DCs (including TLRs and CLRs) to modulate DCs for Th2 polarization via signalling-dependent and -independent mechanisms. ▪ ω-1 is a major antigen expressed by *S. mansoni* eggs that condition DCs for Th2 priming. However, it is not the only Th2-inducing component. Mechanistically, ω-1 is bound and internalized via its glycans by the MR and then interferes with the mRNA activity. ▪ Helminths can modulate host immune responses through promotion of SCFA production by microbiota ▪ SCFAs are metabolites produced by microbiota with known immunomodulatory potential.
	B	**E**
Contribution of this thesis	• Diagnosis based on DNA detection in stool seems a more reliable approach than stool microscopy to study the distribution of helminth infections and to compare different target populations (Chapter 2). • The bead-beating procedure, in particular in combination with ethanol preservation, prior to DNA extraction increases *T. trichiura* DNA yield in human fecal samples (Chapter 3).	▪ SEA and ω-1 alter the DC proteome, with the most pronounced effects on RPLP2 and VAT-1; as well as on proteins involved in antigen presentation (Chapter 5). ▪ Different *S. mansoni* antigens contain different lipid profiles, in which some lipids are known to be associated with Th2 induction(Chapter 4). ▪ *S. mansoni* egg antigens bind to dectin-1/2 on DCs to trigger a signalling axis involving Syk-Erk-cPLA$_2$ and COX1/2 that leads to PGE$_2$ and PGE$_2$ isomers synthesis, which in autocrine manner drive the expression of OX40L by DCs licensing these cell for priming of Th2 responses. (Chapter 6). ▪ This Dectin-Syk signalling cascade is crucially important for Th2 polarization and egg-driven granuloma formation by S. mansoni *in vivo* (Chapter 6). ▪ The SCFA butyrate conditions human DCs to prime IL-10 production Tr1 cells (Chapter 7). ▪ Butyrate depends on the combined action of HDAC inhibition and signalling via GPR109A to promote RALDH activity in DCs to license them to prime Tr1 cells (Chapter 7).
	C	**F**
Future research direction	• How can the operating procedures for helminth diagnosis, which include sample collection, handling, DNA extraction and detection, be standardized across the world? • How to develop a molecular-based rapid diagnostic tool to detect helminth infections?	▪ What is the role of and how does the microenvironment influence DC-mediated T cell priming? ▪ What are the mechanisms of interaction between helminths and microbiota and does their cross-talk lead to induction of regulatory immune responses? ▪ How can integrated –omics approaches be used to study of DC2 and tolDC biology? ▪ Do and how, helminth antigens affect the DC metabolism and does that contribute to their capacity in polarizing T cells?

REFERENCES

1. Hotez, P.J., et al., *Eliminating the Neglected Tropical Diseases: Translational Science and New Technologies.* PLoS Negl Trop Dis, 2016. **10**(3): p. e0003895.
2. Pullan, R.L., et al., *Global numbers of infection and disease burden of soil transmitted helminth infections in 2010.* Parasit Vectors, 2014. **7**: p. 37.
3. van Lieshout, L. and M. Roestenberg, *Clinical consequences of new diagnostic tools for intestinal parasites.* Clin Microbiol Infect, 2015. **21**(6): p. 520-8.
4. van Lieshout, L. and M. Yazdanbakhsh, *Landscape of neglected tropical diseases: getting it right.* Lancet Infect Dis, 2013. **13**(6): p. 469-70.
5. Dunn, J.C., et al., *Epidemiological surveys of, and research on, soil-transmitted helminths in Southeast Asia: a systematic review.* Parasit Vectors, 2016. **9**: p. 31.
6. McCarthy, J.S., et al., *A research agenda for helminth diseases of humans: diagnostics for control and elimination programmes.* PLoS Negl Trop Dis, 2012. **6**(4): p. e1601.
7. Bogoch, II, et al., *Differences in microscopic diagnosis of helminths and intestinal protozoa among diagnostic centres.* Eur J Clin Microbiol Infect Dis, 2006. **25**(5): p. 344-7.
8. Jonker, F.A., et al., *Real-time PCR demonstrates Ancylostoma duodenale is a key factor in the etiology of severe anemia and iron deficiency in Malawian pre-school children.* PLoS Negl Trop Dis, 2012. **6**(3): p. e1555.
9. Siddiqui, A.A. and S.L. Berk, *Diagnosis of Strongyloides stercoralis infection.* Clin Infect Dis, 2001. **33**(7): p. 1040-7.
10. Kunst, H., et al., *Parasitic infections of the lung: a guide for the respiratory physician.* Thorax, 2011. **66**(6): p. 528-36.
11. Greaves, D., et al., *Strongyloides stercoralis infection.* Bmj, 2013. **347**: p. f4610.
12. Campbell, S.J., et al., *Water, Sanitation and Hygiene (WASH) and environmental risk factors for soil-transmitted helminth intensity of infection in Timor-Leste, using real time PCR.* PLoS Negl Trop Dis, 2017. **11**(3): p. e0005393.
13. Basuni, M., et al., *A pentaplex real-time polymerase chain reaction assay for detection of four species of soil-transmitted helminths.* Am J Trop Med Hyg, 2011. **84**(2): p. 338-43.
14. Cimino, R.O., et al., *Identification of human intestinal parasites affecting an asymptomatic peri-urban Argentinian population using multi-parallel quantitative real-time polymerase chain reaction.* Parasit Vectors, 2015. **8**: p. 380.
15. Gordon, C.A., et al., *Multiplex real-time PCR monitoring of intestinal helminths in humans reveals widespread polyparasitism in Northern Samar, the Philippines.* Int J Parasitol, 2015. **45**(7): p. 477-83.
16. Incani, R.N., et al., *Diagnosis of intestinal parasites in a rural community of Venezuela: Advantages and disadvantages of using microscopy or RT-PCR.* Acta Trop, 2017. **167**: p. 64-70.
17. Llewellyn, S., et al., *Application of a Multiplex Quantitative PCR to Assess Prevalence and Intensity Of Intestinal Parasite Infections in a Controlled Clinical Trial.* PLoS Negl Trop Dis, 2016. **10**(1): p. e0004380.
18. Mejia, R., et al., *A novel, multi-parallel, real-time polymerase chain reaction approach for eight gastrointestinal parasites provides improved diagnostic capabilities to resource-limited at-risk populations.* Am J Trop Med Hyg, 2013. **88**(6): p. 1041-7.
19. Wiria, A.E., et al., *The effect of three-monthly albendazole treatment on malarial parasitemia and allergy: a household-based cluster-randomized, double-blind, placebo-controlled trial.* PLoS One, 2013. **8**(3): p. e57899.
20. Easton, A.V., et al., *Multi-parallel qPCR provides increased sensitivity and diagnostic breadth for gastrointestinal parasites of humans: field-based inferences on the impact of mass deworming.* Parasit Vectors, 2016. **9**: p. 38.
21. Tahapary, D.L., et al., *Effect of Anthelmintic Treatment on Insulin Resistance: A Cluster-Randomized Placebo-Controlled Trial in Indonesia.* Clin Infect Dis, 2017.
22. Minetti, C., et al., *Focusing nucleic acid-based molecular diagnostics and xenomonitoring approaches for human helminthiases amenable to preventive chemotherapy.* Parasitology, 2016. **2**: p. 1-17.
23. Everts, B., et al., *Helminths and dendritic cells: sensing and regulating via pattern recognition receptors, Th2 and Treg responses.* Eur J Immunol, 2010. **40**(6): p. 1525-37.
24. Hussaarts, L., M. Yazdanbakhsh, and B. Guigas, *Priming dendritic cells for th2 polarization: lessons learned from helminths and implications for metabolic disorders.* Front Immunol, 2014. **5**: p. 499.
25. Mendez-Samperio, P., *Molecular events by which dendritic cells promote Th2 immune protection in helmith infection.* Infect Dis (Lond), 2016. **48**(10): p. 715-20.
26. Na, H., M. Cho, and Y. Chung, *Regulation of Th2 Cell Immunity by Dendritic Cells.* Immune Netw, 2016. **16**(1): p. 1-12.
27. White, R.R. and K. Artavanis-Tsakonas, *How helminths use excretory secretory fractions to modulate dendritic cells.* Virulence, 2012. **3**(7): p. 668-77.

28. Gundacker, N.C., et al., *Cytoplasmic proteome and secretome profiles of differently stimulated human dendritic cells.* J Proteome Res, 2009. **8**(6): p. 2799-811.
29. Ferret-Bernard, S., et al., *Plasma membrane proteomes of differentially matured dendritic cells identified by LC-MS/MS combined with iTRAQ labelling.* J Proteomics, 2012. **75**(3): p. 938-48.
30. Ferret-Bernard, S., R.S. Curwen, and A.P. Mountford, *Proteomic profiling reveals that Th2-inducing dendritic cells stimulated with helminth antigens have a 'limited maturation' phenotype.* Proteomics, 2008. **8**(5): p. 980-93.
31. Smith, R.D., et al., *An accurate mass tag strategy for quantitative and high-throughput proteome measurements.* Proteomics, 2002. **2**(5): p. 513-23.
32. Strittmatter, E.F., et al., *Proteome analyses using accurate mass and elution time peptide tags with capillary LC time-of-flight mass spectrometry.* J Am Soc Mass Spectrom, 2003. **14**(9): p. 980-91.
33. Zhou, X., et al., *Ribosomal proteins: functions beyond the ribosome.* J Mol Cell Biol, 2015. **7**(2): p. 92-104.
34. Eura, Y., et al., *Identification of a novel protein that regulates mitochondrial fusion by modulating mitofusin (Mfn) protein function.* J Cell Sci, 2006. **119**(Pt 23): p. 4913-25.
35. Constant, S., et al., *Extent of T cell receptor ligation can determine the functional differentiation of naive CD4+ T cells.* J Exp Med, 1995. **182**(5): p. 1591-6.
36. van Panhuys, N., F. Klauschen, and R.N. Germain, *T-cell-receptor-dependent signal intensity dominantly controls CD4(+) T cell polarization In Vivo.* Immunity, 2014. **41**(1): p. 63-74.
37. Bryant, C.*i*.C., F. E. G., *Biochemistry.* Modern parasitology, 2009.
38. Bhure, D.B., et al., *Taxonomic and biochemical studies of piscean nematode Camallanus Jadhavii (Jadhav and Khadap, 2013) parasitic in Wallago Attu (Bleeker, 1857).* World Scientific News, 2016. **34**: p. 98-108.
39. Ferreira, M.S., et al., *Screening the life cycle of Schistosoma mansoni using high-resolution mass spectrometry.* Anal Chim Acta, 2014. **845**: p. 62-9.
40. Kikkawa, U. and Y. Nishizuka, *The role of protein kinase C in transmembrane signalling.* Annu Rev Cell Biol, 1986. **2**: p. 149-78.
41. Pearce, E.J. and A.S. MacDonald, *The immunobiology of schistosomiasis.* Nat Rev Immunol, 2002. **2**(7): p. 499-511.
42. Arima, M. and T. Fukuda, *Prostaglandin D(2) and T(H)2 inflammation in the pathogenesis of bronchial asthma.* Korean J Intern Med, 2011. **26**(1): p. 8-18.
43. de Jong, E.C., et al., *Microbial compounds selectively induce Th1 cell-promoting or Th2 cell-promoting dendritic cells in vitro with diverse th cell-polarizing signals.* J Immunol, 2002. **168**(4): p. 1704-9.
44. Krause, P., et al., *Prostaglandin E(2) enhances T-cell proliferation by inducing the costimulatory molecules OX40L, CD70, and 4-1BBL on dendritic cells.* Blood, 2009. **113**(11): p. 2451-60.
45. Guasconi, L., L.S. Chiapello, and D.T. Masih, *Fasciola hepatica excretory-secretory products induce CD4+T cell anergy via selective up-regulation of PD-L2 expression on macrophages in a Dectin-1 dependent way.* Immunobiology, 2015. **220**(7): p. 934-9.
46. Clarke, D.L., et al., *Dectin-2 sensing of house dust mite is critical for the initiation of airway inflammation.* Mucosal Immunol, 2014. **7**(3): p. 558-67.
47. Laan, L.C., et al., *The whipworm (Trichuris suis) secretes prostaglandin E2 to suppress proinflammatory properties in human dendritic cells.* Faseb j, 2017. **31**(2): p. 719-731.
48. Allen, J.E. and R.M. Maizels, *Diversity and dialogue in immunity to helminths.* Nat Rev Immunol, 2011. **11**(6): p. 375-88.
49. Gause, W.C. and R.M. Maizels, *Macrobiota - helminths as active participants and partners of the microbiota in host intestinal homeostasis.* Curr Opin Microbiol, 2016. **32**: p. 14-8.
50. Zaiss, M.M., et al., *The Intestinal Microbiota Contributes to the Ability of Helminths to Modulate Allergic Inflammation.* Immunity, 2015. **43**(5): p. 998-1010.
51. Reynolds, L.A., B.B. Finlay, and R.M. Maizels, *Cohabitation in the Intestine: Interactions among Helminth Parasites, Bacterial Microbiota, and Host Immunity.* J Immunol, 2015. **195**(9): p. 4059-66.
52. Koh, A., et al., *From Dietary Fiber to Host Physiology: Short-Chain Fatty Acids as Key Bacterial Metabolites.* Cell, 2016. **165**(6): p. 1332-45.
53. Saito, K., et al., *Heat shock protein 90 associates with Toll-like receptors 7/9 and mediates self-nucleic acid recognition in SLE.* Eur J Immunol, 2015. **45**(7): p. 2028-41.
54. Connor, L.M., et al., *Th2 responses are primed by skin dendritic cells with distinct transcriptional profiles.* J Exp Med, 2017. **214**(1): p. 125-142.
55. Everts, B. and E.J. Pearce, *Metabolic control of dendritic cell activation and function: recent advances and clinical implications.* Front Immunol, 2014. **5**: p. 203.
56. Yang, J.Q., et al., *RhoA orchestrates glycolysis for TH2 cell differentiation and allergic airway inflammation.* J Allergy Clin Immunol, 2016. **137**(1): p. 231-45.e4.

57. Yang, K., et al., *T cell exit from quiescence and differentiation into Th2 cells depend on Raptor-mTORC1-mediated metabolic reprogramming*. Immunity, 2013. **39**(6): p. 1043-56.
58. Jha, A.K., et al., *Network integration of parallel metabolic and transcriptional data reveals metabolic modules that regulate macrophage polarization*. Immunity, 2015. **42**(3): p. 419-30.
59. Leon, B., et al., *Regulation of T(H)2 development by CXCR5+ dendritic cells and lymphotoxin-expressing B cells*. Nat Immunol, 2012. **13**(7): p. 681-90.
60. Halim, T.Y., et al., *Group 2 innate lymphoid cells are critical for the initiation of adaptive T helper 2 cell-mediated allergic lung inflammation*. Immunity, 2014. **40**(3): p. 425-35.
61. Oliphant, C.J., et al., *MHCII-mediated dialog between group 2 innate lymphoid cells and CD4(+) T cells potentiates type 2 immunity and promotes parasitic helminth expulsion*. Immunity, 2014. **41**(2): p. 283-95.

Addendum

SUMMARY

Parasitic helminths are important organisms to study because their infections can have both adverse and beneficial effects on the human host. Helminth infections including those caused by soil transmitted helminths (STHs) and schistosomes are considered a burden, as these infections cause significant morbidity in a large proportion of the 1.5 billion people infected worldwide. However, helminth infections, by means of their ability to modify host immune responses can also provide protection against a wide spectrum of inflammatory diseases, such as celiac disease, inflammatory bowel disease, diabetes, and asthma. It is important to better understand the underlying mechanisms of these Yin (positive) and Yang (negative) consequences of helminth infections. The general objective of this thesis is to track helminths at different levels. In Chapter 2 and 3 this is achieved by focusing on molecular diagnostics to detect helminth infections, while in Chapter 4, 5, 6 and 7 the host-parasite interactions and the associated immunological footprint induced by helminths are studied.

Chapter 2
Microscopy-based methods have always been the first-line approach to diagnose helminth infections. However, their limitations and lack of standardization lead to the need for better methods in parasite detection, such as molecular diagnostics. In this chapter, the performance of multiplex real-time PCR and microscopy methods for the detection of STHs (hookworm, *Ascaris lumbricoides* and *Strongyloides stercoralis*) in stool samples between two endemic areas were evaluated. In Indonesia, using a microscopy-based formal ether concentration method (FEC) 35.4% of the study population was found to be positive for helminth infections, while multiplex real-time PCR detected 81.4% was helminths positive. In Mozambique, a combination of microscopy methods (Direct smear, Kato smear, FEC, Baermann method and copro-culture) *versus* a multiplex real-time PCR resulted in 77.9% vs 73.6% positivity for helminths. This work suggests that DNA detection in stool, using multiplex real-time PCR, seems a more reliable approach than stool microscopy in studying the burden and comparing helminth infections in different populations.

Chapter 3
Trichuris trichiura is one of most prevalent STHs worldwide. To date, DNA detection of this parasite from stool has been challenging due to difficulty in extraction of DNA from *T. trichiura* eggs. We optimized the sample preparation procedure for the detection of *T. trichiura* DNA. We found that the combination of ethanol preservation and a bead-beating procedure prior to parasite DNA extraction from stool resulted in a higher sensitivity for detection of *T. trichiura* infection in comparison to a control procedure (without ethanol or bead-beating) in a patient cohort from an endemic region in Indonesia: 55% versus 40% positivity for *T.trichiura*, respectively. Moreover, the optimized method showed significantly higher *T. trichiura* DNA loads. Together the findings demonstrate that this optimized method significantly improved the ability to detect *T. trichiura* infection. Importantly, this optimized procedure had a minor effect on the PCR results of other STHs compared to the control procedure.

Chapter 4
In Chapter 4, we investigated the lipid profile of different life cycle stages (cerariae, worms and eggs) of *Schistosoma mansoni* as well as the lipid profile of the corresponding extracts, to find

potential leads for helminth-derived lipids with immunomodulatory potential. As expected different life cycle stages exhibited distinct lipid signatures. Interestingly the lipid composition of parasite life cycle stages and corresponding extracts were highly similar. The latter mentioned finding validates the use of the widely used parasite preparations such as soluble eggs antigens (SEA) in models to explore host-parasite interactions in immunological studies. A striking finding was the presence of prostaglandins (PGs) specific to egg- and cercarial preparations. Prostaglandins are lipid mediators with known modulatory effects on immune cells. Thus, our lipid profiling study has indicated that such approach could identify immunomodulatory compounds in helminths .

Chapter 5

From detection to characterization of helminths, we moved on to study their detailed interaction with the human immune system. Dendritic cells are central to skewing of immune responses and have often been studied in the context of their interaction with helminths. The maturation of DCs is characterized by changes in expression of a large number of proteins. We aimed to link the expression of proteins to the Th2 priming-capacity of helminth-conditioned DCs. Using a high-throughput mass spectrometry-based method, we explored the proteome of DCs stimulated with *S. mansoni*-derived products, SEA and omega-1 (ω-1). Omega-1 is a glycoprotein derived from SEA and is known as a potent Th2 inducer. We observed an increase in the expression of two proteins involved in ribosome and mitochondrial function indicating that both SEA and ω-1 could affect protein expression and cellular metabolism. Indeed, SEA and ω-1 decreased the expression of proteins related to antigen processing and presentation. These finding, are largely consistent with the hypothesis that the promotion of Th2 responses can result from weaker immunological synapse formation between DCs and T cells.

Chapter 6

Based on the findings in Chapter 4, we sought to dissect the role of lipid mediators in Th2 polarization by SEA via DCs. We found that PGE_2 and its isomers were not only present in SEA but were also synthesized by SEA-conditioned DCs. We found that SEA binds to dectin-1 and dectin-2 receptor in DCs to trigger a signalling pathway involving Syk, ERK, $cPLA_2$ and COX-1 and -2, leading to PGE_2 synthesis. PGE_2 subsequently acts in an autocrine manner to drive expression of OX40L by DCs, which licenses DCs to prime Th2 responses. This Dectin-1/2 induced autocrine PGE_2 signalling axis can fully account for the ω-1 independent ability of SEA to prime Th2 responses. This pathway is also essential for Th2 polarization *in vivo* and for Th2-driven granuloma formation around eggs in the liver during *S. mansoni* infection. Together, we identified in this chapter a novel pathway through which *S. mansoni* conditions DCs to prime Th2 responses.

Chapter 7

Recent studies have shown that helminths are capable of inducing regulatory T cells (Tregs) by promoting production of short chain fatty acids (SCFAs) by microbiota in the gut. In particular butyrate has been shown be an important driver of Treg activation. However, how SCFAs promote this response in humans in less clearly defined. Therefore, we investigated in this chapter whether and through which mechanisms SCFAs can condition human DCs to prime Tregs. We found that butyrate conditions human DCs to prime IL-10 producing type 1 regulatory T cells (Tr1). Butyrate induces RALDH activity, a key enzyme to convert vitamin A into retinoic acid (RA). RALDH-derived

RA acts on DCs themselves to enforce RALDH expression and in T cells to promote Tr1 differentiation. Mechanistically, we found butyrate to depend on the combined action of HDAC inhibition and signalling via GPR109A to promote RALDH activity in DCs and to license these cells to prime Tr1 cells. This provides novel insights in the mechanisms through which helminths are capable of inducing tolerogenic immune responses in humans, by promoting production of SCFAs by gut microbiota.

In conclusion, the studies described in this thesis on the one hand help to improve the detection of helminth infections, essential for the studying helminths and the interaction with their human host. Moreover, the development of more sensitive diagnostics is instrumental for reliably monitoring the distribution of helminth infections, which is key to evaluate the success of programs that aim to eliminative helminth infections, currently underway in many parts of the world. On the other hand, this thesis has generated important new mechanistic insights into how the interplay between helminths and the host immune system results in priming of Th2 and regulatory T cell responses. This could pave the way for the identification of pathways that can be targeted to manipulate these immune responses, as part of developing therapeutics to treat inflammatory disorders characterized by deregulated Th2 and/or Treg responses.

SAMENVATTING

Wereldwijd zijn 1.5 miljard mensen geïnfecteerd met parasitaire wormen (helminthen) waarvan via de bodem overdraagbare helminthen (STH) en schistosomen de meest voorkomende zijn. Een aanzienlijk deel van de aangedane populatie lijdt onder een hoge ziektelast ten gevolge van deze infecties. Maar naast de vaak belichte nadelige gevolgen van wormeninfecties zijn er ook gunstige effecten op het afweersysteem van de gastheer. Parasitaire wormen zijn namelijk meesters in het reguleren van het immuunsysteem van de gastheer met als doel zichzelf te beschermen, maar ook om te voorkomen dat de gastheer zichzelf beschadigt door een overdreven en onnodige afweer. Als gevolg van deze regulatie blijken wormeninfecties bescherming te bieden tegen ontstekingsziektes zoals coeliakie, inflammatoire darmziekten, diabetes en astma. Het doel van dit proefschrift is om de onderliggende mechanismen van zowel de Yin (positieve) en Yang (negatieve) gevolgen van worm infecties beter te begrijpen. In Hoofdstuk 2 en 3 zijn toegespitst op nieuwe moleculaire technieken om wormeninfecties beter vast te kunnen stellen, waarna in Hoofdstuk 4, 5, 6 en 7 de interactie tussen de parasiet en de gastheer op het niveau van het afweersysteem zal worden bestuurd.

Hoofdstuk 2

Microscopische methoden zijn altijd de eerstelijns aanpak geweest bij het diagnosticeren van infecties met helminths. Echter, omdat deze technieken moeilijk zijn te standaardiseren, is er behoefte aan de ontwikkeling van betere detectiemethoden, waarvan moleculaire diagnostiek, wat staat voor de detectie van parasiet-specifiek DNA, er één kan zijn. In dit hoofdstuk wordt de effectiviteit van de multiplex real-time PCR voor de detectie van DNA van STHs (mijnwormen, *Ascaris lumbricoides* en *Strongyloides stercoralis)* vergeleken met de microscopie methode in feces monsters verzameld in twee geheel verschillende endemische gebieden. In de Indonesië populatie testte 35,4% van de bestudeerde personen positief voor helmintheninfecties wanneer één specifieke microscopie methode, de 'formal ether concentratie'-methode (FEC) werd toegepast. In dezelfde populatie testte 81.4% positief met real-time PCR. In Mozambique gaf een combinatie van microscopie methoden (direct uitstrijkje, Kato uitstrijkje, FEC, Baermann methode en copro-kweek) een positieve uitslag van 77,9% terwijl de multiplex real-time PCR 73,6% positief beschouwde. Deze studie suggereert dat DNA detectie in monsters uit feces met behulp van multiplex real-time PCR een meer betrouwbare en beter gestandaardiseerde uitslag geeft dan alleen microscopische analyse van deze monsters.

Hoofdstuk 3

Trichuris trichiura is wereldwijd een van de meest voorkomende bodemoverdraagbare helminthen. Echter, vanwege de moeilijkheid om DNA te extraheren van *T. trichiura* eieren, is het altijd lastig geweest om DNA op eenvoudige wijze te detecteren in fecesmonsters. In deze studie hebben we de opwerkprocedure voor fecesmonsters verder geoptimaliseerd met als doel *T. trichiura* DNA beter te kunnen aantonen in een patiënt cohort uit een endemische regio in Indonesië. Wij concluderen dat de combinatie van ethanol preservatie en een 'bead-beating' procedure (een proces van mechanisch beschadiging) voorafgaand aan DNA extractie uit het fecesmonster resulteerde in een hogere sensitiviteit voor detectie van *T. trichiura* infectie: 55% met de geoptimaliseerde methode versus 40% in de controle procedure (zonder ethanol of 'bead-beating'). Daarbij detecteerde de geoptimaliseerde methode een significant grotere hoeveelheid *T.*

trichiura DNA. Deze bevindingen laten zien dat de geoptimaliseerde methode meer geschikt is voor het detecteren van een *T. trichiura* infectie. Belangrijker, ten opzichte van de voorheen gebruikte methode had de geoptimaliseerde methode slechts een beperkt effect op de PCR resultaten van andere bodem overdraagbare helminthen.

Hoofdstuk 4

In Hoofdstuk 4ier onderzoeken wij het lipiden-profiel van zowel de verschillende levensstadia (cercariae, wormen en eieren) van *Schistosoma mansoni* als de corresponderende extracten om helminth-afgeleide lipiden met potentieel immuunmodulerende werking te vinden. Zoals verwacht vertoonden de verschillende levensstadia een duidelijk verschillende lipide signatuur. Interessant genoeg was de lipide samenstelling van de verschillende levensstadia van de parasiet en hun corresponderende extracten nagenoeg gelijk. Deze overeenkomsten tussen de extracten en de hele organismen valideren het gebruik van de veel gebruikte parasiet preparaties zoals oplosbare ei antigenen (eng: soluble egg antigens, SEA) in modellen om de immunologie van parasiet-gastheer interacties te bestuderen. Een belangrijke bevinding was de aanwezigheid van prostaglandinen (PG) specifiek in ei en cercarielepreparaten. Prostaglandinen zijn lipidendie bekend staan om hun modulerende effecten op immuuncellen. Onze studie naar de lipide profielen van helminthen laat daarmee zien dat deze aanpak mogelijk nog andere immuunmodulerende lipiden zou kunnen identificeren.

Hoofdstuk 5

Na de detectie en karakterisering van helminthen, gaan wij over op het gedetailleerd bestuderen van hun interactie met het menselijke immuunsysteem. Dendritische cellen (DCs) staan centraal in de polarisatie van immuunreacties en zijn vaak bestudeerd in de context van helminthen-infecties. The activering van DCs wordt gekarakteriseerd door verandering in expressie van een groot aantal eiwitten. Ons doel was om om de expressie van eiwitten te correleren aan de Th2-inducerende capaciteit van helminth-geconditioneerde DCs. Met behulp van een op massa-spectometrie gebaseerde methode onderzochten wij het proteoom van DCs gestimuleerd met S. mansoni-afgeleide producten, SEA en omega-1 (ω-1). Omega-1 is een glycoproteïne afgeleid van SEA en staat bekend als factor die een sterke Th2respons kan induceren. Wij observeerden een verhoging van de expressie van twee eiwitten die betrokken zijn bij ribosomale en mitochondriale functie. Dit wijst erop dat zowel SEA als ω-1 een effect kunnen hebben op eiwit-expressie en cellulair metabolisme van DCs. Inderdaad, SEA en ω-1 leidden tot een verlaging van de expressie van eiwitten die betrokken zijn bij antigeenverwerking en presentatie. Deze bevindingen corresponderen grotendeels met de hypothese dat een zwakkere formatie van de immuun synaps tussen DCs en T cellen kan leiden to Th2 differentiatie.

Hoofdstuk 6

Wij probeerden gebaseerd op de bevindingen uit Hoofdstuk 4 een mogelijke rol voor lipide mediatoren te bestuderen in de inductie van Th2 cellen door DCs die met SEA zijn gestimuleerd. Wij vonden dat de lipide mediator PGE_2 en zijn varianten niet alleen aanwezig zijn in SEA, maar ook geproduceerd werden door DCs nadat zij met SEA gestimuleerd waren. SEA bleek te binden aan de receptoren dectin-1 en dectin-2 op DCs, waarna er een signaleringsroute geactiveerd werd bestaande uit de Syk, ERK, $cPLA_2$, COX-1 en COX-2. Het gevolg hiervan was dat PGE_2 geproduceerd en uitgescheiden werd door de DCs. De PGE_2 die geproduceerd werd, werkte

vervolgens terug op de DCs en stimuleerde de expressie van OX40L, een ligand waarvan al langer bekend is dat het DCs de capaciteit geeft om Th2 differentiatie te induceren. Deze as bestaande uit dectin-PGE2-OX40L, verklaart volledig waarom SEA waaruit omega-1 verwijderd is nog steeds DCs de capaciteit geeft om Th2 responsen te induceren. Naast de beschreven in vitro experimenten bleek deze as ook van groot belang voor de inductie van Th2 cellen in vivo en daarmee geassocieerde processen zoals de formatie van granulomen in de lever van met *S. mansoni*-geinfecteerde muizen. Hiermee hebben wij in dit hoofdstuk een nieuwe manier gevonden waarop parasitaire wormen DCs conditioneren om Th2 differentiatie te induceren.

Hoofdstuk 7

Recente studies hebben aangetoond dat helminthen regulatoire T cellen (Tregs) kunnen induceren door de productie van korte-keten vetzuren (eng. Short chain fatty acids, SCFAs) door de samenstelling van microbiota in de darm te veranderen. SCFA butyraat in het bijzonder is een belangrijke drijfveer van Treg activatie. Hoe SCFAs deze regulatoire reactie in mensen teweegbrengen is echter onbekend. Daarom onderzochten bij in dit hoofdstuk óf, en via welke mechanismen, SCFAs menselijke DCs konden conditioneren om Tregs te activeren. Wij vonden dat butyraat humane DCs conditioneert om IL10-producerende type 1 regulatoire T cellen (Tr1) te induceren. Butyraat induceert RALDH activiteit, een enzym belangrijk voor de conversie van vitamine A naar tretinoinezuur (eng. retinoic acid, RA). RA werkt vervolgens op DCs om RALDH expressie te verhogen en direct op T cellen om Tr1 differentiatie te bevorderen. Wij vonden dat butyraat RALDH activiteit in DCs verhoogde door middel van zowelremming van histon deacetylatie als signalering via GRP109A, Deze bevindingen geven nieuwe inzichten in de mechanismen waardoor helminthen tolerogene immuunreacties in mensen kunnen induceren; door het bevorderen van de productie van SCFA door microbiota in de darmen.

De studies beschreven in dit proefschrift helpen om de detectie van helminthen-infecties te verbeteren, wat essentieel is voor het bestuderen van deze parasitaire wormen en hun interactie met de menselijke gastheer. Bovendien is de ontwikkeling van sensitievere diagnostische methoden van groot belang om een beter overzicht te krijgen van de incidentie en prevalentie van helminth infecties, wat cruciaal is om te evalueren of programma's met als doel het elimineren van helminth infecties werken, die op dit moment bezig zijn in verschillende delen van de wereld. Daarnaast heeft dit proefschrift bijgedragen aan het tot stand komen van nieuwe inzichten in de manier waarop het samenspel van worm en het immuunsysteem van de gastheer resulteert in het initiëren van type 2 en regulerende immuunresponsen. Dit draagt bij aan de identificatie van nieuwe druggable targets waarmee die type immuunresponsen gemanipuleerd kunnen worden, en zodoende in de toekomst mogelijk gebruikt kunnen worden voor het ontwikkelen van therapeutische methoden om ontstekingsziektes te behandelen.

CURRICULUM VITAE

Maria Mardalena Martini Kaisar was born on 19th March 1986 in Bengkulu, Indonesia. In 2008 she completed her bachelor of Science with major in Biology at Universitas Indonesia. Her final research project was on *Entamoeba histolytica* and *E. dispar* diagnosis in patients with diarrhea comparing Elisa *versus* real-time polymerase chain reaction. After graduation, she joined Prof. Dr. Taniawati Supali's group at the Department of Parasitology, Medical Faculty, Universitas Indonesia (FKUI). She was involved in several projects funded by the Bill and Melinda Gates Foundation (DOLF) and by The Royal Netherlands Academy of Arts and Sciences (KNAW) special Indonesia program (ImmunoSPIN and SugarSPIN). She has also, conducted fieldwork in rural areas of Flores Island and in Pekalongan, Central Java, Indonesia. In 2009-2010 she participated in a training program in molecular diagnostics for parasitic infections at the Department of Parasitology, Leiden University Medical Center (LUMC) funded by KNAW and Prof. Dr. P. F. C. FLU Foundation. During her training program she was supervised by Dr. Lisette van Lieshout and Dr. Jaco J. Verweij of Department of Parasitology. At the end of 2012, she was awarded a doctoral sholarship by DIKTI-Leiden University program to work on diagnostics and immunology of parasitic infections. Maria Kaisar officially enrolled as a PhD researcher under the supervision of Prof. Dr. Maria Yazdanbakhsh of the Department of Parasitology, LUMC. Dr. Bart Everts became her co-promoter and was responsible for her daily supervision. During her PhD, she received two travel grants from the Erasmus+ program and The Company of Biologists. After finishing her PhD, Maria Kaisar will bring the knowledge she has gained, back to Indonesia to work with the group of Prof. Dr. Taniawati Supali on studies involving cellular and molecular immunology in parasitic infections in particular. Lastly, she is planning to contribute to strengthening basic research in Indonesia and hopes to continue the long-standing collaboration between FKUI and LUMC.

LIST OF PUBLICATIONS

Supali T, Verweij JJ, Wiria AE, Djuardi Y, Hamid F, **Kaisar MMM**, Wammes LJ, van Lieshout L, Luty AJ, Sartono E, Yazdanbakhsh M. *Polyparasitism and its impact on the immune system*. Int J Parasitol 2010; 40:1171-6.

Hamid F, Wiria AE, Wammes LJ, **Kaisar MMM**, Lell B, Ariawan I, Uh HW, Wibowo H, Djuardi Y, Wahyuni S, Schot R, Verweij JJ, van Ree R, May L, Sartono E, Yazdanbakhsh M, Supali T. *A longitudinal study of allergy and intestinal helminth infections in semi urban and rural areas of Flores, Indonesia (ImmunoSPIN Study).* BMC Infect Dis 2011; 11:83.

Wiria AE, Wammes LJ, Hamid F, Dekkers OM, Prasetyani M, May L, **Kaisar MMM**, Verweij JJ, Tamsma JT, Partono F, Sartono E, Supali T, Yazdanbakhsh M, Smit JW. *Relationship between carotid intima media thickness and helminth infections and Flores island, Indonesia*. PLoS One 2013; 8e54855.

Wiria AE, Hamid F, Wammes LJ, **Kaisar MMM**, May L, Prasetyani MA, Wahyuni S, Djuardi Y, Ariawan I, Wibowo H, Lell B, Sauerwein R, Brice GT, Sutanto I, van Lieshout EA, de Craen AJ, van Ree R, Verweij JJ, Tsonaka R, Houwing-Duistermaat JJ, Luty AJ, Sartono E, Supali T, Yazdanbakhsh M. *The effect of three monthly albendazole treatment on malarial parasitemia and allergy: a household-based cluster-randomized double blind, placebo-controlled trial.* PLoS One 2013; 8:e57899.

Wammes LJ, Wiria AE, Toenhake CG, Hamid F, Liu KY, Suryani H, **Kaisar MMM**, Verweij JJ, Sartono E, Supali T, Smits HH, Luty AJ, Yazdanbakhsh M. *Asymptomatic plasmodial infection is associated with increased TNFRII-expressing Tregs and suppressed type 2 immune responses.* J Inf Dis 2013; 207:1590-9.

Kaisar MMM, Supali T, Wiria AE, Hamid F, Wammes LJ, Sartono E, Luty AJ, Brienen EA, Yazdanbakhsh M, van Lieshout L, Verweij JJ. *Epidemiology of Plasmodium infections in Flores Island, Indonesia using real-time PCR*. Malar J 2013; 12:169.

Hamid F, Wiria AE, Wammes LJ, **Kaisar MMM**, Djuardi Y, Versteeg S, Wahyuni S, van Ree R, Sartono E, Supali T, Yazdanbakhsh M. Risk factors associated with the development of atopic sensitization in Indonesia. PLoS One 2013; 8:e67064.

Wiria AE, Hamid F, Wammes LJ, Prasetyani MA, Dekkers OM, May L, **Kaisar MMM**, Verweij JJ, Guigas B, Partono F, Sartono E, Supali T, Yazdanbakhsh M, Smith JW. *Infection with soil-transmitted helminths is associated with increased insulin sensitivity* . PLoS One 2015; 10:e0127746.

Wammes LJ, Hamid F, Wiria AE, May L, **Kaisar MMM**, Prasetyani MA, Djuardi J, Wibowo H, Kruize YCM, Verweij JJ, de Jong SE, Tsonaka R, Houwing-Duistermaat JJ, Sartono E, Luty AJF, Supali T, Yazdanbakhsh M. *Community deworming alleviates geohelminth-induced immune hyporesponsiveness*. PNAS 2016; 113:12526-31.

Prasetyani MA*, de Mast Q*, Afeworki R, **Kaisar MMM**, Stefanie D, Sartono E, Supali T, van der Ven AJ. *Iron supplementation with iron polymaltose is associated with an increased incidence of microscopically detectable malarial parasitemia in Indonesia school children.* Malar J 2017; 16:50.

Kaisar MMM, Brienen EAT, Djuardi Y, Yazdanbakhsh M, Verweij JJ, Supali T, van Lieshout L. *Improved sample preparation for DNA isolation and real-time PCR diagnosis of Trichuris Trichiura and other intestinal parasites in human stool samples*. Parasitology 2017; 144(7):965-974.

Hussaarts L*, **Kaisar MMM***, Guler AT, Dalebout H, Deelder AM, Palmblad M, Yazdanbakhsh M. *Human dendritic cells with Th2-polarizing capacity: analysis using label-free quantitative proteomics.* Int Arch Allergy Immunol 2017.

Budischak SA, Wiria AE, Hamid F, Wammes LJ, **Kaisar MMM**, van Lieshout L, Sartono E, Supali T, Yazdanbakhsh, Graham AL. *Parasites resource requirement predict impact of malaria-helminth co-infection in human host*. Submitted.

Kaisar MMM, Djuardi Y, Mendes F, Hamid F, Wiria AE, Wammes LJ, Brienen EAT, Polderman AM, Sartono E, Yazdanbakhsh M, Verweij JJ, Supali T, van Lieshout L. *Multiplex real-time PCR as opposed to stool microscopy for studying and comparing the distribution of Soil-transmitted helminths within and between population living in endemic regions.* Submitted.

Giera M, **Kaisar MMM**, Derks R, Steenvoorden E, Kruize YCM, Hokke CH, Yazdanbakhsh M, Everts B. *The Schistosoma mansoni lipidome: leads for immunomodulation*. Submitted.

Kaisar MMM, Giera M, Ritter M, del Fresno C, Jónasdóttir H, van der Ham AJ, Pelgrom LR, Schramm G, Layland LE, Sancho D, da Costa CP, Yazdanbakhsh M*, Everts B*. *Dectin-1/2-induced autocrine PGE_2 signalling licenses dendritic cells to prime Th2 responses*. Submitted.

Kaisar MMM, Pelgrom LR, van der Ham AJ, Yazdanbakhsh M*, Everts B*. *Butyrate conditions human dendritic cells to prime type 1 regulatory T cells via histone deacetylase inhibitions and GPR109A signalling*. Submitted.

*these authors contributed equally

ACKNOWLEDGEMENTS

Finally, Hora Est!!!

"Everything is theoretically impossible, until it is done"--Robert A. Heinlein
The works done in this thesis were throretically impossible too without amazing people around to support me.

"A mentor is someone who allows you to see the hope inside yourself"--Oprah Winfrey
My greatest gratitude goes to my promotor Prof. Dr. Maria Yazdanbakhsh ("big" Maria), thank you for introducing me to the complex yet interesting field of immunology and for being a great role model to budding scientists. My sincerest gratitude to my co-promotor Dr. Bart Everts, thanks a lot for transferring a lot of valuable knowledge and simply teaching me how to be positive despite stressful situations. Maria and Bart thank you for making this all possible, and trusting me to do DCs work, all the advice, fruitful discussions and for making me into an immuno-parasitologist. I would like to thank the thesis committee for all the time they invested in reading and commenting on my thesis. I would like to thank other mentors during my PhD: Dr. Lisette van Lieshout and Dr. Jaco. J. Verweij thank you for all the guidance in the field of molecular diagnostics and your excellent mentoring. I am grateful to have had the mentorship of Dr. Erliyani, thank you for all the advice. My gratitude also goes to other mentors in Parasitology: Prof. Dr. Ron Hokke, Dr. Hermelijn, Dr. Bruno, Dr. Angela, Dr. Shahid and Dr. Meta, thank you for all the advice, critical comments and questions. Special thanks goes to Dr. Martin Giera for your excellent guidance in navigating through the world of lipids. I am eternally grateful to have Prof. Dr. Taniawati as my mentor and my advisor; thank you for your support, you have given me the chance to "jump start" to PhD and also simply for believing in me.

"Find a group of people who challenge and inspire you, spend a lot of time, and it will change your life"--Amy Poehler
To Abena and Alwin-my paranymphs, thank you so much for the energy you have put to help me out organizing the final stages of PhD journey. Thanks to Alwin for the pair of hand you gave me in dealing with my DCs experiments. Abena, thanks for sharing the path during my PhD journey; from the discussions about non-sense to making sense of topics. I have learned a lot from you. Super thanks to Yvonne Kruize for always being there whenever I need your help. Thanks to Eric Brienen for helping me "play" with the Hamilton robot and showing me beautiful parasite eggs and larvae. Special thanks goes to Beatrice and Leonard for helping me with my Dutch summary. My gratitude goes to my dear colleagues in the Parasitology Department; from the former to the current T5-48 office-mates: Luciën, Simone, Ulysse, Leonard, Katja, Marijke, Eunice, Beatrice, Dito and Alice. Thanks to my P4 colleges: Dicky--for also sharing the final stage of the PhD journey, Sanne--for all the suggestions and information you have given me, Karin and Dian--for simply sharing the Indonesian "gene", Astrid, Michelle, Yoan, Mathilde, Linh, Jacqueline, Marije, Arifa, Fabrizio, Govert, Syibli, Catherin, Janeke, Pytsje, Laudine, Blandine, Severine, Hans, Jai. Former PARAs: Linda Wammes, Linda May, Honorine, Łucja and Leonie, Noemi, my gratitude to you all. My sincere appreciation goes to former Indonesian PhD colleagues: mbak Yenny--I'll be joining the team soon!! The big brothers kak Daus and kak Eddy. Suzanne, Corrie and Jantien--thanks a lot for helping me deal with all the administrative works. Colleagues in other departments at LUMC: Ivonne Martin--thanks for your time and also sharing PhD-related-unrelated stories, Angga, mbak Nela and Yolanda. CPM colleagues: Magnus, Tugce, Isabelle, Hulda, Marike, Eveline, Rico. Also thanks to my other colleagues: Pavi, Yvonne Aryeetey, Anna, Moustapha Mbow, mbak Ani, William, Moses, Elias and Gyaviira.

"The different shades of colours present cultural diversity"--Laila Gifty Akita

To the DIKTI-LU awardee year of 2012: bu Mega-thank you for your support and advice, mas Wija, mbak Fifi, pak Hari, kak Jermy and kak Santi--thank you for sharing the PhD path with me!! To the Leideners: Julia, mbak Dewi, mbak Ayu, Renzi-Rio, Kang Kur, kak Julinta, Kak Doel, Nazar, Arfian-mbak Nora, mas Nurmaya-teh Tika, mas Syahril, mas Fachrizal, mas Tjahyono, Melita, mbak Isma and all the Leideners who I could not mention here--thanks for fun times in Leiden, mostly eating-related occasions. Special thanks to dearest pak Max (Maxim Henninger) for your hospitality during my stay in Leiden. Thanks to ci Nini, Ro, Gio and Anthony-for the hospitality during my stay in the Netherlands. Pu and Pim--thanks for your help and basically sharing the international experience in Leiden.

I will take this opportunity to thank all my lectures in my undergraduate at Department Biology, FMIPA, especially alm.bu Boen--for being a very inspiring character, bu Mega-for also sharing the PhD business in Leiden, bu Retno, bu Yani, pak Abin, bu Firel, pak Iman, bu Wellyzar, pak Adi, pak Mufti, pak Yasman; pak Jatna, bu Ratna and bu Andi--for your visit to Leiden. Also not to forget, thanks to bu Ros. I must say my undergraduate was the metamorphosis in my life and I am grateful to have all the amazing lecturers who inspire me till now. Makasih buat doa, saran dan waktu sharing dari Bu Stella, jangan bosan ya bu. To the KM.16 team, current and former squad: alm.Prof. Is, pak Heri Wibowo, pak Dirman, pak Warto, kak Tryana, kak Susan, ii Erlinda, Yosi, Difa, Pita, Audi, Femmy, mas Budi, mbak Heni, Puspa, Adi and Eka--for all the memories we shared (and counting) in the fields. I also thank colleagues at the Department of Parasitology, FKUI. Other collugues: Vanya, Arfin, Vito, Lukito, Rosi, Tasya, Arina, mas Farid.

To my old friends: Marta Leni, Silvi, Agustina, Yusvita, alm.Dewi Wulandari--thank you for wonderful experiences. Bu pendeta Hiburyanti Marbun, thank you for being one of my truly special friends. To my E2.lt.4-ladies: Lucyana Siregar, Melani L. Sirait, Santi S. Sagala and Eflina P. Sinulingga, thank you for the colourful memories, you ladies keep me humble and I am glad we are still supporting each other--I am grateful for our friendship. Thanks so so so much to Valentine, my "twin sister" and Melinda Remelia--for being priceless best friends to me, for all the best wishes you sent for me. I am grateful for the friendships in Baliveau (Bio 2004)--especially with the buddies: AE, AP and Banced--we (at least I) never thought we could meet in The Netherlands. Galau United--for sharing random and whatever info.

"Intense love does not measure, it just gives"--Mother Teresa

Mama, papa, mami, papi, Edwar, Erick, Wilfred, Omak, Ama, Kung-kung dan alm.Engkong terima kasih atas semua doa dan dukungannya, uncles-aunties (Semua Apak, Pakme, Engku, Engkim, Kuku, Ii dan Ithio) and my big family thanks for all the support. To my dearest husband, Felix, thanks so much for your love, your endless support, for being patient and for simply being my very best friend.

At the last, for everyone who I cannot mention here, many many many thanks!!!!